Loaded Dice in Monte Carlo

importance sampling in phase space integration and probability distributions for discrepancies

André van Hameren
University of Nijmegen, Nijmegen, the Netherlands
andrevh@sci.kun.nl

PhD thesis

Abstract

Discrepancies play an important rôle in the study of uniformity properties of point sets. Their probability distributions are a help in the analysis of the efficiency of the Quasi Monte Carlo method of numerical integration, which uses point sets that are distributed more uniformly than sets of independently uniformly distributed random points. In this thesis, generating functions of probability distributions of quadratic discrepancies are calculated using techniques borrowed from quantum field theory.

The second part of this manuscript deals with the application of the Monte Carlo method to phase space integration, and in particular with an explicit example of importance sampling. It concerns the integration of differential cross sections of multi-parton QCD-processes, which contain the so-called kinematical antenna pole structures. The algorithm is presented and compared with RAMBO, showing a substantial reduction in computing time.

In behalf of completeness of the thesis, short introductions to probability theory, Feynman diagrams and the Monte Carlo method of numerical integration are included.

This thesis was typeset with LaTeX 2$_\varepsilon$.

Loaded Dice in Monte Carlo

importance sampling in phase space integration and probability distributions for discrepancies

een wetenschappelijke proeve op het gebied van de Natuurwetenschappen, Wiskunde en Informatica

Proefschrift

ter verkrijging van de graad van doctor aan de Katholieke Universiteit Nijmegen, volgens besluit van het College van Decanen in het openbaar te verdedigen op

dinsdag 9 januari 2001
des namiddags om 1.30 uur precies

door

Andreas Ferdinand Willem van Hameren

geboren op 4 december 1973 te Horst

Promotor:	Prof. Dr. R.H.P. Kleiss
Manuscriptcommissie:	Prof. Dr. W.J. Stirling (University of Durham) Prof. Dr. S.J. de Jong Dr. J.D.M. Maassen

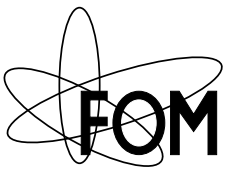

Het werk beschreven in dit proefschrift maakt deel uit van het onderzoeksprogramma van de Stichting voor Fundamenteel Onderzoek der Materie (FOM), die financieel wordt gesteund door de Nederlandse Organisatie voor Wetenschappelijk Onderzoek (NWO).

ISBN 90-9014235-5

Contents

Chapter 1

Introduction

The cement for the subjects this manuscript deals with is the Monte Carlo method of numerical integration. Therefore, the first section is endowed with an introduction to its aspects relevant for the second section, which digresses on the main contents of this thesis.

Contents

1.1 Numerical integration

Numerical integration is an approximation of the solution to an integration problem. An integration problem consists of the task to integrate a function f, the integrand. Sometimes, the integral can be calculated analytically, but in most cases, this is not possible. Let us, for simplicity, assume that the problem can be reduced to that of the calculation of an integral on the s-dimensional hypercube $\mathbf{K} := [0,1]^s$. We denote the Lebesgue integral of the integrand f by

$$\langle f \rangle := \int_{\mathbf{K}} f(x)\,dx \quad . \tag{1.1}$$

With numerical integration, this integral is estimated by a weighted average of f over a finite sample of N points $x_k \in \mathbf{K}$, that is, by

$$\sum_{k=1}^{N} w(x_k) f(x_k) \overset{?}{\approx} \langle f \rangle \quad , \tag{1.2}$$

where the numbers $w(x_k)$ are the weights coming with the particular method. Such a *method* is determined by the choice of the sample and the weights.

In principle, the only restriction on a method to be acceptable is that, with the estimate of the integral, it should give an estimate of the expected error on the result. And of course, this expected error should not be too large. If a certain method cannot give an error estimate, it is useless. In practice, there is another restriction on a method to be acceptable, namely that the computational complexity it introduces should not be too large. It should be possible to do the computation within reasonable time. The computational complexity is due to the generation of the sample, evaluating the weights and evaluating the function values. Naturally, one expects that a result will become more accurate if larger samples are used, because then more information about the integrand is used. But if the evaluation of the function values is very expensive (time consuming), then one would like to use small samples, and indeed, there are methods that need smaller samples than other methods with the same accuracy. For these methods, however, the generation of the samples is more expensive.

In the case of $s = 1$, there are many acceptable and efficient methods. In most of them, the sample is chosen to be distributed evenly over $[0, 1]$, i.e., all the distances between neighbors are the same and the whole of $[0, 1]$ is covered. Different weights can be chosen, depending on the smoothness of the integrand. These methods give an expected error that decreases with the number of points as $1/N^\alpha$, where $\alpha > 0$, with the general rule that α is larger for methods that can be applied to smoother integrands (cf. [1]).

Conceptually, it is a small step to extrapolate these one-dimensional methods to more dimensions: the sample is taken to be the Cartesian product in the coordinates of the one-dimensional samples, and the weights are the products over the coordinates of the one-dimensional weights. Computationally, however, is it a large step, for the expected error decreases with N as $1/N^{\alpha/s}$. So to get an expected error that is of the "one-dimensional order" with N points, you need N^s points. This small disaster is often called the "curse of dimensionality".

A closer look at the choice of the samples reveals the cause of the curse. In one dimension, the even distribution of the points is the most uniform distribution possible. This makes the methods applicable to large classes of functions, because in the choice of the sample no knowledge about the integrand is assumed. As a result of this, the behavior with N of the expected error factorizes. In more dimensions, however, a Cartesian product of these one-dimensional distributions is not at all 'uniform'. The distances between neighbors in different directions are not the same anymore. Therefore, these methods can only be efficient for integrands that have the same kind of Cartesian symmetry. The error estimate, however, includes no knowledge about the integrand, and as a result of this, increases rapidly with the number of dimensions.

1.1.1 Monte Carlo integration

A popular remedy to the curse of dimensionality is the so called Monte Carlo (MC) method of numerical integration [15]. It is based on the belief that the points of the sample will be distributed fairly over $\mathbf{K}$ if they are chosen at random. To be more precise, the points are chosen

at random, independently and uniformly distributed, and the estimate of the integral of a function f is given by the unweighted average

$$\langle f\rangle_N := \frac{1}{N}\sum_{k=1}^{N} f(x_k) \quad . \tag{1.3}$$

With this choice of the samples, the estimate of the integral becomes a random variable, and probability theory can be applied to do statements about it (some relevant topics are reviewed in Section 2.1). For example, the expectation value of $\langle f\rangle_N$ is given by

$$\mathsf{E}(\langle f\rangle_N) = \frac{1}{N}\sum_{k=1}^{N}\langle f\rangle = \langle f\rangle \quad . \tag{1.4}$$

So the expectation value of the estimate of the integral is equal to the integral itself. The variance of $\langle f\rangle_N$ is equal to

$$\mathsf{V}(\langle f\rangle_N) = \mathsf{E}(\langle f\rangle_N^2) - \mathsf{E}(\langle f\rangle_N)^2 = \frac{\langle f^2\rangle - \langle f\rangle^2}{N} \quad , \tag{1.5}$$

where f^2 just denotes pointwise multiplication of f with itself. This means that, if f is square integrable so that $\langle f^2\rangle$ and $\mathsf{V}(\langle f\rangle_N)$ exist, then we can apply the Chebyshev inequality, with the result that for large N, the estimate $\langle f\rangle_N$ converges to $\langle f\rangle$ with an expected error given by $\sqrt{\mathsf{V}(\langle f\rangle_N)}$. This is a very important result, for it states that the Monte Carlo method works in any dimension with the same rate of convergence, given by the $1/\sqrt{N}$-rule. The only restriction is that f has to be square integrable. If this is not the case, the Monte Carlo estimate of an integral cannot be trusted.

1.1.1.1 Error estimation

In practice, one of course does not know $\langle f^2\rangle - \langle f\rangle^2$, so that it has to be estimated. This makes Monte Carlo integration a matter of statistics. A good estimator for the squared error is given by

$$\langle f\rangle_N^{[2]} := \frac{\langle f^2\rangle_N - \langle f\rangle_N^2}{N-1} \quad , \tag{1.6}$$

which satisfies $\mathsf{E}(\langle f\rangle_N^{[2]}) = \mathsf{V}(\langle f\rangle_N)$. To get more confidence in the result, an estimate of the squared error on the estimated squared error can be calculated with

$$\langle f\rangle_N^{[4]} := \frac{\langle f^4\rangle_N - 4\langle f^3\rangle_N\langle f\rangle_N + 3\langle f^2\rangle_N^2}{N(N-2)(N-3)} - \frac{4N-6}{(N-2)(N-3)}\left(\langle f\rangle_N^{[2]}\right)^2 \tag{1.7}$$

which satisfies $\mathsf{E}(\langle f\rangle_N^{[4]}) = \mathsf{V}(\langle f\rangle_N^{[2]})$. Notice that $\langle f^4\rangle$ has to exist in order to credit any value to $\langle f\rangle_N^{[4]}$. One could, in principle, go on calculating higher errors on errors, but their significance becomes less and less, *if* they converge at all.

1.1.1.2 Sample generation

Another question is how to obtain the random points. Monte Carlo integration is preferably done with the help of a computer, and there exist algorithms that produce sequences of numbers between 0 and 1 that are 'as good as random'. They are called *pseudo-random number generators* (c.f. [2]). Since they are implemented on a computer, the algorithms are deterministic, and the numbers they produce cannot be truly random. The sequences, however, 'look random' and are certainly suitable for the use in Monte Carlo integration. Another drawback is that, because computers represent real numbers by a finite number of bits, the algorithms necessarily have a period, that is, they can produce only a finite number of numbers, and if they are recycled, they cannot be considered random anymore. Fortunately, modern random number generators such as `RANLUX` have very large periods, up to 10^{165}.

Finaly, the finiteness of a computer can cause problems when calculating a Lebesgue integral. In the foregoing, we stated that the Monte Carlo method is alway applicable if the integrand f is square integrable. For a computer, however, this is not enough. Consider the function

$$f(x) := \begin{cases} 1 & \text{if } x \in \mathbf{Q} \\ 0 & \text{if } x \notin \mathbf{Q}\,, \end{cases} \tag{1.8}$$

which has Lebesgue integrals $\langle f \rangle = \langle f^2 \rangle = 0$. A computer represents numbers with finite strings of bits, i.e., the numbers are always rational, so that a Monte Carlo estimate will always give $\langle f \rangle_N = 1$. Fortunately, this kind of pathological cases do not appear often in physical applications.

1.1.2 Importance sampling

The original problem is usually not that of the integration of a function on a hypercube. In general, it is the problem of integrating a function F on a more complicated manifold $\mathbf{M}$. As we have seen before, the problem *has* to be reduced to that of integrating a function f on a hypercube $\mathbf{K}$ in order to apply the MC method. This is done with a map $\varphi : \mathbf{K} \mapsto \mathbf{M}$, and sometimes, an invertible map can be found in which cases we simply have

$$\int_{\mathbf{M}} F(y)\,dy = \int_{\mathbf{K}} (F \circ \varphi)(x) |J_\varphi(x)|\,dx \quad , \tag{1.9}$$

where J_φ is the determinant of the Jacobian matrix of φ, so that $f(x) = (F \circ \varphi)(x)|J_\varphi(x)|$. In general however, this is not the case, and a suitable mapping $\varphi : \mathbf{K} \mapsto \mathbf{M}$ and a function $g_\varphi : \mathbf{K} \mapsto \mathbf{R}$ have to be determined such that

$$\int_{\mathbf{K}} g_\varphi(x) \delta(\varphi(x) - y)\,dx = 1 \quad , \tag{1.10}$$

where δ is the Dirac delta-distribution on $\mathbf{M}$ (cf. [4]). The integral of F over $\mathbf{M}$ is then given by

$$\int_{\mathbf{M}} F(y)\,dy = \langle f_\varphi \rangle \quad \text{with} \quad f_\varphi(x) = (F \circ \varphi)(x) g_\varphi(x) \quad . \tag{1.11}$$

If φ is invertible, then $g_\varphi(x) = |J_\varphi(x)|$. We just used the word "suitable" in connection with the determination of φ, and therefore in connection with the determination with the function f_φ, which is not unique. Importance sampling is the effort to choose f_φ such that $\langle f_\varphi^2 \rangle - \langle f_\varphi \rangle^2$ is as small as possible, so that the expected error is as small as possible. The optimal choice would be such that it is zero, but this would mean that $f_\varphi(x) = 1$ for all $x \in \mathbf{K}$ and that the integration problem is solved analytically. In practice, f_φ should be chosen as flat as possible.

1.1.3 Quasi Monte Carlo integration

The Monte Carlo method is very robust, but the $1/\sqrt{N}$ rate of convergence can be considered rather slow: to get one more significant digit in the result, 100 times more sample points are needed. The Quasi Monte Carlo (QMC) method tries to improve this behavior, by using samples the points of which are distributed more uniformly *over* the integration region than independent random points that are distributed uniformly *in* the integration region (cf. [3]).

The previous sentence seems a bit paradoxical, but notice the difference between 'uniformly over' and 'uniformly in'. The latter is meant in the probabilistic sense: a random point is distributed following a distribution *in* an integration region, which can be the uniform distribution. The former is meant for a set of points: the points can be distributed uniformly *over* the integration region. In this case, the word 'uniformly' does not really have a meaning yet, and has to be defined, which is done by introducing measures of rates of uniformity. They are called *discrepancies*, and return a number $D_N(\mathcal{X}_N)$ for a sample, or *point set*, $\mathcal{X}_N = (x_1, x_2, \ldots, x_N)$. The idea is then that, the higher the number $D_N(\mathcal{X}_N)$, the less uniformly the points are distributed.

The task in QMC integration is to find low-discrepancy point sets. The integral of a function f is then estimated again by the unweighted average $\langle f \rangle_N := N^{-1} \sum_{k=1}^{N} f(x_k)$ over the point set. That this approach can indeed improve the convergence of the error is, for example, shown by the Koksma-Hlawka inequality, which states that

$$|\langle f \rangle_N - \langle f \rangle| \;\leq\; V_{HK}[f]\, D_N^*(\mathcal{X}_N) \quad , \tag{1.12}$$

where $D_N^*(\mathcal{X}_N)$ is the so called *star discrepancy* of $\mathcal{X}_N$, and $V_{HK}[f]$ is the variation of f in the sense of Hardy and Krause. It is a complicated function of f that is, however, independent of the point set. This inequality states that the error, made by estimating the integral by an unweighted average over the function values at the points of the point set, decreases with the number of points N at least as quickly as the star discrepancy of the point set.

1.2 Contents of this thesis

The main contents start in Chapter 3, and can be divided into two subjects: the calculation of discrepancy distributions, and phase space integration with the emphasize on a special case of importance sampling. Chapter 2 reviews some topics from probability theory and formalism of Feynman diagrams.

1.2.1 Calculation of discrepancy distributions

As discussed before, the relatively slow convergence of the MC method has inspired a search for other point sets whose discrepancy is lower than that expected for truly random points. The low-discrepancy point sets and *low-discrepancy sequences* have developed into a veritable industry, and sequences with, asymptotically, very low discrepancy are now available, especially for problems for which the dimension of the integration region is very large [16]. For point sets that are extracted as the first N elements of such a sequence, though, one is usually still compelled to compute the discrepancy numerically, and compare it to the expectation for random points in order to show that the point set is indeed 'better than random'. This implies, however, that one has to know, for a given discrepancy, its expectation value for truly random points, or preferably even its probability density (cf. Section 2.1.6).

In Chapter 3, we introduce the formalism of the so-called *quadratic discrepancies*, and derive a formula for the generating function of their probability distribution. Furthermore, we give Feynman rules to calculate the generating function perturbatively using Feynman diagrams, with $1/N$ as expansion parameter. Chapter 4 digresses on the question whether the asymptotic series obtained is correct, and concludes affirmative for two examples of discrepancies, with great confidence in the general case.

In [23, 24, 25] the problem of calculating the probability distribution of quadratic discrepancies under truly random point sets has been solved for large classes of discrepancies. Although computable, the resulting distributions are typically not very illuminating. The exception is usually the case where the number of dimensions of the integration problem becomes very large, in which case a normal distribution often arises [22, 26]. In Chapter 5, we investigate this phenomenon in more detail, and we shall describe the conditions under which this 'law of large dimensions' applies.

Throughout the discussion of Chapter 5, only the asymptotic limit of very large N is considered, which implies that no statements can be done on how the number of points has to approach infinity with respect to the number of dimensions, as was for instance done in [26]. This problem is tackled in Chapter 6, in which the diagrammatic expansions of the generating function is given and calculated to low order for a few examples. For the *Lego discrepancy*, which is equivalent with a χ^2-statistic for N data points distributed over a number of M bins, cases in which N as well as M become large are considered, leading to surprising results. Also the *Fourier diaphony*, for which a limit is derived in [26], is handled, leading to a stronger limit.

1.2.2 Phase space integration

A typical example in which the MC method is the only option is in the problem of *phase space integration*. It occurs in particle physics, where the connection between the model of the particles and the experiments with the particles is made with the help of transition probabilities (cf. [7]). These give the probability to get, under certain conditions, a transition from one certain state of particles (the *initial state*) to another certain state of particles (the *final state*). On one side, these

probabilities can be determined statistically, by performing an experiment several times, starting with the same initial state every time, and by counting the number of times certain final states occur. The probabilities can also be calculated from the model, and then two outcomes can be compared to evaluate the model.

Phase space is the space of all possible momentum configurations of the final-state particles, and particle models predict probability densities on it. Because of the need of very high statistics for acceptable precision, it is usually difficult to determine them experimentally. A solution to this experimental problem is the creation of a mathematical problem: averaging transition probabilities over phase space. In the analysis of the experimental data this just means that final states, that differ only in momentum configuration, are considered equivalent. In the analysis of the model, this means that an integration of the probability density over phase space has to be performed.

The actual quantity that physicists deal with is not the transition probability, but the *cross section*. If the number of initial particles is two, then it is the transition rate per unit of time, normalized with respect to the flux of the initial particles, i.e., the density of the initial particles times their relative velocity. The *differential* cross section $\mathrm{d}\sigma$ of a proces from a two particle initial state to a certain final state is given by

$$\mathrm{d}\sigma(\mathrm{i} \to \mathrm{f}) \;=\; \frac{(2\pi)^4}{v_\mathrm{i}} \, |M_{\mathrm{f,i}}|^2 \, \delta(p_\mathrm{f} - p_\mathrm{i}) \, \mathrm{d}f \quad . \tag{1.13}$$

In this expression, $\mathrm{d}f$ represents the final state degrees of freedom that have to be integrated or summed in order to get the desired cross section σ. This includes the final-state momenta. The delta-distribution represents momentum conservation between the initial and the final states, and v_i is the relative velocity of the initial particles. The characteristics of the particular proces are contained in $M_{\mathrm{f,i}}$, the transition *amplitude* or *matrix element*, and has to be calculated using the particle model in the formalism of quantum field theory. It determines the function that has to be intergrated over phase space.

Besides momentum conservation, there are other restrictions the momenta of the particles have to satisfy, independent of the amplitude. Algorithms that generate random momenta, satisfying these restrictions, are called *phase space generators*, and in Chapter 7 `RAMBO` is described, which generates momenta distibuted uniformly in phase space. This chapter also deals with some techniques that are useful for MC integration in general.

For certain particle processes, the squared amplitude can have complicated peak structures, that make it hard to be integrated if the momenta are generated such that they are distributed uniformly in phase space. This is in particular true if it concernes processes in which the strong interaction is involved, for which the integrand contains peak structures that are governed by the so-called *antenna pole structure*. In Chapter 8, the algorithm `SARGE` is introduced that generates random momenta, satisfying the restrictions that are independent of the amplitude, and such that they are distributed following a density that containes the antenna pole structure. It improves the MC integration process through importance sampling.

Chapter 2

Probability, measures and diagrams

Since this thesis is meant to be read by both theoretical physicists and mathematicians, this chapter elaborates on some subjects that are probably not everyday routine to the one or the other. This concerns probability theory, including a (very) short introduction to martingales, and Feynman diagrams. The hasty reader is advised to read at least Section 2.1.6 and Section 2.1.7.

Contents

2.1 Some probability theory

We start this section ‘at level zero’ with respect to the probability theory, but expect the reader to be familiar with a bit of set theory, logic, measure theory, complex analysis and so on. For more details, we refer to [10], [11] and [12].

2.1.1 Probability space

A probability space consists of a triple $(\Omega, \mathcal{F}, \mathsf{P})$, where Ω is a set, $\mathcal{F}$ a σ-field of subsets of Ω, and P a probability measure defined on $\mathcal{F}$. The collection $\mathcal{F}$ of subsets is called a σ-field if

1. $\emptyset \in \mathcal{F}$;
2. $\mathbf{F} \in \mathcal{F} \Longrightarrow \Omega \backslash \mathbf{F} \in \mathcal{F}$;
3. $\mathbf{F}_1, \mathbf{F}_2, \ldots \in \mathcal{F} \Longrightarrow \bigcup_n \mathbf{F}_n \in \mathcal{F}$,

where, in the last property, the number of sets $\mathbf{F}_n$ has to be countable. The probability measure P is a function $\mathcal{F} \mapsto [0,1]$ with $\mathsf{P}(\Omega) = 1$. We will only consider probability spaces for which Ω is a Lebesgue measurable subset of $\mathbf{R}^n$, $n = 1, 2, \ldots$ and for which P is given by

$$\mathsf{P}(\mathbf{F}) \;=\; \int_{\mathbf{F}} \mathsf{P}(\omega)\, \mathrm{d}\omega \quad , \tag{2.1}$$

where $\mathrm{d}\omega$ stands for the Lebesgue measure on $\Omega \subset \mathbf{R}^n$ and P is a function $\Omega \mapsto [0, \infty)$ with $\int_\Omega \mathsf{P}(\omega)\, \mathrm{d}\omega = 1$. P is called the *probability density* or *probability distribution*, although the latter name is more appropriate for the set of doubles $\{(\mathbf{F}, \mathsf{P}(\mathbf{F})) \mid \mathbf{F} \in \mathcal{F}\}$.

A simple example of a probability distribution is the *uniform* distribution in $[0,1]$, for which $\mathsf{P}(\omega) = 1$. This is often extended to more dimensions, say n, by taking the Cartesian product of independent one-dimensional variables, that is, $\mathsf{P}_n(\omega) = \prod_{k=1}^{n} \mathsf{P}(\omega^{(k)})$, where $\omega = (\omega^{(1)}, \omega^{(2)}, \ldots, \omega^{(n)}) \in [0,1]^n$ and $\mathsf{P}(\omega^{(k)}) = 1$ for all k. We say that ω is distributed uniformly in $[0,1]^n$.

2.1.2 Random variables

A random variable X is a function on Ω. It is an object about which statements Π can be made. These statements are then 'valued' with a number between 0 and 1 by the probability measure. Probability theory concerns itself with the calculation of these numbers; their interpretation depends on the user. It can be a "rate of belief" (the Bayesian interpretation) or a ratio of outcomes in the limit of an infinite number of repetitions of experiments (the frequentist interpretation). In Monte Carlo integration, for example, the latter applies.

Let $\Pi(\mathsf{X})$ denote a statement Π about X, and let $\mathbf{F}_{\Pi(\mathsf{X})} := \{\omega \in \Omega \mid \Pi(\mathsf{X}(\omega)) \text{ is true}\}$ be the subspace of Ω for which $\Pi(\mathsf{X}(\omega))$ is true, then we denote

$$\mathsf{P}(\Pi(\mathsf{X})) := \mathsf{P}(\mathbf{F}_{\Pi(\mathsf{X})}) \quad . \tag{2.2}$$

An important operator in the theory of probability is the expectation value E. It is the average of X over Ω, weighted with P:

$$\mathsf{E}(\mathsf{X}) \;:=\; \int_\Omega \mathsf{X}(\omega)\mathsf{P}(\omega)\, \mathrm{d}\omega \quad . \tag{2.3}$$

Especially expectation values of powers of X are often considered, and they are called the moments of the probability distribution of X. This name anticipates the fact that a random variable has its own probability distribution, which is simply defined through

$$P_X(\Pi(Z)) := P(\mathbf{F}_{\Pi(Z(X))}) \quad , \tag{2.4}$$

where $\mathbf{F}_{\Pi(Z(X))} := \{\omega \in \Omega \mid \Pi(Z(X(\omega)))\,\text{is true}\}$. From now on, we will assume that X is real, and introduce the *cumulative probability distribution* or *distribution function*

$$F_X(x) \;:=\; P(X \leq x) \quad . \tag{2.5}$$

F_X is a monotonously increasing function $\mathbf{R} \mapsto [0,1]$. Its derivative is the probability density P_X, and we have

$$F_X(x) \;=\; \int_{-\infty}^{x} P_X(t)\,dt \quad . \tag{2.6}$$

Discontinuities in F_X are represented by Dirac delta-distributions in P_X. An interesting observation is, furthermore, that if X is distributed following F_X, then the random variable $Y := F_X(X)$ is distributed uniformly in $[0,1]$, since $P(Y \leq y) = P(X \leq F_X^{-1}(y)) = y$.

We proceed with a translation of confidence levels, given by P, into expectation values. This is done by the *Chebyshev inequality*, which states that, for a given number $a > 0$,

$$P(|X| > a) \;\leq\; \frac{E(|X|^s)}{a^s} \quad \text{for any } s \geq 1 \quad . \tag{2.7}$$

Its proof is simple. We have

$$P(|X| > a) \;=\; \int_a^\infty P_X(t)\,dt + \int_{-\infty}^{-a} P_X(t)\,dt \;\leq\; \int_a^\infty \frac{|t|^s}{a^s} P_X(t)\,dt + \int_{-\infty}^{-a} \frac{|t|^s}{a^s} P_X(t)\,dt \quad ,$$

where the inequality holds because $|t|/a \geq 1$ under the integrals. The final expression is smaller than the integral over the whole of $\mathbf{R}$, which is equal to the r.h.s. of Eq.(2.7). An example of its use is an estimate of the probability that a variable X will differ an amount a from its expectation value $E(X)$. The Chebyshev inequality tells us that

$$P(|X - E(X)| > a) \;\leq\; \frac{E(|X - E(X)|^2)}{a^2} \;=\; \frac{V(X)}{a^2} \quad , \tag{2.8}$$

where

$$V(X) \;:=\; E(X^2) - E(X)^2 \tag{2.9}$$

is called the *variance* of X, and its square root $\sigma(X) := \sqrt{V(X)}$ is called the *standard deviation*. So if we take $a = c \cdot \sigma(X)$, then we see that the probability of $|X - E(X)|$ to be larger than $c \cdot \sigma(X)$ is smaller than $1/c^2$.

It is common not to consider the random variable itself, but *standardized variable* which is given by

$$\frac{X - E(X)}{\sigma(X)} \quad . \tag{2.10}$$

It has its expectation value equal to zero and its variance equal to one.

2.1.3 Generating functions

If X is real, its probability density can be calculated as follows. Let θ denote the Heaviside step-function. It can, for example, be represented by the integral in the complex plane

$$\theta(t) \;=\; \frac{-1}{2\pi i}\int_\Gamma \frac{e^{-zt}}{z}\,dz \;\;, \tag{2.11}$$

where the contour Γ is along the line $\mathrm{Re}\,z = -\varepsilon$, and ε is positive and small. If $t > 0$, then the integration contour can be closed to the right and the pole in $z = 0$ contributes with a residue that is equal to -1. An extra minus sign comes from the orientation of the contour. If $t < 0$, then the contour can be closed to the left, giving zero. The probability distribution function F_X is then given by

$$F_X(t) \;=\; \int_\Omega \theta(\,t - X(\omega)\,)P(\omega)\,d\omega \;=\; \frac{-1}{2\pi i}\int_\Gamma \frac{e^{-zt}}{z}\int_\Omega e^{zX(\omega)}P(\omega)\,d\omega\,dz \;\;. \tag{2.12}$$

The integral over Ω just gives the expectation value of e^{zX}, which is called the *moment generating function*

$$G_X(z) := E(\,e^{zX}\,) \;\;. \tag{2.13}$$

It carries this name, because its derivatives in $z = 0$ give the moments $E(X^n)$ of X. In literature, the *characteristic function* is often used, which is just given by $G_X(iz)$. The final result is that F_X is given by

$$F_X(t) \;=\; \frac{-1}{2\pi i}\int_\Gamma \frac{e^{-zt}}{z}\,G_X(z)\,dz \;\;. \tag{2.14}$$

We can translate this into a formula for the probability density P_X by differentiation with respect to t. The result is that

$$P_X(t) \;=\; \frac{1}{2\pi i}\int_\Gamma e^{-zt}\,G_X(z)\,dz \;\;, \tag{2.15}$$

i.e., it is the inverse Laplace transform of the moment generating function of X. Notice that the generating function satisfies $G(0) = 1$, because the probability density P_X is properly normalized: $\int_{\mathbf{R}} P_X(t)\,dt = 1$.

Another generating function that is often used, the cumulant generating function W_X, is simply given by $W_X(z) = \log(G_X(z))$. The first cumulant is equal to $E(X)$ itself, and the second is the variance $V(X)$.

The generating function of the standardized variable can be expressed in terms of the original generating function G_X through

$$E(\,e^{z(X-E(X))\sigma(X)^{-1}}\,) \;=\; e^{-E(X)\sigma(X)^{-1}}G_X(z\sigma(X)^{-1}) \;\;. \tag{2.16}$$

2.1.4 Convergence of random variables and distributions

Sequences $\{X_n \mid n = 1, 2, \ldots\}$ of random variables are often considered in probabilistic analyses, and in particular their limiting behavior. Therefore, notions of convergence are needed, and we distinguish various types. First there is *convergence in probability*, and we write

$$X_n \xrightarrow{p} X \qquad \text{if} \qquad P_n(|X_n - X| \geq \varepsilon) \to 0 \quad \forall\, \varepsilon > 0 \ . \tag{2.17}$$

With the Chebyshev inequality, we see that the requirement for convergence in probability is satisfied if there is a $p \geq 1$ such that $E(|X_n - X|^p)/\varepsilon^p \to 0$ for all $\varepsilon > 0$. This observation suggests to introduce *convergence in* p^{th} *mean*, and we write

$$X_n \xrightarrow{\mathcal{L}_p} X \qquad \text{if} \qquad E(|X_n - X|^p) \to 0 \ . \tag{2.18}$$

The case of $p \to \infty$ can be considered special, and leads to *almost sure convergence*:

$$X_n \xrightarrow{a.s.} X \qquad \text{if} \qquad X_n(\omega) \to X(\omega) \ \text{ for all } \omega \in \Omega \backslash \mathbf{F} \ , \tag{2.19}$$

where $\mathbf{F} \in \mathcal{F}$ with $P(\mathbf{F}) = 0$. To compare these notions of convergence, we note that (cf. [10])

$$X_n \xrightarrow{a.s.} X \quad \Longrightarrow \quad X_n \xrightarrow{p} X \ , \tag{2.20}$$

$$X_n \xrightarrow{\mathcal{L}_p} X \ \text{ for some } p > 0 \quad \Longrightarrow \quad X_n \xrightarrow{p} X \ . \tag{2.21}$$

Finally, there is *convergence in distribution* or *convergence in law*, and we write

$$X_n \xrightarrow{d} X \qquad \text{if} \qquad P_n \Rightarrow P \ , \tag{2.22}$$

where the latter denotes *weak convergence* of the distributions P_n of the variables X_n:

$$P_n \Rightarrow P \qquad \text{if} \qquad E(f(X_n)) \to E(f(X)) \quad \text{for any bounded function } f. \tag{2.23}$$

Notice that, in general, the moments of the variables X_n are not bounded functions. The generating functions $G_n(z)$, however, are bounded for imaginary z. We actually have, (cf. [11])

$$P_n \Rightarrow P \quad \Longleftrightarrow \quad G_n(z) \to G(z) \quad \text{for each imaginary } z. \tag{2.24}$$

The notion of weak convergence is also used in connection with distribution functions, and we write

$$F_n \xrightarrow{w} F \qquad \text{if} \qquad F_n(x) \to F(x) \quad \text{at all continuity points } x \text{ of } F. \tag{2.25}$$

Distribution functions are right-continuous and satisfy $F_n(-\infty) = 0$ and $F_n(\infty) = 1$. Because F does not have to be a distribution function in case of weak convergence, it is useful to define *complete convergence*, and we write

$$F_n \xrightarrow{c} F \qquad \text{if} \qquad F_n \xrightarrow{w} F \ \text{ and } \ F_n(\pm\infty) \to F(\pm\infty) \ . \tag{2.26}$$

We note that weak convergence of a distribution is *not* necessarily equivalent with weak convergence of the density, but that (cf. [10])

$$P_n \Rightarrow P \quad \Longleftrightarrow \quad F_n \xrightarrow{c} F \ , \qquad \text{so that} \qquad X_n \xrightarrow{d} X \quad \text{if} \quad F_n \xrightarrow{c} F \ . \tag{2.27}$$

We end this section with the remark that $X_n \xrightarrow{p} X$ implies $X_n \xrightarrow{d} X$ (cf. [10]), so that

$$X_n \xrightarrow{a.s.} X \quad \Longrightarrow \quad X_n \xrightarrow{p} X \quad \Longrightarrow \quad X_n \xrightarrow{d} X \ . \tag{2.28}$$

2.1.5 Martingales

With a sequence of random variables X_n should come a sequence of σ-fields $\mathcal{F}_n$. A sequence $\{Z_n, \mathcal{F}_n \mid n = 1, 2, \ldots\}$ is called a *martingale* if

1. Z_n is measurable with respect to $\mathcal{F}_n$;
2. $E(|Z_n|) < \infty$;
3. $E(Z_n|\mathcal{F}_m) = Z_m$ with probability one for all $m < n$.

The idea is that Z_n depends on a number of k_n variables ω_i that take their values in Ω. In $E(Z_n|\mathcal{F}_m)$, the first $k_m < k_n$ variables have to be taken fixed, and only the average over the remaining $k_n - k_m$ variables has to be taken. This average can then be considered to depend on the first k_m variables again, and this dependence should be the same as the one of Z_m.

A martingale is called zero-mean if $E(Z_n) = 0$ for all n. Furthermore, it is called square-integrable if $E(Z_n^2)$ exists for all n. A double sequence $\{Z_{n,i}, \mathcal{F}_{n,i} \mid 1 \leq i \leq k_n, n = 1, 2, \ldots\}$ is called a martingale array, if $\{Z_{n,i}, \mathcal{F}_{n,i} \mid 1 \leq i \leq k_n\}$ is a martingale for each $n \geq 1$. The variables $X_{n,i} := Z_{n,i} - Z_{n,i-1}$ are called the martingale differences. These are the ingredients needed for the powerful (c.f. [12])

2.1.5.1 Central Limit Theorem:

Let $\{Z_{n,i}, \mathcal{F}_{n,i} \mid 1 \leq i \leq k_n, n = 1, 2, \ldots\}$ be a zero-mean, square-integrable martingale array with differences $X_{n,i}$, and suppose that

$$\max_i |X_{n,i}| \xrightarrow{p} 0 \ , \tag{2.29}$$

$$\sum_i X_{n,i}^2 \xrightarrow{p} 1 \ , \tag{2.30}$$

$$E(\max_i X_{n,i}^2) \quad \text{is bounded in } n \ , \tag{2.31}$$

$$\mathcal{F}_{n,i} \subseteq \mathcal{F}_{n+1,i} \quad \text{for} \quad 1 \leq i \leq k_n \ , \quad n \geq 1 \ . \tag{2.32}$$

Then $Z_{n,k_n} \xrightarrow{d} Z$, where Z is a normal variable.

A normal variable has a Gaussian distribution with zero mean and unit variance, given by a density $P(t) = (2\pi)^{-1/2} \exp(-\frac{1}{2}t^2)$ and generating function $G(z) = \exp(\frac{1}{2}z^2)$.

2.1.5.2 Adaptive Monte Carlo integration

We apply this theorem to adaptive Monte Carlo integration, as a small exercise. It concerns the problem of calculating the Lebesgue integral $\langle f \rangle_\Omega$ of a function f on an integration region Ω. Let $g_1, g_2, \ldots$ be a sequence of positive functions, where g_k depends on k variables x_i that take their values in Ω. We denote such a set of k variables by $\{x\}_k := \{x_1, \ldots, x_k\}$. Assume that $\int_\Omega g_k(\{x\}_k)\, dx_k = 1$ for all values of $\{x\}_{k-1}$, so that

$$g_{\{x\}_{k-1}} : x_k \mapsto g_k(\{x\}_k) \tag{2.33}$$

is a probability density in x_k. Let us also introduce the functions

$$\bar{g}_k^{-r} : x_k \mapsto \int_{\Omega^{k-1}} \frac{g_1(x_1)\cdots g_{k-1}(\{x\}_{k-1})}{g_k(\{x\}_k)^r}\, dx_1 \cdots dx_{k-1} \quad . \tag{2.34}$$

In adaptive Monte Carlo integration, one generates a random point x_1 in Ω following a density g_1, and with this point a density $g_{\{x\}_1}$ is constructed to generate x_2, so that $g_{\{x\}_2}$ can be constructed to generate x_3 and so on. Then, one tries to estimate the integral $\langle f \rangle_\Omega$ with

$$\langle f \rangle_n \;:=\; \frac{1}{n} \sum_{k=1}^{n} \frac{f(x_k)}{g_{\{x\}_{k-1}}(x_k)} \quad . \tag{2.35}$$

The expectation value and the variance of $\langle f \rangle_n$ can easily be calculated, with the result that $E(\langle f \rangle_n) = \langle f \rangle_\Omega$ and $V(\langle f \rangle_n) = V_n[f]/n$, where

$$V_n[f] \;:=\; \frac{1}{n} \sum_{k=1}^{n} \langle \bar{g}_k^{-1} f^2 \rangle_\Omega - \langle f \rangle_\Omega^2 \quad . \tag{2.36}$$

Monte Carlo integration is based on the observation that if $\langle \bar{g}_k^{-1} f^2 \rangle_\Omega$ exists for every k, so that $V_n[f]$ is a finite number, the Chebyshev inequality gives

$$P(\, |\langle f \rangle_n - \langle f \rangle_\Omega| > \varepsilon \,) \;\le\; \frac{V_n[f]}{\varepsilon^2 n} \qquad \Longrightarrow \qquad \langle f \rangle_n \;\xrightarrow{p}\; \langle f \rangle_\Omega \quad , \tag{2.37}$$

which suggests to use $\langle f \rangle_n$ as an estimator of $\langle f \rangle_\Omega$, and to interpret $V_n[f]/n$ as the square of the expected integration error.

We shall prove[1] now, that $\langle f \rangle_n$ converges to $\langle f \rangle_\Omega$ with Gaussian confidence levels. Except of the existence of $\langle \bar{g}_k^{-1} f^2 \rangle_\Omega$, we shall need some more requirements, but first let us introduce the variables

$$Z_{n,i} := \sum_{k=1}^{i} \bar{X}_{n,k} \quad , \qquad \bar{X}_{n,k} := \frac{X_k}{\sqrt{n V_n[f]}} \quad , \qquad X_k := \frac{f(x_k)}{g_{\{x\}_{k-1}}(x_k)} - \langle f \rangle_\Omega \quad .$$

Because we define the variables $Z_{n,i}$ explicitly as the sum of the differences $\bar{X}_{n,k}$, we are clearly dealing with a martingale array (with $k_n = n$) satisfying (2.32). It obviously is zero mean, and

[1] This is a correction of the erroneous proof in the original thesis.

it is square integrable by the requirement that $\langle \bar{g}_k^{-1} f^2 \rangle_\Omega$ exists for all k. For the proof, we shall furthermore need the requirements that

$$\lim_{n\to\infty} \frac{1}{n^2} \sum_{i=1}^{n} E(X_i^4) = 0 \qquad \text{and} \qquad \lim_{n\to\infty} \frac{1}{n^2} \sum_{i\neq j}^{n} \left| E(X_i^2 X_j^2) - E(X_i^2) E(X_j^2) \right| = 0 \ . \tag{2.38}$$

The first one is satisfied if $E(X_i^4)$ exists for all i, which can be translated in the demand that $\langle \bar{g}_k^{-2} f^3 \rangle_\Omega$ and $\langle \bar{g}_k^{-3} f^4 \rangle_\Omega$ exist for all k. The second one puts a restriction on how strong the dependencies between the variables may be. This demand is, for example, satisfied if for every n there are numbers $K_n(i,j)$ such that

$$\int_{\Omega^{j-i}} \left| \int_{\Omega^i} \frac{g_1 g_2 \cdots g_{j-1} f_j^2}{g_j} \, dx_1 \cdots dx_i - \frac{g_{i+1} \cdots g_{j-1} f_j^2}{g_j} \right| dx_{i+1} \cdots dx_j \ < \ K_n(i,j) \tag{2.39}$$

and that satisfy $\lim_{n\to\infty} \frac{1}{n} \sum_{j=i+1}^{n} K_n(i,j) = 0$. This is, for example, the case if $K_n(i,j) \sim 1/|i-j|$. We prove along the line of argument as presented in [26], that the first three requirements of the theorem are satisfied. First we observe that the martingale is constructed such that

$$\sum_{i=1}^{n} E(\bar{X}_{n,i}^2) \ = \ \frac{1}{n V_n[f]} \sum_{i=1}^{n} E(X_i^2) \ = \ \frac{1}{n V_n[f]} \sum_{i=1}^{n} \left(\langle \bar{g}_i^{-1} f^2 \rangle_\Omega - \langle f \rangle_\Omega^2 \right) \ = \ 1 \ , \tag{2.40}$$

so that, for requirement (2.31), we have $E(\max_i \bar{X}_{n,i}^2) \leq \sum_{i=1}^{n} E(\bar{X}_{n,i}^2) = 1$. For (2.29) we use the Chebyshev inequality to find that

$$P(\max_i |\bar{X}_{n,i}| > \varepsilon) \ \leq \ \sum_{i=1}^{n} P(|\bar{X}_{n,i}| > \varepsilon) \ \leq \ \frac{1}{\varepsilon^4} \sum_{i=1}^{n} E(\bar{X}_{n,i}^4) \ = \ \frac{1}{\varepsilon^4 V_n[f]^2 n^2} \sum_{i=1}^{n} E(X_i^4) \ ,$$

which goes to zero for all $\varepsilon > 0$ by (2.38). Requirement (2.30) goes the same way:

$$\begin{aligned} P\Big(\Big| \sum_{i=1}^{n} \bar{X}_{n,i}^2 - 1 \Big| > \varepsilon \Big) &\leq \frac{1}{\varepsilon^2} \Big(\sum_{i,j=1}^{n} E(\bar{X}_{n,i}^2 \bar{X}_{n,j}^2) - 2 \sum_{i=1}^{n} E(\bar{X}_{n,i}^2) + 1 \Big) \\ &= \frac{1}{\varepsilon^2 V_n[f]^2 n^2} \Big(\sum_{i=1}^{n} \left(E(X_i^4) - E(X_i^2)^2 \right) \\ &\qquad + \sum_{i\neq j}^{n} \left(E(X_i^2 X_j^2) - E(X_i^2) E(X_j^2) \right) \Big) \ , \end{aligned}$$

where we used (2.40) again. The final expression goes to zero for all $\varepsilon > 0$ by (2.38). The result is that, because the variables $Z_{n,n}$ converge to a Gaussian variable with zero-mean and variance one, the random variables

$$\langle f \rangle_n \ = \ \sqrt{\frac{V_n[f]}{n}} \, Z_{n,n} + \langle f \rangle_\Omega \tag{2.41}$$

converge to a Gaussian variable with mean $\langle f \rangle_\Omega$ and variance $V_n[f]/n$. Note that for non-adaptive Monte Carlo integration, for which the densities g_k are equal to a fixed density g for all k, the Lévy Central Limit Theorem applies (cf. [10]) and only the existence of $\langle f^2/g \rangle_\Omega$ is needed.

2.1.6 Hypothesis testing, qualification and discrepancies

Probability theory is extensively used in the field of statistics. Statisticians try to derive probability distributions from empirical data, which are believed to be distributed following an existing, but unknown, distribution. In this section, some statistical procedures and their relevance to the main subjects of this thesis are discussed.

2.1.6.1 Hypothesis testing

One way to test a model of a physical system is by deriving from this model the probability distribution according to which certain data from the system are supposed to be distributed. Then a test has to be developed, which measures the deviation between the probability distribution from the model, and the empirical distribution of the data. Because the actual probability distribution that the data seem to be drawn from is not known, this procedure belongs to the field of statistics, and it goes under the name of *hypothesis testing*.

Let $\mathcal{X}_N = \{x_1, \ldots, x_N\}$ be a sample of physical data, P_N the probability density derived from the model (the hypothesis), and T_N the statistical test. In order for the test to be suitable, it should be developed such that, if $\mathcal{X}_N$ is distributed following P_N, then

$$\lim_{N\to\infty} T_N(\mathcal{X}_N) = 0 \quad . \tag{2.42}$$

The idea is then that, for a finite number of data, $T_N(\mathcal{X}_N)$ also has to be small if $\mathcal{X}_N$ is distributed following P_N. If $T_N(\mathcal{X}_N)$ happens to be to large, the hypothesis has to be rejected. The question is now: what is *small* or *large*? In order to answer this question, the probability distribution of T_N under P_N has to be calculated. The probability distribution function $F_{T,N}$ is given by

$$F_{T,N}(t) \;:=\; \int_{\Omega_N} \theta(\, t - T_N(\omega)\,) P_N(\omega)\, d\omega \quad , \tag{2.43}$$

where Ω_N is the space the data $\mathcal{X}_N$ can take their values in. The generic shape of $F_{T,N}$ and its derivative, the probability density, are depicted in Fig.2.1. They tell us what the probability would be to find certain values for $T_N(\mathcal{X}_N)$ if $\mathcal{X}_N$ would be distributed following the hypothesis, i.e., they give the *confidence levels*. For example, we can read off the first graph that the probability for $T_N(\mathcal{X}_N)$ to be larger than 0.80 is about $1 - 0.95 = 0.05$. This means that it is not very probable to find a value for $T_N(\mathcal{X}_N)$ this large, so that this number *can* be considered large.

2.1.6.2 Qualification of samples

Instead of for hypothesis testing, a test T_N can also be used to *qualify* a sample of data $\mathcal{X}_N$. Suppose that there is a notion of *good* and *bad* samples, and that this notion is translated into the test T_N: if $T_N(\mathcal{X}_N)$ is small, then $\mathcal{X}_N$ is *good*, and if $T_N(\mathcal{X}_N)$ is large, then $\mathcal{X}_N$ is *bad*. A first question can be whether the test makes sense, and an answer can again be given by the probability distribution. Suppose that the information available about the source of the data leads to a probability density P_N according to which the data seem to be randomly distributed. If the

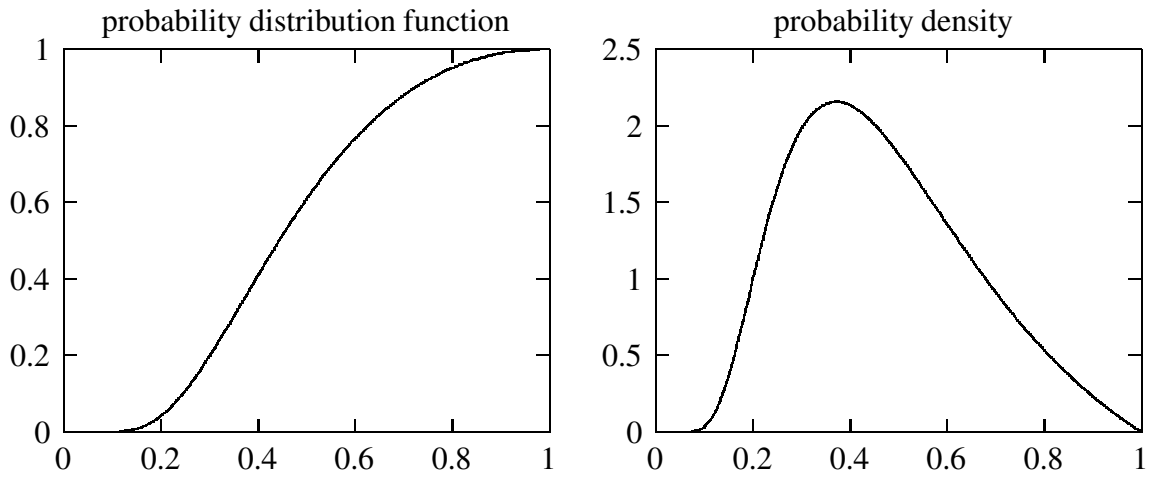

Figure 2.1: A probability distribution function and the probability density.

probability density of T_N looks like the one in Fig. 2.1, i.e., if it goes to zero for small values of $T_N(\mathcal{X}_N)$, then the test makes sense. It means that the test is capable of distinguishing between *good* samples and the kind of samples that occur most often. The next question is then: what *are* small values of $T_N(\mathcal{X}_N)$? The answer is that values are small if it is improbable to find them.

2.1.6.3 Qualification of algorithms and discrepancy

It can also be the case that the data come from an (expensive) algorithm that was specially designed to produce *good* samples (for example integration points for numerical integration), and the question is whether the algorithm makes sense. Suppose there is another (cheap) algorithm that produces data distributed with density P_N. The probability distribution of T_N determines the notion of *smallness* for the values of $T_N(\mathcal{X}_N)$ again, and the expensive algorithm only makes sense if it produces samples with low values of $T_N(\mathcal{X}_N)$ that are improbable to find. In the mentioned case of numerical integration, *good* samples are the point sets that are distributed uniformly over the integration space, and the tests are called *discrepancies* (Section 3.1).

Discrepancies have the structure of tests that measure the deviation between the empirical distribution of the point set, and the uniform distribution in the integration space. Algorithms to generate point sets following the uniform distribution (cf. [2]) can be considered 'cheap' compared to the special algorithms developed for numerical integration (cf. [16]). This seems paradoxical, since numerical integration asks for point sets that are distributed over the integration space as uniformly as possible (Section 1.1.3). The clue is that (random) point sets, generated following the uniform distribution, are not necessarily those that are distributed over the integration space as uniformly as possible. A simple example is one-dimensional space. For a given number of points, the most uniform distribution possible clearly is the one for which all distances between the points are the same. However, if the points are distributed randomly following the uniform distribution, this situation will never occur.

The example above gives a simple algorithm to generate *good* samples in one-dimensional space. Algorithms become 'expensive' if they have to be generated in more-dimensional spaces.

2.1.7 Calculation of probability distributions

In statistics, probability distributions are used, and in probability theory, they are calculated. Part of this thesis deals with their calculation for discrepancies. The way this will be done is by calculating the generating function. The probability density can then be found using the inverse Laplace transform (Eq.(2.15)), which can, if necessary, be calculated through a numerical integral over a contour in the complex plane.

The distribution is often calculated in certain limits, such as an infinite number of random variables or degrees of freedom. This is, in most cases, done because it simplifies the calculation. These limits can, however, often be considered as the limiting cases in certain stochastic processes: in Monte Carlo integration, for example, the limit of an infinite number of integration points can be interpreted as the limit of an infinite run-time for a computer.

If the generating function is considered, these limits correspond with weak convergence. However, if the generating function is calculated through all moments of the distribution, this corresponds with a stronger convergence: if $z \mapsto \sum_{p=0}^{\infty} a_p z^p/p!$ is a generating function and

$$E(X_n^p) \to a_p \ , \quad p = 0, 1, 2, \ldots \qquad \text{then} \qquad G_n(z) \to \sum_{p=0}^{\infty} \frac{a_p z^p}{p!} \ , \tag{2.44}$$

but the opposite does not have to be true. The moments might even go to infinity, while the generating function converges to an analytic function, and we will encounter an explicit example in which this happens.

2.2 Feynman diagrams and Gaussian measures

Part of this thesis deals with the calculation of probability distributions of measures of non-uniformity of point sets $\{x_1, \ldots, x_N\}$ in an integration space. The measures that are considered can be written in terms of two-point functions as $N^{-1} \sum_{k,l}^{N} \mathcal{B}(x_k, x_l)$. Consequently, the calculation of the moments of the distributions involves the calculation of multiple convolutions of these two-point functions, and Feynman diagrams can be of help.

2.2.1 Feynman diagrams

Feynman diagrams are drawings obtained by connecting vertices following some rules. Let us illustrate this with an example, in which three vertices are connected to a diagram:

(2.45)

The vertices have a number of legs and, in this case, there are two kinds of legs. The rule to get from these vertices to the particular diagram could be that legs of the same kind have to be connected. One rule that will always apply to cases we consider is that *all legs have to be connected to other legs*. Notice that, with this rule and the one that connected legs have to be of the same kind, the diagram drawn above is not the only possible one. Also

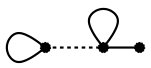

(2.46)

is a permitted diagram. The vertices in the diagrams are connected by *lines*. The previous two diagrams we also call *connected* as a whole, because one can walk from any vertex to any other vertex over lines. An example of a *disconnected* diagram can be obtained with twice as many vertices:

(2.47)

This is a possible diagram if the previous rules are applied.

If there are also rules how to assign a number to a diagram, these, together with the rules how to construct the diagrams, are called the *Feynman rules*. The Feynman rules make the diagrams of practical use. Certain calculations can be reduced to the assignment of numbers to a set of diagrams, which then have to be added to finish the whole calculation. We call such a number the *contribution* of the diagram, but this word shall often be omitted, and we will refer to 'sums of diagrams' instead of 'sums of contributions of diagrams'. In the following sections, we will give some examples, but first we derive

2.2.1.1 A few general relations

Let $\eta_1, \eta_2, \eta_3, \ldots$ be elements of a commutative algebra over $\mathbf{C}$, and assume that there is an operation $\langle\!\langle \cdot \rangle\!\rangle : \prod_i \eta_{k_i} \mapsto \langle\!\langle \prod_i \eta_{k_i} \rangle\!\rangle \in \mathbf{C}$ which is linear over $\mathbf{C}$. Suppose that every η_k

represents a type of vertex, and that

$$\frac{\langle\!\langle\, \eta_1^{p_1}\, \eta_2^{p_2} \cdots \eta_n^{p_n} \,\rangle\!\rangle}{p_1! \cdot p_2! \cdots p_n!} \tag{2.48}$$

can be interpreted as the sum of all possible diagrams with p_1 vertices of type η_1, p_2 vertices of type η_2 and so on. Then, the sum of all possible diagrams is given by

$$\sum_n \sum_{p(n)} \frac{\langle\!\langle\, \eta_1^{p_1(n)}\, \eta_2^{p_2(n)} \cdots \eta_n^{p_n(n)} \,\rangle\!\rangle}{p_1(n)! \cdot p_2(n)! \cdots p_n(n)!} \quad , \tag{2.49}$$

where the second sum is over all partitions $p(n)$ of n. Using the combinatorial rule of Eq.(2.91), which is derived in Appendix 2A, and the linearity of $\langle\!\langle \cdot \rangle\!\rangle$, we find that this is equal to

$$\sum_{m=1}^{\infty} \frac{1}{m!} \sum_{k_1,\ldots,k_m} \langle\!\langle \eta_{k_1} \cdots \eta_{k_m} \rangle\!\rangle \;=\; \sum_{m=1}^{\infty} \frac{1}{m!} \langle\!\langle \Big(\sum_k \eta_k \Big)^m \rangle\!\rangle \;=\; \langle\!\langle \exp\Big(\sum_k \eta_k \Big) \rangle\!\rangle - 1 \quad , \tag{2.50}$$

so that

$$G(\{\eta\}) \;:=\; 1 + \textit{the sum of all possible diagrams} \;=\; \langle\!\langle \exp\Big(\sum_k \eta_k \Big) \rangle\!\rangle \quad . \tag{2.51}$$

Now, we show that the sum of all possible connected diagrams is given by $\log G(\{\eta\})$. Define

$$G_n[\eta_m] \;:=\; \frac{1}{n!} \langle\!\langle\, \eta_m^n \exp\Big(\sum_{k \neq m} \eta_k \Big) \,\rangle\!\rangle \quad , \tag{2.52}$$

so that

$$G(\{\eta\}) \;=\; \sum_{n=0}^{\infty} G_n[\eta_m] \quad . \tag{2.53}$$

$G_n[\eta_m]$ contains all diagrams with n vertices of type η_m. The sum of all diagrams for which these n vertices are contained in the same connected piece is denoted $C_n[\eta_m]$, so that

$$G_n[\eta_m] \;=\; \sum_{p(n)} \prod_{i=1}^{n} \frac{C_i[\eta_m]^{p_i(n)}}{p_i(n)!} \quad , \tag{2.54}$$

where the sum in the r.h.s. is over all partitions $p(n)$ of n. Using Eq.(2.91) again, we find that

$$G(\{\eta\}) \;=\; \sum_{n=0}^{\infty} \frac{1}{n!} \sum_{i_1,\ldots,i_n=1}^{\infty} C_{i_1}[\eta_m] \cdots C_{i_n}[\eta_m] \;=\; \exp(W[\eta_m]) \quad , \tag{2.55}$$

where

$$W[\eta_m] \;:=\; \sum_{n=1}^{\infty} C_n[\eta_m] \tag{2.56}$$

is the sum of all diagrams for which all vertices of the kind η_m are contained in the same connected piece. Because we can take any kind of vertex for η_m, the sum of all diagrams has to be given by the exponential of the sum of all connected diagrams, and we find that

$$\log G(\{\eta\}) \;=\; \textit{the sum of all possible connected diagrams.} \tag{2.57}$$

2.2.2 Gaussian measures

An example of the use of Feynman diagrams is in calculations with Gaussian measures. We refer to [4] for more details about the formalism used.

We are going to look at measures on spaces C of real bounded functions on a subset $\mathbf{K}$ of $\mathbf{R}^s$, where $s = 1, 2, \ldots$. The Lebesgue measure on $\mathbf{K}$ we just denote dx. $\mathbf{K}$ can also be a finite set, in which case the Lebesgue integral becomes a finite sum. A measure on C will be denoted μ, and for, not necessarily linear, functionals $\eta_1, \eta_2, \ldots, \eta_n$ on C, we denote

$$\langle \eta_1 \eta_2 \cdots \eta_n \rangle_\mu := \int_C \eta_1[\phi]\eta_2[\phi]\cdots\eta_n[\phi]\, d\mu[\phi] \quad . \tag{2.58}$$

The space of continuous linear functionals on C is denoted C', and a typical member is the Dirac measure δ_x, which is for every $x \in \mathbf{K}$ defined by

$$\delta_x[\phi] := \phi(x) \quad . \tag{2.59}$$

Furthermore, we introduce the so called n-point functions, which are given by

$$\mathcal{G}_n(x_1, x_2, \ldots, x_n) := \langle \delta_{x_1} \delta_{x_2} \cdots \delta_{x_n} \rangle_\mu \quad . \tag{2.60}$$

Notice that they are symmetric in their arguments. We will always assume that μ is normalized, so that $\mathcal{G}_0 := \int_C d\mu[\phi] = 1$. For linear functionals, we will use the notation

$$\eta[\phi] = \int_{\mathbf{K}} \eta(x)\phi(x)\, dx \quad , \tag{2.61}$$

although '$\eta(x)$' cannot always be seen as a function value. For example, $\delta_x(x)$ does not exist. If we combine this notation with the notation of Eq.(2.60), we can write

$$\langle \eta_1 \eta_2 \cdots \eta_n \rangle_\mu = \int_{\mathbf{K}^n} \mathcal{G}_n(x_1, x_2, \ldots, x_n)\eta_1(x_1)\eta_2(x_2)\cdots\eta_n(x_n)\, dx_1 dx_2 \cdots dx_n \quad . \tag{2.62}$$

The Fourier transform of a measure μ on C is the function on C' given by

$$\eta \mapsto \langle \exp(i\eta) \rangle_\mu \quad , \tag{2.63}$$

and μ is *Gaussian* if there is a quadratic form $\mathcal{Q}$ on C' such that the Fourier transform is given by

$$\langle \exp(i\eta) \rangle_\mu = \exp(-\tfrac{1}{2}\mathcal{Q}[\eta]) \quad . \tag{2.64}$$

$\mathcal{Q}$ can be written in terms of the two-point function, for take $\eta := \lambda\zeta$, where λ is a real variable, and differentiate Eq.(2.64) twice with respect to λ before putting it to zero. Then it is easy to see that

$$\mathcal{Q}[\zeta] = \langle \zeta\, \zeta \rangle_\mu = \int_{\mathbf{K}} \zeta(x_1)\mathcal{G}_2(x_1, x_2)\zeta(x_2)\, dx \quad . \tag{2.65}$$

With this result, we can express the n-point functions in terms of the two-point function. If we take $\eta := \sum_{i=1}^{n} \lambda_i \delta_{x_i}$, where λ_i, $i = 1, \ldots, n$ are real variables, and differentiate Eq. (2.64) once with respect of each of these variables before putting them to zero, we find that, for odd n, $\mathcal{G}_n = 0$, and for even n that

$$\mathcal{G}_n(x_1, x_2, \ldots, x_n) = \sum_{\text{pairs } (i<j)} \mathcal{G}_2(x_i, x_j) \quad , \tag{2.66}$$

where the sum is over all pairs (i, j) for which $i < j$.

2.2.2.1 Diagrams

The previous formula suggests to interpret $\mathcal{G}_2(x_i, x_j)$ as a *line* that connects the arguments x_i and x_j, so that the r.h.s. consists of all possible ways to connect the arguments $x_1, x_2, \ldots, x_n$ in pairs with lines. If there is a prescription to identify a number of $m \leq n$ arguments, then they can represent a vertex. The number of arguments in a vertex, the number of legs, we call the *order* of the vertex.

A typical case in which arguments are identified is when integrals of the following type are calculated. Let $\eta_1, \eta_2, \eta_3, \ldots$ be a sequence of functionals acting on C as

$$\eta_k[\phi] := \int_{\mathbf{K}^k} \eta_k(x_1, \ldots, x_k)\, \phi(x_1) \cdots \phi(x_k)\, dx_1 \cdots dx_k \quad . \tag{2.67}$$

Let, furthermore, $k_1, \ldots, k_m$ be a set of integers larger than zero, and denote $k_{(i)} = \sum_{j=1}^{i} k_j$. The integrals we want to consider are given by

$$\langle \eta_{k_1} \cdots \eta_{k_m} \rangle_\mu = \int_{\mathbf{K}^{k_{(m)}}} \mathcal{G}_{k_{(m)}}(\{x\}_0^{k_{(m)}})\, \eta_{k_1}(\{x\}_0^{k_{(1)}}) \cdots \eta_{k_m}(\{x\}_{k_{(m-1)}}^{k_{(m)}})\, dx_1 \cdots dx_{k_{(m)}} \quad , \tag{2.68}$$

where we use the notation $\{x\}_j^i = \{x_{j+1}, x_{j+2}, \ldots, x_i\}$. The set of arguments that are the integration variables of the same η_i can be considered identical. As a result, the whole integral is given by the sum of all possible diagrams with the m vertices of the orders $k_1, \ldots, k_m$. The contribution of a diagram is obtained by convoluting the two-point functions with the functionals η_{k_i} in the vertices.

The question we want to answer now is, given the Gaussian measure μ and the functionals η_k, what the sum of all possible diagrams is. Because $\mathcal{G}$ is symmetric, it suffices to consider the integrals

$$\langle\, \eta_1^{p_1}\, \eta_2^{p_2}\, \cdots\, \eta_n^{p_n}\, \rangle_\mu \quad . \tag{2.69}$$

The diagrams that contribute have p_1 vertices of order 1, p_2 vertices of order 2 and so on. In the set of diagrams that contribute to this integral, there are many diagrams that look exactly the same because they only differ in the exchange of integration variables of the same vertex, or in the exchange of vertices of the same order. We do not want to count them separately, and

therefor include in the contribution of a diagram the number of ways it can be obtained. We turn this number into a *symmetry factor*, by considering

$$\frac{\langle\, \bar\eta_1^{p_1}\, \bar\eta_2^{p_2}\, \cdots\, \bar\eta_n^{p_n}\,\rangle_\mu}{p_1!\cdot p_2!\cdots p_n!}\quad,\qquad \bar\eta_k := \frac{\eta_k}{k!}\quad, \tag{2.70}$$

instead of (2.69). As a consequence, every vertex of order k accounts for a factor $1/k!$, and the set of vertices of order k accounts for a factor $1/p_k!$. The contribution of a diagram is then given by the number obtained calculating the convolutions of the η_k's, represented by the vertices, with the $\mathcal{G}_2$'s, represented by the lines, multiplied with the symmetry factor. This factor is the number of ways the diagram can be obtained, considering all vertices and all legs of vertices distinct, divided by $\prod_i p_i!(i!)^{p_i}$, where p_i is the number of vertices of order i. We can use the results of Section 2.2.1 now and find that

$$1 + \textit{the sum of all possible diagrams} \;=\; \langle\, \exp\Big(\sum_{k=1}^{\infty}\frac{\eta_k}{k!}\Big)\,\rangle_\mu\quad, \tag{2.71}$$

and that this equal to the exponential of the sum of all connected diagrams.

2.2.3 Falling powers, diagrams and Grassmann variables

Another, small, example of the use of Feynman diagrams is in the representation of the numbers

$$N^{\underline{k}} := N(N-1)(N-2)\cdots(N-k+1)\quad,\quad N,k\in\mathbf{N}\quad. \tag{2.72}$$

It can be derived from the relation

$$N^{\underline{k}} \;=\; \sum_{i_1,\ldots,i_k=1}^{N}\;\sum_{\pi\in S_k}\mathrm{sgn}(\pi)\,\delta_{i_1,i_{\pi(1)}}\delta_{i_2,i_{\pi(2)}}\cdots\delta_{i_k,i_{\pi(k)}}\quad, \tag{2.73}$$

where the second sum on the r.h.s. is over all permutations of $(1,2,\ldots,k)$. This relation is derived in Appendix 2A. It allows for following diagrammatic interpretation.

Consider 'arrowed' vertices of order two, that is, vertices of order two with distinct legs: one incoming and one outgoing. They can be connected with the rule that outgoing legs may only be connected to incoming legs and vice versa. The legs are connected with an 'arrowed' line, representing a δ_{i_1,i_2}, and the vertices represent the convolution $\sum_{i_2=1}^{N}\delta_{i_1,i_2}\delta_{i_2,i_3}$ of the two lines arriving at and starting from that vertex. Up to an overall minus sign, the r.h.s. of Eq. (2.73) is equal to the sum of all possible diagrams with k distinct 'arrowed' vertices, with the extra rule that every closed loop gives a factor -1. The overall minus sign is equal to $(-1)^k$. For example,

$(-1)^3N^{\underline{3}} =$ 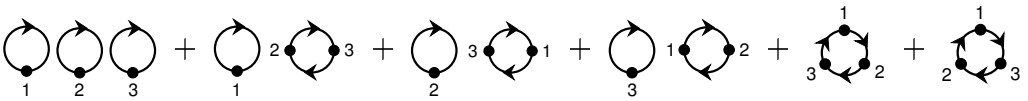

$$= -N^3 + 3N^2 - 2N\quad. \tag{2.74}$$

It is useful to consider diagrams that look exactly the same as one diagram again. In the example above, this applies to the last two diagrams, and to the second, the third and the fourth diagram. The extra number the contribution of a diagram has to be multiplied with is turned into a symmetry factor by considering $(-1)^kN^{\underline{k}}/k!$ instead of $(-1)^kN^{\underline{k}}$.

2.2.3.1 Grassmann variables

The numbers $(-1)^k N^{\underline{k}}$ can also be written in another way. We introduce $2N$ *Grassmann variables* ψ_i and $\bar{\psi}_i$, $i = 1, \ldots, N$. They all anti-commute with each other and commute with complex numbers:

$$\bar{\psi}_i\bar{\psi}_j + \bar{\psi}_j\bar{\psi}_i = 0\ ,\ \ \bar{\psi}_i\psi_j + \psi_j\bar{\psi}_i = 0\ ,\ \ \psi_i\psi_j + \psi_j\psi_i = 0 \qquad i,j = 1,2,\ldots,N \tag{2.75}$$

$$c\bar{\psi}_i - \bar{\psi}_i c = 0\ ,\ \ c\psi_i - \psi_i c = 0 \qquad i = 1,2,\ldots,N\ \ ,\ \ \ c \in \mathbf{C}\ . \tag{2.76}$$

These variables are nilpotent, i.e., $\psi_i\psi_i = \bar{\psi}_i\bar{\psi}_i = 0$ for all i. Products of even numbers of these variables commute with all other combinations. Furthermore, we introduce the 'integral' of these variables, which maps sums of products of them onto $\mathbf{C}$. It is linear over $\mathbf{C}$ and defined by the relations

$$\int [d\bar{\psi}\,d\psi]\,\psi_{i_1}\psi_{i_2}\cdots\psi_{i_k}\,\bar{\psi}_{j_1}\bar{\psi}_{j_2}\cdots\bar{\psi}_{j_l} \ :=\ 0 \quad \text{if } k,l < N\ \ , \tag{2.77}$$

$$\int [d\bar{\psi}\,d\psi]\,\psi_1\bar{\psi}_1\,\psi_2\bar{\psi}_2\cdots\psi_N\bar{\psi}_N \ :=\ 1\ \ . \tag{2.78}$$

Notice that the first integral is also zero if $k > N$, because then there has to be a pair (ψ_{i_r}, ψ_{i_s}) with $i_r = i_s$ in the product of ψ's, so that $\psi_{i_r}\psi_{i_s} = 0$. The same holds if $l > N$. A useful calculation of such an integral is

$$\begin{aligned}\int [d\bar{\psi}\,d\psi]\Big(\sum_{i=1}^N \bar{\psi}_i\psi_i\Big)^N \ &=\ \sum_{\pi\in S_N}\int [d\bar{\psi}\,d\psi]\,\bar{\psi}_{\pi(1)}\psi_{\pi(1)}\,\bar{\psi}_{\pi(2)}\psi_{\pi(2)}\cdots\bar{\psi}_{\pi(N)}\psi_{\pi(N)} \\ &=\ \sum_{\pi\in S_N}(-1)^N \mathrm{sgn}(\pi)^2 \ =\ (-1)^N N!\ \ .\end{aligned} \tag{2.79}$$

Another useful relation is the following. If A is a complex number, then

$$\int [d\bar{\psi}\,d\psi]\ \exp\Big(-\sum_{j=1}^N \bar{\psi}_j\psi_j A\Big) \ =\ \sum_{k=0}^N \frac{(-)^k A^k}{k!}\int [d\bar{\psi}\,d\psi]\Big(\sum_{i=1}^N \bar{\psi}_i\psi_i\Big)^k \ =\ A^N\ , \tag{2.80}$$

since only the term with $k = N$ is non-zero. Let us now introduce the 'measure' $\langle\cdot\rangle_\psi$, defined by

$$\langle f\rangle_\psi \ :=\ \int [d\bar{\psi}\,d\psi]\,f(\psi_1,\ldots,\psi_N,\bar{\psi}_1,\ldots,\bar{\psi}_N)\ \exp\Big(-\sum_{j=1}^N \bar{\psi}_j\psi_j\Big)\ \ . \tag{2.81}$$

Using the result of the previous calculations, we find

$$\langle\Big(\sum_{i=1}^N \bar{\psi}_i\psi_i\Big)^k\rangle_\psi \ =\ \sum_{m=0}^N \frac{(-1)^m}{m!}\int [d\bar{\psi}\,d\psi]\Big(\sum_{i=1}^N \bar{\psi}_i\psi_i\Big)^{k+m} \ =\ (-)^k N^{\underline{k}}\ \ , \tag{2.82}$$

since only the term with $m = N - k$ contributes. If we combine the two representations of the numbers $(-)^k N^{\underline{k}}$, we can draw the conclusion that

$$\frac{1}{k!}\langle\Big(\sum_{i=1}^N \bar{\psi}_i\psi_i\Big)^k\rangle_\psi \ =\ \textit{the sum of all possible diagrams with } k \textit{ 'arrowed' two-point vertices.} \tag{2.83}$$

2.2.4 Gaussian measures and Grassmann variables

As a final application, we are going to combine the previous two examples. Let μ be a Gaussian measure on a space of real bounded functions on a subset $\mathbf{K}$ of $\mathbf{R}^s$, let ψ_i and $\bar{\psi}_i$, $i = 1, \ldots, N$ be a set of Grassmann variables, and let us denote

$$\langle\!\langle\, \chi \,\rangle\!\rangle \;:=\; \langle \langle\, \chi \,\rangle_\psi \rangle_\mu \;=\; \langle \langle\, \chi \,\rangle_\mu \rangle_\psi \quad . \tag{2.84}$$

If $\eta_1, \eta_2, \eta_3, \ldots$ is a sequence of functionals acting on C as

$$\eta_k[\phi] \;:=\; \int_{\mathbf{K}^k} \eta_k(x_1, \ldots, x_k)\, \phi(x_1) \cdots \phi(x_k)\, dx_1 \cdots dx_k \quad , \tag{2.85}$$

then

$$\frac{\langle\, \eta_1^{p_1}\, \eta_2^{p_2}\, \cdots\, \eta_n^{p_n} \,\rangle_\mu}{p_1! \cdot p_2! \cdots p_n!} \tag{2.86}$$

can be calculated using diagrams with p_1 vertices of type η_1, p_2 vertices of type η_2 and so on, as described in Section 2.2.2. If we apply the results of Section 2.2.3, we see that

$$\frac{(-1)^{p_{(n)}} N^{\underline{p_{(n)}}}\, \langle\, \eta_1^{p_1}\, \eta_2^{p_2}\, \cdots\, \eta_n^{p_n} \,\rangle_\mu}{p_1! \cdot p_2! \cdots p_n!} \quad , \qquad p_{(n)} := p_1 + p_2 + \cdots + p_n \quad , \tag{2.87}$$

can be calculated by attaching an incoming and an outgoing 'arrowed' leg to each type of vertex, and using the Feynman rules of Section 2.2.3. Furthermore, we see that

$$(-1)^{p_{(n)}} N^{\underline{p_{(n)}}}\, \langle\, \eta_1^{p_1}\, \eta_2^{p_2}\, \cdots\, \eta_n^{p_n} \,\rangle_\mu \;=\; \langle\!\langle\, \chi_1^{p_1}\, \chi_2^{p_2}\, \cdots\, \chi_n^{p_n} \,\rangle\!\rangle \quad , \quad \chi_k := \eta_k \sum_{i=1}^{N} \bar{\psi}_i \psi_i \quad . \tag{2.88}$$

Each χ_k represents a vertex of the kind η_k, with attached to it an incoming and an outgoing 'arrowed' leg. Now, we can apply the relations of Section 2.2.1 to arrive at the result that

$$\begin{aligned} G(\{\chi\}) \;&:=\; 1 + \textit{the sum of all possible diagrams with } \chi_k\textit{-vertices} \\ &=\; \langle\!\langle\, \exp\Big(\sum_k \frac{\chi_k}{k!} \Big) \,\rangle\!\rangle \quad , \end{aligned} \tag{2.89}$$

and that the sum of the connected diagrams is equal to $\log G(\{\chi\})$.

Appendix 2A: Some combinatorial relations

Consider a sequence $f_1, f_2, f_3, \ldots$ of functions of integer arguments that are completely symmetric in those arguments. We want to establish a relation of the kind

$$\sum_{m=1}^{\infty} \sum_{k_1, \ldots, k_m = 1}^{\infty} f_m(k_1, \ldots, k_m) \;\stackrel{?}{=}\; \sum_{n=1}^{\infty} \sum_{p(n)} f_n(\overbrace{1, \ldots, 1}^{p_1(n)}, \overbrace{2, \ldots, 2}^{p_2(n)}, \ldots, \overbrace{n}^{p_n(n)}) \quad , \tag{2.90}$$

where the second sum on the r.h.s. is over all partitions $p(n)$ of n. Put like this, the relation is obviously incorrect, since on the l.h.s. all permutations $f_m(\pi(1), \pi(2), \ldots, \pi(m))$ are counted separately, whereas on the r.h.s., only $f_m(1, 2, \ldots, m)$ is counted. At first instance, it seems natural to correct for this by including a factor $1/m!$ on the l.h.s.. This is, however, too crude, because permutations of equal k_i's are not counted separately. This can again be cured by including a factor $p_1(n)! \cdot p_2(n)! \cdots p_n(n)!$ on the r.h.s., and we arrive at

$$\sum_{m=1}^{\infty} \sum_{k_1,\ldots,k_m=1}^{\infty} \frac{f_m(k_1, \ldots, k_m)}{m!} = \sum_{n=1}^{\infty} \sum_{p(n)} \frac{f_n(\overbrace{1, \ldots, 1}^{p_1(n)}, \overbrace{2, \ldots, 2}^{p_2(n)}, \ldots, \overbrace{n}^{p_n(n)})}{p_1(n)! \cdot p_2(n)! \cdots p_n(n)!} \quad . \tag{2.91}$$

Note that $p_n(n)$ is equal to 0 or 1.

Consider the $k \times k$ matrix $A(\{i\}^k)$, depending on k integer variables $\{i\}^k := \{i_1, i_2, \ldots, i_k\}$ that run from 1 to N. The matrix is defined by

$$A_{r,s}(\{i\}^k) := \delta_{i_r, i_s} := \begin{cases} 1 & \text{if } i_r = i_s \ , \\ 0 & \text{if } i_r \neq i_s \ . \end{cases} \tag{2.92}$$

Every diagonal element of this matrix is equal to 1 for every configuration $\{i\}$, because $i_r = i_s$ if $r = s$. Now consider a configuration $\{i\}$ for which all i's are not equal, except of one pair $i_r = i_s$ with $r \neq s$. Then $A_{r,s}(\{i\}^k) = A_{s,r}(\{i\}^k) = 1$, and we see that row r and row s are the same, so that $\det A(\{i\}^k) = 0$. It is easy to see that this will always be the case if there are pairs $i_r = i_s$ with $r \neq s$. The number of configurations $\{i\}$ for which all i's are not equal is precisely $N^{\underline{k}}$, so that we can write down the following identity

$$N^{\underline{k}} = \sum_{i_1,\ldots,i_k=1}^{N} \det A(\{i\}^k) = \sum_{i_1,\ldots,i_k=1}^{N} \sum_{\pi \in S_k} \operatorname{sgn}(\pi) \delta_{i_1, i_{\pi(1)}} \delta_{i_2, i_{\pi(2)}} \cdots \delta_{i_k, i_{\pi(k)}} \quad , \tag{2.93}$$

where the second sum on the r.h.s. is over all permutations of $(1, 2, \ldots, k)$. We just used the formula $\det A = \sum_{\pi \in S_k} \operatorname{sgn}(\pi) \prod_{r=1}^{k} A_{r,\pi(r)}$ to arrive at this result.

Chapter 3

The formalism of quadratic discrepancies

Discrepancies are measures of non-uniformity of point sets in subsets of s-dimensional Euclidean space. They are interesting in connection with numerical integration, because the integration error can be estimated in terms of the discrepancy of the point set used (Section 1.1.3). Their definition will be given in the first section of this chapter. An interesting feature of discrepancies is their probability distribution (Section 2.1.6), and large part of this chapter concerns with techniques, borrowed from quantum field theory, to calculate them for the so called quadratic discrepancies. In the last section, some examples of quadratic discrepancies are given.

Contents

3.1 Definition of discrepancy

The only subspace of $\mathbf{R}^s$, $s = 1, 2, \ldots$ that will be considered is the s-dimensional unit hypercube $\mathbf{K} := [0,1]^s$ since, in practice, an integration problem can always be reduced to one on $\mathbf{K}$. A point set $\mathcal{X}_N$ consists of N points $x_k \in \mathbf{K}$, $1 \le k \le N$. The coordinates of the points will be labeled with an upper index as x_k^ν, $1 \le \nu \le s$. For an arbitrary subset $\mathbf{A}$ of $\mathbf{K}$, we define the characteristic function $\vartheta_\mathbf{A}$ such that

$$\vartheta_\mathbf{A}(x) := \begin{cases} 1 & \text{if } x \in \mathbf{A} \\ 0 & \text{if } x \notin \mathbf{A} \end{cases} . \tag{3.1}$$

The integral of a function f, Lebesgue integrable on $\mathbf{K}$, we denote by

$$\langle f \rangle := \int_\mathbf{K} f(x)\, dx , \tag{3.2}$$

so that the Lebesgue measure of a region $\mathbf{A} \subset \mathbf{K}$ is given by $\langle \vartheta_\mathbf{A} \rangle$. For every point set $\mathcal{X}_N$, we introduce the estimate $\langle f \rangle_N$ of $\langle f \rangle$ using $\mathcal{X}_N$ by

$$\langle f \rangle_N := \frac{1}{N} \sum_{i=1}^{N} f(x_i) . \tag{3.3}$$

3.1.1 The original definition

Naturally, a discrepancy of the point set is defined with respect to a certain family $\mathcal{A}$ of measurable subsets of $\mathbf{K}$ as follows

$$D_N^{[\mathcal{A}]}(\mathcal{X}_N) := \sup_{\mathbf{A} \in \mathcal{A}} \left| \langle \vartheta_\mathbf{A} \rangle_N - \langle \vartheta_\mathbf{A} \rangle \right| . \tag{3.4}$$

It is the largest absolute error one makes if one tries to estimate the measure of every subset $\mathbf{A} \in \mathcal{A}$ by counting the number of points from $\mathcal{X}_N$ in the subset. The idea is that, if a point set is suitable for estimating the measures of all subsets well, so that $D_N^{[\mathcal{A}]}(\mathcal{X}_N)$ is small, then the point set must be distributed very "uniformly" over $\mathbf{K}$. In order to arrive at a natural notion of uniformity, the family $\mathcal{A}$ of subsets has to be chosen sensibly. In principle, for every finite point set a subset of $\mathbf{K}$ can be found, such that the discrepancy takes its maximum value, which is 1. A first restriction on the subsets one can for example take is that they have to be convex, i.e., for every x_1, x_2 in $\mathbf{A}$ and every $t \in [0,1]$ also $tx_1 + (1-t)x_2$ is in $\mathbf{A}$.

This restriction still leaves many possible choices for the subsets, leading to different discrepancies (cf. [6]). An important example is the so called *star discrepancy*, denoted by D_N^*, for which the family $\mathcal{A}^*$ consists of all subsets

$$\mathbf{A}_y := [0, y^1) \times [0, y^2) \times \cdots \times [0, y^s) , \quad y \in \mathbf{K} . \tag{3.5}$$

It consists of all hyper-rectangles spanned by the origin and points $y \in \mathbf{K}$. For this discrepancy, various theorems are derived (cf. [6]), such as Koksma-Hlawka's inequality (Eq. (1.12)). In one

dimension, D_N^* is equal to the statistic of the Kolmogorov-Smirnov test for the hypothesis that the points are distributed randomly following the uniform distribution (cf. [2]).

In order to proceed in a direction that leads to a definition of discrepancy that we will use, we introduce the L_p^*-*discrepancy*. If we denote $\vartheta_y := \vartheta_{\mathbf{A}_y}$, then

$$D_N^{[p]}(\mathcal{X}_N) := \left(\int_{\mathbf{K}} \left| \langle \vartheta_y \rangle_N - \langle \vartheta_y \rangle \right|^p dy \right)^{1/p} . \tag{3.6}$$

It is the average over A^* of the p^{th} power of the error made by estimating the measures of the subsets using $\mathcal{X}_N$. This definition assures the limit $D_N^*(\mathcal{X}_N) = \lim_{p\to\infty} D_N^{[p]}(\mathcal{X}_N)$. Furthermore, it satisfies the bounds

$$D_N^{[p]}(\mathcal{X}_N) \le D_N^*(\mathcal{X}_N) \le c(s,p) D_N^{[p]}(\mathcal{X}_N)^{\frac{p}{p+1}} , \tag{3.7}$$

where $c(s,p)$ is independent of the point set [6]. For us, the case of $p = 2$ is in particular interesting. The expression for $D_N^{[2]}(\mathcal{X}_N)$ can be evaluated further, with the result that

$$D_N^{[2]}(\mathcal{X}_N) = \left(\frac{1}{N^2} \sum_{k,l=1}^{N} \mathcal{B}(x_k, x_l) \right)^{1/2} , \tag{3.8}$$

where

$$\mathcal{B}(x_k, x_l) = \mathcal{C}(x_k, x_l) - \int_{\mathbf{K}} \mathcal{C}(x_k, y)\, dy - \int_{\mathbf{K}} \mathcal{C}(y, x_l)\, dy + \int_{\mathbf{K}^2} \mathcal{C}(y_1, y_2)\, dy_1 dy_2 , \tag{3.9}$$

and

$$\mathcal{C}(x_k, x_l) = \int_{\mathbf{K}} \vartheta_y(x_k)\vartheta_y(x_l)\, dy = \prod_{\nu=1}^{s} \min(1 - x_k^\nu, 1 - x_l^\nu) . \tag{3.10}$$

In this case of $p = 2$, the discrepancy is called *quadratic*, and is completely determined by the two-point function $\mathcal{C}$.

3.1.2 Quadratic discrepancies

The quadratic discrepancy invites generalizations. The number $\mathcal{B}(x_1, x_2)$ can be interpreted as a correlation between the points x_1 and x_2, and the discrepancy is a function of the sum over all correlations in the point set. Various quadratic discrepancies can be defined by choosing different, and sensible, two-point correlation functions. The two-point functions can, however, also be interpreted differently, leading to another approach to quadratic discrepancies. This approach is based on the insight by H. Woźniakowski [17], that $D_N^{[2]}$ can be written as an *average case complexity*. We will demonstrate this here by constructing the probability measure with respect to which the discrepancy can be written as an average. For more details about the formalism, we refer to [4].

Consider the Hilbert space $H := L_2(\mathbf{K})$ of (equivalence classes of almost everywhere equal) real quadratically integrable functions on $\mathbf{K}$. We denote the inner product and the norm on H by

$$\langle f\, h\rangle \;:=\; \int_{\mathbf{K}} f(x)h(x)\,dx \quad , \qquad \|f\| := \sqrt{\langle f\, f\rangle} \quad \text{for real } f \quad . \tag{3.11}$$

Let us, as before, denote $\vartheta_y(x) = \prod_{\nu=1}^{s} \theta(y^\nu - x^\nu)$ and let $\mathcal{P}$ be the "primitivation" operator, defined by

$$(\mathcal{P}f)(x) \;:=\; \int_{\mathbf{K}} \vartheta_y(x) f(y)\,dy \quad . \tag{3.12}$$

$\mathcal{P}$ is a continuous linear map from H to the space C_W of continuous functions that vanish if any coordinate $x^\nu = 1$. It even is a Hilbert-Schmidt operator: if $\{u_n\}$ is a basis of H, then $\sum_n \|\mathcal{P}u_n\|^2 < \infty$.

The dual space C'_W, i.e. the space of all continuous linear functionals on C_W, consists of all bounded measures on $[0,1)^s$. For such a measure η, we will use the notation

$$\eta[f] \;:=\; \int_{\mathbf{K}} f(x)\eta(x)\,dx \quad , \tag{3.13}$$

although "$\eta(x)$" cannot always be seen as a function value. The transposed $\tilde{\mathcal{P}}$, which acts on C'_W through the definition $(\tilde{\mathcal{P}}\eta)[f] := \eta[\mathcal{P}f]$, is then simply given by

$$(\tilde{\mathcal{P}}\eta)(x) \;=\; \int_{\mathbf{K}} \vartheta_x(y)\eta(y)\,dy \quad , \tag{3.14}$$

and $\tilde{\mathcal{P}}\eta$ *is* a bounded function. Notice that, because H is isomorphic to its dual, we can make the straightforward identification $\tilde{\mathcal{P}} = \mathcal{P}^\dagger$, where $\mathcal{P}^\dagger$ is the adjoint of $\mathcal{P}$. There is a unique Gaussian probability measure μ_W on C_W which has Fourier transform

$$\int_{C_W} \exp(i\eta[\phi])\,d\mu_W[\phi] \;=\; \exp(-\tfrac{1}{2}\langle\, (\tilde{\mathcal{P}}\eta)^2\,\rangle) \quad . \tag{3.15}$$

It is going to serve as the probability measure mentioned before. In literature, it is known as the *Wiener sheet measure*. By taking $\eta := \lambda(\lambda_1\delta_{x_1} + \lambda_1\delta_{x_1})$, where $\lambda, \lambda_1, \lambda_2$ are real variables and δ_x denotes the Dirac measure $\delta_x[\phi] := \phi(x)$, and differentiating the above equation twice with respect to λ, it is easy to see that μ_W has two point function

$$\int_{C_W} \phi(x_1)\phi(x_2)\,d\mu_W[\phi] \;=\; \langle \tilde{\mathcal{P}}\delta_{x_1}\, \tilde{\mathcal{P}}\delta_{x_2}\rangle \;=\; \prod_{\nu=1}^{s} \min(1-x_1^\nu, 1-x_2^\nu) \quad . \tag{3.16}$$

So the two-point function with which the discrepancy is defined, is the two-point function of the Gaussian measure μ_W on C_W. Using this equation and Eq. (3.8) and Eq. (3.9), it is easy to see that

$$\big(\, D_N^{[2]}(\mathcal{X}_N)\,\big)^2 \;=\; \int_{C_W} \big|\langle\phi\rangle_N - \langle\phi\rangle\big|^2\,d\mu_W[\phi] \quad . \tag{3.17}$$

So we can identify the square of the discrepancy as the average case complexity, defined as the squared integration error averaged over C_W.

The particular choice of $\mathcal{P}$ led to the Wiener sheet measure. In principle, any Hilbert-Schmidt operator can be used, leading to another Gaussian measure μ. We want to apply this generalization. For further analysis, it will therefore appear to be convenient to use the square, as it stands on the l.h.s., as definition for quadratic discrepancy. Furthermore, the definition of discrepancy is such, that it goes to zero, if the number of points in a uniformly distributed point set goes to infinity. This is immediately clear from inequality (1.12), the l.h.s. of which goes to zero if $\mathcal{X}_N$ consists of independent random points and N goes to infinity. In fact, Monte Carlo integration tells us that it goes to zero as $1/\sqrt{N}$. Therefore, it seems natural to use N times the square of the original definition of the quadratic discrepancy, especially since we want to calculate probability distributions of discrepancies for large N. This multiplication with the factor N is equivalent with considering $\sqrt{N}$ times the average of N random variables (with zero mean) when applying the central limit theorem in probabilistic analyses.

3.1.2.1 Definition quadratic discrepancy

We conclude this section with the definition of discrepancy we will further use. Given a Hilbert-Schmidt operator $\mathcal{P}$ on $H := L_2(\mathbf{K})$, there is a Gaussian measure $\mu_{\mathcal{P}}$ on H with Fourier transform

$$\int_H \exp(i\eta[\phi])\, d\mu_{\mathcal{P}}[\phi] \;=\; \exp(-\tfrac{1}{2}\langle\, (\tilde{\mathcal{P}}\eta)^2\,\rangle) \quad . \tag{3.18}$$

In the case of the Wiener sheet measure, it even is a measure on a space of continuous functions, but for the general case this is not necessary. The operator $\mathcal{P}$ should only be such, that it maps H continuously on a space C of continuous functions, so that there is a number p such that $\sup_{x\in\mathbf{K}} |(\mathcal{P}f)(x)| \le p\|f\|$ for any $f \in H$. In Appendix 3A, we show that in that case the Dirac measure can be properly defined under the measure $\mu_{\mathcal{P}}$, which we will need. We shall omit the label H at the integral symbol from now on.

We define the discrepancy of a point sets $\mathcal{X}_N$ in $\mathbf{K}$ as the quadratic integration error, made by using $\mathcal{X}_N$, averaged under $\mu_{\mathcal{P}}$ over H:

$$D_N(\mathcal{X}_N) \;:=\; N\int \left|\langle\phi\rangle_N - \langle\phi\rangle\right|^2 d\mu_{\mathcal{P}}[\phi] \quad . \tag{3.19}$$

From now on, we will omit the argument $\mathcal{X}_N$ when we denote the discrepancy. Using this definition, the discrepancy can again be written in terms of two-point functions. With the Hilbert-Schmidt operator comes a two-point function

$$C_{\mathcal{P}}(x_1,x_2) \;:=\; \int \phi(x_1)\phi(x_2)\, d\mu_{\mathcal{P}}[\phi] \;=\; \langle \tilde{\mathcal{P}}\delta_{x_1}\, \tilde{\mathcal{P}}\delta_{x_2}\rangle \quad . \tag{3.20}$$

Because the combination $\phi - \langle\phi\rangle$ appears in the average, it is useful to introduce the notation

$$\widehat{\phi}(x) \;:=\; \phi(x) - \langle\phi\rangle \quad , \tag{3.21}$$

and the *reduced* two-point function

$$\mathcal{B}_{\mathcal{P}}(x_1, x_2) \;:=\; \int \widehat{\phi}(x_1)\widehat{\phi}(x_2)\, d\mu_{\mathcal{P}}[\phi] \quad , \tag{3.22}$$

which can be written in terms of $\mathcal{C}_{\mathcal{P}}$ like in Eq.(3.9). It has the important feature that it integrates to zero with respect to each of its arguments. The discrepancy is given by

$$D_N \;=\; \frac{1}{N}\sum_{k,l=1}^{N} \mathcal{B}_{\mathcal{P}}(x_k, x_l) \quad , \tag{3.23}$$

i.e., as a sum over two-point correlations between the points of $\mathcal{X}_N$. The correlation function $\mathcal{B}_{\mathcal{P}}$ is determined by the operator $\mathcal{P}$ in this formulation.

3.2 The generating function

When $\mathcal{X}_N$ consists of uniformly distributed random points, then the discrepancy D_N is a random variable with a certain probability density. In [22, 23, 24], the generating function

$$G(z) := E(\, e^{zD_N}\,) \tag{3.24}$$

has been used to calculate it. We will also concentrate on the calculation of $G(z)$. Given G, the probability density can then be calculated by the inverse Laplace transform (Section 2.1.3).

It will turn out that it is far to complicated to calculate $G(z)$ analytically. For large number N of points, however, a series expansion in $1/N$ can be made which can be calculated term by term. We intend to calculate the generating function from an explicit expression in terms of $\mu_{\mathcal{P}}$, which we will now derive.

3.2.1 The generating function as an average over functions

First, we introduce the following bounded measure on $\mathbf{K}$, which consists of a sum of Dirac measures, centered around the points of the point set, minus one:

$$\eta_N(x) \;:=\; \frac{1}{N}\sum_{k=1}^{N} [\delta_{x_k}(x) - 1] \quad . \tag{3.25}$$

The integration error of a function ϕ and the discrepancy can be written in terms of η_N:

$$\langle\phi\rangle_N - \langle\phi\rangle = -i\eta_N[\phi] \qquad \text{and} \qquad D_N = -N\langle\, (\tilde{\mathcal{P}}\eta_N)^2\,\rangle \quad . \tag{3.26}$$

Using this expression for the discrepancy and the relation of Eq.(3.18), we can write

$$\exp(zD_N) \;=\; \exp(-zN\langle\, (\tilde{\mathcal{P}}\eta_N)^2\,\rangle) \;=\; \int \exp\left(\sqrt{2zN}\,\eta_N[\phi]\right) d\mu_{\mathcal{P}}[\phi] \quad . \tag{3.27}$$

If now the definition of η_N is used, and the integrals over $x_1, \ldots, x_N$ are performed on the l.h.s. and the r.h.s., we arrive at

$$G(z) \;=\; \int \langle\, e^{g\widehat{\phi}} \,\rangle^N d\mu_{\mathcal{P}}[\phi] \quad , \qquad g \;=\; \sqrt{\frac{2z}{N}} \;, \tag{3.28}$$

where we denote

$$\langle\, e^{g\widehat{\phi}} \,\rangle := \int_{\mathbf{K}} \exp(\, g\widehat{\phi}(x)\,)\, dx \;. \tag{3.29}$$

3.2.2 Gauge freedom

For the calculation of the generating function of the probability density of the discrepancy, there exists a freedom in the choice of the operator $\mathcal{P}$ with which the measure is defined, as we will show now. Let $\mathcal{T}$ act on $H := L_2(\mathbf{K})$ such that $\mathcal{T}\mathcal{P}$ is a Hilbert-Schmidt operator on H that maps H continuously on a space of continuous functions. For each functional F on H there is a functional $F \circ \mathcal{T}$ which maps $\phi \in H$ onto $F[\mathcal{T}\phi]$. We use this to define the measure $\mu_{\mathcal{T}\mathcal{P}}$ by

$$\int F[\phi]\, d\mu_{\mathcal{T}\mathcal{P}}[\phi] \;:=\; \int (F \circ \mathcal{T})[\phi]\, d\mu_{\mathcal{P}}[\phi] \;, \tag{3.30}$$

so that its Fourier transform is given by

$$\int \exp(i\eta[\phi])\, d\mu_{\mathcal{T}\mathcal{P}}[\phi] \;=\; \exp(-\tfrac{1}{2}\langle\, (\tilde{\mathcal{P}}\tilde{\mathcal{T}}\eta)^2 \,\rangle) \;, \tag{3.31}$$

and its two-point function is given by

$$\mathcal{C}_{\mathcal{T}\mathcal{P}}(x_1, x_2) \;=\; \langle \tilde{\mathcal{P}}\tilde{\mathcal{T}}\delta_{x_1}\, \tilde{\mathcal{P}}\tilde{\mathcal{T}}\delta_{x_2} \rangle \;. \tag{3.32}$$

If $\mathcal{T}$ is such that $\widehat{\mathcal{T}\phi} = \widehat{\phi}$ for all ϕ, then

$$G(z) \;=\; \int \langle\, e^{g\widehat{\phi}} \,\rangle^N d\mu_{\mathcal{P}}[\phi] \;=\; \int \langle\, e^{g\widehat{\phi}} \,\rangle^N d\mu_{\mathcal{T}\mathcal{P}}[\phi] \;, \tag{3.33}$$

and we call this property the *gauge freedom*. It leads to a freedom in the choice of the operator $\mathcal{P}$ with which the measure is defined, and we call these choices the *gauges*. Most *gauge transformations* $\mathcal{T}$ we consider are *global translations* that are characterized by a functional $t : H \mapsto \mathbf{R}$, and are given by $(\mathcal{T}\phi)(x) := \phi(x) + t[\phi]$ for all x. They trivially satisfy $\widehat{\mathcal{T}\phi} = \widehat{\phi}$.

An example of a gauge transformation that satisfies the criteria is simply given by $\mathcal{T}\phi := \widehat{\phi}$. It results in the *Landau gauge*, for which all ϕ satisfy $\langle\phi\rangle = 0$. This is, actually, the natural gauge to choose, because it restricts the analysis to functions that integrate to zero, so that the integration error becomes equal to the average of the function over the point set. The existence of the gauge freedom originates from the fact that the integration error is the same for integrands that differ only by a constant. The two-point function is equal to the reduced two-point function in the Landau gauge: $\mathcal{C}_{\mathcal{T}\mathcal{P}} = \mathcal{B}_{\mathcal{T}\mathcal{P}}$.

From now on, we will omit the label '$\mathcal{P}$' in the notation of the measures and the two-point functions.

3.2.3 The path integral, perturbation theory and instantons

The connection of the foregoing with Euclidean quantum field theory is made via the path integral formulation. The emphasis is put on the use of perturbation theory.

3.2.3.1 The path integral

We want to express the generating function, as given by Eq.(3.28), in terms of a *Euclidean path integral* (cf. [8]). We have to introduce the *free action*, which is a quadratic functional

$$S_0[\phi] \;:=\; \tfrac{1}{2}\langle\,(\mathcal{P}^{-1}\phi)^2\,\rangle \quad , \tag{3.34}$$

and we arrive at the path integral formulation of the measure μ by making the identification

$$d\mu[\phi] \;=\; [d\phi]\exp(-S_0[\phi]) \quad . \tag{3.35}$$

It is a formal expression, where $[d\phi]$ represents the product over the whole of $\mathbf{K}$ of the "infinitesimal volume elements" $d\phi(x)$. This is, of course, ill-defined, and it gets even worse since the set of functions ϕ, for which $S_0[\phi]$ is finite, in general has measure zero.

One thing we want to be more precise about is the fact that, in first instance, $\mathcal{P}^{-1}$ is only well-defined on the image $\mathcal{P}H$ of $H := L_2(\mathbf{K})$ under $\mathcal{P}$, while this set has measure zero. The members of the subsets of H that do not have measure zero, however, usually *do* satisfy the boundary conditions imposed by $\mathcal{P}$. We assume that these boundary conditions can be expressed by a finite number of linear equations

$$\Upsilon_i[\phi] = 0 \quad , \quad i = 1, 2, \ldots \quad . \tag{3.36}$$

Then, the action should be extended as follows:

$$S_0[\phi] \;=\; \tfrac{1}{2}\langle\,(\mathcal{P}^{-1}\phi)^2\,\rangle + \sum_i \tfrac{1}{2}M_i\Upsilon_i[\phi]^2 \quad , \tag{3.37}$$

where $M_i \to \infty$ for all labels i. The "infinitesimal volume element" $[d\phi]$ gets a factor $\sqrt{2\pi/M_i}$ for every i in order for the measure to stay normalized to one. The extra terms in the action assure that the measure is zero if a function does not satisfy the boundary conditions. Notice that the action is still quadratic in ϕ.

If we apply all this to the expression of Eq.(3.28) for the generating function, we find that

$$G(z) \;=\; \int [d\phi]\exp(-S[\phi]) \quad , \tag{3.38}$$

with an action S given by

$$S[\phi] \;=\; S_0[\phi] - N\log\langle\, e^{g\widehat{\phi}}\,\rangle \quad , \qquad g = \sqrt{\frac{2z}{N}} \quad . \tag{3.39}$$

3.2.3.2 Perturbation theory and instantons

In the action of Eq. (3.39), g appears to be a natural expansion parameter if N is large. An expansion around $g = 0$ will automatically result in an expansion of the generating function around $z = 0$. Furthermore, it corresponds to an expansion of the action around $\phi = 0$. An expansion of the action to evaluate the generating function, however, only makes sense when it is an expansion around a minimum, so that it represents a saddle point approximation of the path integral. Therefore, a straightforward expansion such as just proposed, is only correct if it is an expansion around the minimum of the action, that is, if the trivial solution $\phi = 0$ gives the only minimum of the action. General extrema of the action are given by solutions of the *field equation*

$$(\Lambda\phi)(x) + Ng - Ng\frac{e^{g\phi(x)}}{\langle e^{g\phi}\rangle} \;=\; 0 \;\;, \tag{3.40}$$

where Λ represents the self-adjoint operator $(\mathcal{P}^{-1})^\dagger\mathcal{P}^{-1}$ including the boundary conditions Υ_i *and* possible boundary conditions coming from the fact that $\mathcal{P}^{-1}$ is not necessarily self-adjoint [1]. Depending on the value of z, non-trivial solutions may also exist. At this point it can be said that, because $\Lambda\phi$ is real, non-trivial solutions only exist if z is real and non-zero so that $g \in \mathbf{R}$. In the analysis of the solutions we therefore can do a scaling $\phi(x) \mapsto \phi(x)/g$ so that the action for these solutions is given by

$$\Sigma[\phi] \;:=\; \frac{1}{N}S[\tfrac{1}{g}\,\phi] \;=\; \frac{1}{2}\,\frac{\langle\phi\, e^{\phi}\rangle}{\langle e^{\phi}\rangle} + \frac{1}{2}\langle\phi\rangle - \log\langle e^{\phi}\rangle \;\;. \tag{3.41}$$

These non-trivial solutions we call instantons (cf. [9]), although this may not be a rigorously correct nomenclature, in the field theoretical sense, for all situations we will encounter. Notice that instantons under different gauges only differ by a constant: if two gauges are connected by a global translation $\mathcal{T}$, and ϕ is an instanton in the $\mathcal{P}$-gauge, then $\mathcal{T}\phi$ is an instanton in the $\mathcal{TP}$-gauge. The values of z for which they appear and the value of the action are gauge invariant, as can be concluded from Eq.(3.40) and Eq.(3.41).

If N becomes large, then the contribution of an instanton to the path integral will behave as $e^{-N\Sigma[\phi]}$, where $\Sigma[\phi]$ does not depend on N (Notice that $\phi(x)$ does not depend on N because the field equation for these rescaled functions does not depend on N.). The $e^{-N\Sigma[\phi]}$-like behavior of the instanton contribution makes it invisible in the perturbative expansion around $1/N = 0$. If $\Sigma[\phi]$ is larger than zero, this will not be a problem, because the contribution will be very small. If, however, $\Sigma[\phi]$ is equal to zero, then the contribution will be more substantial, and it will even explode if $\Sigma[\phi]$ is negative. Notice that, to be able to do make a perturbation series around $\phi = 0$, the action has to be zero for this solution, for else the terms would all become zero or would explode for large N.

The escape from this possible disaster is given by the fact that z has to be real and larger than zero for instantons to exist, and we want to integrate $G(z)$ along the imaginary z-axis (Section 2.1.3). Also in the end, when we want to close the integration contour in the complex z-plane

[1] For example, if $\mathcal{P}^{-1}\phi = \phi' := \frac{d\phi}{dx}$ and $\Upsilon[\phi] = \phi(0)$, then $\langle\,(\mathcal{P}^{-1}\phi)^2\,\rangle = \phi(1)\phi'(1) - \langle\phi\,\phi''\rangle$, so that the extra boundary condition is $\phi'(1) = 0$.

to the right, we will not meet the problem, because the function we want to integrate is an expansion in z around $z = 0$ that can be integrated term by term. Problems might only occur when instantons exist for values of z that are arbitrarily close to 0. We will confirm for a few cases that this does not happen.

3.2.4 Feynman rules to calculate the $1/N$ corrections

We just suggested a straight-forward expansion in $1/N$ of $\exp(-S)$ to calculate G perturbatively. This way, however, the calculation of the perturbation series becomes very cumbersome, and the reason for this is the following. We want to use the fact that an expansion in $1/N$ corresponds to an expansion around $\phi = 0$ of the part of the action that is non-quadratic in ϕ. The subsequent terms in the expansions are therefore proportional to moments of a Gaussian measure, and can be calculated using diagrams (Section 2.2.2). These diagrams, the *Feynman diagrams*, consist of lines representing two-point functions and vertices representing convolutions of two-point functions. Because the action is non-local, i.e. it cannot be written as a single integral over a Lagrangian density because of the logarithm in Eq. (3.39), the total path integral, thus the total sum of all diagrams, cannot be seen as the exponential of all *connected* diagrams, and it is this that makes the calculations difficult.

In order to circumvent this obstacle, we first of all use the Landau gauge, so that $\widehat{\phi} = \phi$ for all ϕ. Secondly, we introduce $2N$ Grassmann variables $\bar{\psi}_i$ and ψ_i, $i = 1, 2, \ldots, N$, as in Section 2.2.3, so that we can write

$$G(z) \;=\; \int \langle\, e^{g\phi} \,\rangle^N \, d\mu[\phi] \;=\; \int\int [d\bar{\psi}\, d\psi] \exp\Big(- \sum_{i=1}^{N} \bar{\psi}_i \psi_i \,\langle\, e^{g\phi} \,\rangle \Big)\, d\mu[\phi] \quad . \tag{3.42}$$

If we now define

$$\eta_k[\phi] := -g^k \langle \phi^k \rangle \quad , \quad \chi_k := \eta_k \sum_{i=1}^{N} \bar{\psi}_i \psi_i \quad , \tag{3.43}$$

and

$$\langle\!\langle\, f \,\rangle\!\rangle \;:=\; \int\int [d\bar{\psi}\, d\psi]\, f(\{\chi\}) \, \exp\Big(- \sum_{i=1}^{N} \bar{\psi}_i \psi_i \Big)\, d\mu[\phi] \quad , \tag{3.44}$$

we can write

$$G(z) \;=\; \langle\!\langle \exp\Big(\sum_{k=2}^{\infty} \frac{\chi_k}{k!} \Big) \rangle\!\rangle \quad , \tag{3.45}$$

which has exactly the form of the r.h.s. of Eq. (2.89). Because the functionals η_k are also of the kind of Eq. (2.85), we can use the statement of Eq. (2.89), that $G(z)$ is equal to the sum of the contributions of all Feynman diagrams that can be constructed with the vertices

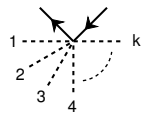

$$, \quad k \geq 2 \quad , \tag{3.46}$$

and with the rules that all incoming legs have to be connected to outgoing legs and vice versa, and all dashed legs have to be connected to dashed legs. The lines in the obtained diagrams stand for *propagators*:

$$\text{boson propagator:} \quad x \cdots\cdots y \;=\; \mathcal{B}(x,y) \;; \tag{3.47}$$

$$\text{fermion propagator:} \quad i \longrightarrow\!\!\!\!\!\!\!\!\longrightarrow j \;=\; \delta_{i,j} \;, \tag{3.48}$$

and to calculate the contribution of a diagram, boson propagators have to be convoluted in the vertices as $\int_{\mathbf{K}} \mathcal{B}(y,x_1)\mathcal{B}(y,x_2)\cdots\mathcal{B}(y,x_k)\,dy$, fermion propagators as $\sum_{j=1}^{N} \delta_{i_1,j}\delta_{j,i_2}$, and then these convolutions have to be multiplied. To get the final result for a diagram, a factor $-g^k$ has to be included for every vertex of order k, and the symmetry factor has to be included.

The contribution of the fermionic part can easily be determined, for every fermion loop only gives a factor $-N$. The main problem is to calculate the bosonic part. Furthermore, only the connected diagrams have to be calculated, since the sum of their contributions is equal to

$$W(z) := \log G(z) \;. \tag{3.49}$$

Because every vertex carries a power of g that is equal to its order, the expansion in g is an expansion in the complexity of the diagrams, which can be systematically evaluated.

3.2.5 Gaussian measures on a countable basis

Because $\mathcal{P}$ is a Hilbert-Schmidt operator on $H := L_2(\mathbf{K})$, $\mathcal{P}^\dagger\mathcal{P}$ is a self adjoint compact operator on H, and there exists an orthonormal basis $\{u_n\}$ of H, consisting of eigenvectors of $\mathcal{P}^\dagger\mathcal{P}$. If we denote the eigenvalues by σ_n^2, then the eigenvalue equation is given by

$$(\mathcal{P}^\dagger\mathcal{P}u_n)(x) \;=\; \int_{\mathbf{K}} \mathcal{C}(x,y)u_n(y)\,dy \;=\; \sigma_n^2 u_n(x) \;. \tag{3.50}$$

As the notation suggests, they are positive since $0 < \|\mathcal{P}u_n\|^2 = \langle u_n\, \mathcal{P}^\dagger\mathcal{P}u_n\rangle = \sigma_n^2$. Notice that, because $\mathcal{P}$ is Hilbert-Schmidt, $\sum_n \sigma_n^2\|u_n\|^2 < \infty$, and this leads immediately to the spectral decomposition of $\mathcal{C}$, which is simply given by

$$\mathcal{C}(x,y) \;=\; \sum_n \sigma_n^2 u_n(x)u_n(y) \;. \tag{3.51}$$

In principle, the basis and the eigenvalues can be used as an alternative definition of a quadratic discrepancy. They naturally introduce the spectral decomposition of a two-point function and a reduced two-point function. The reasonable requirement of the existence of $E(D_N)$ leads to

$$E(D_N) \;=\; \sum_n \sigma_n^2 \left(\|u_n\|^2 - \langle u_n\rangle^2\right) \;<\; \infty \;, \tag{3.52}$$

which is satisfied if $\mathcal{C}$ comes from a Hilbert-Schmidt operator. If we denote the expansion of a function $\phi \in H$ by

$$\phi(x) \;=\; \sum_n \phi_n u_n(x) \;, \quad \phi_n \in \mathbf{R} \;, \tag{3.53}$$

then the probability measure μ can be written as

$$d\mu[\phi] \;=\; \prod_n \frac{\exp(-\phi_n^2/2\sigma_n^2)}{\sqrt{2\pi\sigma_n^2}}\, d\phi_n \quad , \quad \sigma_n \in \mathbf{R} \quad . \tag{3.54}$$

The basis functions will often be refered to as *modes*, originating from an example of a quadratic discrepancy (the Fourier diaphony), for which the basis is the Fourier basis without the constant mode.

With different gauges come different bases and strengths. We call a gauge in which the basis is orthonormal a *Feynman* gauge. If the Landau gauge is used, in which $\langle \phi \rangle = 0$, then the basis functions have to integrate to zero:

$$\langle\, u_n^{(L)} \,\rangle \;=\; 0 \quad \forall\, n \quad , \tag{3.55}$$

where the label L indicates the Landau gauge. These functions are the solutions of the eigenvalue equation

$$\int_{\mathbf{K}} \mathcal{B}(x,y)\, u_n^{(L)}(y)\, dx \;=\; \sigma_{L,n}^2 u_n^{(L)}(x) \quad . \tag{3.56}$$

It will not always be possible to find the Landau basis. In terms of a basis that is not in the Landau gauge, $\mathcal{B}$ is given by

$$\mathcal{B}(x,y) \;=\; \sum_n \sigma_n^2 (u_n(x) - \langle u_n \rangle)(u_n(y) - \langle u_n \rangle) \quad . \tag{3.57}$$

3.3 Examples

Some explicit, and well known, examples of quadratic discrepancies are introduced, and cast in the formalism of this chapter.

3.3.1 The L_2^*-discrepancy

In our definition, the L_2^*-discrepancy is N times the square of the case of $p = 2$ in Eq.(3.6). The operator $\mathcal{P}$ and the two-point function $\mathcal{C}$ are given by

$$(\mathcal{P}\phi)(x) := \int_{\mathbf{K}} \vartheta_y(x)\phi(y)\, dy \quad , \quad \mathcal{C}(x_1,x_2) \;=\; \prod_{\nu=1}^{s} \min(1-x_1^\nu, 1-x_2^\nu) \quad , \tag{3.58}$$

where $\vartheta_y(x) := \prod_{\nu=1}^{s} \theta(y^\nu - x^\nu)$. The boundary conditions imposed by $\mathcal{P}$ are given by $\phi(x) = 0$ if at least one of the coordinates $x^\nu = 1$. The basis functions can now be found by solving the eigenvalue equation $\int_{\mathbf{K}} \mathcal{C}(x,y)u(y) = \sigma^2 u(x)$. The equation factorizes for the different coordinates, and is most easily solved by differentiating twice on the l.h.s. and the r.h.s.. The one-dimensional solutions, that satisfy the boundary conditions, are

$$u_n(x^\nu) = \sqrt{2}\, \cos\left((n+\tfrac{1}{2})\pi x^\nu\right) \quad , \quad \sigma_n^2 = \pi^{-2}(n+\tfrac{1}{2})^{-2} \quad , \quad n = 0,1,2,\ldots \quad . \tag{3.59}$$

The set $\{u_n\}$ clearly is orthonormal, and it is the basis in the one-dimensional case. For $s > 1$, the basis and the strengths are given by all possible products

$$u_{\vec{n}}(x) \;=\; 2^{s/2} \prod_{\nu=1}^{s} \cos\left((n_\nu + \tfrac{1}{2})\pi x^\nu\right) \quad , \quad \sigma^2_{\vec{n}} \;=\; \pi^{-2s} \prod_{\nu=1}^{s} (n_\nu + \tfrac{1}{2})^{-2} \quad , \tag{3.60}$$

where $\vec{n} := (n_1, n_2, \ldots, n_s)$ and $n_\nu = 0, 1, 2, \ldots$ for $\nu = 1, \ldots, s$. The reduced two-point function is given by

$$\mathcal{B}(x_1, x_2) \;=\; \prod_{\nu=1}^{s} \min(1 - x_1^\nu, 1 - x_2^\nu) - (\tfrac{1}{2})^s \prod_{\nu=1}^{s} (1 - (x_1^\nu)^2) - (\tfrac{1}{2})^s \prod_{\nu=1}^{s} (1 - (x_2^\nu)^2) + (\tfrac{1}{3})^s \quad . \tag{3.61}$$

In one dimension, the eigenfunctions and eigenvalues are

$$u_n^{(L)}(x) = \sqrt{2}\,\cos(n\pi x) \quad , \quad \sigma^2_{L,n} = \pi^{-2} n^{-2} \quad , \quad n = 1, 2, \ldots \quad . \tag{3.62}$$

For $s > 1$, it is difficult to find all solutions to the eigenvalue equation, and we will address this problem in Section 5.2.2.

3.3.2 The Cramér-von Mises goodness-of-fit test

The L_2^*-discrepancy is equivalent with the statistic of the Cramér-von Mises goodness-of-fit test, which tests the hypotheses that N data x_k are distributed independently following a cumulative distribution function F (cf. [2, 18]). Consider, for simplicity, the one-dimensional case, so that $x_k \in \mathbf{R}$, and denote $\vartheta_{x_1}(x_2) := \theta(x_1 - x_2)$ and $\langle \phi \rangle_N := N^{-1} \sum_{k=1}^{N} \phi(x_k)$. The statistic is given by

$$W_N^2 \;:=\; N \int_{\mathbf{R}} \left| \langle \vartheta_x \rangle_N - F(x) \right|^2 dF(x) \quad , \tag{3.63}$$

where we put the extra factor N again, just as in the case of the discrepancies. Because F is a cumulative distribution function, its inverse $F^{-1} : [0,1] \mapsto \mathbf{R}$ is uniquely defined, and we can re-write the statistic as

$$W_N^2 \;=\; N \int_{\mathbf{K}} \left| \langle \vartheta_{F^{-1}(y)} \rangle_N - y \right|^2 dy \quad , \tag{3.64}$$

where we denote $\mathbf{K} := [0,1]$. But $\vartheta_{F^{-1}(y)}(x) = \vartheta_y(F(x))$, so that W_N^2 is equal to the L_2^*-discrepancy of the points $F(x_k)$. The interpretation of the statistic is slightly different from the L_2^*-discrepancy, but the probability distribution is exactly the same.

3.3.3 The Fourier diaphony

For the Fourier diaphony, $\mathcal{P}$ should impose periodic boundary conditions. In one dimension, a simple Hilbert-Schmidt operator that achieves this is given by

$$(\mathcal{P}\phi)(x) \;:=\; \frac{\sqrt{3}}{\pi} \int_{\mathbf{K}} k_1(x - y)\phi(y)\, dy \quad , \qquad k_1(x) := 2\pi(\{x\} - \tfrac{1}{2}) \quad , \tag{3.65}$$

where $\{x\} := x \bmod 1$. The term of a half in the integration kernel assures that $\mathcal{P}\phi$ integrates to zero, so that the discrepancy is formulated in the Landau gauge from the start. The choice of the factors seems odd, but will appear to be the natural choice for the extension to more dimensions. The two-point function is given by

$$\mathcal{B}(x_1, x_2) \;=\; \langle \tilde{\mathcal{P}}\delta_{x_1}\, \tilde{\mathcal{P}}\delta_{x_2} \rangle \;=\; 1 - 6\{x_1 - x_2\}(1 - \{x_1 - x_2\}) \quad . \tag{3.66}$$

Notice that the two-point function only depends on $x_1 - x_2$ and therefore is translation invariant, i.e., $\mathcal{B}(x_1 + a, x_2 + a) \;=\; \mathcal{B}(x_1, x_2)$ for all $a \in [0, 1]$. As a result of this, all information about $\mathcal{B}$ is contained in the function $\mathcal{B}_1 : x \mapsto \mathcal{B}(x, 0)$, and we have

$$\mathcal{B}(x_1, x_2) \;=\; \mathcal{B}_1(x_1 - x_2) \quad . \tag{3.67}$$

The factor $\sqrt{3}/\pi$ was chosen such, that $\mathcal{B}_1(0) = 1$. The set $\{u_n\}$ of solutions of the eigenvalue equation $\int_{\mathbf{K}} \mathcal{B}(x, y)u(y)\,dy \;=\; \sigma^2 u(x)$ is just the Fourier basis on $[0, 1]$ without the constant mode:

$$u_{2n-1}(x) = \sqrt{2}\sin(2\pi n x) \quad , \quad u_{2n}(x) = \sqrt{2}\cos(2\pi n x) \quad , \quad n = 1, 2, \ldots \quad , \tag{3.68}$$

with eigenvalues

$$\sigma^2_{2n-1} = \sigma^2_{2n} \;=\; 3\,\pi^{-2} n^{-2} \quad , \quad n = 1, 2, \ldots \quad . \tag{3.69}$$

The function $u_0 : x \mapsto 1$ is not a member of the basis because of the Landau gauge. Only functions that integrate to zero are present.

In $s > 1$ dimensions, the operator $\mathcal{P}$ is extended as follows. Let $\ominus$ denote coordinate wise subtraction, then

$$(\mathcal{P}\phi)(x) \;:=\; \frac{1}{\sqrt{(1 + \pi^2/3)^s - 1}} \int_{\mathbf{K}} k_s(x \ominus y)\phi(y)\,dy \quad , \tag{3.70}$$

with

$$k_s(x) \;:=\; -1 + \prod_{\nu=1}^{s} [1 + k_1(x^\nu)] \quad . \tag{3.71}$$

The s-dimensional integration kernel is obtained from the one-dimensional one by adding the constant mode and taking the product over the coordinates. The extra term of -1 assures that the constant mode in s dimensions disappears again. The new factor assures that the s-dimensional two-point function is equal to one in the origin:

$$\mathcal{B}_s(x) \;=\; \frac{1}{(1 + \pi^2/3)^s - 1} \left(-1 + \prod_{\nu=1}^{s} \left[1 + \frac{\pi^2}{3}\,\mathcal{B}_1(x^\nu) \right] \right) \quad . \tag{3.72}$$

The basis in s-dimensions consists of all products over coordinates of the one-dimensional basis including the constant mode u_0. The only product that does not appear is, of course,

$\prod_{\nu=1}^{s} u_0(x^\nu)$. The eigenvalue coming with u_0 is determined by the choice of k_s, and equal to 1. The eigenvalues in s dimensions are just the properly normalized products of the one-dimensional ones. If we denote $\vec{n} = (n_1, n_2, \ldots, n_s)$ and introduce

$$k_\nu(\vec{n}) := \begin{cases} \frac{1}{2}n_\nu & \text{if } n_\nu \text{ is even,} \\ \frac{1}{2}(n_\nu + 1) & \text{if } n_\nu \text{ is odd,} \end{cases} \tag{3.73}$$

then

$$\sigma^2_{\vec{n}} \;:=\; \sigma^2(\vec{k}(\vec{n})) \;:=\; \frac{1}{(1+\pi^2/3)^s - 1} \prod_{\nu=1}^{s} \frac{1}{r(k_\nu)^2} \quad , \qquad r(k_\nu) = \begin{cases} k_\nu & \text{if } k_\nu \neq 0\,, \\ 1 & \text{if } k_\nu = 0\,. \end{cases} \tag{3.74}$$

The Fourier diaphony is often written in terms of the complex Fourier basis of $\mathbf{K}$. Then, it attains the form

$$D_N \;=\; \frac{1}{N} \sum_{\vec{k}} \sigma^2(\vec{k}\,) \left| \sum_{l=1}^{N} e^{2i\pi \vec{k}\cdot x_l} \right|^2 \quad , \tag{3.75}$$

where $\vec{k} \cdot x := k_1 x^1 + k_2 x^2 + \cdots + k_s x^s$, and the first sum is over all $\vec{k} \in \mathbf{Z}^s$ except the constant mode $\vec{k} = (0, 0, \ldots, 0)$. Introduced as in this section, the diaphony is again N times the square of the definition as given in, for example, [19].

3.3.4 The Lego discrepancy and the χ^2-statistic

For the Lego discrepancy, the image $C := \mathcal{P}H$ is a finite dimensional vector space. It is obtained by dividing $\mathbf{K}$ into M disjoint 'bins' $\mathbf{A}_n$ with $\bigcup_{n=1}^{M} \mathbf{A}_n = \mathbf{K}$, and taking

$$(\mathcal{P}\phi)(x) \;:=\; \sum_{n=1}^{M} \frac{\sigma_n}{\sqrt{w_n}}\, \vartheta_n(x) \langle \vartheta_n\, \phi \rangle \quad , \tag{3.76}$$

where

$$\vartheta_n := \vartheta_{\mathbf{A}_n} \quad , \qquad w_n := \langle \vartheta_n \rangle \quad , \tag{3.77}$$

and, in first instance, the strengths σ_n are not specified. $\mathcal{P}$ maps H onto the space of functions that are defined with a precision up to the size of the bins $\mathbf{A}_n$. Notice that $\vartheta_n \vartheta_m = \delta_{n,m}\vartheta_m$ where $\delta_{n,m}$ is the Kronecker delta symbol, and that $\sum_{n=1}^{M} \vartheta_n = 1$, $\sum_{n=1}^{M} w_n = 1$. The two-point function is given by

$$C(x_1, x_2) \;=\; \sum_{n=1}^{M} \sigma_n^2 \vartheta_n(x_1)\vartheta_n(x_2) \quad . \tag{3.78}$$

Clearly, this model is dimension-independent, in the sense that the only information on the dimension of $\mathbf{K}$ is that contained in the value of M: if the dissection of $\mathbf{K}$ into bins is of the

hyper-cubic type with p bins along each axis, then we shall have $M = p^s$. Also, a general area-preserving mapping of $\mathbf{K}$ onto itself will leave the discrepancy invariant: it will lead to a distortion (and possibly a dissection) of the various bins, but this influences neither w_n nor (by definition) σ_n. Owing to the finiteness of M, a finite point set can, in fact, have zero discrepancy in this case, namely if every bin $\mathbf{A}_n$ contains precisely $w_n N$ points (assuming this number to be integer for every n).

Because C is M-dimensional, it is easiest to formulate everything in $\mathbf{R}^M$. We define

$$\phi^v := (\phi_1, \phi_2, \ldots, \phi_n) \quad , \qquad \phi_n = \frac{1}{w_n} \langle \vartheta_n \, \phi \rangle \quad , \tag{3.79}$$

and divide H into equivalence classes by the prescription that $\phi \sim \varphi$ if $\phi^v = \varphi^v$. This space is C, and it is isomorphic to $\mathbf{R}^M$ with inner product $\langle \phi^v \, \varphi^v \rangle := \sum_{n=1}^{M} w_n \phi_n \varphi_n$. The operator $\mathcal{P}$ restricted to $\mathbf{R}^M$ is given by

$$(\mathcal{P}\phi^v)_n = \frac{\sigma_n}{\sqrt{w_n}} \, \phi_n \quad . \tag{3.80}$$

Notice that $\mathcal{P}$ is self adjoint. The Gaussian measure μ can now be defined rigorously in terms of a finite-dimensional path integral. If F is a functional on C, then

$$\int_C F[\phi] \, d\mu[\phi] \;=\; \int [d\phi^v] \, F\Big[\sum_{n=1}^{M} \phi_n \vartheta_n \Big] \, \exp(-S_0[\phi^v]) \quad , \tag{3.81}$$

with

$$[d\phi^v] \;=\; \prod_{n=1}^{M} \frac{d\phi_n}{\sqrt{2\pi\sigma_n^2}} \qquad \text{and} \qquad S_0[\phi^v] \;=\; \frac{1}{2} \sum_{n=1}^{M} \frac{1}{\sigma_n^2} \, \phi_n^2 \quad . \tag{3.82}$$

The two-point function and the reduced two-point function can be written in terms of matrices as

$$\mathcal{C}(x_1, x_2) = \sum_{n,m=1}^{M} \mathcal{C}_{n,m} \vartheta_n(x_1) \vartheta_m(x_2) \quad , \quad \mathcal{B}(x_1, x_2) = \sum_{n,m=1}^{M} \mathcal{B}_{n,m} \vartheta_n(x_1) \vartheta_m(x_2) \quad , \tag{3.83}$$

with

$$\mathcal{C}_{n,m} = \sigma_n^2 \delta_{n,m} \quad , \quad \mathcal{B}_{n,m} = \sum_{k=1}^{M} (\sigma_n \delta_{n,k} - \sigma_k w_k)(\sigma_m \delta_{m,k} - \sigma_k w_k) \quad . \tag{3.84}$$

In the path integral formulation of the generating function, $\langle \, e^{g\widehat{\phi}} \, \rangle$ occurs, and the series expansion of exp and the properties of the characteristic functions tell us that $\langle e^{g\phi} \rangle = \sum_{n=1}^{M} w_n e^{g\phi_n}$, so that the generating function is given by

$$G(z) \;=\; \int [d\phi^v] \, \exp\left(-S_0[\phi^v] - gN \sum_{n=1}^{M} w_n \phi_n + N \log\Big(\sum_{n=1}^{M} w_n e^{g\phi_n} \Big) \right) \quad . \tag{3.85}$$

The discrepancy itself can be written as

$$D_N = \frac{1}{N}\sum_{k,l=1}^{N} \mathcal{B}(x_k, x_l) = \frac{1}{N}\sum_{n,m=1}^{M} \mathcal{S}_n \mathcal{B}_{n,m} \mathcal{S}_m \quad , \quad \text{where} \quad \mathcal{S}_n := \sum_{k=1}^{N} \vartheta_n(x_k) \tag{3.86}$$

is the number of points in bin $\mathbf{A}_n$.

3.3.4.1 The χ^2-statistic

We did not yet specify the strengths σ_n, but we will in particular look at the choice for which $\sigma_n^2 w_n = 1$ for all $n = 1, 2, \ldots, M$. In this case, C consists of functions in which the largest fluctuations appear over the smallest intervals. Although not a priori attractive in many cases, this choice is actually quite appropriate for, e.g. particle physics where cross sections display precisely this kind of behavior. The reduced two-point function attains the simple form $\mathcal{B}_{n,m} = \frac{1}{w_n}\delta_{n,m} - 1$ and the discrepancy becomes

$$D_N \;=\; \sum_{n=1}^{M} \frac{(\mathcal{S}_n - w_n N)^2}{w_n N} \quad , \tag{3.87}$$

which is nothing but the χ^2-statistic for N data points distributed over M bins with expected number of points $w_n N$ (cf. [2]).

3.4 Appendices

Appendix 3A

Let $H := L_2(\mathbf{K})$ be the Hilbert space of (equivalence classes of almost everywhere equal) real quadratically integrable functions on $\mathbf{K}$, with inner product and norm

$$\langle f, g\rangle \;:=\; \int_{\mathbf{K}} f(x) g(x)\, dx \quad , \qquad \|f\|_2 \;:=\; \sqrt{\langle f, f\rangle} \ . \tag{3.88}$$

A Hilbert space is self-dual, i.e. there is an isomorphism between H and its dual space $\tilde{H}$ of continuous linear functions $H \mapsto \mathbf{R}$. It induces an invertible mapping $\tilde{H} \ni \eta \mapsto f_\eta \in H$ such that $\langle f_\eta, g\rangle = \eta[g]$ for all $g \in H$, and we write $\|\eta\|_2 := \|f_\eta\|_2$.

Let $\mathcal{P}$ be a Hilbert-Schmidt operator on H, and $\tilde{\mathcal{P}}$ its transposed which acts on $\tilde{H}$ through the definition $\tilde{\mathcal{P}}\eta := \eta \circ \mathcal{P}$. It is easy to see that $\tilde{\mathcal{P}}$ is a Hilbert-Schmidt operator on $\tilde{H}$ and that $\|\tilde{\mathcal{P}}\eta\|_2 = \|\mathcal{P}^\dagger f_\eta\|_2$ exists for every $\eta \in \tilde{H}$. Furthermore, it is well known (cf. [4]) that there exists a Gaussian measure μ on H with Fourier transform

$$\int_H \exp(i\eta[f])\, d\mu[f] \;=\; \exp(-\tfrac{1}{2}\|\tilde{\mathcal{P}}\eta\|_2^2) \ . \tag{3.89}$$

By inserting $\lambda\eta$ where λ is a real variable, and differentiating the above equation twice with respect to λ before putting it to zero, one obtains the relation

$$\int_H \eta[f]^2 \, d\mu[f] \;=\; \|\tilde{\mathcal{P}}\eta\|_2^2 \;. \tag{3.90}$$

With μ, a Hilbert space $L_2(H,\mu)$ can be defined, where the norm is given by

$$\|\eta\|_\mu \;:=\; \left(\int_H \eta[f]^2 \, d\mu[f]\right)^{1/2} \;. \tag{3.91}$$

It is clear that a mapping $\mathcal{N} : \tilde{H} \mapsto L_2(H,\mu)$ can directly be defined on the whole of $\tilde{H}$, but we need more: we want to apply it to Dirac-measures, which $\tilde{H}$ does not contain. Consider therefore the Hilbert space $H_{\tilde{\mathcal{P}}}$, which is the completion of $\tilde{H}$ under the norm

$$\|\eta\|_{\tilde{\mathcal{P}}} \;:=\; \|\tilde{\mathcal{P}}\eta\|_2 \;. \tag{3.92}$$

$\tilde{\mathcal{P}}$ can be interpreted as a continuous mapping from $H_{\tilde{\mathcal{P}}}$ to $\tilde{H}$, with $\tilde{\mathcal{P}}H_{\tilde{\mathcal{P}}} = \tilde{H}$. Furthermore, $\mathcal{N}$ can be extended to the whole of $H_{\tilde{\mathcal{P}}}$ since it is an isometry:

$$\forall\, \eta \in H_{\tilde{\mathcal{P}}} : \quad \|\mathcal{N}\eta\|_\mu^2 \;=\; \int_H (\mathcal{N}\eta)[f]^2 \, d\mu[f] \;=\; \|\tilde{\mathcal{P}}\eta\|_2^2 \;=\; \|\eta\|_{\tilde{\mathcal{P}}}^2 \;. \tag{3.93}$$

Now, suppose that $\mathcal{P}$ maps H continuously onto a space C of continuous functions, such that

$$\|\mathcal{P}f\|_\infty := \sup_{x\in\mathbf{K}} |(\mathcal{P}f)(x)| \le p\|f\|_2 \quad \text{for some } p > 0. \tag{3.94}$$

The dual space $\tilde{C}$ of C consists of bounded measures on $\mathbf{K}$, and containes the Dirac-measures. Then we have for every $\eta \in \tilde{C}$ and every $f \in H$:

$$\left|(\tilde{\mathcal{P}}\eta)[f]\right| \;=\; \left|\eta[\mathcal{P}f]\right| \;\le\; \|\eta\|\cdot\|\mathcal{P}f\|_\infty \;\le\; p\|\eta\|\cdot\|f\|_2 \;, \tag{3.95}$$

so that $\tilde{\mathcal{P}}$ maps $\tilde{C}$ continuously onto $\tilde{H}$. Therefore, $\tilde{C} \subset H_{\tilde{\mathcal{P}}}$, and $\mathcal{N}$ can be applied to $\tilde{C}$.

Appendix 3B

For the proof that (3.94) holds in case of the Fourier diaphony, we use that there is obviously a number p such that

$$\left|\frac{k_s(x \ominus y)}{\sqrt{(1+\pi^2/3)^s - 1}}\right| \le p \quad \text{for all } x, y \in \mathbf{K}, \tag{3.96}$$

so that

$$|(\mathcal{P}f)(x)| \;\le\; p\int_{\mathbf{K}} |f(y)|\, dy \quad \text{for all } x \in \mathbf{K}. \tag{3.97}$$

Now, we can apply the Cauchy-Schwarz inequality, with the result that for all $x \in \mathbf{K}$

$$|(\mathcal{P}f)(x)| \;\le\; p\left(\int_{\mathbf{K}} 1\, dy\right)^{1/2}\left(\int_{\mathbf{K}} |f(y)|^2\, dy\right)^{1/2} \;=\; p\,\|f\|_2 \;. \tag{3.98}$$

Chapter 4

Instantons for discrepancies

It is mentioned in Section 3.2.3 that an expansion of the path integral representation of the generating function of quadratic discrepancies around the trivial solution of the field equation is only correct, if this solution gives the minimum of the action. Furthermore, it is suggested that the non-trivial solutions, called *instantons*, might spoil the perturbation expansion if they exist for real values of the order parameter z of the generating function that are arbitrarily close to 0. In this chapter, we take a closer look at the issue for the Lego discrepancy and the L_2^*-discrepancy in one dimension, and show that instantons exist but do not threaten the perturbative expansion.

For the the L_2^*-case, a method had to be developed to analyze the singularity structures of the solutions of implicit function equations with numerical help of a computer which is presented in Section 4.4.

Contents

4.1 An alternative derivation of the path integral formulation

We start with an alternative derivation of the representation of the generating function as a path integral. For the Lego discrepancy, this goes as follows. We consider the case for which $\sigma_n^2 w_n = 1$ for all $n = 1, \ldots, M$, so that the discrepancy is just the χ^2-statistic

$$D_N = \frac{1}{N} \sum_{n=1}^{M} \frac{S_n^2}{w_n} - N \quad , \quad \text{where} \quad S_n := \sum_{k=1}^{N} \vartheta_n(x_k) \tag{4.1}$$

is the number of points x_k in bin n. If the points x_k are truly randomly distributed, the variables S_n are distributed according to a multinomial distribution, so that the generating function is given by

$$E(e^{zD_N}) = \sum_{\{S_n\}} \frac{N!}{S_1! \cdots S_M!} w_1^{S_1} \cdots w_M^{S_M} \exp\left(\frac{z}{N} \sum_{n=1}^{M} \frac{S_n^2}{w_n} - zN \right) \quad , \tag{4.2}$$

where the summation is over all configurations $\{S_n\}$ which satisfy $\sum_{n=1}^{M} S_n = N$. Notice that $E(e^{zD_N}) > w_n^N \exp(zN/w_n - zN)$ for every n, so that the generating function is not defined if $N \to \infty$ for the values of z with $\mathrm{Re}\, z > \frac{w_n}{w_n - 1} \log w_n$. Using Gaussian integration rules and the generalized binomial theorem, it is easy to see that Eq.(4.2) can be written as

$$E(e^{zD_N}) = e^{-zN} \left(\prod_{n=1}^{M} \frac{w_n}{2\pi} \right)^{\frac{1}{2}} \int_{\mathbf{R}^M} \exp\left(-\frac{1}{2} \sum_{n=1}^{M} w_n y_n^2 \right) \left(\sum_{n=1}^{M} w_n e^{g y_n} \right)^N d^M y \quad , \tag{4.3}$$

with $g = \sqrt{2z/N}$. By writing the N-th power as a power of e and substituting $y_n = \phi_n + Ng$, the path integral of Eq.(3.85) is obtained.

For the L_2^*-discrepancy in one dimension, $\mathcal{P}^{-1}\phi = \phi' := \frac{d\phi}{dx}$ with the boundary condition that $\phi(1) = 0$ (Section 3.3.1). The action is therefore given by

$$S[\phi] = \tfrac{1}{2} \langle (\phi')^2 \rangle + \tfrac{1}{2} M \phi(1)^2 - N \log \langle e^{g\widehat{\phi}} \rangle \quad , \tag{4.4}$$

where $M \to \infty$. We show now that there is a naïve continuum limit with this result. We use the fact that the discrepancy can be defined as the naïve continuum limit of

$$D_N^{(M)} = \frac{1}{N} \sum_{\rho=1}^{M} \sigma_\rho^2 \left(\sum_{k=1}^{N} \sum_{n=1}^{M} K_n^\rho \left[\vartheta_n(x_k) - w_n \right] \right)^2 \quad , \tag{4.5}$$

where

$$\vartheta_n = \vartheta_{[\frac{n-1}{M}, \frac{n}{M})} \quad , \quad w_n = \langle \vartheta_n \rangle \quad , \quad K_n^\rho = \theta(n - \rho) \quad , \quad \text{and} \quad \sigma_\rho^2 = \frac{1}{M} \quad . \tag{4.6}$$

$D_N^{(M)}$ is the discretized version of the L_2^*-discrepancy, obtained when in Eq.(3.6) the average over a finite number of points y_n, $n = 1, \ldots, M$ is taken, instead of the average over the whole of

K. Notice that a whole class of 'discrete' discrepancies can be written as Eq.(4.5), by choosing different expressions for the K_n^ρ and the σ_ρ^2. Just like the Lego discrepancy, such a discrepancy can be written in terms of variables S_n that count the number of points x_k in bin n:

$$D_N^{(M)} \;=\; \frac{1}{N}\sum_{n,m=1}^{M} R_{nm}S_nS_m - 2\sum_{n=1}^{M} T_nS_n + NU \quad , \tag{4.7}$$

with

$$R_{nm} = \sum_{\rho=1}^{M} \sigma_\rho^2 K_n^\rho K_m^\rho \quad , \quad T_n = \sum_{m=1}^{M} R_{nm}w_m \quad , \quad \text{and} \quad U = \sum_{n,m=1}^{M} R_{nm}w_nw_m \quad . \tag{4.8}$$

In the case of the L_2^*-type discrepancy, the matrix R is given by $R_{nm} = \min(M-n, M-m)/M$. The generating function is again given as the expectation value under the multinomial distribution. If we assume that the matrix R is invertible and positive definite, as it is for the L_2^*-type discrepancy, use the Gaussian integration rules and the generalized binomial theorem and do the appropriate coordinate transformations, we find

$$G(z) \;=\; \sqrt{\frac{\det R^{-1}}{(2\pi)^M}} \int_{\mathbf{R}^M} \exp\left(-S[\phi]\right) d^M\phi \quad , \tag{4.9}$$

with

$$S[\phi] \;=\; \frac{1}{2}\sum_{n,m=1}^{M} R^{-1}_{nm}\phi_n\phi_m + Ng\sum_{n=1}^{M} w_n\phi_n - N\log\Big(\sum_{n=1}^{M} w_n e^{g\phi_n}\Big) \quad . \tag{4.10}$$

For the L_2^*-type discrepancy the inverse R^{-1} of the matrix R is easy to find and we get

$$\sum_{n,m=1}^{M} R^{-1}_{nm}\phi_n\phi_m \;=\; M\phi_M^2 + M\sum_{n=1}^{M-1}(\phi_{n+1}-\phi_n)^2 \quad , \tag{4.11}$$

so that a naïve continuum limit clearly produces Eq.(4.4).

4.2 Instantons for the Lego discrepancy

We start this section with a repetition of the statement that non-trivial instanton solutions only exist if $z \in [0,\infty)$ (Section 3.2.3). In order to investigate the instantons, we analyze the action in terms of the variables $y_n = g\phi_n + 2z$, that is, we consider the integral $\int_{\mathbf{R}^M} \exp(-N\Sigma[y])\, d^My$, with

$$\Sigma[y] \;=\; z + \frac{1}{4z}\sum w_n y_n^2 - \log\Big(\sum w_n e^{y_n}\Big) \quad . \tag{4.12}$$

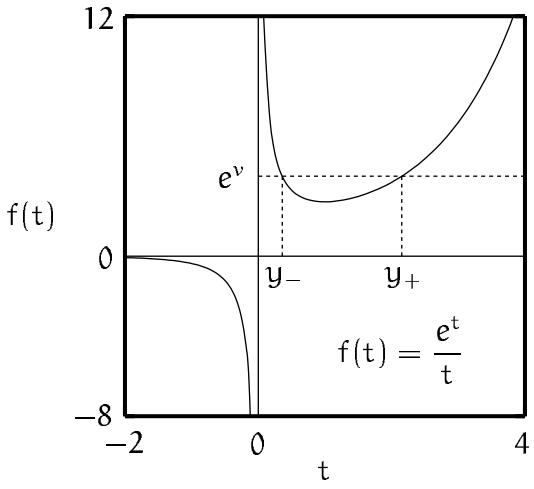

Figure 4.1: y_- and y_+.

The sum is over $n = 1, \ldots, M$. We are interested in the minima of Σ. The 'perturbative' minimum $\phi_n = 0$, $n = 1, \ldots, M$ corresponds to $y_n = 2z$, $n = 1, \ldots, M$, and general extrema of Σ are situated at points y which are solutions of the equations

$$\frac{\partial \Sigma}{\partial y_k}(y) = 0 \quad \Leftrightarrow \quad \frac{e^{y_k}}{y_k} = \frac{1}{2z} \sum w_n e^{y_n} \quad , \quad k = 1, \ldots, M \quad . \tag{4.13}$$

If z is positive, e^{y_k}/y_k, and therefore y_k, has to be positive for every k. The result is that the y_k can take at most two values in one solution y (Fig.4.1). If they all take the same value, this value is $2z$, and we get the perturbative solution. If they take two values, one of them, y_+, is larger that 1 and the other, y_-, is smaller than 1. With these results, and the fact that Eq.(4.13) implies that

$$\sum w_n y_n = 2z \quad , \tag{4.14}$$

we see that there are no solutions but the perturbative one if $2z < w_{\min}$, where $w_{\min} = \min_n w_n$.

In the next section, the other extremal points will be analyzed and it will appear that minima occur with $\Sigma[y] < 0$. This means that, in the limit of $N \to \infty$, the integral of $\exp(-N\Sigma)$ is not defined; there is a 'wall' in the complex z plane along the positive real side of the imaginary axis, to the right of which the generating function is not defined. That this is not an artifact of our approach, can be seen in the expression of the generating function given by Eq. (4.2). It is shown there that the generating function is not defined if $\mathrm{Re}\, z > \frac{w_n}{w_n - 1} \log w_n$ for any one of the w_n.

We know (Section 6.2) that, at the perturbative level, the generating function has a singularity at $z = \frac{1}{2}$, but the instanton contributions cannot correspond with it, because they will appear already for $\mathrm{Re}\, z < \frac{1}{2}$. However, in order to calculate the probability density H with the Laplace transform using the perturbative expression of $G(z)$, we can just calculate the contribution of the singularity at $z = \frac{1}{2}$, for *that is* the contribution to the perturbative expansion of $H(t)$.

4.2.1 The wall

To expose the nature of the extrema of Σ, we have to investigate the eigenvalues λ of the second derivative matrix Δ of Σ in the extremal points. This matrix is given by

$$\Delta_{k,l}(y) \;:=\; \frac{\partial^2\Sigma}{\partial y_k \partial y_l}(y) \;=\; a_k(y)\delta_{k,l} + b_k(y)b_l(y) \quad , \tag{4.15}$$

with

$$a_k(y) = \frac{w_k}{2z}(1-y_k) \quad \text{and} \quad b_k(y) = \frac{w_k y_k}{2z} \quad . \tag{4.16}$$

To show that Σ becomes negative, we only use its minima, and these correspond with extremal points in which all eigenvalues of Δ are positive. According to Appendix 4A, we are therefore only interested in cases where the degeneracy of negative a_k is one, for else $\lambda = a_k$ would be a solution. We further are only interested in cases where there is only one negative a_k, for if there where more, say a_k and a_{k+1} with $a_k < a_{k+1}$, then there would be a solution $a_k < \lambda < a_{k+1} < 0$. So we see that the only extremal points we are interested in have all co-ordinates y_k equal, or have one $y_k = y_+$ and the others equal to y_-. If they are all equal, then they have to be equal to $2z$, and for the extremal point to be a minimum $2z$ has to be smaller than 1. This is the perturbative minimum. Whether the other extremal points are minima depends on whether $\det\Delta$ is positive in these points. The determinant can be written as

$$\det\Delta(t) \;=\; \frac{\prod_n w_n}{(2z)^{M+1}}\,(1-y_-)^{M-1}(y_+-1)\left(\frac{w_+y_+}{y_+-1} + \frac{(1-w_+)y_-}{y_--1}\right) \quad . \tag{4.17}$$

Now we notice that all extremal points can be labeled with a parameter ν by defining

$$\frac{e^{y_\pm(\nu)}}{y_\pm(\nu)} \;=\; e^{\nu} \quad \text{with} \quad \nu \in (1,\infty) \quad . \tag{4.18}$$

We see that $y_\pm$ is a continuous and differentiable function of ν and we have that $dy_\pm/d\nu = y_\pm/(y_\pm - 1)$. This parameterization induces a parameterization of $2z$, and with the help of Eq.(4.14) we see that

$$\frac{d(2z)}{d\nu} \;=\; \frac{w_+y_+}{y_+-1} + \frac{(1-w_+)y_-}{y_--1} \quad . \tag{4.19}$$

So we see that the sign of $\det\Delta$ is the same as the sign of $d(2z)/d\nu$: if an extremal point is a minimum, then $d(2z)/d\nu > 0$. The minimal value that ν can take to represent a solution is 1, which corresponds to $y_+ = y_- = 1$ and $2z = 1$. It is easy to see that $d(2z)/d\nu \to -\infty$ if $\nu \downarrow 1$ and $w_+ < \frac{1}{2}$, where w_+ is the value of the weight belonging to the co-ordinate with the value y_+. This means that if ν starts from $\nu = 1$ and increases, then it will represent solutions with $d(2z)/d\nu < 0$, which are local maxima. We know that, if $\nu \to \infty$, then $y_- \to 0$, $y_+ \to \infty$ and $2z = w_+y_+ + (1-w_+)y_- \to \infty$, so that $d(2z)/d\nu$ has to become larger than 0 at some point. The first point where $2z$ becomes equal to 1 again we call ν_c (Fig.4.2), so

$$z(\nu_c) = z(1) = \tfrac{1}{2} \quad . \tag{4.20}$$

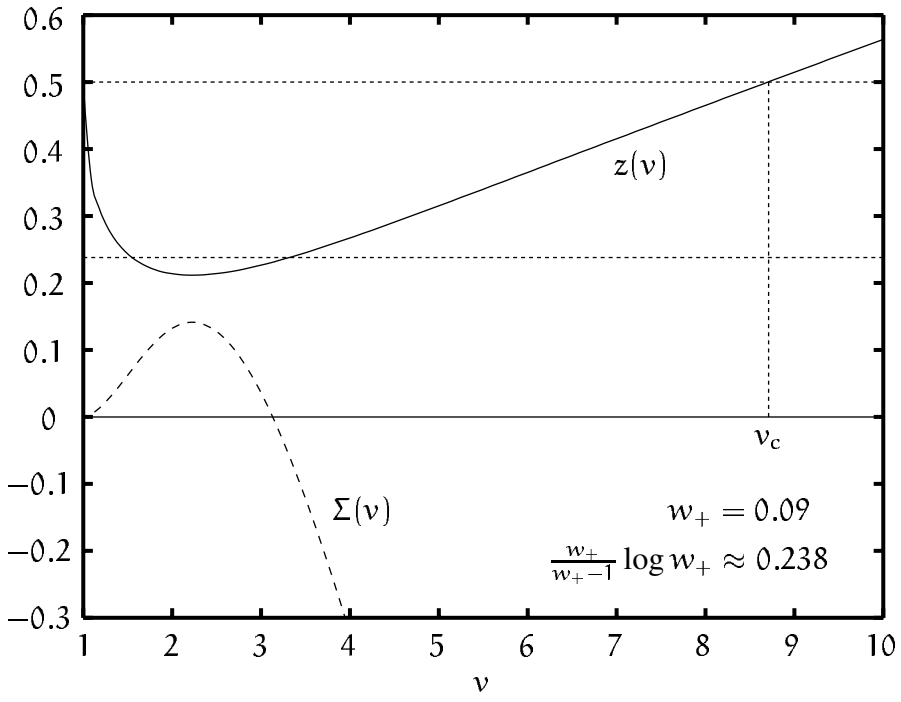

Figure 4.2: Σ and z for instanton solutions parameterized with ν.

Also the function Σ itself can be written in terms of $z(\nu)$ in the extremal points. We use that

$$\frac{d}{d\nu}[w_+ y_+^2 + (1-w_+)y_-^2] \;=\; 4z + 4\frac{dz}{d\nu} \tag{4.21}$$

and that $w_+ y_+^2 + (1-w_+)y_-^2 = 1$ if $\nu = 1$, so that

$$\Sigma(\nu) \;=\; z(\nu) + \frac{1}{z(\nu)}\int_1^\nu z(x)\,dx + 1 - \frac{1}{4z(\nu)} - \nu - \log(\,2z(\nu)\,) \quad . \tag{4.22}$$

Now the problem arises. From the previous analysis of $z(\nu)$ we know that, if $1 \le \nu \le \nu_c$, then $z(\nu) < \frac{1}{2}$ so that

$$\Sigma(\nu_c) \;=\; 1 - \nu_c + 2\int_1^{\nu_c} z(x)\,dx \;<\; 0 \quad . \tag{4.23}$$

Furthermore, we find that

$$\frac{d\Sigma}{d\nu} = \left[1 - \frac{1}{4z^2}\left(w_+ y_+^2 + (1-w_+)y_-^2\right)\right]\frac{dz}{d\nu} = -\frac{w_+(1-w_+)(y_+ - y_-)^2}{4z^2}\,\frac{dz}{d\nu} \quad , \tag{4.24}$$

so that also $d\Sigma/d\nu < 0$ in ν_c. So there clearly is a region in $[1,\nu_c]$ where $dz/d\nu > 0$ and $\Sigma(\nu) < 0$. This means that in the region $\frac{1}{2}w_{\min} < z < \frac{1}{2}$ there are instanton solutions with negative action. The situation is shown in Fig.4.2 for $w_{\min} = 0.09$. A region where $dz/d\nu > 0$ and $S(\nu) < 0$ is clearly visible in $[1,\nu_c]$.

4.3 Instantons for the L_2^*-discrepancy

In order to investigate the instantons for the L_2^*-discrepancy in one dimension, we analyze $\Sigma[\phi] := S[\phi/g]/N$, with S as Eq.(4.4), because this new action does not depend on N:

$$\Sigma[\phi] \;=\; \frac{1}{4z}\langle\,(\phi')^2\,\rangle + \frac{1}{4z}M\phi(1)^2 - \log\langle\,e^{\widehat{\phi}}\,\rangle \;\;, \tag{4.25}$$

where $2z = Ng^2$ and $M \to \infty$. Extremal points of this action are solutions of the field equation

$$-\frac{1}{2z}\,\phi''(x) + 1 - \frac{e^{\phi(x)}}{\langle\,e^{\phi}\,\rangle} \;=\; 0 \tag{4.26}$$

that also satisfy the boundary conditions, which are $\phi(0) = \phi'(1) = 0$ at this point. We proceed however by applying the gauge transformation $\mathcal{T} : \phi \mapsto \phi - \log\langle\,e^{\phi}\,\rangle$, so that $\langle\,e^{\mathcal{T}\phi}\,\rangle = 1$ and, in this gauge, the equation becomes

$$-\frac{1}{2z}\,\phi''(x) + 1 - e^{\phi(x)} \;=\; 0 \;\;, \quad \text{with} \;\; \phi'(1) = 0 \;\; \text{and} \;\; \langle\,e^{\phi}\,\rangle = 1 \;\;. \tag{4.27}$$

Integration over $\mathbf{K}$ of this equation leads to the identity $\phi'(0) = 0$. The problem is now reduced to that of the motion of a classical particle with a mass $1/\sqrt{4z}$ in a potential

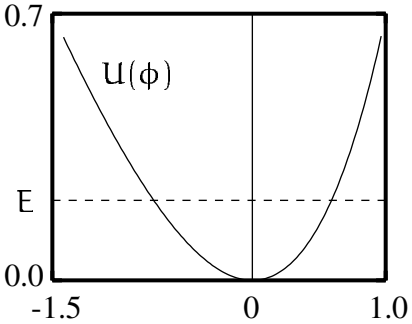

$$U(\phi) \;=\; e^{\phi} - \phi - 1 \;\;, \tag{4.28}$$

and the solution can be written implicitly as

$$\sqrt{4z}\,\frac{dx}{d\phi} \;=\; \frac{1}{\sqrt{E - U(\phi)}} \;\;, \tag{4.29}$$

where the integration constant E, the *energy*, has to be larger than zero for solutions to exist. It is easy to see that the solutions are oscillatory and that, if $\phi(x)$ is a solution with one bending point, then also

$$\phi_k(x) \;=\; \begin{cases} \phi(kx - p) & \frac{p}{k} \le x \le \frac{p+1}{k} \;\; p \text{ even} \\ \phi(1 + p - kx) & \frac{p}{k} \le x \le \frac{p+1}{k} \;\; p \text{ odd} \end{cases} \;\;, \quad p = 0, 1, \ldots, k-1 \;\;, \tag{4.30}$$

is a solution for $k = 2, 3, \ldots$. These new solutions have the same energy, but a larger number of bending points, namely k, and the value of z increases by a factor k^2. Hence, we can classify the solutions according to the energy and the number bending points. This classification in terms of

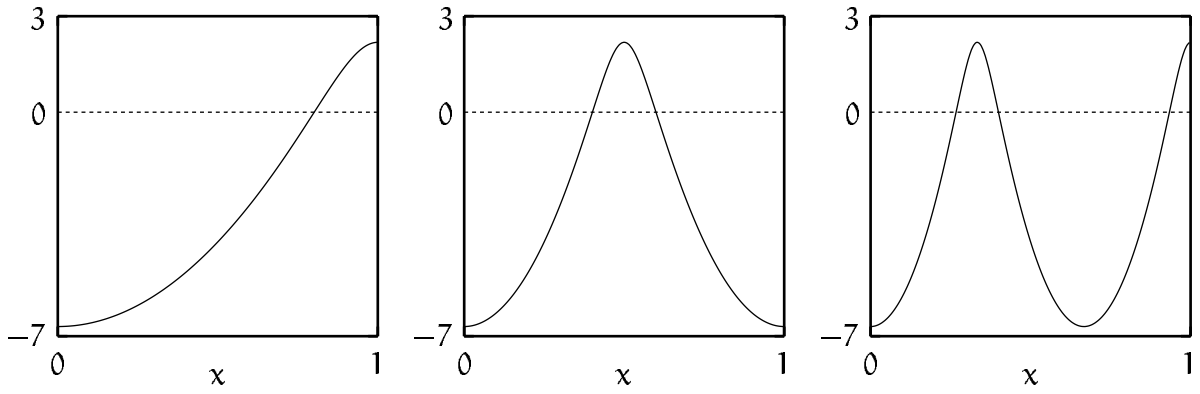

Figure 4.3: Instanton solutions $\phi_k(x)$ with $E = 5.7$ and number of bending points $k = 1, 2, 3$.

the number of bending points is quite natural and this can best be understood by looking at the limit of $N \to \infty$. Then, the equation becomes

$$-\phi''(x) - 2z\widehat{\phi}(x) \;=\; 0 \quad , \tag{4.31}$$

with $\phi(0) = \phi'(1) = 0$, and the solutions are given by

$$\phi_k(x) = \sqrt{\tfrac{2}{3}}\,[1 - \cos(k\pi x)] \quad , \quad 2z = k^2\pi^2 \quad , \quad k = 1, 2, \ldots \quad , \tag{4.32}$$

so that the instantons are completely classified with the number of bending points k. If N becomes finite, these solutions are deformed but keep the same value of k (Fig. 4.3). For given k there are infinitely many solutions classified by E.

4.3.1 Existence of instantons

We now concentrate on the instantons with one bending point, because the numerical value of the action is independent of the number of bending points. Those instantons are completely characterized by their energy. The values of z for which these instantons exist are defined as a function of E by Eq. (4.29), which states that

$$T(E) \;:=\; \sqrt{4z} \;=\; \int_{\phi_-}^{\phi_+} \frac{d\phi}{\sqrt{E - U(\phi)}} \quad , \tag{4.33}$$

where ϕ_- and ϕ_+ are the classical turning points. They are solutions of $U(\phi_\pm) = E$ with $\phi_- < 0 < \phi_+$. In classical mechanics, $T(E)$ is proportional to the period of a particle in the potential U (cf. [13]).

The function T cannot be expressed in terms of elementary functions, but a number of its properties can be derived, as we shall now discuss. For small E, a quadratic approximation of the potential can be made with $\phi_\pm = \pm\sqrt{2E}$ with the result that

$$\lim_{E \downarrow 0} T(E) \;=\; \pi\sqrt{2} \quad \Longrightarrow \quad \lim_{E \downarrow 0} z(E) \;=\; \tfrac{1}{2}\pi^2 \quad . \tag{4.34}$$

The question is now whether z is increasing as a function of E. To calculate $T(E)$ for large E, $U(\phi)$ can be approximated by $-1-\phi$ for $\phi<0$ and by e^{ϕ} for $\phi>0$, so that

$$T(E\to\infty) \;\approx\; 2\sqrt{E+1}+\frac{2}{\sqrt{E}}\log\left(\sqrt{E}+\sqrt{E-1}\right) \quad , \tag{4.35}$$

so $T(E)$ is clearly increasing for large E. To analyze $T(E)$ for small E, we make an expansion in powers of E. Therefore, we write

$$T(E) \;=\; \int_0^{\sqrt{2E}} \left(E-\tfrac{1}{2}v^2\right)^{-1/2} \frac{d}{dv}\left[f(v)-f(-v)\right]\,dv \quad , \tag{4.36}$$

where f is a continuous solution of the implicit equation

$$e^{f(v)}-f(v)-1=\tfrac{1}{2}v^2 \quad , \tag{4.37}$$

with $f(v)\sim v$ for small v. In Section 4.4 it is shown that it is given by the function values on the principal Riemann sheet of the general continuous solution and that is has an expansion $f(v)=\sum_{n=0}^{\infty}\alpha_n v^n$ with the coefficients α_n given by

$$\alpha_1=1 \quad\text{and}\quad \alpha_n=-\frac{1}{n+1}\left[\tfrac{1}{2}(n-1)\alpha_{n-1}+\sum_{k=2}^{n-1}k\alpha_k\alpha_{n+1-k}\right] \quad\text{for}\quad n>1 \quad , \tag{4.38}$$

and with the radius of convergence equal to $\sqrt{4\pi}$. If we substitute the power series into Eq.(4.36) and integrate term by term, we obtain the following power series for $|E|<2\pi$:

$$T(E) \;=\; \sum_{n=1,\ n\,\text{odd}}^{\infty} \frac{\Gamma(\frac{1}{2})\Gamma(\frac{n}{2})}{\Gamma(\frac{n+1}{2})}\,n\alpha_n\,2^{\frac{n}{2}}E^{\frac{n-1}{2}} \quad . \tag{4.39}$$

The first few terms in this expansion are

$$T(E) \;=\; \pi\sqrt{2}\left[1+\frac{E}{12}+\frac{1}{4}\left(\frac{E}{12}\right)^2-\frac{139}{180}\left(\frac{E}{12}\right)^3-\frac{571}{2880}\left(\frac{E}{12}\right)^4+\mathcal{O}(E^5)\right] \quad . \tag{4.40}$$

The asymptotic behavior of the coefficients α_n will be determined in Section 4.4, with the result that, for large and integer k,

$$\alpha_n \;\sim\; \frac{1}{(4\pi)^{\frac{n}{2}}\,n^{\frac{3}{2}}}\times\begin{cases}-2(-)^k & \text{if } n=4k\\ 0 & \text{if } n=4k+1\\ -2(-)^k & \text{if } n=4k+2\\ +2\sqrt{2}(-)^k & \text{if } n=4k+3\end{cases} \tag{4.41}$$

The results are summarized in Fig.4.4. Depicted are the behavior for large E, the expansion for small E and a numerical evaluation of the integral of Eq.(4.33). Notice the strong deviation of the expansion from the other curves for $E>2\pi$, the radius of convergence. For this plot the first 50 terms were used. It appears that T is indeed an increasing function of E.

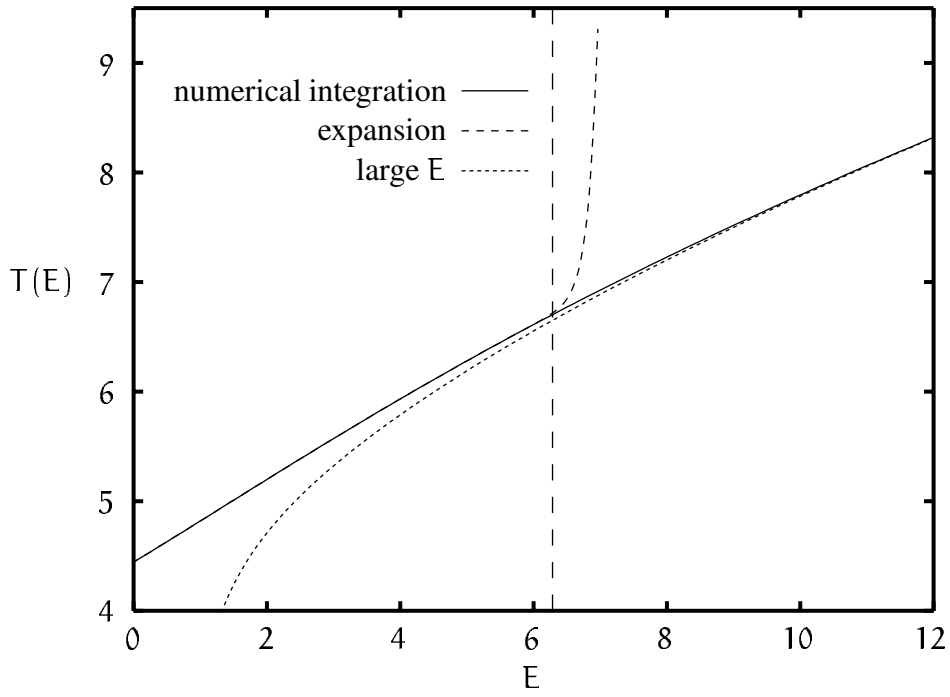

Figure 4.4: $T(E)$ computed by numerical integration, as an expansion around $E = 0$ and as an approximation for large E. The expansion is up to and including $\mathcal{O}(E^{49})$.

4.3.2 The wall

We now turn to the analysis of the value of the action for an instanton. In the foregoing, we have shown for which positive values of z no instantons exist. Now we will show that the action indeed becomes negative for z positive and large enough. For an instanton solution with one bending point, the action is given by

$$S(E) \;=\; \frac{1}{4z(E)} \int_0^1 \phi''(x)\,dx + \int_0^1 \phi(x)\,dx \;=\; E + 2\,\frac{T_1(E)}{T(E)} \quad , \tag{4.42}$$

$$T_1(E) \;=\; \int_{\phi_-}^{\phi_+} \frac{\phi\,d\phi}{\sqrt{E - U(\phi)}} \quad . \tag{4.43}$$

With the use of the same approximations for $U(\phi)$ as in the derivation of Eq.(4.35), it is easy to see that, for large E, $T_1(E)$ is bounded by

$$-\frac{4}{3}(E+1)^{3/2} + \frac{2\log E}{\sqrt{E}} \log\left(\sqrt{E} + \sqrt{E-1}\right) \quad , \tag{4.44}$$

so that $S(E)$ clearly becomes negative for large E.

To investigate the behavior of $S(E)$ for small E, we use an expansion again. It can be obtained using Eq.(4.42) and the relation

$$\frac{dT_1}{dE}(E) \;=\; -\frac{1}{2}\,T(E) - E\,\frac{dT}{dE}(E) \quad . \tag{4.45}$$

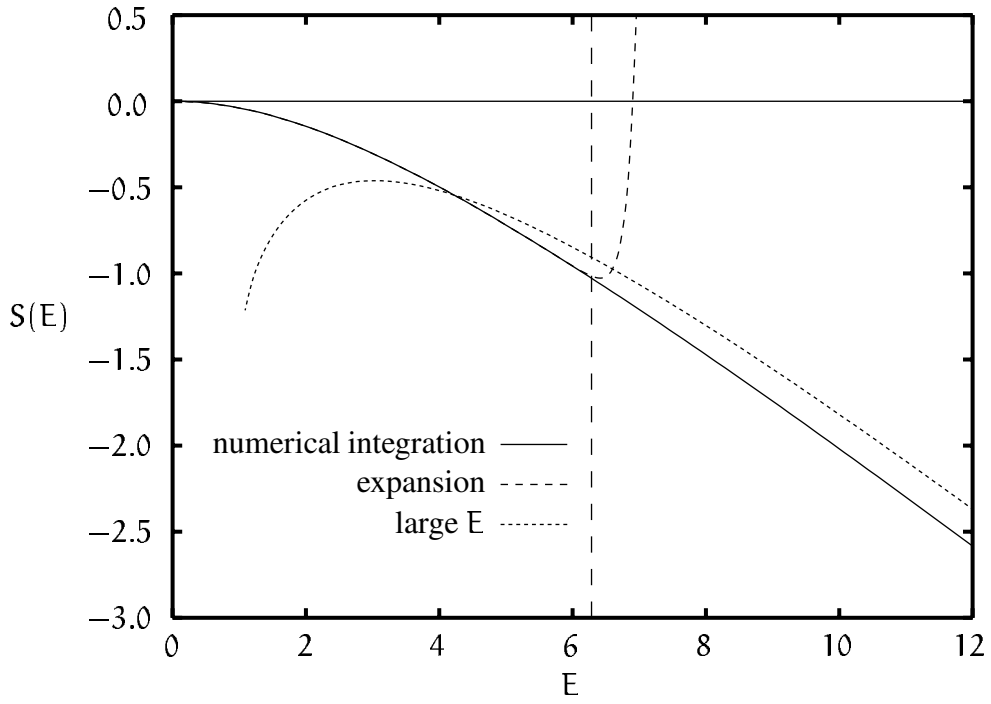

Figure 4.5: $S(E)$ computed by numerical integration and as an expansion around $E = 0$. The expansion is up to and including $\mathcal{O}(E^{48})$ and its radius of convergence is 2π. The curve for large E is the upper bound of Eq.(4.44).

A derivation of this relation is given in Appendix 4B. For $E \downarrow 0$ a quadratic approximation of the potential $U(\phi)$ can be used in Eq.(4.43) and we find that $T_1(0) = 0$, so that the expansion of $T(E)$ can be substituted in Eq.(4.45) and an expansion of $T_1(E)$ can be obtained by integrating term by term. The expansions of $T(E)$ and $T_1(E)$ can then be used to find the expansion of $S(E)$ using Eq.(4.42). The first few terms are

$$T_1(E) = \pi\sqrt{2}\left[-\frac{E}{2} - \frac{E^2}{16} - \frac{5\,E^3}{3456} + \frac{973\,E^4}{2488320} + \mathcal{O}(E^5)\right] \quad , \tag{4.46}$$

$$S(E) = -\frac{E^2}{24} + \frac{E^3}{432} + \frac{89\,E^4}{414720} + \mathcal{O}(E^5) \quad . \tag{4.47}$$

In Fig.4.5, we plot $S(E)$ as obtained from the series expansion, from the asymptotic behavior, and from numerical integration. The conclusion is that $S(E)$ is always negative.

4.4 Computer-aided analysis of Riemann sheet structures

In the previous section, we encountered the problem of finding solutions to the implicit function equation (4.37), or at least series expansions of solutions. It can be classified as a particular case of slightly more general problems one encounters in theoretical physics that are formulated as

follows: consider an entire function $F : \mathbf{C} \mapsto \mathbf{C}$ such that

$$F(y) \sim y^m \quad \text{as } y \to 0 \ , \tag{4.48}$$

with nonnegative integer m (in practice, we have met cases with $m = 1$ and $m = 2$). The task at hand is then to find information about $y : \mathbf{C} \mapsto \mathbf{C}$ such that

$$F(\, y(x)\,) = x^m \ . \tag{4.49}$$

In general, both the form of the series expansion of $y(x)$ around $x = 0$ and the nature of its singularities are of interest. Apart from Section 4.3, such questions arise, for instance, in the combinatorial problem of determining the number of Feynman diagrams contributing to given scattering amplitudes in various quantum field theories [27], in the statistical bootstrap model for hot hadronic matter (refs. in [28]), and in renormalization theory connected with the 't Hooft transformation [29]. An important and interesting example, studied in detail in [28], is the so-called *bootstrap equation*:

$$F_b(y) = 2y + 1 - e^y \ , \tag{4.50}$$

which obviously has $m = 1$. We shall consider functions F of the more general form

$$F(y) = P(y) + Q(y)\, e^y \ , \tag{4.51}$$

where P and Q are polynomials of finite degree $d_P > 0$ and $d_Q \geq 0$, respectively, with real coefficients. As our working example, taken from Section 4.3, we shall consider the function F_w defined as

$$F_w(y) = -2 - 2y + 2e^y \ , \tag{4.52}$$

for which $m = 2$. It is, in fact, closely related to the bootstrap equation (4.50): by substituting, in Eq.(4.50), $y \to \log 2 + y$ and $x \to 2\log 2 - 1 - x^2$, we obtain Eq.(4.52). Its Riemann sheet structure, however, is quite different, as we shall see. We shall concentrate on the analysis of the Riemann sheet structure of those solutions of these equations that have a series expansion around $x = 0$. To determine the asymptotic behavior of these expansions, the nature of the singularities will be analyzed numerically. The results are justified by the fact that, in our calculations, only finite computer accuracy is required, as we shall demonstrate.

4.4.1 Identification of the Riemann sheets

As a first step we identify the various Riemann sheets by their value of $y(0)$: the sheet labeled s will have $y(0) = Y_s$ for that sheet. Obviously, $y(0) = 0$ is a solution with multiplicity m. In general, there will be d_P solutions if $Q(y) = 0$, and infinitely many if Q is non-vanishing. It will be helpful if we can identify the Riemann sheet on which pairs $(x, y(x))$ lie when x is small

s	Y_s/π
1	(0.0000, 0.0000)
3	(0.6649, 2.3751)
5	(0.8480, 4.4178)
7	(0.9633, 6.4374)
9	(1.0478, 8.4490)
11	(1.1145, 10.4567)

Table 4.1: The first few Riemann sheet solutions for $F_w(Y_s) = 0$.

but nonzero. This is indeed possible, and we shall illustrate it using F_w. Let us write $y = \xi + i\eta$ with ξ and η real numbers. We are then looking for solutions of $F_w(\xi + i\eta) = 0$, or

$$\xi = \log\left(\frac{\eta}{\sin\eta}\right) \quad , \tag{4.53}$$

$$0 = 1 + \log\left(\frac{\eta}{\sin\eta}\right) - \frac{\eta}{\tan\eta} \quad . \tag{4.54}$$

Inspecting the left-hand side of the last equation, we can immediately see that its zeroes are quite nicely distributed. We can usefully enumerate them as $\mathrm{Im}(Y_s) = u_s$, where the sheet number s takes only the odd integer values $\pm1, \pm3, \pm5, \ldots$. For positive s, the zero u_s is certainly located in the interval where $\sin u_s > 0$, i.e. $(s-1)\pi \le u_s < s\pi$, and $u_{-s} = -u_s$. We have $u_1 = u_{-1} = 0$, and for increasing s the zero u_s moves upwards in its interval, until asymptotically we have $u_s \sim a_s - (\log a_s)/a_s$ with $a_s = (s - 1/2)\pi$. In Tab. 4.1 we give the values of Y_s for F_w, for the first few values of s. Because the values Y_s fall in disjoint intervals, for small x we need to know $y(x)$ only to a limited accuracy in order to be able to identify its Riemann sheet. The only nontrivial case is that of sheets -1 and 1, where it is sufficient to consider the complex arguments: for $\arg(x) - \arg(y) = 0$ we are on sheet 1, for $|\arg(x) - \arg(y)| = \pi$ we are on sheet -1. Again, limited computer accuracy is acceptable here, and for larger m we simply have m different values of the argument, distinguished in an analogous manner. Note that of course the labeling of the sheets is rather arbitrary: we have chosen the odd integers in order to emphasize that both sheet 1 and -1 can be considered the principal Riemann sheet. For the bootstrap equation (4.50) it is more natural to label the single principal Riemann sheet with $y(0) = 0$ as sheet number zero.

4.4.2 Series expansion

We want to compute $y(x)$ as a Taylor series around $x = 0$:

$$y(x) = \sum_{n\ge0} \alpha_n x^n \quad . \tag{4.55}$$

Obviously, α_0 can be chosen as one of the u_s above. On principal sheets, with $\alpha_0 = 0$, we also have immediately that α_1 must be chosen out of the m possibilities with $\alpha_1^m = 1$. The other

coefficients must then be computed (algebraically or numerically) by some recursive method, which we shall now discuss.

It would be straightforward to plug the expansion (4.55) into Eq.(4.49) and equate the powers of x on both sides, but notice that, for Q non-vanishing, the number of possible products of coefficients grows very rapidly, so that the computer time needed to find the first N coefficients grows exponentially with N. As already mentioned in [28], the better way is to differentiate Eq.(4.49) with respect to x so that we obtain the nonlinear differential equation

$$y'(x)\,[P'(y)Q(y) + (Q(y) + Q'(y))(x^m - P(y))] = mx^{m-1}Q(y) \quad . \tag{4.56}$$

This equation yields a recursion relation involving products of at most $d_P + d_Q + 1$ coefficients, so that a truncated power series can be computed in polynomial time. As an example, for F_w we find the following differential equation:

$$y'(x)(x^2 + 2y(x)) = 2x \quad , \tag{4.57}$$

and the following recursion relation:

$$\begin{aligned} &\alpha_0\alpha_1 = 0 \quad , \quad 2\alpha_0\alpha_2 + \alpha_1^2 - 1 = 0 \quad , \\ &n\alpha_0\alpha_n + (n-2)\alpha_{n-2} + 2\sum_{p=1}^{n-1} p\,\alpha_p\,\alpha_{n-p} = 0 \quad , \quad n \geq 3 \quad . \end{aligned} \tag{4.58}$$

We see immediately that $y(x)$ is necessarily even in x if $\alpha_0 \neq 0$, i.e. on the non-principal Riemann sheets. In that case, we also see that if α_n, $n = 0, 2, \ldots$ is a solution, then also α_n^*, $n = 0, 2, \ldots$ is a solution, where the asterix stands for complex conjugation. This is a result of the fact that if $y(x)$ is a solution of Eq.(4.52), then also $y^*(x^*)$ is a solution. In practice, these solutions give the function values on the different Riemann sheets of one solution. The analysis of the previous section proves that $y_s(0) = y_{-s}(0)^*$ so that the solutions satisfy $y_s^*(x) = y_{-s}(x^*)$ and the expansion coefficients satisfy

$$\alpha_n^{(s)} = (\alpha_n^{(-s)})^* \quad . \tag{4.59}$$

On the principal Riemann sheets we have $\alpha_0 = 0$ and $\alpha_1^2 = 1$ as mentioned, and the two solutions on sheet 1 and sheet -1 are related by $y_{-1}(x) = y_1(-x)$. For $y_1(x)$ we find, finally:

$$\alpha_n = -\frac{1}{2(n+1)}\left[(n-1)\alpha_{n-1} + 2\sum_{p=2}^{n-1} p\,\alpha_p\,\alpha_{n+1-p}\right] \quad , \tag{4.60}$$

for $n \geq 2$. Using this relation we have been able to compute many thousands of terms. The recursion appears to be stable in the forward direction, but we have not tried to prove this or examine the stability in the general case.

In series expansions it is of course always important to know the convergence properties or, equivalently, the asymptotic behavior of α_n as n becomes very large. In the next section, we therefore turn to the singularity structure of $y(x)$.

4.4.3 Singularities and branches

In order to find information about the singularity structure of $y(x)$, we employ the techniques developed in [27], which we recapitulate here. Singularities are situated at those values y_k of y where

$$F'(y_k) = 0 \quad . \tag{4.61}$$

Since F is entire we also know that these singular points must form an enumerable set, i.e. we can find, and label, them as distinct points. We shall assume that these singularities are square-root branch points, for which it is necessary that

$$F''(y_k) \neq 0 \quad , \tag{4.62}$$

If F'' vanishes at y_k but F''' does not, we have a cube-root branch point, and so on. If, for non-vanishing Q, all derivatives vanish (as for instance when $F(y) = e^y$) we have, of course, a logarithmic branch point. We know that $y = -\infty$ corresponds to a logarithmic branch point, and it is to remove this to infinity in the x plane that we have required $d_P > 0$. In our examples all the singularities at finite x will be square-root branch points. The position of the singularity in the x plane, x_k, is of course given by

$$F(y_k) = x_k^m \quad , \tag{4.63}$$

so that there are m different possible positions, lying equally spaced on a circle around the origin. We shall denote them by $x_{k,p}$ with $p = 1, 2, \ldots, m$. Note that, in first instance, it is not clear at all whether $x_{k,p}$ for certain k and p is indeed a singular point on a specific Riemann sheet. Later on, we shall describe how to determine this numerically. For values of x close to an observed singular point $x_{k,p}$ we may expand the left-hand and right-hand side of Eq.(4.49) to obtain

$$\frac{1}{2}(y - y_k)^2 F''(y_k) \sim mF(y_k)\left(\frac{x}{x_{k,p}} - 1\right) \quad , \tag{4.64}$$

where we have dropped the higher derivative terms. Very close to the branch point we may therefore approximate $y(x)$ by

$$y(x) \sim y_k + \beta_{k,p}\left(1 - \frac{x}{x_{k,p}}\right)^{1/2} \quad , \quad \beta_{k,p}^2 := -\frac{2mF(y_k)}{F''(y_k)} \quad . \tag{4.65}$$

Note that there are only two possible values for $\beta_{k,p}$, and each singular point $x_{k,p}$ goes with one or the other of these. Again numerical methods will help in determining which one of the two is the correct choice.

We are now in a position to compute the asymptotic behavior of the coefficients α_n. To find it, we first determine, *for a given Riemann sheet*, which are the $x_{k,p}$ that lie closest to the origin: this gives us the radius of convergence of the expansion of $y(x)$ in that Riemann sheet. We then have to determine those p for which $x_{k,p}$ is actually a singular point. We shall do this

numerically, in the way described in the following section. Let us denote the set of values of p for which this is the case by **P**. Now, we may use the fact that

$$\sqrt{1-x} = 1 - \sum_{n\geq 1} \gamma_n x^n \quad , \quad \gamma_n = \frac{(2n-2)!}{2^{2n-1}(n-1)!n!} \overset{n\to\infty}{\sim} \frac{1}{\sqrt{4\pi}} n^{-3/2} + \mathcal{O}(n^{-5/2}) \ , \quad (4.66)$$

where we have chosen that square root that is real and positive for $1-x$ real and positive. The asymptotic behavior of α_n as $n \to \infty$ must therefore be given by

$$\alpha_n \sim \frac{-1}{n^{3/2}\sqrt{4\pi}} \sum_{p\in\mathbf{P}} \frac{\beta_{k,p}}{x_{k,p}^n} \quad . \quad (4.67)$$

Amongst other things, this provides a powerful numerical check on the accuracy of the α_n as computed by the recursive technique. We shall now discuss how the singularity structure of our problem can be investigated numerically.

4.4.4 Computer searches for sheet structures

The main tool we use for our computer studies is a method for taking small steps over a Riemann sheet, that is, given the fact that for some value x_1 the point $y_1 = y(x_1)$ is determined to belong to a certain Riemann sheet, we perform a small step Δx to a point x_2 and find the point $y_2 = y(x_2)$ on the same Riemann sheet. Our method to do this is nothing but Newton-Raphson iteration: we simply iterate the mapping

$$y \leftarrow y - \frac{F(y) - x_2^m}{F'(y)} \quad , \quad (4.68)$$

until satisfactory convergence is obtained. The starting value for this iteration is just the point y_1. A few remarks are in order here. In the first place, it must be noted that for this method to work, y_1 must be in the basin of attraction of y_2. Since, except at the branch points, which we shall expressly avoid, $y(x)$ is a continuous and differentiable function of x, this can always be arranged by taking Δx small enough. In the second place, the accuracy with which y_1 is actually a solution of Eq.(4.49) is not important as long as it is in the basin of attraction of y_2: therefore, there is no buildup of numerical errors in this method if we restrict ourselves to just keeping track of which Riemann sheet we are on. Finally, problems could arise if two Riemann sheet values of y for the same x are very close. But, since F is an entire function, we know that the solutions of Eq.(4.49) must either completely coincide or be separated by a finite distance, any inadvertent jump from one sheet to another can be detected and cured by, again, taking a small enough Δx.

We have applied the following method for detecting and characterizing the various singular points. We start on a Riemann sheet s_1 at a value x close to zero, and determine $y(x)$ on that Riemann sheet. We then let the parameter x follow a prescribed contour that circles a selected would-be singularity $x_{k,p}$ once (and no other singularities), and then returns to the starting point close to the origin. We then determine to which Riemann sheet the resulting y belongs. In this way we can find whether $x_{k,p}$ is, in fact, a singular point for the starting sheet, and, if so, which

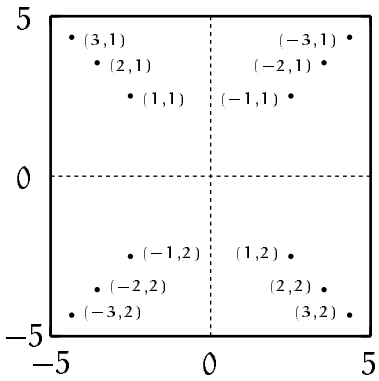

Figure 4.6: The numbering (k, p) of the singularities.

two sheets are connected there. It is also possible, of course, to certify the square-root branch point nature of a singular point by circling twice around it, and checking that one returns to the original Riemann sheet.

One important remark is in order here. In our tracking over the Riemann sheet, it is necessary that we do not cross branch cuts (except of course the one connected to the putative singularity). Since these branch cuts can be moved around in the complex x plane, *the contour chosen defines the (relative) position of the branch cuts*. The sheets that are said to be connected at a particular branch cut are therefore also determined by the choice of contour. Of course, choosing a different contour will change the whole system of interconnected sheets in a consistent manner, so that in fact, given one choice of contour and its system of sheets, we can work out what system of sheets will correspond to another choice of contour. We shall illustrate this in the following.

Suppose, now, that $x_{k,p}$ is one of the singular points on a certain sheet that is closest to the origin. We can then follow, on that sheet, a straight line running from x_1 close to the origin to a point x_2 for which $x_2/x_{k,p}$ is real and just a bit smaller than one. Since $x_{k,p}$ is by assumption closest to the origin, there is then no ambiguity involved in determining which one of the two possible complex arguments of $\beta_{k,p}$ we have to take. Thus, we can find all the information needed to compute the asymptotic behavior of α_n on that sheet.

4.4.5 An example

Having established the necessary machinery, we shall now discuss a concrete example of our method. For this, we have taken the function F_w of Eq.(4.52), which is closely related to the very well-understood bootstrap equation (4.50), as we have shown. Note that the origin $x = 0, y = 0$ for F_w corresponds to the first singularity in F_b.

4.4.5.1 The singularities

The values of $y(0)$ on the different Riemann sheets for F_w, namely Y_s for $s = \pm 1, \pm 3, \ldots$ have already been discussed above. The singular values y_k are simply given by

$$F_w'(y_k) = 2e^{y_k} - 2 = 0 \quad \Rightarrow \quad y_k = 2i\pi k \ , \tag{4.69}$$

so that the possible singular points $x_{k,p}$ satisfy

$$x_{k,p}^2 = -4i\pi k \quad . \tag{4.70}$$

Note that $k = 0$ does not correspond to a singular point. The positions of the possible singularities in the complex x plane are therefore as follows. For positive integer k:

$$\begin{aligned} x_{k,1} = iz_k \quad , \quad x_{k,2} = -iz_k \quad , \\ x_{-k,1} = z_k \quad , \quad x_{-k,2} = -z_k \quad , \qquad z_k = (1+i)\sqrt{2\pi k} \quad . \end{aligned} \tag{4.71}$$

At all these various possible singularities, we have

$$\beta_{k,p}^2 = 8i\pi k \quad , \tag{4.72}$$

and therefore we may write

$$\begin{aligned} \text{for } k > 0: \quad \beta_{k,p} = \epsilon_{k,p}(1+i)\sqrt{4\pi|k|} \quad , \\ \text{for } k < 0: \quad \beta_{k,p} = \epsilon_{k,p}(1-i)\sqrt{4\pi|k|} \quad , \end{aligned} \tag{4.73}$$

where the only number to be determined is $\epsilon_{k,p} \in \{-1, 1\}$. It must be kept in mind that the value of ϵ depends of course on the sheet: we take the convention that we work on the sheet with the lowest number (in absolute value). When viewed from the other sheet, the value of ϵ is simply opposite.

4.4.5.2 The Riemann sheet structure

We now have to discuss how the branch cuts should run in the complex x plane. There are two simple options (and an infinity of more complicated ones): in the first option (I), we choose to let the branch cuts extend away from the origin parallel to the real axis. This corresponds to tracking a contour that, say, first moves in the imaginary direction, and then in the real direction, to arrive close to the chosen singularity. The other option (II) is to take the cuts parallel to the imaginary axis, so that a contour that does not cross branch cuts *en route* first goes in the real direction, and then in the imaginary direction. Note that these two alternatives do, indeed, correspond to different implied relative positionings of the branch cuts.

In Fig.4.7.a we show the contour used in examining singularity $x_{2,1}$ under option I.

The contour starts on sheet number 1 close to the origin (so that y is close to Y_1), moves upwards and then to the left, circles the singularity once anti-clockwise, and returns to its starting point by the same route in order to enable us to determine the resulting Riemann sheet number. Fig.4.7.b shows the corresponding path in the y plane. It ends again close to Y_1 so that, *for this choice of contour and its induced branch structure* (indicated in the figure), sheet 1 does not have a branch point at $x_{2,1}$. Fig. 4.7.c shows what happens if, instead of sheet number 1, we start at sheet number 3: the y track starts then at close to Y_3, but ends up close to Y_5, so that we conclude that sheets 3 and 5 are connected at $x_{2,1}$. If we run through the whole contour twice, we get the y

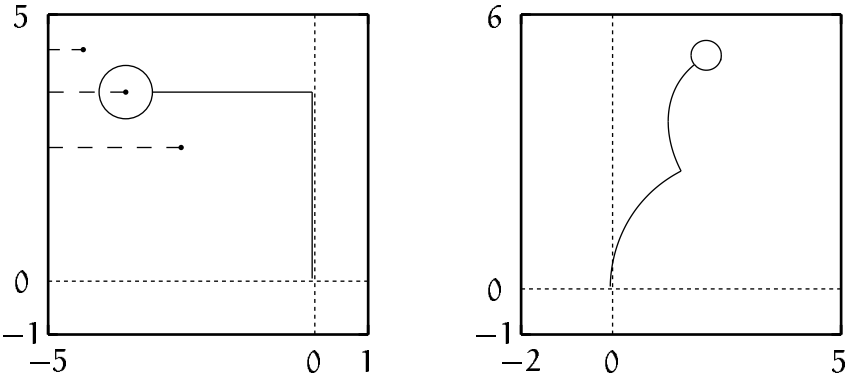

a: the x-plane b: sheet 1, single loop

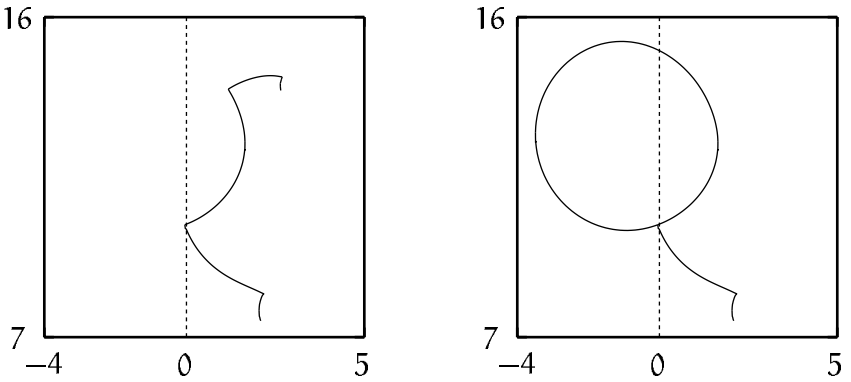

c: sheet 3, single loop d: sheet 3, double loop

Figure 4.7: Loops around $x_{2,1}$ under option I.

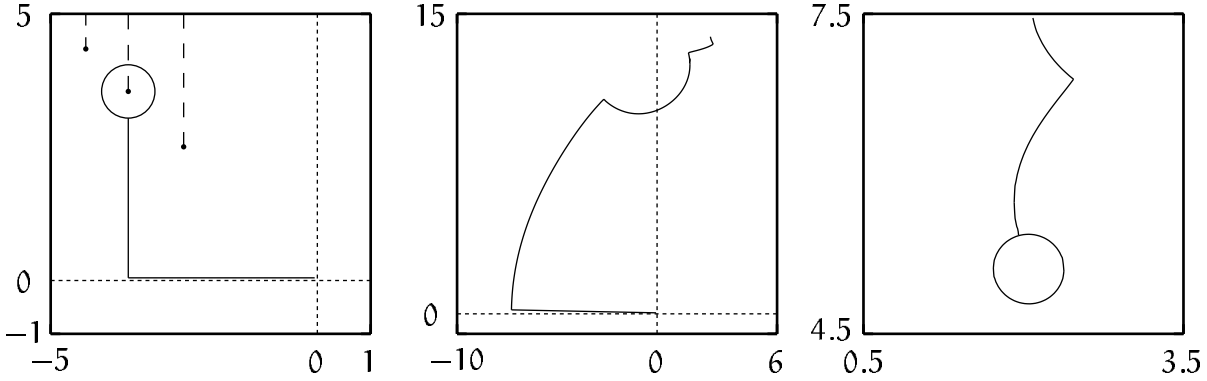

a: the x-plane b: sheet 1, single loop c: sheet 3, single loop

Figure 4.8: Loops around $x_{2,1}$ under option II.

k	$x_{k,1}$	$\epsilon_{k,1}$	$x_{k,2}$	$\epsilon_{k,2}$	$x_{-k,1}$	$\epsilon_{-k,1}$	$x_{-k,2}$	$\epsilon_{-k,2}$
1	(1,3)	-1	(-1,3)	-1	(-1,-3)	-1	(1,-3)	-1
2	(3,5)	-1	(3,5)	-1	(-3,-5)	-1	(-3,-5)	-1
3	(5,7)	-1	(5,7)	-1	(-5,-7)	-1	(-5,-7)	-1
4	(7,9)	-1	(7,9)	-1	(-7,-9)	-1	(-7,-9)	-1
5	(9,11)	-1	(9,11)	-1	(-9,-11)	-1	(-9,-11)	-1

Table 4.2: The first few sheets and singularities (option I), and the corresponding value for ϵ.

k	$x_{k,1}$	$\epsilon_{k,1}$	$x_{k,2}$	$\epsilon_{k,2}$	$x_{-k,1}$	$\epsilon_{-k,1}$	$x_{-k,2}$	$\epsilon_{-k,2}$
1	(1,3)	-1	(-1,3)	-1	(-1,-3)	-1	(1,-3)	-1
2	(1,5)	-1	(-1,5)	-1	(-1,-5)	-1	(1,-5)	-1
3	(1,7)	-1	(-1,7)	-1	(-1,-7)	-1	(1,-7)	-1
4	(1,9)	-1	(-1,9)	-1	(-1,-9)	-1	(1,-9)	-1
5	(1,11)	-1	(-1,11)	-1	(-1,-11)	-1	(1,-11)	-1

Table 4.3: The first few sheets and singularities (option II), and the corresponding value for ϵ.

track presented in Fig. 4.7.d, where the y track ends up again at Y_3 as expected for a square root branch cut.

Under option II, we rather use the contour indicated in Fig. 4.8.a, which first moves to the left and then upwards. Fig. 4.8.b shows the resulting y path, which does not return to Y_1 but rather to Y_5, indicating that under this choice of contour the sheets labeled 1 and 5 are connected at $x_{2,1}$. Fig. 4.8.c shows that, now, sheet 3 is insensitive to this singularity.

In this way we have mapped the various singularities around the origin. In Tab. 4.2 we present the pairs of sheets that are pairwise connected at the first few singularities, under option I, and the observed value for ϵ, which turns out to be -1 in all cases. We point out that at each singularity only two sheets out of all infinitely many are connected. Note the somewhat atypical situation at the lowest-lying singularities $x_{1,\pm1}$ and $x_{-1,\pm1}$. The alternative option II results in Tab. 4.3. Note that the higher-lying singularities now show a sheet structure similar to the lowest ones. In fact, this is the choice that corresponds most directly to the analysis of the sheet structure of the bootstrap equation in [28], with of course the extra complication in the fact that the bootstrap equation (4.50) has $m = 1$ while for F_w, $m = 2$. Note that, once again, $\epsilon = -1$ in all cases.

4.4.5.3 Asymptotic behavior of the series expansion coefficients

We shall now illustrate how the information on the $x_{k,p}$ and $\beta_{k,p}$ allows us to compute the asymptotic behavior of the series expansion coefficients α_n.

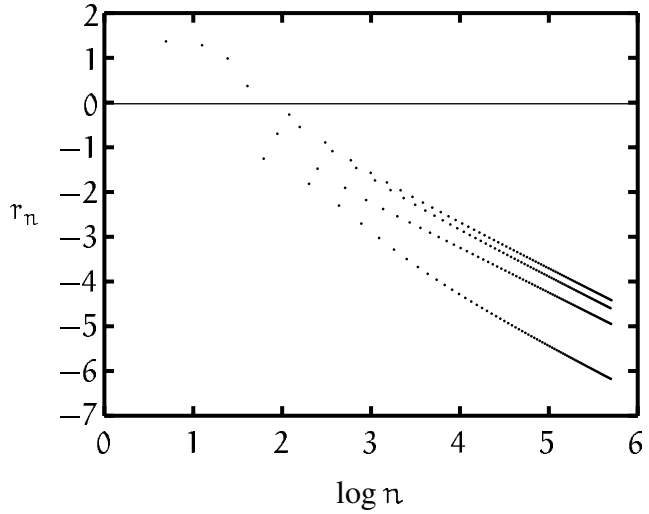

Figure 4.9: r_n, defined in Eq.(4.76), as function of $\log n$.

First Riemann sheet. In this sheet, the singularities closest to the origin, and their corresponding β's are

$$\begin{aligned} x_{1,1} &= \sqrt{4\pi}\exp(3i\pi/4) \quad , \quad \beta_{1,1} = \sqrt{8\pi}\exp(-3i\pi/4) \quad , \\ x_{-1,2} &= \sqrt{4\pi}\exp(-3i\pi/4) \quad , \quad \beta_{-1,2} = \sqrt{8\pi}\exp(3i\pi/4) \quad . \end{aligned} \tag{4.74}$$

Using Eq.(4.67), we see that the asymptotic form of the coefficients on sheet 1 is given by

$$\begin{aligned} &\alpha_n^{(1)} \sim \alpha_n^{\text{asym}} \quad , \\ &\alpha_n^{\text{asym}} = \frac{2}{n^{3/2}(4\pi)^{n/2}}\, c_n \quad , \\ &c_n = -\sqrt{2}\cos\left(\frac{3n\pi}{4} + \frac{3\pi}{4}\right) = \begin{cases} (-)^p & n = 4p \\ 0 & n = 4p+1 \\ (-)^{p+1} & n = 4p+2 \\ (-)^p\sqrt{2} & n = 4p+3 \end{cases} \quad , \end{aligned} \tag{4.75}$$

with integer p. In Fig.4.9 we have plotted the observed behavior of

$$r_n = \log\left(\frac{(4\pi)^{n/2} n^{3/2}}{2}\left|\alpha_n - \alpha_n^{\text{asym}}\right|\right) \tag{4.76}$$

on the first Riemann sheet, against $\log n$. The coefficients clearly converge to the computed behavior, and we can even distinguish that the leading corrections go as $n^{-5/2}$; the four separate lines that emerge are just the four different forms of c_n. The series expansion for Riemann sheet -1 are simply obtained from

$$\alpha_n^{(-1)} = (-)^n \alpha_n^{(1)} \quad . \tag{4.77}$$

Higher Riemann sheets. We first consider positive sheet label $s = 3, 5, 7, \ldots$ and put $k = (s-1)/2$. We then have

$$x_{k,1} = -x_{k,2} = \sqrt{4\pi k}\exp(i\pi/4) \quad , \quad \beta_{k,1} = \beta_{k,2} = (1+i)\sqrt{4\pi k} \ . \tag{4.78}$$

As we have already seen α_n vanishes for odd n, and for even n we have the following asymptotic form:

$$\alpha^{(s)}_{4p} \sim \frac{2(1+i)\sqrt{k}}{(4\pi k)^{2p}}(-)^{p+1} \quad , \quad \alpha^{(s)}_{4p+2} \sim \frac{2(1-i)\sqrt{k}}{(4\pi k)^{2p+1}}(-)^{p} \quad , \tag{4.79}$$

for integer p. For negative s, we use Eq.(4.59), which also holds asymptotically.

4.5 Conclusions

For the L_2^*-discrepancy and the Lego discrepancy, we have addressed the problem that non-trivial extremal points of the the action in the path integral representation of the generating function of quadratic discrepancies, called instantons, might spoil the saddle point approximation around the trivial extremal point. We have shown that instantons appear in both cases, but only if the order parameter z of the generating function G is larger then a certain positive value. In the Lego-case this value is half of the size of the smallest bin, and in the L_2^*-case it is $\frac{1}{2}\pi^2$, the smallest positive value of z at which $G(z)$ in the limit of an infinite number of random points N has a singularity. Although the instantons do not threaten the perturbation expansion, they cause $G(z)$ to be undefined for asymptotically large N when the real part of z is larger then the mentioned values.

For the analyses in the L_2^*-case, a numerical method to investigate the Riemann sheet structure of the solution of certain algebraic complex equations is used, which is treated in Section 4.4. The method is in particular suitable for the determination of the series expansions around the origin on the different sheets and the asymptotic behavior of their coefficients. The results of the numerical analyses have been justified by the fact that only finite computer accuracy was required in the specific calculations.

4.6 Appendices

Appendix 4A: Matrices of the form $A_{n,m} = a_n\delta_{n,m} + \epsilon b_n b_m$

The eigenvalues λ of a real-valued matrix A are given by the zeros of the characteristic polynomial P_A. If A is an $M \times M$ matrix with matrix elements

$$A_{n,m} \;=\; a_n\delta_{nm} + \epsilon\, b_n b_m \;\;,\quad a_n, b_n \in \mathbf{R}\;,\;\; n = 1,\ldots,M \;\;,\quad \epsilon = \pm 1 \;\;, \tag{4.80}$$

then the characteristic polynomial P_A is given by

$$P_A(x) \;=\; Q_A(x)\prod_{n=1}^{M}(a_n - x) \;\;,\quad Q_A(x) \;=\; 1 + \epsilon\sum_{m=1}^{M}\frac{b_m^2}{a_m - x} \;\;, \tag{4.81}$$

which is easily derived using $P_A(x) = \sum_{\pi\in S_M}\prod_{n=1}^{M}[A_{n,\pi(n)} - x\delta_{n,\pi(n)}]$, where the sum is over all permutations of $(1,\ldots,M)$. Without loss of generality, we assume that the coefficients a_n are ordered such that $a_1 \le a_2 \le \cdots \le a_M$. If a number of d_n coefficients a_n take the same value, that is, if a_n is d_n-fold degenerate, then a $(d_n - 1)$-fold degenerate eigenvalue of A is given by $\lambda = a_n$. The remaining eigenvalues are given by the zeros of the function Q_A. Except of the poles at $x = a_n$, $n = 1,\ldots,M$, this function is continuous and differentiable on the whole of $\mathbf{R}$. Furthermore, the sign of the derivative is equal to ϵ. This means that for each zero λ of Q_A except one, there is an n, such that $a_n < \lambda < a_{n+m}$ for the nearest and non-equal neighbor a_{n+m} of a_n. The one other zero is smaller than a_1 if $\epsilon = -1$, and larger than a_M if $\epsilon = 1$. This is easy to see because $\lim_{x\to\infty} Q_A(x) = \lim_{x\to-\infty} Q_A(x) = 1$.

Appendix 4B: Derivation of Eq.(4.45)

We use the definitions of $T(E)$ as the r.h.s. of Eq.(4.33) and $T_1(E)$ as given in Eq.(4.43):

$$T(E) = \int_{\phi_-}^{\phi_+} \frac{d\phi}{\sqrt{E-U(\phi)}}\,, \quad T_1(E) = \int_{\phi_-}^{\phi_+} \frac{\phi\, d\phi}{\sqrt{E-U(\phi)}}\,, \quad U(\phi) = e^{\phi} - \phi - 1\,. \tag{4.82}$$

Because the end points ϕ_+ and ϕ_- depend on E such that $E - U(\phi_\pm) = 0$, we can use Leibnitz's rule for differentiation under the integral sign to write

$$T(E) = 2\frac{d}{dE}\int_{\phi_-}^{\phi_+} \sqrt{E-U(\phi)}\, d\phi \quad . \tag{4.83}$$

Now we write $\sqrt{E-U(\phi)} = (E - e^{\phi} + \phi + 1)(E-U(\phi))^{-1/2}$ and use that $1 - e^{\phi} = dU/d\phi$, so that

$$T(E) = 2\frac{d}{dE}\left(ET(E) + T_1(E) - \int_{\phi_-}^{\phi_+} \frac{1}{\sqrt{E-U(\phi)}}\frac{dU}{d\phi}\, d\phi \right) \quad . \tag{4.84}$$

But the last integral is equal to zero, and as a result, we obtain Eq.(4.45).

Chapter 5

Gaussian limits for discrepancies

This chapter deals with the calculation of the generating function of the probability densities of quadratic discrepancies in the limit of a large number of truly random points. These densities depend on the dimension s of the integration region, or, in the case of the Lego discrepancy, on the number of bins M the integration region is dissected in. We will derive a 'Law of Large Number of Modes', which describes the conditions under which these densities approaches a normal density if s or M become large. Throughout this discussion, we shall only consider the asymptotic limit of a very large number of random points. This implies that, in this chapter, we cannot make any statements on how the number of points has to approach infinity with respect to s or M, as was for instance done in [26].

Contents

5.1 The generating function

We want to calculate the the probability density H of quadratic discrepancies in the limit of $N \to \infty$, where N is the number of points in the point set. We will use the generating function in this limit, that we denote by

$$G_0(z) := \lim_{N\to\infty} E(e^{zD_N}) \quad , \tag{5.1}$$

so that the probability density is given by the inverse Laplace transform of G_0 (Section 2.1.3). It results in the weak limit of H. Starting from Eq.(3.28), it is easy to see that G_0 is given by

$$G_0(z) = \int \exp(z\langle\phi^2\rangle + z\langle\phi\rangle^2) \, d\mu[\phi] \quad . \tag{5.2}$$

In the Landau gauge, the boundary conditions on the functions ϕ that give a contribution are such that $\langle\phi\rangle = 0$ (notice that G_0 contains the same gauge freedom as G). We can apply the formalism of Section 2.2.2, and conclude that $\log G_0(z)$ is equal to the sum of the contributions of all possible connected diagrams consisting only of vertices with two legs. Consequently, they are of the form

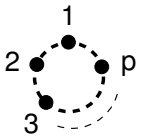

, (5.3)

and carry a symmetry factor equal to $1/2p$, where p is the number of vertices. Every vertex contributes with a factor $2z$, and represents a convolution of reduced two-point functions $\mathcal{B}$, so that

$$\log G_0(z) = \sum_{p=1}^{\infty} \frac{(2z)^p}{2p} R_p \quad , \tag{5.4}$$

with

$$R_p := \int_{\mathbf{K}^p} \mathcal{B}(x_1,x_2)\mathcal{B}(x_2,x_3)\cdots\mathcal{B}(x_{p-1},x_p)\mathcal{B}(x_p,x_1)\, dx_1 dx_2 \cdots dx_{p-1} dx_p \quad . \tag{5.5}$$

The coefficients R_p can be written in terms of the eigenfunctions u_n and the eigenvalues σ_n^2 of the two-point function $\mathcal{C}$ interpreted as an integration kernel (Section 3.2.5). We can use the expression of Eq.(3.57) for $\mathcal{B}$, which tells us that we have to repeatedly calculate the integral

$$\Gamma_{n,m} := \int_{\mathbf{K}} \sigma_n(u_n(x) - \langle u_n\rangle)\sigma_m(u_m(x) - \langle u_m\rangle)\, dx = \sigma_n^2\delta_{n,m} - \sigma_n\langle u_n\rangle\sigma_m\langle u_m\rangle \quad . \tag{5.6}$$

Γ is an infinite dimensional matrix, and the coefficients R_p can be written in terms of Γ through

$$R_p = \mathrm{Tr}(\Gamma^p) \quad , \tag{5.7}$$

where Γ^p denotes the p-fold matrix product, and Tr the trace, i.e., the sum over the diagonal elements. The generating function itself can also be expressed directly in terms of Γ, since

$$\log G_0(z) \;=\; \sum_{p=1}^{\infty} \frac{(2z)^p}{2p}\,\mathrm{Tr}(\Gamma^p) \;=\; \mathrm{Tr}\left(\sum_{p=1}^{\infty} \frac{(2z\Gamma)^p}{2p}\right) \;=\; -\mathrm{Tr}(\,\tfrac{1}{2}\log(1-2z\Gamma)\,)\;, \qquad (5.8)$$

so that

$$G_0(z) = (\,\det(1-2z\Gamma)\,)^{-1/2}\;, \qquad (5.9)$$

where we used the well known rule that, for a general matrix A, $\det(e^A) = e^{\mathrm{Tr}(A)}$. In Appendix 5A, it is shown how G_0 can be written in terms of the strengths σ_n and the weights $\langle u_n\rangle$, with the result that

$$G_0(z) \;=\; \frac{e^{\psi(z)}}{\sqrt{\chi(z)}}\;, \qquad (5.10)$$

where

$$\psi(z) \;=\; -\sum_n \tfrac{1}{2}\log(1-2z\sigma_n^2)\;, \qquad \text{and} \qquad \chi(z) \;=\; 1+\sum_n \frac{\langle u_n\rangle^2}{1-2z\sigma_n^2}\;. \qquad (5.11)$$

Notice that if the basis is in the Landau gauge, then $\langle u_n\rangle = 0$ for all functions and $\chi(z) = 1$, so that the generating function is just given by $\prod_n (1-2z\sigma_n^2)^{-1/2}$. In the Landau gauge, the matrix Γ is diagonal, so that this result follows directly from Eq.(5.9). If the eigenvalues of Γ, in a general gauge, are denoted λ_n, then the generating function is given by $\prod_n (1-2z\lambda_n)^{-1/2}$.

5.1.1 Standardized variables and the Gaussian limit

We have now derived the expression for $G_0(z)$ in the large-N limit. Given the form of Γ, we can now compute $H(t)$ for given discrepancy t, if only numerically; in fact this was done for the L_2^*-discrepancy in [22] for several dimensionalities. In some special cases, $H(t)$ can even be given as an analytic expression [23, 24]. Here, however, we are interested in possible Gaussian limits, and therefore it is useful use the standardized variable instead of the discrepancy itself (Section 2.1.2). Notice that the expectation value and the variance of the discrepancy are just given by

$$E(D_N) = R_1 \qquad \text{and} \qquad V(D_N) \overset{N\to\infty}{\longrightarrow} 2R_2\;. \qquad (5.12)$$

The generating function $\hat{G}$ of the standardized variable is given by

$$\hat{G}_0(z) \;=\; \exp\left(\tfrac{1}{2}z^2 + \sum_{p=3}^{\infty} \frac{(\sqrt{2}\,z)^p}{2p}\,\sqrt{\gamma_p}\right)\;, \qquad \text{with} \qquad \gamma_p := \frac{R_p^2}{R_2^p}\;. \qquad (5.13)$$

All information on the particulars of the discrepancy are now contained in the constants γ_p, and we have that *the standardized probability density approaches the normal density whenever* $\gamma_p \to 0$ *for all* $p \geq 3$. It remains to examine under what circumstances this can happen.

5.1.2 A Law of Large Number of Modes

Since we know that $G_0(z)$ has no singularities for negative values of $\mathrm{Re}\, z$, the eigenvalues of Γ are also nonnegative, and we may write

$$\mathrm{Tr}(\Gamma^k) \;=\; \sum_n \lambda_n^k \quad , \quad \gamma_k \;=\; \left(\sum_n \lambda_n^k\right)^2 \left(\sum_n \lambda_n^2\right)^{-k} \quad , \quad \lambda_n \geq 0 \;\; , \tag{5.14}$$

where the various eigenvalues have been denoted by λ_n. Note that the sum may run over a finite or an infinite number of eigenvalues, but all these sums must converge since $\mathsf{E}(D_N)$ is finite. Note, moreover, that γ_k is homogeneous of degree zero in the λ_n: therefore, any scaling of the eigenvalues by a constant does not influence the possible Gaussian limit (although it will, of course, affect the mean and variance of D_N).

We now proceed by noting that $\gamma_{k+1} \leq \gamma_k$, because

$$\left(\sum_n \lambda_n^{k+1}\right)^2 \;\leq\; \left(\sum_n \lambda_n^{2k}\right)\left(\sum_n \lambda_n^2\right) \;\leq\; \left(\sum_n \lambda_n^k\right)^2 \left(\sum_n \lambda_n^2\right) \quad , \tag{5.15}$$

where the first inequality is simply the Schwarz inequality, and the second one holds because the λ_n are nonnegative. This means that γ_k will approach zero for $k > 3$, whenever γ_3 approaches zero. To see when this happens we define

$$\rho_n \;:=\; \frac{\lambda_n}{\sqrt{\sum_m \lambda_m^2}} \qquad \text{and} \qquad \rho_s := \sup_n \rho_n \quad , \tag{5.16}$$

so that $\sum_n \rho_n^2 = 1$. It is then trivial to see that

$$\rho_s^3 \;\leq\; \gamma_3^{1/2} \;\leq\; \rho_s \quad , \tag{5.17}$$

from which we derive that *the necessary and sufficient condition for the discrepancy distribution, in the limit of an infinite number of points in the point set, to approach a Gaussian is that*

$$\frac{\lambda_s^2}{\sum_n \lambda_n^2} \;\to\; 0 \quad , \quad \lambda_s := \sup_n \lambda_n \quad . \tag{5.18}$$

The Gaussian limit is thus seen to be equivalent to the statement that even the largest eigenvalue becomes unimportant.

Clearly, a necessary condition for this is that the total number of non-vanishing eigenvalues (number of *modes*) approaches infinity. Incidentally, the condition (5.18) also implies that

$$\lambda_s \;\to\; 0 \;\; , \qquad \sum_n \lambda_n^2 \;\to\; 0 \;\; , \tag{5.19}$$

for all those discrepancies that have $\mathsf{E}(D_N) = \sum_n \lambda_n = 1$. This is eminently reasonable, since a distribution centered around 1 and (by construction) vanishing for negative argument can only

approach a normal distribution if its variance approaches zero. On the other hand, the condition $\lambda_s \to 0$ is by itself *not* sufficient, as proven by a counterexample given in Appendix 5B.

Another piece of insight can be obtained if we allow the eigenvalues to take on random values. We may introduce the rather dizzying concept of *an ensemble of different definitions of discrepancy,* each characterized by its set of eigenvalues (all nonnegative) $\vec{\lambda} = \{\lambda_1, \lambda_2, \ldots, \lambda_M\}$, with the usual constraint that they add up to 1; we keep M finite for simplicity. A natural probability measure on this ensemble is given by the probability density $P_\lambda(\vec{\lambda})$ of the random vector λ:

$$P_\lambda(\vec{\lambda}) \;:=\; \Gamma(M)\,\delta\left(\sum_{n=1}^{M}\lambda_n - 1\right) \quad . \tag{5.20}$$

Here Γ denotes Euler's gamma-function and δ stands for the Dirac delta-distribution. It is easily computed that the expectation and variance of $R_k = \sum_n \lambda_n^k$ are given, for large M, by

$$E(R_k) \sim \frac{k!}{M^{k-1}} \quad , \quad V(R_k) \sim \frac{(2k)! - (1+k^2)(k!)^2}{M^{2k-1}} \quad , \tag{5.21}$$

so that the R_k become sharply peaked around their expectation for large M. In that case, we have

$$\gamma_3 \;\sim\; \frac{9}{2M} \quad , \tag{5.22}$$

and we see that, in the above sense, almost all discrepancies have a Gaussian distribution in the limit where M, the number of modes, approaches infinity.

5.2 Applications to different examples

5.2.1 Fastest approach to a Gaussian limit

We now examine the various definitions of discrepancies, and assert their approach to a Gaussian limit. Usually this is envisaged, for instance in [26], as the limit where the dimensionality of the integration region becomes very large. But, as we have shown, this is only a special case of the more general situation where the number of relevant modes becomes very large: another possible case is that where, in one dimension, the number of modes with essentially equal strength σ_n becomes very large. As an illustration, consider the case where the basis functions with the Gaussian measure are orthonormal and M of the nontrivial modes have equal strength $\sigma_n^2 = 1/M$, and the rest have strength zero. The moment-generating function then takes on a particularly simple form, and so does the discrepancy distribution [24]:

$$\log G_0(z) \;=\; -\frac{M}{2}\log\left(1 - \frac{2z}{M}\right) \quad , \quad H(t) \;=\; \frac{(M/2)^{M/2}}{\Gamma(M/2)}\,t^{M/2-1}e^{-tM/2} \quad . \tag{5.23}$$

It is easily seen that the gamma-distribution $H(t)$ approaches a normal one when M becomes very large. At the same time, we see the 'physical' reason behind this: it is the fact that the

singularity of $G_0(z)$ in the complex plane (in the more general case, the singularity nearest to $z = 0$) moves away to infinity. One observation is relevant here: in the inverse Laplace transform, to go from G_0 to H, we have kept the integration along the imaginary axis $\mathrm{Re}\, z = 0$. We might consider performing a saddle-point integration, with a non-vanishing value of $\mathrm{Re}\, z$. That may give us, for a finite number of modes, a good approximation to the actual form of $H(t)$. It is quite possible, and, indeed, it happens in the above equal-strength model, that this approximation is already quite similar to a Gaussian. In the equal-strength model, a saddle-point approximation for $H(t)$ gives precisely the form of Eq. (5.23), the only difference being that $\Gamma(M/2)$ is replaced by its Stirling approximation. On the other hand, for not-so-large M, this form is not too well approximated by a Gaussian centered around $t = 1$, since the true maximum resides at $t = 1 - 2/M$. Nevertheless, in this chapter we are only interested in the limiting behavior of $H(t)$, and we shall stick to the use of condition (5.18) as an indicator of the Gaussian limit.

One interesting remaining observation is the following. For any finite number M of eigenvalues λ_n ($n = 1, 2, \ldots, M$), the *smallest* value of the indicator $\lambda_s^2 / \sum_n \lambda_n^2$ is obtained when $\lambda_n = 1/M$ for all n. In this sense, the equal-strengths model gives, for finite M, that discrepancy distribution that is closest to a Gaussian.

5.2.2 The L_2^*-discrepancy

Here we shall discuss the standard L_2^*-discrepancy (Section 3.3.1). The eigenfunctions $u_{\vec{n}}$ are equal to $2^{s/2} \prod_{\nu=1}^{s} \cos\left((n_\nu + \frac{1}{2})\pi x^\nu\right)$ so that $\langle u_{\vec{n}} \rangle = 2^{s/2} \sigma_{\vec{n}}$ where the strengths, and the matrix Γ, are given by

$$\Gamma_{\vec{m},\vec{n}} \;=\; \sigma_{\vec{m}}^2 \delta_{\vec{m},\vec{n}} - 2^s \sigma_{\vec{m}}^2 \sigma_{\vec{n}}^2 \;, \qquad \sigma_{\vec{n}}^2 \;=\; \left(\frac{4}{\pi^2}\right)^s \prod_{\nu=1}^{s} \frac{1}{(2n_\nu + 1)^2} \;. \tag{5.24}$$

The components n_ν of the integer vector $\vec{n}$ can take all non-negative integer values, including zero. The eigenvalue equation for the eigenvalues λ of Γ can be written down easily:

$$\prod_{\vec{n}} (\sigma_{\vec{n}}^2 - \lambda) \left[1 - 2^s \sum_{\vec{m}} \frac{\sigma_{\vec{m}}^4}{\sigma_{\vec{m}}^2 - \lambda} \right] \;=\; 0 \;. \tag{5.25}$$

The strengths $\sigma_{\vec{n}}$ are degenerate in the values they take. Labeling the strengths with different values by σ_p with $p = \prod_{\nu=1}^{s} (2n_\nu + 1)$, the degeneracy is given by

$$Q_w(p) \;:=\; \sum_{\vec{n} \geq 0} \theta\left(p = \prod_{\nu=1}^{s} (2n_\nu + 1) \right) \;. \tag{5.26}$$

We introduced the logical step function here, which is simply defined by

$$\theta(\Pi) \;:=\; \begin{cases} 1 & \text{if } \Pi \text{ is true} \;, \\ 0 & \text{if } \Pi \text{ is false} \;. \end{cases} \tag{5.27}$$

So $\lambda = \sigma_p^2$ is a solution to the eigenvalue equation with a $(Q_w(p) - 1)$-fold degeneracy. If we factorize these solutions we obtain the following equation for the remaining eigenvalues:

$$1 - 2^s \sum_p Q_w(p) \frac{\sigma_p^4}{\sigma_p^2 - \lambda} = 0 \ . \tag{5.28}$$

Some assertions concerning the remaining eigenvalues can be made using this equation. On inspection, it can be seen that there are no negative solutions, nor solutions larger than σ_1^2, so that σ_1^2 can be used as an upper bound of the eigenvalues of Γ. If we order the λ such that $\lambda_1 \geq \lambda_3 \geq \ldots$, then $\sigma_1^2 \geq \lambda_1 \geq \sigma_3^2 \geq \lambda_3 \geq \ldots$. This implies that $\mathrm{Tr}(\Gamma^k) = \sum_p Q_w(p)\, \sigma_p^{2k} - \epsilon$ where $0 \leq \epsilon \leq \sigma_1^{2k}$. Now we have

$$\sum_p Q_w(p)\, \sigma_p^{2k} = \left(\frac{4}{\pi^2}\right)^{ks} \xi(2k)^s \quad , \quad \xi(p) = \sum_{n \geq 0} \frac{1}{(2n+1)^p} \ , \tag{5.29}$$

and therefore, for $k \geq 3$, that

$$\gamma_k \leq \left(\frac{\xi(2k)^2}{\xi(4)^k}\right)^s \left(1 - 2\left(\frac{4}{5}\right)^s + \left(\frac{2}{3}\right)^s\right)^{-k} \ . \tag{5.30}$$

The second factor decreases monotonically from $(15)^k$ for $s = 1$ to one as $s \to \infty$; for the first factor, we note that $1 < \xi(2k) < \xi(4)$ for all $k > 2$. Therefore γ_k can be made arbitrarily small by choosing s large enough, and the Gaussian limit of high dimensionality is proven. Note, however, that the approach is not particularly fast: for large s, we have $\gamma_3 \sim (24/25)^s \sim \exp(-s/25)$, so that s has to become of the order of one hundred or so to make the Gaussian behavior manifest. In fact, this was already noted by explicit numerical computation in [22].

5.2.3 The Fourier diaphony

In the case of the Fourier diaphony (Section 3.3.3), the eigenfunctions are in the Landau gauge by definition, so that the matrix Γ is just given by

$$\Gamma_{\vec{m},\vec{n}} = \sigma_{\vec{n}}^2 \delta_{\vec{m},\vec{n}} \ , \tag{5.31}$$

with the strengths $\sigma_{\vec{n}}$ as in Eq.(3.74). The normalization of the strengths ensures that $E(D_N) = 1$, independent of s. In this case, keeping in mind that sines and cosines occur in the eigenfunctions with equal strength, we have to consider the multiplicity function

$$Q_F^{\Pi}(p) := \sum_{\vec{n} \geq 0} \theta\left(p = \prod_\nu r(k_\nu(\vec{n}))\right) \ , \tag{5.32}$$

Actually, before assigning a strength $\sigma_{\vec{n}}$, or rather σ_p^2, we have to know the behavior of $Q_F^{\Pi}(p)$ in order to ensure convergence of $E(D_N)$. In order to do so, we introduce the Dirichlet generating function for $Q_F^{\Pi}(p)$:

$$F_s^{[1]}(x) := \sum_{p>0} \frac{Q_F^{\Pi}(p)}{p^x} = (1 + 2\zeta(x))^s \ , \tag{5.33}$$

where we use the Riemann ζ function. Since this function (and, therefore, $F_s^{[1]}(x)$ as well), converges for all $x > 1$, we are ensured that $Q_F^{\Pi}(p)$ exceeds the value $cp^{1+\epsilon}$ at most for a finite number of values of p, for all positive c and ϵ. This is proven in Appendix 5C. It is therefore sufficient that σ_p^2 decreases as a power (larger than 1) of p. In fact, taking

$$\sigma_p^2 \;=\; cp^{-\beta} \quad , \quad \beta \;>\; 1 \;\; , \tag{5.34}$$

we immediately have that

$$R_k \;=\; \sum_{\vec{n}>0} \sigma_{\vec{n}}^{2k} \;=\; \sum_{p>0} Q_F^{\Pi}(p)\sigma_p^{2k} - \sigma_1^{2k} \;=\; c^k\left[(1+2\zeta(k\beta))^s - 1\right] \;\; , \tag{5.35}$$

which, for given β, fixes c such that $R_1 = E(D_N) = 1$, and, moreover, gives

$$\gamma_3 \sim a(\beta)^s \quad \text{as} \quad s \to \infty \quad , \quad a(\beta) \;=\; \frac{(1+2\zeta(3\beta))^2}{(1+2\zeta(2\beta))^{-3}} \;\; . \tag{5.36}$$

In Section 3.3.3, the value $\beta = 2$ is used, with $a(2) \sim 0.291$. The supremum of $a(\beta)$ equals $1/3$, as $\beta \to \infty$, and the (more interesting) infimum is $a(1)$, about 0.147. We conclude that, for all diaphonies of the above type, the Gaussian limit appears for high dimensionality. For large β, where the higher modes are greatly suppressed, the convergence is slowest, in accordance with the observation that the 'equal-strength' model gives the fastest convergence; however, the convergence is still much faster than for the L_2^*-discrepancy, and the Gaussian approximation is already quite good for $s \sim 4$. The *fastest* approach to the Gaussian limit occurs when we force all modes to have as equal a strength as is possible within the constraints on the β. The difference between the supremum and infimum of $a(\beta)$ is, however, not much more than a factor of 2.

Another possibility would be to let σ_p^2 depend exponentially on p. In that way one can ensure convergence of the R_k while at the same time enhancing as many low-frequency modes as possible. It is proven in Appendix 5C that the function

$$F_s^{[2]}(x) \;:=\; \sum_{p>0} Q_F^{\Pi}(p)\, x^p \tag{5.37}$$

has radius of convergence equal to one, and therefore we may take $\sigma_p^2 = (\beta')^p$ with β' between zero and one. If we choose β' to be very small, we essentially keep only the modes with $p = 1$, and therefore in that case we have $\gamma_3 \sim 1/(3^s - 1)$. This is of course in reality the same type of discrepancy as the above one, with $\beta \to \infty$. On the other hand, taking $\beta' \to 1$ we arrive at $\gamma_3 \to 0$ (see, again, Appendix 5C). The difference with the first model is, then, that we can approach the Gaussian limit arbitrarily fast, at the price, of course, of having a function $\mathcal{B}(x_k, x_l)$ that is indistinguishable from a Dirac δ-distribution in $x_k - x_l$, and hence meaningless for practical purposes.

5.2.3.1 Fourier diaphony with sum clustering

In the above, we have let the strength $\sigma_{\vec{n}}$ depend on the *product* of the various $r(n_\nu)$. This can be seen as mainly a matter of expediency, since the generalization to $s > 1$ is quite simple

in that case. From a more 'physical' point of view, however, this grouping of the σ is not so attractive, if we keep in mind that each $\vec{n}$ corresponds to a mode with wave vector $\vec{k}(\vec{n})$. Under the product rule, wave vectors differing only in their direction but with equal length may acquire vastly different weights: for instance, $\vec{k} = (m\sqrt{s}, 0, 0, \dots)$ and $\vec{k} = (m, m, m, \dots)$ have equal Euclidean length, $m\sqrt{s}$, but their strengths under the product rule are $1/(sm^2)$ and $1/(m^{2s})$, respectively. This lack of 'rotational' symmetry could be viewed as a drawback in a discrepancy distinguished by its nice 'translational' symmetry. One may attempt to soften this problem by grouping the strengths $\sigma_{\vec{n}}$ in another way, for instance by taking

$$\sigma_{\vec{n}} \;=\; \sigma\left(\sum_{\nu} k(n_\nu)\right) \quad , \tag{5.38}$$

so that σ depends on the sum of the components rather than on their product. The multiplicity of a given strength now becomes, in fact, somewhat simpler:

$$Q_F^{\Sigma}(p) \;:=\; \sum_{\vec{n}>0} \theta\left(p = \sum_{\nu=1}^{s} k(n_\nu)\right) \;=\; \sum_{m\geq 0} \binom{s}{m}\binom{s-1+p-m}{p-m} \quad , \tag{5.39}$$

where the last identity follows from the generating function

$$F_s^{[3]}(x) \;:=\; \sum_{p\geq 0} Q_F^{\Sigma}(p)\, x^p \;=\; \left(\frac{1+x}{1-x}\right)^s \quad . \tag{5.40}$$

This also immediately suggests the most natural form for the strength: $\sigma_{\vec{n}}^2 = \beta^p$, where p is $\sum_\nu k(n_\nu)$ as above. We see that R_1 converges as long as $\beta < 1$, and moreover,

$$\gamma_3 \;=\; \frac{\left[\left(\frac{1+\beta^3}{1-\beta^3}\right)^s - 1\right]^2}{\left[\left(\frac{1+\beta^2}{1-\beta^2}\right)^s - 1\right]^3} \;\sim\; a(\beta)^s \quad , \tag{5.41}$$

where $a(\beta)$ has supremum $a(0) = 1$, and decreases monotonically with increasing β. For β close to one, we have $a(\beta) \sim 4(1-\beta)/9$, so that the Gaussian limit can be reached as quickly as desired (again with the reservations mentioned above). At the other extreme, note that for very small β we shall have

$$\gamma_3 \;\sim\; \frac{1}{2s} \quad \text{if} \quad s\beta^2 \ll 1 \quad . \tag{5.42}$$

This just reflects the fact that, for extremely small β, only the $2s$ lowest nontrivial modes contribute to the discrepancy; and even in that case the Gaussian limit is attained, although much more slowly. The criterion that determines whether the behavior of γ_3 with s and β is exponential or of type $1/(2s)$ is seen to be whether $s\beta^2$ is considered to be large or small, respectively.

Another alternative might be a power-law-like behavior of the strengths, such as $\sigma_p^2 = 1/p^\alpha$. Also in this case we may compute the R_k, as follows:

$$R_k \;=\; \sum_{p>0} Q_F^{\Sigma}(p)\,\frac{1}{p^{k\alpha}} \;=\; \frac{1}{\Gamma(k\alpha)}\int_0^\infty z^{k\alpha-1}\left(F_s^{[3]}(e^{-z}) - 1\right)\,dz \quad , \tag{5.43}$$

from which it follows that $\alpha > s$ to ensure convergence of $\mathsf{E}(D_N)$. In the large-s limit, we therefore find that, also in this case, $\gamma_3 \to 1/(2s)$.

5.2.3.2 Fourier diaphony with spherical clustering

A clustering choice which is, at least in principle, even more attractive from the symmetry point of view than sum clustering, is to let $\sigma_{\vec{n}}$ depend on $|\vec{k}(\vec{n})|^2$, hence assuring the maximum possible amount of rotational invariance under the constraint of translational invariance. We therefore consider the choice

$$\sigma_{\vec{n}}^2 \;=\; \exp\left(-\alpha \sum_{\nu} k(n_\nu)^2\right) \quad . \tag{5.44}$$

For the function $\mathcal{B}(x_1, x_2) = \mathcal{B}(x_1 - x_2)$ we now have the following two alternative forms, related by Poisson summation:

$$\begin{aligned} \mathcal{B}(x) \;&=\; -1 + \prod_{\nu=1}^{s} \left(\sum_{k=-\infty}^{+\infty} e^{-\alpha k^2} \cos(2\pi k x^\nu) \right) \\ &=\; -1 + \left(\frac{\pi}{\alpha}\right)^{s/2} \sum_{\vec{m}} \exp\left(-\frac{\pi^2(\vec{x}+\vec{m})^2}{\alpha}\right) \quad , \end{aligned} \tag{5.45}$$

of which the first converges well for large, and the second for small, values of α; the sum over $\vec{m}$ extends over the whole integer lattice. The R_k are, similarly, given by

$$\begin{aligned} R_k \;&=\; \left(\sum_{q=-\infty}^{+\infty} e^{-k\alpha q^2} \right)^s - 1 \\ &=\; \left(\frac{\pi}{k\alpha}\right)^{s/2} \left(\sum_{m=-\infty}^{+\infty} e^{-\pi^2 m^2/k\alpha} \right)^s - 1 \quad . \end{aligned} \tag{5.46}$$

For large α (where, again, only the first few modes really contribute) we recover, again, the limit $\gamma_3 \to 1/(2s)$ as $s \to \infty$: for small α we have, again, an exponential approach to the Gaussian limit:

$$\gamma_3 \sim \left(\frac{8\alpha}{9\pi}\right)^{s/2} \qquad \text{as} \quad s \to \infty \quad . \tag{5.47}$$

The distinction between the two limiting behaviors is now the magnitude of the quantity $se^{-2\alpha}$, which now takes over the rôle of the $s\beta^2$ of the previous paragraph.

5.2.4 The Walsh diaphony

Another type of diaphony is based on Walsh functions, which are defined as follows. Let, in one dimension, the real number x be given by the decomposition

$$x \;=\; 2^{-1}x_1 + 2^{-2}x_2 + 2^{-3}x_3 + \cdots \quad , \quad x_i \in \{0,1\} \quad , \tag{5.48}$$

and let the nonnegative integer n be given by the decomposition

$$n \;=\; n_1 + 2n_2 + 2^2 n_3 + 2^3 n_4 + \cdots \quad , \quad n_i \in \{0,1\} \;\; . \tag{5.49}$$

Then, the n^{th} Walsh function $W_n(x)$ is defined as

$$W_n(x) \;:=\; (-1)^{(n_1 x_1 + n_2 x_2 + n_3 x_3 + \cdots)} \;\; . \tag{5.50}$$

The extension to the multidimensional case is of course straightforward, and it is easily seen that the Walsh functions form an orthonormal set. The Walsh diaphony is then given by

$$D_N \;=\; \frac{1}{N} \sum_{\vec{n}>0} \sigma_{\vec{n}}^2 \left| \sum_{k=1}^{N} W_{\vec{n}}(x_k) \right|^2 \;\; . \tag{5.51}$$

In [20], the following choice is made:

$$\begin{aligned} \sigma_{\vec{n}}^2 \;&:=\; \frac{1}{3^s - 1} \prod_{\nu=1}^{s} \frac{1}{r(n_\nu)^2} \;\; , \\ r(n) \;&:=\; \theta(n=0) + \theta(n>0) \sum_{p \geq 0} 2^p \, \theta\left(2^p \leq n < 2^{p+1}\right) \;\; . \end{aligned} \tag{5.52}$$

Note that, in contrast to the Fourier case where each mode of frequency n contains two basis functions (one sine and one cosine), the natural requirement of 'translational invariance' in this case requires that the Walsh functions from 2^p up to 2^{p+1} get equal strength. The clusterings are therefore quite different from the Fourier case. We slightly generalize the notions of [26], and write

$$\begin{aligned} \sigma_{\vec{n}}^2 \;&=\; \prod_{\nu=1}^{s} \frac{1}{r(n_\nu)^2} \;\; , \\ r(n) \;&=\; \theta(n=0) + \theta(n>0) \sum_{p \geq 0} (\alpha \beta^p)^{-1/2} \, \theta\left(2^p \leq n < 2^{p+1}\right) \;\; . \end{aligned} \tag{5.53}$$

Here, we have disregarded the overall normalization of the σ's since it does not influence the Gaussian limit. It is an easy matter to compute the R_k; we find

$$R_k \;=\; \sum_{\vec{n}>0} \sigma_{\vec{n}}^{2k} \;=\; \left(1 + \frac{\alpha^k}{1 - 2\beta^k}\right)^s - 1 \;\; , \tag{5.54}$$

so that the requirement $E(D_N) = R_1 < \infty$ implies that we must have $\beta < 1/2$. Therefore, for not too small values of α, we have

$$\gamma_3 \;\sim\; a(\alpha,\beta)^s \quad , \quad a(\alpha,\beta) \;=\; \frac{(1 + \alpha^3/(1-2\beta^3))^2}{(1 + \alpha^2/(1-2\beta^2))^3} \;\; . \tag{5.55}$$

The choice made in [20] corresponds to $\alpha = 1$ and $\beta = 1/4$, for which we find $a(1,1/4) \sim 0.4197$. The Gaussian limit should, therefore, be a good approximation for s larger than 6 or so.

An interesting observation is that for fixed β, $a(\alpha,\beta)$ attains a minimum at $\alpha = (1-2\beta^3)/(1-2\beta^2)$, so that the choice $\beta = 1/4$ could in principle lead to $a(31/28, 1/4) = 0.4165$ with a marginally faster approach to the Gaussian. The overall infimum is seen to be $a(3/2, 1/2) = 2/11 \sim 0.182$. As in the Fourier case with product clustering and a power-law strength, there is a limit on the speed with which the Gaussian is approached: in both cases this is directly related to the type of clustering.

At the other extreme, for very small α we find the limiting behavior

$$\gamma_3 \;\sim\; \frac{(1-2\beta^2)^3}{(1-2\beta^3)^2}\,\frac{1}{s} \quad \text{if} \quad s\alpha^2 \ll 1 \;\; . \tag{5.56}$$

Again in this case, the slowest possible approach to the Gaussian limit is like $1/s$, directly related to the symmetry of the discrepancy definition with respect to the various coordinate axes.

5.2.5 The Lego discrepancy

In the case of the Lego discrepancy (Section 3.3.4), the matrix $\Gamma_{m,n}$ has indices that label the bins $\mathbf{A}_n$ ($n = 1, 2, \ldots M$) the hypercube is dissected into, where M is the total number of bins. Because the characteristic functions of the bins are not normalized, the matrix looks a bit different:

$$\Gamma_{m,n} \;=\; \sigma_m \sigma_n \left(w_m \delta_{m,n} - w_m w_n\right) \;\; , \tag{5.57}$$

where $w_n := \langle \vartheta_n \rangle$ is the volume of bin $\mathbf{A}_n$. This matrix satisfies $\mathrm{Tr}(\Gamma^p) = R_p$ for all $p > 0$. We shall now examine under what circumstances the criterion (5.18) for the appearance of the Gaussian limit is fulfilled. The eigenvalues λ_i of the matrix $\Gamma_{m,n}$ are given as the roots of the eigenvalue equation

$$\left(\prod_{m=1}^{M} (\lambda_i - \sigma_m^2 w_m)\right)\left(\sum_{n=1}^{M} \frac{w_n \lambda_i}{\lambda_i - \sigma_n^2 w_n}\right) \;=\; 0 \;\; . \tag{5.58}$$

It is seen that there is always one zero eigenvalue (the corresponding eigenvector has $1/\sigma_m$ for its m^{th} component). Furthermore the eigenvalues are bounded by $\max_m(\sigma_m^2 w_m)$, and this bound is an eigenvalue if there is more than one m for which the maximum is attained. At any rate, we have for our criterion, that

$$\rho_s \;:=\; \frac{\lambda_s^2}{\sum_i \lambda_i^2} \;\le\; \frac{\max_m(\sigma_m^2 w_m)^2}{\mathrm{Tr}(\Gamma^2)} \;=\; \frac{\max_m(\sigma_m^2 w_m)^2}{\sum_m \sigma_m^4 w_m^2 (1-2w_m) + (\sum_m \sigma_m^2 w_m)^2} \;\; . \tag{5.59}$$

Since the generality of the Lego discrepancy allows us to choose from a multitude of possibilities for the σ's and w's, we now concentrate on a few special cases.

1. *All w_m equal.* This models integrands whose local details are not resolved within areas smaller than $1/M$, but whose magnitude may fluctuate. In that case, we have

$$\rho_s \;<\; \frac{1}{1-2/M}\,\frac{(\max_m \sigma_m)^4}{\sum_n \sigma_n^4} \;\; , \tag{5.60}$$

and a sufficient condition for the Gaussian limit is for this bound to approach zero. Note that here, as in the general case, only bins m with $\sigma_m \neq 0$ contribute to the discrepancy as well as to the criterion ρ_s, so that one has to be careful with models in which the integrand is fixed at zero in a large part of the integration region: this type of model was, for instance, examined in [21].

2. *All σ_m equal.* In this case, the underlying integrands have more or less bounded magnitude, but show finer detail in some places (with small w) than in other places (with larger w). Now, it is simple to prove that

$$\rho_s \leq \frac{M\bar{w}^2}{1 - 2\bar{w} + 1/M} \quad , \quad \bar{w} := \max_m w_m \quad , \tag{5.61}$$

so that a sufficient condition is that $M\bar{w}^2$ should approach zero.

3. *All $\sigma_m^2 w_m$ equal.* In this case, the discrepancy is the χ^2-statistic for the data points distributed over the bins with expected fraction of points w_n. We simply have

$$\rho_s = \frac{1}{(M+2)(M-1)} \quad , \tag{5.62}$$

and the Gaussian limit follows whenever $M \to \infty$.

5.3 Conclusions

We derived the probability distribution, in the limit of a large number of points, over the ensemble of truly random point-sets of quadratic discrepancies. We have shown under what conditions this distribution tends to a Gaussian. In particular, the question of the limiting behavior of a given distribution can be reduced to solving an eigenvalue problem. Using the knowledge of the eigenvalues for a given function class it is possible to determine under which conditions and how fast the Gaussian limit is approached. Finally, we have investigated the limiting behavior of the probability distribution for the discrepancy of several function classes explicitly.

The discrepancy that fastest approaches the Gaussian limit is obtained for the model in which the number of modes with non-zero equal strength goes to infinity, while the sum of the strengths is fixed. In fact, we give an argument why we cannot improve much on this limit. However, a drawback of this model is that the discrepancy itself becomes a sum of Dirac δ-distributions in this limit: it only measures whether points coalesce, and is therefore not very useful in practice.

Secondly we looked at the L_2^*-discrepancy. Here a Gaussian distribution appears in the limit of a large number of dimensions. It is however a very slow limit: only when the number of dimensions becomes of the order $\mathcal{O}\left(10^2\right)$ does the Gaussian behavior become manifest.

For the different diaphonies the choice of the mode-strengths is more arbitrary. The strengths we discuss are chosen on the basis of some preferred global properties of the diaphony, such as translation- and/or rotation-invariance. Again for large dimensions the Gaussian limit is attained, either as a power-law or inverse of the number of dimension. It is possible to choose the

strengths in such a way that the Gaussian limit is approached arbitrarily fast. But the diaphony corresponding to that case again consists of a sum of Dirac δ-distributions.

Finally, for the Lego-discrepancy, we can assign strengths to the different modes in several ways. One example is to keep the product of the squared strength and volume of the modes fixed, then the Gaussian limit is reached for a large number of modes.

All these results have been derived in the limit of large number of points. It remains to be seen however whether this is reasonable in practice. To determine when the asymptotic regime sets in, i.e. for which value of N, it is necessary to take into account the next-to-leading contributions, which will be calculated in the following chapter.

5.4 Appendices

Appendix 5A: The form of $G_0(z)$

In this Appendix, we derive the result (5.10) for the form of $G_0(z)$. We introduce the notation $[BA^kB] := \sum_{m,n} B_m (A^k)_{m,n} B_n$ for matrices A and vectors B, and the general form of the matrix Γ:

$$\Gamma_{m,n} = A_{m,n} - B_m B_n \quad . \tag{5.63}$$

The k^{th} power of this matrix has the general form

$$(\Gamma^k)_{m,n} = (A^k)_{m,n} - \sum_{p,q,\nu_{0,1,2,\ldots}\geq 0} \frac{(\sum_{r\geq 0}\nu_r)!}{\nu_0!\nu_1!\nu_2!\cdots} (A^p B)_m (BA^q)_n \prod_{r\geq 0} (-[BA^r B])^{\nu_r} \quad , \tag{5.64}$$

with the constraint $k-1 = p+q+\nu_0+2\nu_1+3\nu_2+\cdots$. The combinatorial factor follows directly from the possible positionings of the dyadic factors $-B_m B_n$. Multiplying by $(2t)^{k-1}$ and summing over the k then gives us immediately

$$\mathrm{Tr}\left(\frac{\Gamma}{1-2t\Gamma}\right) = \sum_{k\geq 1} (2t)^{k-1} \mathrm{Tr}(A^k) - \frac{\sum_{r\geq 0}(r+1)(2t)^r [BA^r B]}{1+\sum_{n\geq 1}(2t)^n [BA^{n-1}B]} \quad , \tag{5.65}$$

where the factor with $r+1$ comes from the double sum over p and q with $p+q=r$. Upon integration of this result over t from 0 to z we find

$$\begin{aligned} \log G_0(z) &= \sum_{n>0} \frac{(2z)^n}{2n} \mathrm{Tr}(\Gamma^n) \\ &= \sum_{n>0} \frac{(2z)^n}{2n} \mathrm{Tr}(A^n) - \frac{1}{2}\log\left(1+\sum_{n>0}(2z)^n [BA^{n-1}B]\right) \quad . \end{aligned} \tag{5.66}$$

If we now take $A_{m,n} = \sigma_n^2 \delta_{m,n}$ and $B_n = \sigma_n \langle u_n \rangle$, we obtain (5.10) with (5.11). This result has, in fact, already been obtained for the case of the L_2^*-discrepancy in [22], but here we demonstrate

its general validity for more general discrepancy measures. In those cases where $B_m = 0$, the second term vanishes of course.

Appendix 5B: A counterexample

In this Appendix we prove that the condition (5.18) for the occurrence of a Gaussian limit is, in a sense, the best possible. Namely, consider a set of eigenvalues λ_n, again adding up to unity as usual, defined as follows: let λ be a positive number, and take

$$\lambda_1 = \lambda \quad , \quad \lambda_n = \begin{cases} (1-\lambda)/(M-1) & \text{for } n = 2, 3, \ldots, M \ , \\ 0 & \text{for } n > M \ . \end{cases} \tag{5.67}$$

Clearly, λ will indeed be the maximal eigenvalue as long as $M > 1/\lambda$. Now,

$$\frac{\lambda^2}{\sum_n \lambda_n^2} = \frac{\lambda^2}{\lambda^2 + (1-\lambda)^2/(M-1)} \ , \tag{5.68}$$

and this ratio can be driven as close to unity as desired by choosing M sufficiently large. This shows that the simple condition $\lambda \to 0$ is not always enough to ensure the Gaussian limit.

Appendix 5C: The magnitude of $Q_F^{\Pi}(p)$

Here we present the proofs of our various statements about the multiplicity function $Q_F^{\Pi}(p)$ of Eq. (5.37). In the first place, we know that its Dirichlet generating function, $F^{[1]}(x)$, converges for all $x > 1$. Now suppose that $Q_F^{\Pi}(p)$ exceeded cp^{α} an infinite number of times, with $c > 0$ and $\alpha > 1$. The Dirichlet generating function would then contain an infinite number of terms all larger than c, for $1 < x < \alpha$, and therefore would diverge, in contradiction with its convergence for all $x > 1$.

In the second place, consider the 'standard' generating function, $F_s^{[2]}(x)$. By inspecting how many of the vector components n_ν of $\vec{n}$ are zero, we see that we may write, for $p > 1$,

$$Q_F^{\Pi}(p) = \sum_{t=1}^{s} \binom{s}{t} 2^t d_t(p) \quad , \quad d_t(p) := \sum_{\vec{n} \geq 0} \theta\left(p = \prod_{\nu=1}^{t} n_\nu \right) \ , \tag{5.69}$$

so that $d_t(p)$ counts in how many ways the integer p can be written as a product of t factors, including ones; this function is discussed, for instance, in [14]. Now, for p prime, we have $d_t(p) = t$, and therefore

$$Q_F^{\Pi}(p) \geq 2s(3^{s-1}) \quad , \quad \text{equality for } p \text{ prime.} \tag{5.70}$$

The radius of convergence of $F_s^{[2]}(x)$ is therefore *at most* equal to unity. On the other hand, we can obtain a very crude, but sufficient, upper bound on $Q_F^{\Pi}(p)$ as follows. Since $d_t(p)$ is a nondecreasing function of t, we may bound $Q_F^{\Pi}(p)$ by $(3^s - 1)d_s(p)$. Now let k_p be the number of prime factors in p; then k_p cannot exceed $\log(p)/\log(2)$, and only is equal to this when p is

a pure power of 2. Also, the number of ways to distribute k object in s groups (which may be empty) is at most s^k, and is smaller if some of the objects are equal. Therefore, $d_s(p)$ is at most s^{k_p}, and we see that

$$Q_F^{\prod}(p) \;<\; (3^s - 1)p^{\log(s)/\log(2)} \quad , \tag{5.71}$$

or, in short, is bounded[1] by a polynomial in p. Therefore, the radius of convergence of $F_s^{[2]}(x)$ is also *at least* unity, and we have proven the assertion in Section 5.2.3.

Finally, we consider the limit

$$\lim_{\beta' \to 1} \gamma_3 \;=\; \lim_{x \to 1} \frac{\left(F_s^{[2]}(x^3)\right)^2}{\left(F_s^{[2]}(x^2)\right)^3} \quad . \tag{5.72}$$

The same reasoning that led us to the radius of convergence shows that, for x approaching 1 from below, the function $F_s^{[2]}(x)$ behaves as $(1-x)^{-c}$, with $c \geq 1$. Therefore, γ_3 will behave as $(8(1-x)/9)^c$, and approach zero as $x \to 1$. Note that the upper bound on $Q_F^{\prod}(p)$ is extremely loose: but it is enough.

[1] Note that equality cannot occur in this case since the two requirements are mutually exclusive.

Chapter 6

Finite-sample corrections to discrepancy distributions

This chapter deals with the calculation of the $1/N$-corrections to the asymptotic probability distributions of quadratic discrepancies in the limit of an infinite number of random points N. In Section 6.1, the explicit diagrammatic expansion of the logarithm of the generating function up to and including $\mathcal{O}(1/N^2)$ will be given. For the Lego discrepancy, the L_2^*-discrepancy in one dimension and the Fourier diaphony in one dimension, the explicit $1/N$-correction is calculated.

In Chapter 5, criteria were given for the asymptotic probability distribution of several quadratic discrepancies to become Gaussian when a certain free parameter becomes infinitely large. This parameter often is the dimension s of the integration region. In the case of the Lego discrepancy, it is the number of bins M. In [26], it is shown that for the *Fourier diaphony* a Gaussian limit is obtained when both N and s go to infinity such that $c^s/N \to 0$, where c is some constant larger than 1. This theorem clearly gives more information about the behavior of the probability distribution, for it relates s and N, whereas in Chapter 5 the limit of $N \to \infty$ is assumed before considering the behavior with respect to s or M. However, the techniques of this chapter to calculate $1/N$-corrections to the asymptotic distributions *give* the opportunity to relate s or M with N. In Section 6.2, this leads to limits for the Lego discrepancy, which is equivalent with a χ^2-statistic for N data points distributed over M bins, if M as well as N become infinite. In Section 6.3, a Gaussian limit is derived for the Fourier diaphony, which is stronger than the one in [26] in the sense that it provides convergence of the moments of the distribution, whereas the limit in [26] is weak.

Contents

6.1 The first few orders

The Feynman diagrams that contribute to the first few orders in the $1/N$-expansion of the generating function $G(z)$ of the probability distribution of quadratic discrepancies are determined, and are used in a few examples.

6.1.1 The diagrammatic expansion

To calculate a term in the $1/N$-expansion of G, the contribution of all diagrams that can be drawn using the Feynman rules, as given in Section 3.2.4, and carry the right power of $1/N$ has to be included. We want to stress again that we only need to calculate the connected diagrams without external lines. The sum of the contributions of all these diagrams gives

$$W(z) := \log G(z) = W_0(z) + \frac{1}{N} W_1(z) + \frac{1}{N^2} W_2(z) + \cdots \quad . \tag{6.1}$$

Usually, a Feynman diagram is a mnemonic representing a certain contribution to a term in a series expansion, i.e. a label. We will use the same drawing for the contribution itself, apart of the symmetry factor of the diagram. For example, the contribution of the diagram  is equal to $\frac{1}{2} N g^2 \int_K \mathcal{B}(x,x)\,dx$ and its symmetry factor is equal to $\frac{1}{2}$, so that we write

$$\frac{1}{2} \quad = \quad \frac{N g^2}{2} \int_K \mathcal{B}(x,x)\,dx \quad . \tag{6.2}$$

6.1.1.1 The zeroth order

The contribution to the zeroth order in $1/N$ can only come from diagrams in which the power of $1/N$ coming from the vertices cancels the power of N, coming from the fermion loops. This only happens in diagrams with vertices with two bosonic legs only, and in which the fermion lines begin and end on the same vertex. To write down their contribution, we introduce the two-point functions $\mathcal{B}_p$, $p = 1, 2, \ldots$, defined by

$$\mathcal{B}_1(x_1, x_2) := \mathcal{B}(x_1, x_2) \quad , \quad \mathcal{B}_{p+1}(x_1, x_2) := \int_{\mathbf{K}} \mathcal{B}_p(x_1, y,)\mathcal{B}(y, x_2)\, dy \quad . \tag{6.3}$$

The zeroth order term $W_0(z)$ is given by

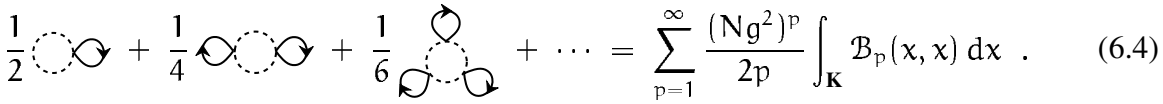

$$= \sum_{p=1}^{\infty} \frac{(Ng^2)^p}{2p} \int_{\mathbf{K}} \mathcal{B}_p(x, x)\, dx \quad . \tag{6.4}$$

The factor $1/2p$ is the symmetry factor of this type of diagram with p fermion "leaves". If we substitute $g = \sqrt{2z/N}$ in this expression, we find exactly the result of Eq.(5.4).

6.1.1.2 The first order

As we have seen before, bosonic two-point vertices with a closed single fermion line contribute with a factor $2z$, and without any dependence on N. Therefore, it is useful to introduce the following effective vertex

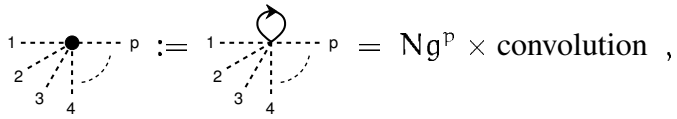

$$= Ng^p \times \text{convolution} \quad , \tag{6.5}$$

and the following *dressed* boson propagator

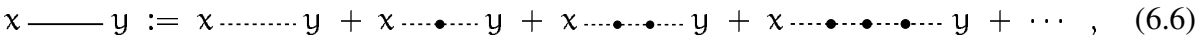

$$\mathcal{G}_z(x, y) := \sum_{p=1}^{\infty} (2z)^{p-1} \mathcal{B}_p(x, y) \quad . \tag{6.7}$$

In terms of the basis in the Landau gauge, it is given by

$$\mathcal{G}_z(x, y) = \sum_{n} \frac{\sigma_{L,n}^2}{1 - 2z\sigma_{L,n}^2} u_n^{(L)}(x) u_n^{(L)}(y) \quad , \tag{6.8}$$

which is, apart of a factor $2z$, the same expression as in Eq. (67) in [23]. Notice that $\mathcal{G}_z$ and $\mathcal{B}$ satisfy the relation

$$\lim_{z \to 0} \mathcal{G}_z(x, y) = \mathcal{G}_{z=0}(x, y) = \mathcal{B}(x, y) \quad \forall x, y, \in \mathbf{K} \quad . \tag{6.9}$$

Furthermore, notice that $\mathcal{G}_z$ and W_0 satisfy

$$\frac{\partial}{\partial z} W_0(z) \;=\; \int_{\mathbf{K}} \mathcal{G}_z(x,x)\,dx \quad , \tag{6.10}$$

and that this relation determines W_0 uniquely, because we know that $W_0(0)$ has to be equal to 0 in order for the asymptotic probability distribution to be normalized to 1.

The first order term in the expansion of $W(z)$ is

$$\frac{1}{N} W_1(z) \;=\; \frac{1}{8} + \frac{1}{8} + \frac{1}{4} + \frac{1}{8} + \frac{1}{12} \quad , \tag{6.11}$$

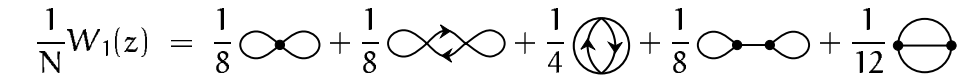

or, more explicitly,

$$\begin{aligned} W_1(z) \;=\; & \frac{z^2}{2}\int_{\mathbf{K}} \mathcal{G}_z(x,x)^2\,dx \;-\; \frac{z^2}{2}\left(\int_{\mathbf{K}} \mathcal{G}_z(x,x)\,dx\right)^2 \;-\; z^2\int_{\mathbf{K}^2} \mathcal{G}_z(x,y)^2\,dxdy \\ & + z^3\int_{\mathbf{K}^2} \mathcal{G}_z(x,x)\mathcal{G}_z(x,y)\mathcal{G}_z(y,y)\,dxdy \;+\; \frac{2z^3}{3}\int_{\mathbf{K}^2} \mathcal{G}_z(x,y)^3\,dxdy \quad . \end{aligned} \tag{6.12}$$

6.1.1.3 The second order

The second order term in the expansion of $W(z)$ is denoted $\frac{1}{N^2}W_2(z)$ and is given by

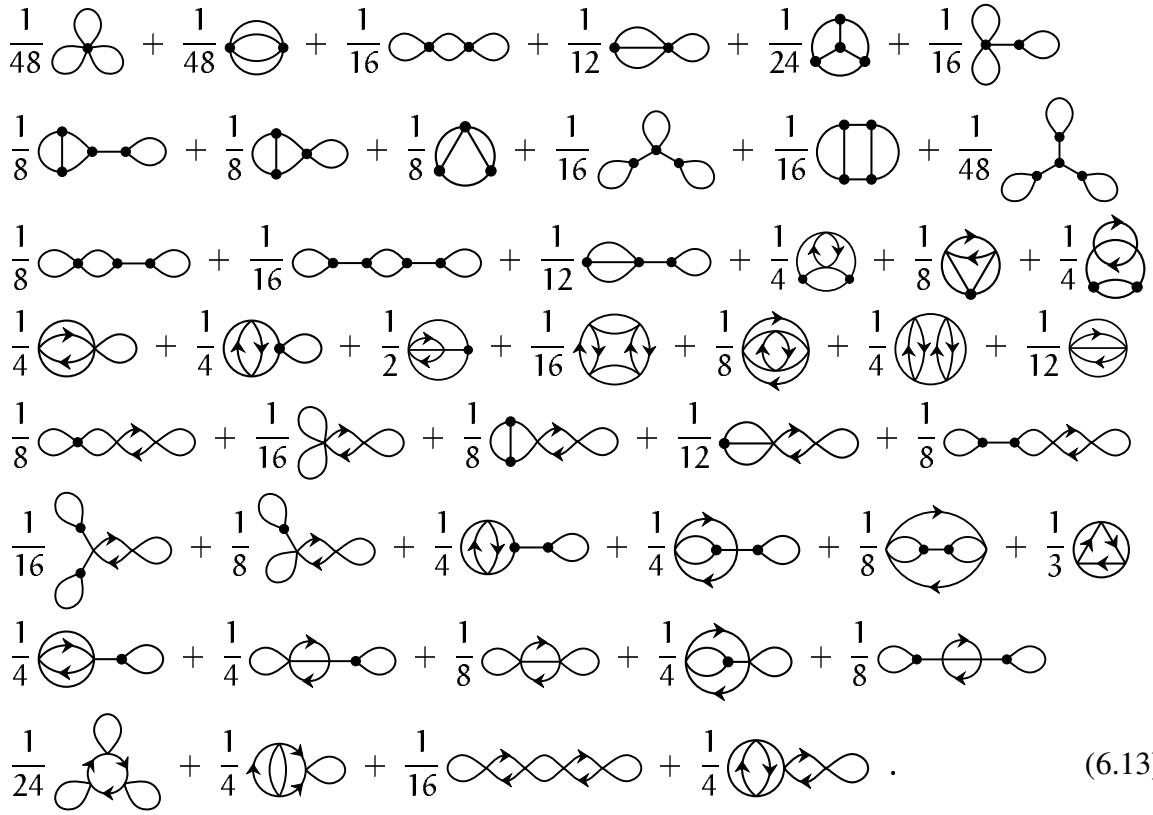

$$\begin{aligned} & \frac{1}{48} + \frac{1}{48} + \frac{1}{16} + \frac{1}{12} + \frac{1}{24} + \frac{1}{16} \\ & + \frac{1}{8} + \frac{1}{8} + \frac{1}{8} + \frac{1}{16} + \frac{1}{16} + \frac{1}{48} \\ & + \frac{1}{8} + \frac{1}{16} + \frac{1}{12} + \frac{1}{4} + \frac{1}{8} + \frac{1}{4} \\ & + \frac{1}{4} + \frac{1}{4} + \frac{1}{2} + \frac{1}{16} + \frac{1}{8} + \frac{1}{4} + \frac{1}{12} \\ & + \frac{1}{8} + \frac{1}{16} + \frac{1}{8} + \frac{1}{12} + \frac{1}{8} \\ & + \frac{1}{16} + \frac{1}{8} + \frac{1}{4} + \frac{1}{4} + \frac{1}{8} + \frac{1}{3} \\ & + \frac{1}{4} + \frac{1}{4} + \frac{1}{8} + \frac{1}{4} + \frac{1}{8} \\ & + \frac{1}{24} + \frac{1}{4} + \frac{1}{16} + \frac{1}{4} \quad . \end{aligned} \tag{6.13}$$

6.1.1.4 One-vertex decomposability

For some discrepancies, the contribution of a bosonic part of a diagram that consists of two pieces connected by *only one* vertex, is equal to the product of the contribution of those pieces. Such diagrams we call *one-vertex reducible*, and discrepancies with this property we call *one-vertex decomposable*. Examples of such discrepancies are those for which $\mathcal{B}$ is translation invariant, i.e., $\mathcal{B}(x,y) = \mathcal{B}(x+a, y+a)\ \forall\, x,y,a \in \mathbf{K}$, such as the Fourier diaphony. Also the Lego discrepancy with equal bins is one-vertex decomposable. In contrast, the L_2^*-discrepancy is not one-vertex decomposable.

As a result of the one-vertex decomposability, many diagrams cancel or give zero. For example, the first and the second diagram in (6.11) cancel, and the fourth gives zero, so that

$$\frac{1}{N}W_1(z) \;=\; \frac{1}{4}$$ 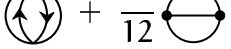 $$+\; \frac{1}{12}$$ $$\;. \tag{6.14}$$

To second order, only the following remains:

$$\frac{1}{N^2}W_2(z) \;=\; \frac{1}{48}$$  $$+\; \frac{1}{24}$$  $$+\; \frac{1}{8}$$  $$+\; \frac{1}{2}$$  $$+\; \frac{1}{8}$$  $$+\; \frac{1}{4}$$  $$+\; \frac{1}{4}$$ 

$$+\; \frac{1}{16}$$  $$+\; \frac{1}{16}$$  $$+\; \frac{1}{8}$$  $$+\; \frac{1}{4}$$  $$+\; \frac{1}{12}$$  $$+\; \frac{1}{3}$$  $$\;. \tag{6.15}$$

We now derive a general rule of diagram cancellation. First, we extend the notion of one-vertex reducibility to complete diagrams, including the fermionic part, with the rule that the two pieces both must contain a bosonic part. Consider the following diagram

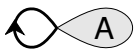

. (6.16)

The only restriction we put one the "leave" A is that it must be one-vertex irreducible with respect to the vertex that connects it to the fermion loop. For the rest, it may be anything. We define the contribution of the leave by the contribution of the whole diagram divided by $-N$, and denote it with $C(A)$. This contribution includes internal symmetry factors. Now consider a diagram consisting of a fermion loop as in diagram (6.16) with attached to the one vertex n_1 leaves of type A_1, n_2 leaves of type A_2, and so on, up to n_p leaves of type A_p. The extra symmetry factor of such a diagram is $(n_1!n_2!\cdots n_p!)^{-1}$, and, for one-vertex decomposable discrepancies, the contribution is equal to the product of the contributions of the leaves, so that the total contribution is given by

$$-N\prod_{q=1}^{p}\frac{C(A_q)^{n_q}}{n_q!}\;. \tag{6.17}$$

Now we sum the contribution of all possible diagrams of this kind that can made with the p leaves, and denote the result by

 $$= -N\sum_{n_1,n_2,\ldots\geq 1}\prod_{q=1}^{p}\frac{C(A_q)^{n_q}}{n_q!} \;=\; -N\Big(\exp\Big(\sum_{q=1}^{p}C(A_q)\Big)-1\Big)\;. \tag{6.18}$$

Because the little square in l.h.s. of Eq. (6.18) represents all possible ways to put the leaves together onto one vertex, the sum of all possible ways to put the leaves onto one fermion loop is given by

$$= -N \sum_{n=1}^{\infty} \frac{(-1)^{n-1}}{n} \Big(\exp\Big(\sum_{q=1}^{p} C(A_q) \Big) - 1 \Big)^n \quad . \tag{6.19}$$

The $(-1)^{n-1}$ in the sum comes from the vertices and $1/n$ is the extra symmetry factor of such diagram with n squares. The sum can be evaluated further and is equal to

$$-N \log \Big(\exp\Big(\sum_{q=1}^{p} C(A_q) \Big) \Big) \;=\; -N \sum_{q=1}^{p} C(A_q) \quad , \tag{6.20}$$

i.e., the sum of all possible ways to put p different leaves onto one fermion loop is equal to the sum of all leaves, each of them put onto its own fermion loop. This means that diagrams, consisting of two or more leaves put onto one fermion loop, cancel.

Now consider the following equation, which holds for every one-vertex decomposable discrepancy:

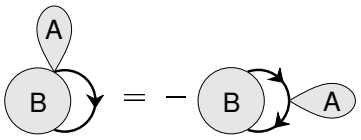

, (6.21)

where we only assume that B is not of the type on the l.h.s. of Eq.(6.19). The minus sign comes from the fact that the first diagram has one vertex less. Because the number of fermion lines a fermion loop consists of is equal to the number of vertices it contains, we can always pair the diagrams into one diagram of the l.h.s. type and one of the r.h.s. type so that they cancel. We can summarize the result with the rule that

for one-vertex decomposable discrepancies,
only the one-vertex irreducible diagrams contribute. (6.22)

6.1.2 Applications

We apply the general formulae given above to the Lego discrepancy, the L_2^*-discrepancy in one dimension and the Fourier diaphony in one dimension.

6.1.2.1 The Lego discrepancy

We take the strengths σ_n equal to $1/\sqrt{w_n}$, so that the discrepancy is just the χ^2-statistic that determines how well the points are distributed over the bins (Section 3.3.4). The propagator is given by

$$\mathcal{B}(x,y) \;=\; \sum_{n=1}^{M} \frac{\vartheta_n(x)\vartheta_n(y)}{w_n} - 1 \quad , \tag{6.23}$$

and it is easy to see that $\mathcal{B}_p(x,y) = \mathcal{B}(x,y)$, $p = 2,3,\ldots$, so that the dressed propagator is given by

$$\mathcal{G}_z(x,y) \;=\; \frac{1}{1-2z}\,\mathcal{B}(x,y) \quad . \tag{6.24}$$

The zeroth order term can be found with the relation of Eq.(6.10), which results in the following expression

$$W_0(z) \;=\; -\frac{1}{2}\log(1-2z)\int_{\mathbf{K}} \mathcal{B}(x,x)\,dx \;=\; -\frac{M-1}{2}\log(1-2z) \quad , \tag{6.25}$$

which is exactly the logarithm of the generating function of the χ^2-distribution (notice that this is by definition the distribution of the χ^2-statistic in the limit of an infinite number of random data). To write down the first order term, we introduce

$$M_2 = \sum_{n=1}^{M} \frac{1}{w_n} \quad , \quad \text{and} \quad \eta(z) = \frac{2z}{1-2z} \quad , \tag{6.26}$$

so that

$$W_1(z) \;=\; \frac{1}{8}\left(M_2 - M^2 - 2M + 2\right)\eta(z)^2 + \frac{1}{24}\left(5M_2 - 3M^2 - 6M + 4\right)\eta(z)^3 \quad . \tag{6.27}$$

If the bins are equal, so that $w_n = 1/M$ $n = 1,2,\ldots,M$, then only the contribution of the diagrams of Eq.(6.16) remains, and the result is

$$W_1(z) \;=\; -\frac{1}{4}E\eta(z)^2 + \frac{1}{12}(E^2 - E)\eta(z)^3 \quad , \tag{6.28}$$

where we denote

$$E = M - 1 \quad . \tag{6.29}$$

To second order in $1/N$, the contribution comes from the diagrams in Eq.(6.15), and is given by

$$\begin{aligned} W_2(z) \;=\; & (5E^3 - 12E^2 + 7E)\frac{\eta(z)^6}{48} \;+\; (E^3 - 6E^2 + 5E)\frac{\eta(z)^5}{8} \\ & +\; (E^3 - 28E^2 + 43)\frac{\eta(z)^4}{48} \;+\; (-E^2 - 5E)\frac{\eta(z)^3}{12} \quad . \end{aligned} \tag{6.30}$$

In Appendix 6A, we present the expansion of $G(z)$ in the case of equal bins, up to and including the $1/N^4$ term. It is calculated using the path integral expression (3.85) of $G(z)$ and computer algebra. The reader may check that this expression for $G(z)$ and the above terms of $W(z)$ satisfy $G(z) = e^{W(z)}$ up to the order of $1/N^2$.

6.1.2.2 The L_2^*-discrepancy

In one dimension, the basis in the Landau gauge is given by the set of functions $\{\sqrt{2}\cos(n\pi x), n = 1, 2, \ldots\}$ (Section 3.3.1), so that the propagator is given by

$$\mathcal{B}(x,y) \;=\; \sum_{n=1}^{\infty} \frac{2\cos(n\pi x)\cos(n\pi y)}{n^2\pi^2} \;=\; \min(1-x,1-y) + \tfrac{1}{2}x^2 + \tfrac{1}{2}y^2 - \tfrac{2}{3} \quad . \tag{6.31}$$

The dressed propagator is given by

$$\mathcal{G}_z(x,y) \;=\; \sum_{n=1}^{\infty} \frac{2\cos(n\pi x)\cos(n\pi y)}{n^2\pi^2 - 2z} \tag{6.32}$$

$$\;=\; \frac{1}{u^2} - \frac{1}{2u\sin u}\{\cos[u(1-|x+y|)] \;+\; \cos[u(1-|x-y|)]\} \quad , \tag{6.33}$$

with

$$u = \sqrt{2z} \quad . \tag{6.34}$$

The zeroth order term can be obtained using Eq.(6.10):

$$W_0(z) \;=\; -\frac{1}{2}\log\left(\frac{\sin u}{u}\right) \quad , \tag{6.35}$$

which is the well-known result. After some algebra, also the first order term follows:

$$W_1(z) \;=\; \frac{1}{288}\left(24 - 8\frac{u}{\sin u} - 7\frac{u^2}{\sin^2 u} - 7\frac{u}{\tan u} - 2\frac{u^2}{\tan^2 u}\right) \quad . \tag{6.36}$$

6.1.2.3 The Fourier diaphony

We consider the one-dimensional case, with a slightly different definition than the one given in Section 3.3.3: we multiply the discrepancy with a factor $\pi^2/3$, so that the propagator is given by

$$\mathcal{B}(x,y) \;=\; \sum_{n=1}^{\infty} \frac{2\cos(2n\pi\{x-y\})}{n^2} \;=\; \frac{\pi^2}{3}\left[1 - 6\{x-y\}(1-\{x-y\})\right] \quad , \tag{6.37}$$

where we use the notation $\{x\} = x \mod 1$. The dressed propagator is given by

$$\mathcal{G}_z(x,y) \;=\; \sum_{n=1}^{\infty} \frac{2\cos(2n\pi\{x-y\})}{n^2 - 2z} \;=\; \frac{\pi^2}{\nu^2}\left(1 - \frac{\nu\cos[\nu(2\{x-y\}-1)]}{2\sin\nu}\right) \quad , \tag{6.38}$$

where

$$\nu = \sqrt{2\pi^2 z} \quad . \tag{6.39}$$

This two-point function is, apart of a factor π^2/ν^2, the same as the one in Eq. (26) in [24]. The zeroth order term can easily be obtained from the dressed propagator and is given by

$$W_0(z) \;=\; -\log\left(\frac{\sin\nu}{\nu}\right) \quad , \tag{6.40}$$

which is in correspondence with Eq. (21) in [24]. Because the propagator is translation invariant, i.e., $\mathcal{B}(x+a, y+a) = \mathcal{B}(x,y)\ \forall\, x, y, a \in \mathbf{K}$, the contributions of the first two diagrams in Eq. (6.11) cancel, and the contribution of the fourth diagram is zero. The contribution of the remaining diagrams gives

$$W_1(z) \;=\; \frac{1}{36}\left(3+\nu^2-3\frac{\nu^2}{\sin^2\nu}\right) \quad . \tag{6.41}$$

6.2 Scaling limits for the Lego discrepancy

In this section, we take a closer look at the Lego discrepancy in the case that it is equivalent with a χ^2-statistic for N data points distributed over M bins (Section 3.3.4). First, we will show that the natural expansion parameter in the calculation of the moment generating function is M/N, and calculate a few terms. We will see, however, that a strict limit of $M \to \infty$ does not exist, and, in fact, this is well known because the χ^2-distribution, which gives the lowest order term in this expansion, does not exist if the number of degrees of freedom becomes infinite. We overcome this problem by going over to the standardized variable, which is obtained from the discrepancy by shifting and rescaling it such that it has zero expectation and unit variance. In fact, it is this variable for which the results in [26] and Chapter 5 were obtained. In this section, we derive similar results for the Lego discrepancy, depending on the behavior of the sizes of the bins if M goes to infinity. We will see that various asymptotic probability distributions occur if $M, N \to \infty$ such that $M^\alpha/N \to$ *constant* with $\alpha \geq 0$. If, for example, the bins become asymptotically equal and $\alpha > \frac{1}{2}$, then the probability distribution becomes Gaussian. Notice that this includes limits with $\alpha < 1$, which is in stark contrast with the rule of thumb that, in order to trust the χ^2-distribution, each bin has to contain at least a few, say five (see e.g. [2]), data points. Our result states that, for large M and N, the majority of bins is allowed to remain empty!

6.2.1 Sequences and notation

In the following, we will investigate limits in which the number of bins M goes to infinity. Note that for each value of M, we have to decide on the values of the volumes w_n of the bins. They clearly have to scale with M, because their sum has to be equal to one. There are, of course, many possible ways for the measures to scale, i.e., many double-sequences $\{w_n^{[M]}, 1 \leq n \leq M, M > 0\}$ of positive numbers with

$$\sum_{n=1}^{M} w_n^{[M]} \;=\; 1 \quad \forall\, M > 0 \qquad \text{and} \qquad \lim_{M\to\infty} \sum_{n=1}^{M} w_n^{[M]} \;=\; 1 \quad . \tag{6.42}$$

We, however, want to restrict ourselves to discrepancies in which the relative sizes of the bins stay of the same order, i.e., sequences for which

$$\inf_{n,M} M w_n^{[M]} > 0 \qquad \text{and} \qquad \sup_{n,M} M w_n^{[M]} < \infty \quad . \tag{6.43}$$

It will appear to be appropriate to specify the sequences under consideration by another criterion, which is for example satisfied by the sequences mentioned above. It can be formulated in terms of the objects

$$M_p \;:=\; \sum_{n=1}^{M} \left(w_n^{[M]}\right)^{1-p} \quad , \quad p \geq 1 \quad , \tag{6.44}$$

and is given by the demand that

$$h_p \in [1,\infty) \quad \forall\, p \geq 1 \quad , \quad \text{where} \quad h_p := \lim_{M\to\infty} \frac{M_p}{M^p} \quad . \tag{6.45}$$

Within the set of sequences we consider, there are those with for which the bins become asymptotically equal, i.e., sequences with

$$w_n^{[M]} = \frac{1+\varepsilon_n^{[M]}}{M} \qquad \text{with} \qquad \lim_{M\to\infty} \max_{1\leq n\leq M} \left|\varepsilon_n^{[M]}\right| = 0 \quad , \tag{6.46}$$

and $\varepsilon_n^{[M]} > -1$, $1 \leq n \leq M$ of course. They belong to the set of sequences with $h_p = 1\;\forall\, p \geq 1$, which will allow for special asymptotic probability distributions.

In the following analysis, we will consider functions of M and their behavior if $M \to \infty$. To specify relative behaviors, we will use the symbols "$\sim$", "$\asymp$" and "$\prec$". The first one is used as follows:

$$f_1(M) \sim f_2(M) \quad \Longleftrightarrow \quad \lim_{M\to\infty} \frac{f_1(M)}{f_2(M)} \;=\; 1 \quad . \tag{6.47}$$

If a limit as above is not necessarily equal to one and not equal to zero, then we use the second symbol:

$$f_1(M) \asymp f_2(M) \quad \Longleftrightarrow \quad f_1(M) \sim c f_2(M) \quad , \quad c \in (0,\infty) \quad . \tag{6.48}$$

We only use this symbol for those cases in which $c \neq 0$. For the cases in which $c = 0$ we use the third symbol:

$$f_1(M) \prec f_2(M) \quad \Longleftrightarrow \quad \lim_{M\to\infty} \frac{f_1(M)}{f_2(M)} \;=\; 0 \quad . \tag{6.49}$$

We will also use the $\mathcal{O}$-symbol, and do this in the usual sense. We can immediately use the symbols to specify the behavior of M_p with M, for the criterion of Eq.(6.45) tells us that

$$M_p \asymp M^p \quad , \tag{6.50}$$

and that

$$M_p \sim M^p \quad \text{if} \quad h_p = 1 \ . \tag{6.51}$$

In our formulation, also the number of data points N runs with M. We will, however, never denote the dependence of N on M explicitly and assume that it is clear from now on. Also the upper index at the measures w_n we will omit from now on.

6.2.2 Feynman rules

The Feynman rules to calculate the generating function $G(z)$ in a diagrammatic expansion are given in Section 3.2.4. The boson propagator is a matrix in this case, i.e.,

$$\text{boson propagator:} \quad n \cdots\cdots m \ = \ \mathcal{B}_{n,m} = \frac{\delta_{n,m}}{w_n} - 1 \ , \tag{6.52}$$

and boson propagators are convoluted as $\sum_{m=1}^{M} w_m \mathcal{B}_{m,n_1} \mathcal{B}_{m,n_2} \cdots \mathcal{B}_{m,n_p}$ in the vertices. Only *connected* diagrams have to be calculated, since

$$\log G(z) \ = \ \textit{the sum of the connected vacuum diagrams.} \qquad \text{rule 1}$$

Furthermore, the bosonic part of each diagram decouples completely from the fermionic part, and the contribution of the fermionic part can easily be determined, for

$$\textit{every fermion loop only gives a factor} -N. \qquad \text{rule 2}$$

Because of the rather simple expression for the bosonic propagator, we are able to deduce from the basic Feynman rules some effective rules for the bosonic parts of the Feynman diagrams. Remember that the bosonic parts decouples completely from the fermionic parts. The following rules apply after having counted the number of fermion loops and the powers of g coming from the vertices, and after having calculated the symmetry factor of the original diagram. When we mention the *contribution* of a diagram in this section, we refer to the contribution apart from the powers of g and symmetry factors. This contribution will be represented by the same drawing as the diagram itself.

The first rule is a consequence of the fact that

$$\sum_{n=1}^{M} w_m \mathcal{B}_{n_1,m} \mathcal{B}_{m,n_2} \ = \ \mathcal{B}_{n_1,n_2} \tag{6.53}$$

and states that

$$\textit{all vertices with only two legs that do not form a single loop can be removed.} \qquad \text{rule 3}$$

The second rule is a consequence of the fact that for any $M \times M$-matrix f

$$\sum_{n,m=1}^{M} w_n w_m f_{n,m} \mathcal{B}_{n,m} \ = \ \sum_{n=1}^{M} w_n f_{n,n} - \sum_{n,m=1}^{M} w_n w_m f_{n,m} \ , \tag{6.54}$$

and states that the contribution of a diagram is the same as that of the diagram in which a boson line is contracted and the two vertices, connected to that line, are fused together to form one vertex, minus the contribution of the diagram in which the line is simply removed and the vertices replaced by vertices with one boson leg less. This rule can be depicted as follows

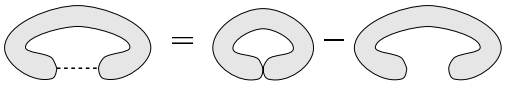

rule 4

By repeated application of these rules, we see that the contribution of a connected bosonic diagram is equal to the contribution of a sum of products of so called *daisy* diagrams [1], which are of the type

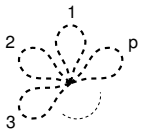

. (6.55)

They are characterized by the fact that all lines begin and end on the same vertex and form single loops. The contribution of such a diagram is given by

$$d_p(M) \;=\; \sum_{n=1}^{M} w_n \mathcal{B}^p_{n,n} \;=\; \sum_{q=0}^{p} \binom{p}{q} (-1)^{p-q} M_q \;=\; M_p[1 + \mathcal{O}(M^{-1})] \;, \tag{6.56}$$

where the last equation follows from Eq. (6.50). The maximal number of leaves in a product in the sum of daisy diagrams is equal to the number of loops L_b in the original diagram, so that

the contribution of a diagram with L_b boson loops is $M_{L_b}[1 + \mathcal{O}(M^{-1})]$. rule 5

The leading order contribution of a diagram with L_b boson loops is thus of the order of M^{L_b}.

6.2.2.1 Extra rule if $h_p = 1$

If $h_p = 1 \;\forall\, p \geq 1$, then all kind of cancellations between diagrams occur, because in those cases $M_p \sim M^p \;\forall\, p \geq 1$. As a result of this, the contribution of a daisy diagram is $d_p(M) \sim M^p$, and we can deduce the following rule: the contribution of a diagram that falls apart in disjunct pieces if a vertex is cut, is equal to the product of the contributions of those disjunct pieces times one plus vanishing corrections. Diagrammatically, the rule looks like

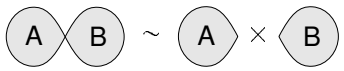

, (6.57)

In Section 6.1.1.4 we called discrepancies for which Eq. (6.57) is exact one-vertex decomposable, and have shown that for those discrepancies only the *one-vertex irreducible* diagrams contribute, i.e., diagrams that do not fall apart in pieces containing bosonic parts if a vertex is cut. The previous rule tells us that, if $h_p = 1 \;\forall\, p \geq 1$, then

$$\log G(z) \;\sim\; \textit{sum of all connected one-vertex irreducible diagrams.} \qquad \text{rule 6}$$

The connected one-vertex irreducible diagrams we call *relevant* and the others *irrelevant*.

[1] For example 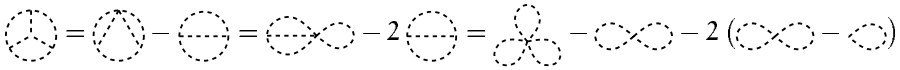

6.2.3 Loop analysis

We want to determine the contribution of the diagrams in this section, and in order to do that, we need to introduce some notation:

$$L_b := \text{the number of boson loops} ; \tag{6.58}$$
$$L_f := \text{the number of fermion loops} ; \tag{6.59}$$
$$L := \text{the total number of loops} ; \tag{6.60}$$
$$I_b := \text{the number of bosonic lines} ; \tag{6.61}$$
$$I_f := \text{the number of fermionic lines} ; \tag{6.62}$$
$$v := \text{the number of vertices} ; \tag{6.63}$$
$$L_m := L - L_b - L_f = \text{number of mixed loops} . \tag{6.64}$$

These quantities are in principle functions of the diagrams, but we will never denote this dependence explicitly, for it will always be clear which diagram we are referring to when we use the quantities.

With the foregoing, we deduce that the contribution C_Δ of a connected diagram Δ with no external legs satisfies

$$C_\Delta \asymp M^{L_b} N^{L_f} g^{2I_b} . \tag{6.65}$$

The Feynman rules and basic graph theory tell us that, for connected diagrams with no external legs, $v = I_f$ and $L = I_b + I_f - v + 1$, so that

$$I_b = L - 1 = L_b + L_f + L_m - 1 . \tag{6.66}$$

If we furthermore use that $g = \sqrt{2z/N}$, we find that the contribution is given by

$$C_\Delta \asymp \frac{M^{L_b}}{N^{L_m} N^{L_b - 1}} (2z)^{I_b} . \tag{6.67}$$

Notice that this expression does not depend on L_f. Furthermore, it is clear that, for large M and N, the largest contribution comes from diagrams with $L_m = 0$. Moreover, we see that we must have $N = \mathcal{O}(M)$, for else the contribution of higher-order diagrams will grow with the number of boson loops, and the perturbation series becomes completely senseless. If, however, $N \asymp M$, then the contribution of each diagram with $L_m = 0$ is more important than the contribution of each of the diagrams with $L_m > 0$. Finally, we also see that the contribution of the $\mathcal{O}(M^{-1})$-corrections of a diagram (Eq.(6.56)) is always negligible compared to the leading contribution of each diagram with $L_m = 0$. These observations lead to the conclusion that, if N and M become large with $N \asymp M$, then the leading contribution to $\log G(z)$ comes from the diagrams with $L_m = 0$, and that there are no corrections to these contributions. If we assume that M/N is small, then the importance of these diagrams decreases with the number of boson loops L_b as $(M/N)^{L_b}$.

6.2.3.1 The loop expansion of $\log G(z)$

Now we calculate the first few terms in the loop expansion of $\log G(z)$. We start with the diagrams with one loop (remember that it is an expansion in boson loops and that we only have to calculate *connected* diagrams for $\log G(z)$). The sum of all 1-loop diagrams with $L_m = 0$ is given by the l.h.s. of Eq. (6.4), resulting in the r.h.s. of Eq. (6.25). To calculate the higher loop diagrams, we introduce the effective vertex of Eq. (6.5) and the partly re-summed propagator

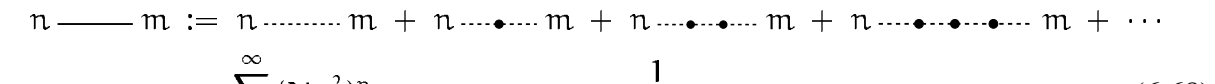

$$= \sum_{p=0}^{\infty} (Ng^2)^p \times$$

$$= \frac{1}{1-2z} \times$$

$$. \qquad (6.68)$$

The contribution of the 2-loop diagrams with $L_m = 0$ is given by

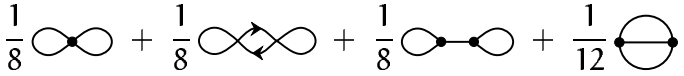

$$= \left[-\frac{1}{8}\frac{Ng^2M^2}{(1-2z)^2} + \frac{1}{8}\frac{Ng^2M_2}{(1-2z)^2} + \frac{1}{8}\frac{(Ng^3)^2(M_2-M^2)}{(1-2z)^3} + \frac{1}{12}\frac{(Ng^3)^2M_2}{(1-2z)^3} \right] [1 + \mathcal{O}(M^{-1})]$$

$$= \frac{1}{N}\left[\frac{1}{8}(M_2 - M^2)\eta(z)^2 + \left(\frac{5M_2}{24} - \frac{M^2}{8} \right) \eta(z)^3 \right] [1 + \mathcal{O}(M^{-1})] \ , \qquad (6.69)$$

where we define

$$\eta(z) \ = \ \frac{2z}{1-2z} \ . \qquad (6.70)$$

Notice that the first three diagrams vanish if $h_p = 1 \ \forall \, p \geq 1$. The contribution of the 3-loop diagrams with $L_m = 0$ is given by

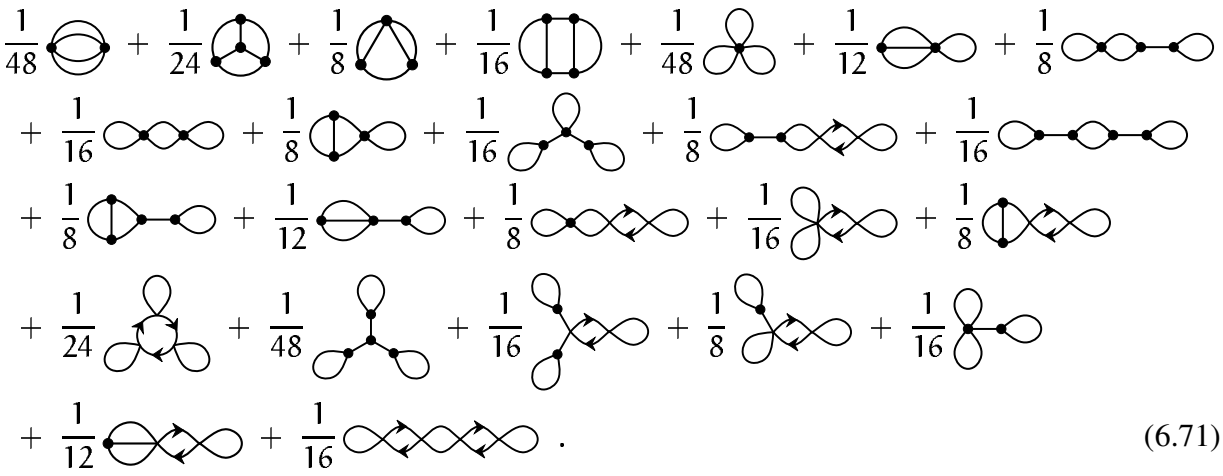

$$. \qquad (6.71)$$

If $h_p = 1 \ \forall \, p \geq 1$, then only the first four diagrams are relevant, and their contribution C satisfies

$$C \ \sim \ \frac{M^3}{N^2}\left[\frac{1}{48}\eta(z)^4 \ + \ \frac{1}{8}\eta(z)^5 \ + \ \frac{5}{48}\eta(z)^6 \right] \ . \qquad (6.72)$$

6.2.4 Various limits

In the previous calculations, M/N was the expansion parameter and the expansion of the generating function only makes sense if it is considered to be small. Furthermore, a limit in which $M \to \infty$ does not exist, because the zeroth order term is proportional to M. In order to analyze limits in which M as well as N go to infinity, we can go over to the standardized variable $(D_N - E)/\sqrt{V}$ of the discrepancy (Section 2.1.2), where

$$E := E(D_N) = M - 1 \tag{6.73}$$

$$V := V(D_N) = 2(M-1) + \frac{M_2 - M^2 - 2(M-1)}{N} \quad . \tag{6.74}$$

The generating function of the probability distribution of the standardized variable is given by

$$\hat{G}(\xi) = E\left(\exp\left(\xi \frac{D_N - E}{\sqrt{V}} \right) \right) = \exp\left(-\frac{E\xi}{\sqrt{V}} \right) G\left(\frac{\xi}{\sqrt{V}} \right) \quad . \tag{6.75}$$

Instead of the parameter z, the parameter $\xi = z\sqrt{V}$ is considered to be of $\mathcal{O}(1)$ in this perspective, in the sense that it are these values of ξ that give the important contribution to the inverse Laplace transform to get from the generating function to the probability density, and the contribution of a diagram changes from (6.67) to

$$C_\Delta \asymp \frac{M^{L_b}}{N^{L_m} N^{L_b - 1} V^{\frac{1}{2}(L_b + L_f + L_m - 1)}} (2\xi)^{I_b} \quad . \tag{6.76}$$

In the following we will investigate limits of $M \to \infty$ with, at first instance, the criterion of Eq.(6.45) as only restriction. The fact that the variance V shows up explicitly in the contribution of the diagrams, forces us to specify the behavior of M_2 more precisely. We will take

$$M_2 - M^2 \asymp M^\gamma \quad , \quad 0 \leq \gamma \leq 2 \quad . \tag{6.77}$$

Notice that $h_2 = 1$ if $\gamma < 2$ and that h_2 does not exist if $\gamma > 2$. Furthermore, we cannot read off the natural expansion parameter from the contribution of the diagrams anymore, and have to specify the behavior of N. We will only consider limits in which

$$N \asymp M^\alpha \quad , \quad \alpha > 0 \quad . \tag{6.78}$$

Although they are a small subset of possible limits, those that can be specified by a pair (α, γ) show an interesting picture. We will derive the results in the next section, but present them now in the following phase diagram:

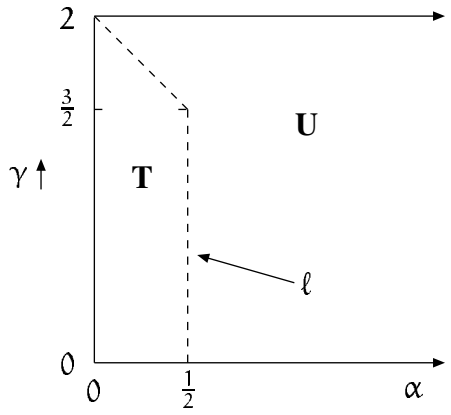

It shows the region $\mathbf{S} = \{(\alpha, \gamma) \in \mathbf{R}^2 \mid \alpha \in [0, \infty),\ \gamma \in [0, 2]\}$ of the real (α, γ)-plane. In this region, there is a *critical line* ℓ, given by

$$\ell := \{(f_\ell(t), t) \in \mathbf{S} \mid t \in [0, 2]\} \quad \text{with} \quad f_\ell(t) := \begin{cases} \frac{1}{2} & \text{if } 0 \leq t \leq \frac{3}{2} \ , \\ 2 - t & \text{if } \frac{3}{2} \leq t \leq 2 \ . \end{cases} \tag{6.79}$$

It separates **S** into two regions **T** and **U**, neither of which contains ℓ. Our results are the following. Firstly,

in the region **T**, *the limit of* $M \to \infty$ *is not defined.* (6.80)

In this region, the standardized variable is not appropriate, and we see that there are too many diagrams that grow indefinitely with M. Secondly,

in the region **U**, *the limit of* $M \to \infty$ *gives a Gaussian distribution.* (6.81)

Because we used the standardized variable, this distribution has necessarily zero expectation and unit variance. Finally,

on the line ℓ, *various limits exist, depending on the behaviour of* M_p, $p > 2$. (6.82)

One of these limits we were able to calculate explicitly. It appears if $M_p - M^p \prec M^{p-\frac{1}{2}}\ \forall p \geq 1$, which is, for example, satisfied in the case of equal binning. In this limit, the generating function is given by

$$\log \hat{G}(\xi) \ = \ \frac{1}{\lambda^2}\left(e^{\lambda\xi} - 1 - \lambda\xi\right) \quad , \quad \lambda := \lim_{M\to\infty} \frac{\sqrt{2M}}{N} \ . \tag{6.83}$$

In Appendix 6B, we show that the probability distribution $\hat{H}$ belonging to this generating function, which is the inverse Laplace transform, is given by

$$\hat{H}(\tau) \ = \ \sum_{n\in\mathbf{N}} \delta\left(\tau - \left[n\lambda - \frac{1}{\lambda}\right]\right) \frac{1}{n!}\left(\frac{1}{\lambda^2}\right)^n \exp\left(-\frac{1}{\lambda^2}\right) \ . \tag{6.84}$$

It consists of an infinite number of Dirac delta-distributions, weighed with a Poisson distribution. The delta-distributions reveal the fact that, for finite N and M, the Lego discrepancy, and also the χ^2-statistic, can only take a finite number of values, so that the probability density *should* consist of a sum of delta-distributions. In the usual limit of $N \to \infty$, the discrete nature of the random variable disappears, and the χ^2-distribution is obtained. In our limit, however, the discrete nature does not yet disappear. A continuous distribution is obtained if $\lambda \to 0$, which corresponds with going over from $\alpha = \frac{1}{2}$ to $\alpha > \frac{1}{2}$. Then $\hat{G}(\xi) \to \exp(\frac{1}{2}\xi^2)$.

6.2.5 Derivation of the various limits

We will deal with the cases $\gamma = 2$, $\gamma - \alpha \leq 1$ and $\gamma - \alpha > 1$ separately.

6.2.5.1 $\gamma = 2$

We distinguish the three cases $0 < \alpha < 1$, $\alpha = 1$ and $\alpha > 1$.

If $\alpha > 1$, then $V \asymp M$, and the contribution C_Δ of a diagram Δ satisfies $C_\Delta \asymp M^\beta$, with

$$\beta \;=\; (\tfrac{1}{2} - \alpha)L_b - \tfrac{1}{2}L_f + (\alpha + \tfrac{1}{2})(1 - L_m) \quad . \tag{6.85}$$

A short analysis shows that only diagrams with $(L_b, L_f, L_m) = (1, 1, 0)$ or $(L_b, L_f, L_m) = (1, 2, 0)$ give a non-vanishing contribution, and those diagrams are

$$\frac{1}{2}\;\bigcirc\!\!\circlearrowright \;=\; \frac{1}{2}\,\frac{N(M-1)2\xi}{N\sqrt{V}} \;=\; \frac{E\xi}{\sqrt{V}} \tag{6.86}$$

$$\frac{1}{4}\;\circlearrowleft\!\!\bigcirc\!\!\circlearrowright \;=\; \frac{1}{4}\,\frac{N^2(M-1)4\xi^2}{N^2V} \;=\; \frac{\xi^2}{2} + \mathcal{O}(M^{-1}) \quad . \tag{6.87}$$

The first diagram gives a contribution that is linear in ξ and cancels with the exponent in Eq.(6.75). This has to happen for every value of α, and as we will see, this diagram will occur always. Notice that the diagrams above are the first two diagrams in the series on the l.h.s of Eq. (6.4). The logarithm of the generating function becomes quadratic, so that the probability distribution becomes Gaussian.

If $\alpha = 1$, then again $V \asymp M$, so that $\beta = -\frac{1}{2}(L_b + L_f) + \frac{3}{2}(1 - L_m)$, and we have to add the diagrams with $(L_b, L_f, L_m) = (2, 1, 0)$:

$$\frac{1}{8}\;\circlearrowleft\!\!\bigcirc \;+\; \frac{1}{8}\;\bigcirc\!\!\circlearrowright\!\!\bigcirc \;=\; \frac{1}{8}\,\frac{N(M_2 - M^2)4\xi^2}{N^2V} \;=\; \frac{(M_2 - M^2)\xi^2}{2NV} \quad . \tag{6.88}$$

If $0 < \alpha < 1$, then $V \asymp M^{2-\alpha}$ and $\beta = -\frac{\alpha}{2}L_b - (1 - \frac{\alpha}{2})L_f - (\frac{\alpha}{2} + 1)L_m + \frac{\alpha}{2} + 1$, so that, besides the diagram of Eq.(6.86), only the diagrams of Eq.(6.88) give a non-vanishing contribution, and this contribution is equal to $\xi^2/2$.

6.2.5.2 $\gamma - \alpha \leq 1$

In this case, $V \asymp M$, and the contribution C_Δ of a diagram Δ satisfies $C_\Delta \asymp M^\beta$ with

$$\beta \;=\; (\tfrac{1}{2} - \alpha)L_b - \tfrac{1}{2}L_f + (\alpha + \tfrac{1}{2})(1 - L_m) \quad . \tag{6.89}$$

If $\alpha < \frac{1}{2}$, then β increases with the number of boson loops L_b, and we are not able to calculate the limit of $M \to \infty$.

If $\alpha > \frac{1}{2}$, then the only diagrams that have a non-vanishing contribution are those with $(L_b, L_f, L_m) = (1,1,0)$, $(1,2,0)$ or $(2,1,0)$. These are exactly the diagrams of Eq. (6.86), Eq.(6.87) and Eq.(6.88). Notice, however, that the diagrams of Eq.(6.88) cancel if $\gamma - \alpha < 0$: then they are *irrelevant*. The resulting asymptotic distribution is Gaussian again.

If $\alpha = \frac{1}{2}$, then L_b disappears from the equation for β, and we obtain a non-Gaussian asymptotic distribution. The diagrams that contribute are those with $(L_f, L_m) = (1,0)$ or $(2,0)$. There is, however, only one *relevant* diagram with $(L_f, L_m) = (1,0)$, namely the diagram of Eq.(6.86) that gives the linear term. We have to be careful here, because the other diagrams with $(L_f, L_m) = (1,0)$ still might be non-vanishing. A short analysis shows that they are given by the sum of all ways to put daisy diagrams to one fermion loop, and that their contribution is given by

$$C_1(M) \;=\; N \log\left(1 + \sum_{p=1}^{\infty} \frac{(\frac{1}{2}g^2)^p d_p(M)}{p!}\right) \quad . \tag{6.90}$$

We know that, if $h_p = 1$, then $d_p(M) = M^p[1 + \varepsilon_p(M)]$ with $\lim_{M\to\infty} \varepsilon_p(M) = 0$, so that

$$C_1(M) \;=\; \tfrac{1}{2}NMg^2 + N \log\left(1 + e^{-\frac{1}{2}Mg^2} \sum_{p=1}^{\infty} \frac{(\frac{1}{2}Mg^2)^p \varepsilon_p(M)}{p!}\right) \quad . \tag{6.91}$$

The first term gives the leading contribution; the contribution of the relevant diagram, which consists of a boson loop and a fermion loop attached to one vertex. The second term is irrelevant with respect to the first, but can still be non-vanishing, depending on the behavior of $\varepsilon_p(M)$. Remember that $\alpha = \frac{1}{2}$ and $V \asymp M$, so that $Mg^2 = 2\xi M/(N\sqrt{V}) \to$ *constant*, and we can see that the contribution is only vanishing if

$$\lim_{M\to\infty} N\varepsilon_p(M) \;=\; 0 \quad \forall\, p \geq 1 \quad \Longleftrightarrow \quad M_p - M^p \prec M^{p-\frac{1}{2}} \quad \forall\, p \geq 1 \quad . \tag{6.92}$$

For $p = 1$ this relation is satisfied because $\varepsilon_1(M) = 0$. For $p = 2$ this relation is also satisfied if $\gamma < \frac{3}{2}$.

If the relation is also satisfied for the other values of p, then the only diagrams that contribute to the generating function are the relevant diagrams with $(L_f, L_m) = (2,0)$:

 , (6.93)

where we used the effective vertex (6.5) again. The contribution of a diagram of this type with p boson lines is given by

$$\frac{1}{2\,p!}\left(\frac{2\xi}{N\sqrt{V}}\right)^p N^2 M_p[1+\mathcal{O}(M^{-1})] \;\sim\; \frac{N^2}{2M}\frac{1}{p!}\left(\frac{2M\xi}{N\sqrt{V}}\right)^p . \tag{6.94}$$

The factor $1/2\,p!$ is the symmetry factor of this type of diagram. If we sum the contribution of these diagrams and use that $V \sim 2M$, we obtain

$$\log \hat{G}(\xi) \;\sim\; \frac{1}{\lambda^2}\left(e^{\lambda\xi} - 1 - \lambda\xi\right) \quad , \quad \lambda := \lim_{M\to\infty} \frac{\sqrt{2M}}{N} \quad . \tag{6.95}$$

6.2.5.3 $\gamma - \alpha > 1$

In this case, $V \asymp M^{\gamma-\alpha}$ and the contribution C_Δ of a diagram Δ satisfies $C_\Delta \asymp M^\beta$ with

$$\beta \;=\; (1-\tfrac{\gamma+\alpha}{2})L_b - \tfrac{\gamma-\alpha}{2}L_f + \tfrac{\gamma+\alpha}{2}(1-L_m) \quad . \tag{6.96}$$

If $\gamma+\alpha < 2$, then β increases with the number of boson loops L_b, and we are not able to calculate the limit of $M \to \infty$.

If $\gamma+\alpha > 2$, then the only diagrams that have a non-vanishing contribution are those with $(L_b, L_f, L_m) = (1,1,0)$, $(1,2,0)$ or $(2,1,0)$. These are exactly the diagrams of Eq.(6.86), Eq.(6.87) and Eq.(6.88). Notice, however, that the diagrams of Eq.(6.88) cancel if $\gamma-\alpha < 0$: then they are *irrelevant*. The resulting asymptotic distribution is Gaussian.

If $\gamma+\alpha = 2$, then $\beta = (\alpha-1)L_f + 1 - L_m$. Because $\gamma-\alpha > 1$, we have $\alpha < \frac{1}{2}$, and non-vanishing diagrams have $(L_f, L_m) = (1,0)$. Their contribution is given by the r.h.s. of Eq.(6.91), the first term of which gives the term linear in ξ. The second term is non-vanishing, because $Mg^2 \asymp M^{1-(\gamma+\alpha)/2} \to$ *constant* and $N\varepsilon_2(M) \asymp M^{\alpha+\gamma-2} \to$ *constant*.

6.3 Stronger-than-weak limits for diaphony

In [26], it is proven that the standardized variable of the Fourier diaphony (Section 3.3.3) converges in distribution to a Gaussian variable if the number N of points in the point set, and with it the number s_N of dimensions of the integration region, goes to infinity such that $c_w^{s_N}/N$ goes to zero, where

$$c_w \;=\; \frac{\sqrt{1+\frac{2\pi^4}{15}+\frac{8\pi^6}{945}+\frac{\pi^8}{945}}}{1+\frac{\pi^4}{45}} \;=\; 1.79218\cdots \quad . \tag{6.97}$$

To be more precise, if $s_1, s_2, \ldots$ is a nondecreasing sequence such that

$$\limsup_N \frac{c_w^{s_N}}{N} = 0 \qquad \text{then} \qquad \frac{D_N - E(D_N)}{\sqrt{V(D_N)}} \;\xrightarrow{d}\; \text{Normal} \quad , \tag{6.98}$$

where we include in the notation "D_N" the dependence on N through s_N. The proof makes use of the Central Limit Theorem as given in Section 2.1.5.1, and is, roughly speaking, based on the fact that the conditions in the theorem are satisfied if $E(D_N^4)/V(D_N)^2 \to 0$.

6.3.1 The observation

The Central Limit Theorem provides a weak limit for the distribution, which becomes dramatically clear in a short calculation. The expectation value and the variance of the diaphony are given by $\mathsf{E}(D_N) = \int_{\mathbf{K}} \mathcal{B}(x,x)\,dx$ and $\mathsf{V}(D_N) = 2\frac{N-1}{N}\int_{\mathbf{K}} \mathcal{B}(x,y)^2\,dxdy$, leading to

$$E := \mathsf{E}(D_N) = 1 \quad , \qquad V_N := \mathsf{V}(D_N) = 2\,\frac{N-1}{N}\,\frac{\left(1+\frac{\pi^4}{45}\right)^{s_N} - 1}{\left[\left(1+\frac{\pi^2}{3}\right)^{s_N} - 1\right]^2} \quad . \tag{6.99}$$

The moments of the diaphony contain contributions of all kind of convolutions of the reduced two-point function $\mathcal{B}$. One such convolution for the fifth moment $\mathsf{E}(D_N^5)$ is given by

$$\begin{aligned}\int_{\mathbf{K}} \mathcal{B}(x,y)^5\,dxdy \;=\; &\left[\left(1+\tfrac{2\pi^4}{9}+\tfrac{4\pi^6}{189}+\tfrac{\pi^8}{189}+\tfrac{4\pi^{10}}{18711}\right)^{s_N} - 5\left(1+\tfrac{2\pi^4}{15}+\tfrac{8\pi^6}{945}+\tfrac{\pi^8}{945}\right)^{s_N}\right.\\ &\left. + 10\left(1+\tfrac{\pi^4}{15}+\tfrac{2\pi^6}{945}\right)^{s_N} - 10\left(1+\tfrac{\pi^4}{45}\right)^{s_N} + 4\right]\left[\left(1+\tfrac{\pi^2}{3}\right)^{s_N} - 1\right]^{-5} .\end{aligned}$$

If s_N becomes large, the leading contribution in the expression above is given by the first term. The convolution contributes to $\mathsf{E}(D_N^5)$ with a third power of $1/N$, and this means that the fifth moment of the standardized variable behaves at least as

$$\frac{\left(1+\frac{2\pi^4}{9}+\frac{4\pi^6}{189}+\frac{\pi^8}{189}+\frac{4\pi^{10}}{18711}\right)^{s_N}}{\left[\left(1+\frac{\pi^2}{3}\right)^{s_N} - 1\right]^5 N^3 V_N^{5/2}} \;>\; \left(\frac{N}{2(N-1)}\right)^{5/2}\left(\frac{(1.85)^{s_N}}{N}\right)^3$$

if N becomes large, and calculation of the other contributions to $\mathsf{E}(D_N^5)$ shows that this behavior is not canceled. So clearly, the fifth moment of the standardized variable may explode in the weak limit of (6.98).

6.3.2 The statement

In this section, we derive a limit in which all moments of the standardized variable converge to the moments of a normal variable, which is therefore 'stronger' than the weak limit, in the sense that if s_N grows with N such that the 'strong' limit appears, it grows such that the criterion of (6.98) is certainly satisfied (Section 2.1.7). Actually, we will see that the 'strong' limit appears under the same type of condition, but of course with a constant $c_s > c_w$. Our exact statement shall be that *if* $s_N \to \infty$ *as* $N \to \infty$ *such that*

$$\limsup_N \frac{c_s^{s_N}}{N} = 0 \tag{6.100}$$

then all moments of the standardized variable converge to the moments of a normal variable. We shall show that it works for $c_s \geq \alpha^{4/3}$ and probably even for $\alpha \leq c_s < \alpha^{4/3}$, where

$$\alpha = \left(1+\tfrac{\pi^2}{3}\right)\left(1+\tfrac{\pi^4}{45}\right)^{-1/2} \quad . \tag{6.101}$$

Note that $\alpha = 2.41146\cdots$ and $\alpha^{4/3} = 3.23376\cdots$.

6.3.3 The scenario

The logarithm $\hat{W} := \log \hat{G}$ of the generating function of the standardized variable is given by

$$\hat{W}(\xi) \;=\; \log \mathsf{E}\left(\exp\left(\xi\,\frac{D_N - E}{\sqrt{V_N}}\right)\right) \;=\; -\frac{E\xi}{\sqrt{V_N}} + W\left(\frac{\xi}{\sqrt{V_N}}\right) \quad , \tag{6.102}$$

where $W := \log G$ is the logarithm of the generating function of the probability distribution of D_N. So $\hat{W}$ can be calculated using the Feynman rules of Section 3.2.4 if $g := \sqrt{2z/N}$ is replaced by $g := \sqrt{2\xi/(N\sqrt{V_N})}$. This is equivalent with using $g := \sqrt{2\xi/N}$ and replacing the propagator $\mathcal{B}$ by $\hat{\mathcal{B}} := \mathcal{B}/\sqrt{V_N}$, and it is this what we shall do. Only connected diagrams contribute to $\hat{W}(\xi)$, and there is only one diagram that gives a contribution linear in ξ, namely

$$\frac{1}{2}\;\bigcirc\!\!\!\!\circlearrowright \;=\; \frac{Ng^2}{2}\int_{\mathbf{K}} \hat{\mathcal{B}}(x,x)\,dx \;=\; \frac{E\xi}{\sqrt{V_N}} \quad , \tag{6.103}$$

which cancels against the term $-E\xi/\sqrt{V_N}$ in Eq.(6.102). The second-order in ξ is given by

$$\frac{1}{4}\;\circlearrowright\!\circlearrowleft \;+\; \frac{1}{4}\;\bigcirc\!\!\!\!\circlearrowright \;+\; \frac{1}{8}\;\infty \;+\; \frac{1}{8}\;\circlearrowright\!\bigcirc\!\circlearrowleft \;=\; \frac{(N^2-N)g^4}{4}\int_{\mathbf{K}} \hat{\mathcal{B}}(x,y)^2\,dx\,dy \;=\; \frac{\xi^2}{2}\,. \tag{6.104}$$

Note that the third and the fourth diagram cancel each other. These results for the first two orders in ξ are in correspondence with the fact that we use the standardized variable. If we find a criterion dictating how $s_N \to \infty$ as $N \to \infty$ such that the contribution of all other diagrams vanishes, regardless of the value of ξ, then this vanishing happens order by order in ξ because each order consists of a sum of diagrams. This then implies that all moments of the standardized variable converge to the moments of a normal variable.

6.3.4 The calculation

In order to calculate the diagrams, we expand $\hat{\mathcal{B}}$ in terms of the complex Fourier basis

$$\hat{\mathcal{B}}(x,y) \;=\; \sum_{\vec{n}} \hat{\sigma}^2_{\vec{n}}\, e^{2\pi i \vec{n}\cdot(x-y)} \quad , \tag{6.105}$$

where the sum is over all $\vec{n} \in \mathbf{Z}^s$ except the constant mode $\vec{n} = (0,0,\ldots,0)$, and we denote $\vec{n}\cdot x := \sum_{\nu=1}^{s} n_\nu x^\nu$. The strengths $\hat{\sigma}_{\vec{n}}$ are given by

$$\hat{\sigma}^2_{\vec{n}} \;=\; \frac{1}{\sqrt{\tau_N}} \prod_{\nu=1}^{s} \frac{1}{r(n_\nu)^2} \quad , \qquad r(n_\nu) = \begin{cases} n_\nu & \text{if } n_\nu \neq 0\,, \\ 1 & \text{if } n_\nu = 0\,, \end{cases} \tag{6.106}$$

where

$$\tau_N \;:=\; \rho_N\left[\left(1+\tfrac{\pi^4}{45}\right)^s - 1\right] \quad , \qquad \rho_N := 2\left(1-\frac{1}{N}\right) \quad . \tag{6.107}$$

Notice that, because we absorbed the factor $\sqrt{V_N}$ in $\hat{\mathcal{B}}$, the strengths depend on N. Because we expanded $\hat{\mathcal{B}}$ in terms of the complex exponentials, convolutions of this two-point function can be calculated as sums over products of the strengths $\hat{\sigma}^2_{\vec{n}}$. As a result of this, we can go over to another boson propagator

$$\vec{n} \cdots\cdots \vec{m} \;=\; \hat{\sigma}^2_{\vec{n}}\, \delta_{\vec{n},-\vec{m}} \quad , \tag{6.108}$$

and the rule that in a vertex with k boson legs, boson propagators have to be convoluted as

$$\sum_{\vec{n}_1,\vec{n}_2,\ldots,\vec{n}_k} \hat{\sigma}^2_{\vec{n}_1}\, \delta_{\vec{n}_1,-\vec{m}_1}\, \hat{\sigma}^2_{\vec{n}_2}\, \delta_{\vec{n}_2,-\vec{m}_2} \cdots \hat{\sigma}^2_{\vec{n}_k}\, \delta_{\vec{n}_k,-\vec{m}_k}\, \theta(\vec{n}_1 + \vec{n}_2 + \cdots + \vec{n}_k = 0) \quad , \tag{6.109}$$

where the logical θ-function expresses that the sum of the labels has to be zero. These Feynman rules give the same result as the original rules.

Because the Fourier diaphony is translation invariant, it is *one-vertex decomposable*, so that we only have to consider *one-vertex irreducible* (1VI) diagrams (Section 6.1.1.4). The other diagrams cancel exactly. For each 1VI diagram that has vertices that are not of the type of Eq.(6.5), there exists a diagram that has exactly the same bosonic part, but only effective vertices of the type of Eq.(6.5), and therefore carries a smaller power of $1/N$. Combining this with the fact that we only have to consider connected diagrams to calculate $\hat{W}(\xi)$, we see that

for the limit of large N*, we only have to consider connected 1VI diagrams with all vertices of the type of Eq.(6.5), which we call relevant.* (6.110)

The power of $1/N$ that is carried by a relevant diagram is given by $1/N^{p/2-\nu}$, where p is the sum of all bosonic legs of all vertices, and ν the number of vertices. Basic graph theory tells us that the number of bosonic lines I is equal to $p/2$, and the number of bosonic loops L is equal to $I - \nu + 1$, so that

the power of $1/N$ *carried by a relevant diagram is* $1/N^{L-1}$*, where* L *is the number of bosonic loops.* (6.111)

So the natural way to order the diagrams is by number of bosonic loops. From now on, the drawing of a diagram only represents the contribution coming from the bosonic part of the diagram, stripped from its factors of $g = \sqrt{2\xi/N}$, its factors of N coming from the fermionic piece, and the symmetry factors, which we call the *bare* contribution.

6.3.4.1 One loop

Diagrams with no loops do not exist (because of the Landau gauge), and the relevant diagrams with only one loop contribute with

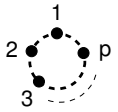

$$\;=\; \sum_{\vec{n}} \hat{\sigma}^{2p}_{\vec{n}} \;=\; \tau_N^{-p/2}\left[\left(1 + \sum_{n=1}^{\infty} \frac{2}{n^{2p}}\right)^s - 1\right] \;\overset{s,N\to\infty}{\longrightarrow}\; \gamma_p^s \tag{6.112}$$

where

$$\gamma_p \;=\; \Big(1+\sum_{n=1}^{\infty}\frac{2}{n^{2p}}\Big)\Big(1+\sum_{n=1}^{\infty}\frac{2}{n^{4}}\Big)^{-p/2} \quad . \tag{6.113}$$

Using the line of argument with Eq. (5.14) and Eq. (5.15), we derive that $\gamma_{p+1} < \gamma_p$. Explicit calculation shows that $\gamma_3 = (\frac{2\pi^6}{945}+1)(\frac{\pi^4}{45}+1)^{-3/2} < 1$, so that $\gamma_p < 1$ for all $p > 2$, and

the contribution of all one-loop diagrams with more than two vertices vanishes if $N \to \infty$ *and* $s \to \infty$. (6.114)

The diagrams with one or two vertices contribute to the first two powers in ξ (Eq. (6.103) and Eq.(6.104)). If $N \to \infty$ and s stays finite, only one-loop diagrams do not vanish, and the analysis above was just a repetition of what was done in Chapter 5.

6.3.4.2 More than one loop

In order to estimate the contribution of the higher-loop diagrams, we observe that, because $0 < \hat\sigma^2_{\vec n} < 1$ for all $\vec n$ and all values of N,

$$\begin{aligned}\sum_{\vec m_1,\vec m_2}\theta(\vec n_1+\vec m_1=0)\,\hat\sigma^2_{\vec m_1}\,\delta_{\vec m_1,-\vec m_2}\,\theta(\vec n_2+\vec m_2=0) \;&<\; \sum_{\vec m}\theta(\vec n_1+\vec m=0)\,\theta(\vec n_2-\vec m=0)\\ &=\; \theta(\vec n_1+\vec n_2=0)\quad .\end{aligned} \tag{6.115}$$

As a result of this, the bare contribution of a relevant diagram can be estimated by repeated application of the operation

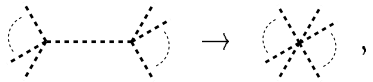 , (6.116)

until only one vertex remains. This operation leaves the number of loops L invariant, so that the bare contribution of a relevant diagram is smaller than

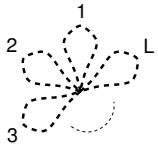

$$\;=\; \Big(\sum_{\vec n}\hat\sigma^2_{\vec n}\Big)^{L} \;=\; \Big(\rho_N^{-1/2}\,d(N)\Big)^{L}\quad , \tag{6.117}$$

where

$$d(N) := \Big(\frac{\rho_N}{\tau_N}\Big)^{1/2}\Big[\Big(1+\sum_{n=1}^{\infty}\frac{2}{n^2}\Big)^{s}-1\Big] = \Big[\Big(1+\tfrac{\pi^2}{3}\Big)^{s}-1\Big]\Big[\Big(1+\tfrac{\pi^4}{45}\Big)^{s}-1\Big]^{-1/2}. \tag{6.118}$$

Using this result, (6.110) and (6.111), we conclude that if $s, N \to \infty$, then the behavior of the contribution of any 1VI diagram with $L > 1$ loops is dominated by

$$\frac{(\alpha^s)^L}{N^{L-1}} \qquad \text{where} \qquad \alpha := \Big(1+\tfrac{\pi^2}{3}\Big)\Big(1+\tfrac{\pi^4}{45}\Big)^{-1/2}\quad , \tag{6.119}$$

so that all diagrams with more than one loop vanish if $s = s_N \to \infty$ as $N \to \infty$, such that

$$\limsup_N \frac{c_s^{s_N}}{N} = 0 \qquad \text{where} \qquad c_s = \alpha^2 \ . \tag{6.120}$$

We have already established that, in the expansion of $\hat{W}(\xi)$ in ξ, there is no linear term, and the quadratic term is given by $\xi^2/2$, as demanded by the fact that we are dealing with the standardized variable. The one-loop diagrams contributing to the higher powers vanish if $s, N \to \infty$, and all other diagrams vanish if (6.120) holds.

6.3.4.3 Leading contributions

In the previous section we have put a bound on the contribution of each diagram, which resulted in (6.120). This result comes from the bound on the two-loop diagrams. For the lower-loop diagrams, however, the determination of the *actual* leading behavior is attainable. There is, for example, only one relevant two-loop diagram, which has the following bosonic structure:

 . (6.121)

Its bare contribution is

$$\int_K \hat{\mathcal{B}}(x,y)^3 \, dxdy \ = \ \frac{\left(1 + \frac{\pi^4}{15} + \frac{2\pi^6}{945}\right)^{s_N} - 3\left(1 + \frac{\pi^4}{45}\right)^{s_N} + 2}{\rho_N^{3/2}\left[\left(1 + \frac{\pi^4}{45}\right)^{s_N} - 1\right]^{3/2}} \ \to \ \frac{b_3^{s_N}}{2^{3/2}} \ , \tag{6.122}$$

where

$$b_3 \ := \ \left(1 + \frac{\pi^4}{15} + \frac{2\pi^6}{945}\right)\left(1 + \frac{\pi^4}{45}\right)^{-3/2} \ < \ \alpha^{3/2} \ , \tag{6.123}$$

so that it suffices to take $c_s = \alpha^{3/2}$ in (6.120). The relevant three-loop diagrams have bosonic parts

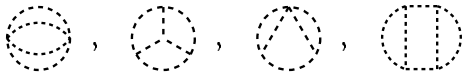 , (6.124)

and using (6.115), we immediately see that the last two diagrams are bounded by the first, which has a bare contribution

$$\int_K \hat{\mathcal{B}}(x,y)^4 \, dxdy \ = \ \frac{\left(1 + \frac{2\pi^4}{15} + \frac{8\pi^6}{945} + \frac{\pi^8}{945}\right)^{s_N} - 4\left(1 + \frac{\pi^4}{15} + \frac{2\pi^6}{945}\right)^{s_N} + 6\left(1 + \frac{\pi^4}{45}\right)^{s_N} - 3}{\rho_N^2\left[\left(1 + \frac{\pi^4}{45}\right)^{s_N} - 1\right]^2}$$

$$\to \ \frac{1}{4}\left[\left(1 + \frac{2\pi^4}{15} + \frac{8\pi^6}{945} + \frac{\pi^8}{945}\right)\left(1 + \frac{\pi^4}{45}\right)^{-2}\right]^{s_N} := \ \frac{1}{4} b_4^{s_N} \ . \tag{6.125}$$

Application of (6.115) shows also that the bare contribution of the second diagram is bounded by

$$\int_{\mathbf{K}} \hat{\mathcal{B}}(x,y)^3 \hat{\mathcal{B}}(z,z)\,dx dy dz \;\to\; \tfrac{1}{4}\left[\left(1+\tfrac{\pi^4}{15}+\tfrac{2\pi^6}{945}\right)\left(1+\tfrac{\pi^2}{3}\right)\left(1+\tfrac{\pi^4}{45}\right)^{-2}\right]^{s_N} \;:=\; \tfrac{1}{4}m^{s_N}\,, \tag{6.126}$$

and we have $b_4^{1/2} < \alpha^{4/3}$ and $m^{1/2} < \alpha^{4/3}$, so that $c_s = \alpha^{4/3}$ also suffices in (6.120). We suspect that this works to all loop-orders, and that we can actually take $c_s = \alpha$.

6.4 Conclusions

We have presented finite-sample corrections to the probability distributions of quadratic discrepancies under sets of N random points. The corrections are terms in an $1/N$ expansion of the generating function of the probability distribution, consisting of the contribution of a finite number of Feynman diagrams. We presented the diagrams up to and including the order of $1/N^2$ for the general case, and derived a rule of diagram cancellation in the case of special discrepancies, which we call one-vertex decomposable. We have applied the formalism to the Lego discrepancy, the L_2^*-discrepancy in one dimension and the Fourier diaphony in one dimension, and calculated the first two terms in the expansion. For the Lego discrepancy, this resulted in Eq.(6.25) and Eq.(6.27), for the L_2^*-discrepancy in Eq.(6.35) and Eq.(6.36), and for the Fourier diaphony in Eq.(6.40) and Eq.(6.41). The Fourier diaphony and the Lego discrepancy with equal binning are one-vertex decomposable. For the latter, we also calculated the $1/N^2$-term, which is in correspondence with the result of an alternative calculation up to the order of $1/N^4$, given in Appendix 6A.

In the second part of the chapter, we focused on the variant of the Lego discrepancy that is equivalent with a χ^2-statistic of N data points distributed over M bins. We have presented a procedure to calculate the generating function perturbatively if M and N become large. The natural expansion parameter we have identified to be M/N, and we have calculated the first few terms in the series explicitly.

In order to calculate limits for the Lego discrepancy in which $N, M \to \infty$, we have introduced the objects of Eq.(6.44) and restricted the behavior of the size of the bins such that they satisfy Eq.(6.45). Furthermore, we have gone over to the standardized variable of the discrepancy. For this variable, we have derived a phase diagram, representing the limits specified by Eq.(6.77) and Eq.(6.78). We have formulated the results in (6.80), (6.81) and (6.82). On of these results is that there are non-trivial limits if $N, M \to \infty$ such that $M^\alpha/N \to$ *constant* with $\alpha < 1$. This result is in stark contrast with the rule of thumb that, in order to trust the χ^2-distribution, each bin has to contain at least a few data points.

Finally, we have derived a limit in which all the moments of the standardized variable of the Fourier diaphony converge to the moments of a normal variable, which is given in (6.100).

6.5 Appendices

Appendix 6A

If we define, for the Lego discrepancy with equal bins, $E = M - 1$, $\eta(z) = 2z/(1-2z)$ and

$$(1-2z)^{E/2} G(z) \;=\; \sum_{n,p \geq 0} \frac{\eta(z)^p}{N^n}\, C_n^{(p)}(E) \quad , \tag{6.127}$$

then the only non-zero $C_n^{(p)}(E)$ up to $n = 4$ are given by

$$\begin{aligned}
C_1^{(2)}(E) &= -\frac{1}{4}E \\
C_1^{(3)}(E) &= E\left(\frac{1}{12}E - \frac{1}{12}\right) \\
C_2^{(3)}(E) &= E\left(-\frac{1}{12}E + \frac{5}{12}\right) \\
C_2^{(4)}(E) &= E\left(\frac{1}{48}E^2 - \frac{53}{96}E + \frac{43}{48}\right) \\
C_2^{(5)}(E) &= E\left(\frac{5}{48}E^2 - \frac{35}{48}E + \frac{5}{8}\right) \\
C_2^{(6)}(E) &= E\left(\frac{1}{288}E^3 + \frac{7}{72}E^2 - \frac{71}{288}E + \frac{7}{48}\right) \\
C_3^{(4)}(E) &= E\left(-\frac{1}{48}E^2 + \frac{7}{12}E - \frac{61}{48}\right) \\
C_3^{(5)}(E) &= E\left(\frac{1}{240}E^3 - \frac{17}{30}E^2 + \frac{583}{120}E - \frac{1451}{240}\right) \\
C_3^{(6)}(E) &= E\left(\frac{53}{576}E^3 - \frac{1153}{384}E^2 + \frac{7423}{576}E - \frac{527}{48}\right) \\
C_3^{(7)}(E) &= E\left(\frac{1}{576}E^4 + \frac{461}{1152}E^3 - \frac{6581}{1152}E^2 + \frac{8663}{576}E - \frac{467}{48}\right) \\
C_3^{(8)}(E) &= E\left(\frac{11}{1152}E^4 + \frac{85}{144}E^3 - \frac{5125}{1152}E^2 + \frac{1555}{192}E - \frac{17}{4}\right) \\
C_3^{(9)}(E) &= E\left(\frac{1}{10368}E^5 + \frac{29}{3456}E^4 + \frac{955}{3456}E^3 - \frac{12475}{10368}E^2 + \frac{953}{576}E - \frac{53}{72}\right) \\
C_4^{(5)}(E) &= E\left(-\frac{1}{240}E^3 + \frac{37}{80}E^2 - \frac{337}{80}E + \frac{1397}{240}\right) \\
C_4^{(6)}(E) &= E\left(\frac{1}{1440}E^4 - \frac{349}{960}E^3 + \frac{7193}{720}E^2 - \frac{15283}{320}E + \frac{67021}{1440}\right) \\
C_4^{(7)}(E) &= E\left(\frac{49}{960}E^4 - \frac{29069}{5760}E^3 + \frac{372169}{5760}E^2 - \frac{571727}{2880}E + \frac{21503}{144}\right)
\end{aligned}$$

$$C_4^{(8)}(E) = E\left(\frac{13}{23040}E^5 + \frac{13979}{23040}E^4 - \frac{2290601}{92160}E^3 + \frac{1446743}{7680}E^2 - \frac{9583187}{23040}E + \frac{294773}{1152}\right)$$

$$C_4^{(9)}(E) = E\left(\frac{73}{6912}E^5 + \frac{35077}{13824}E^4 - \frac{781079}{13824}E^3 + \frac{993515}{3456}E^2 - \frac{564301}{1152}E + \frac{24607}{96}\right)$$

$$C_4^{(10)}(E) = E\left(\frac{1}{13824}E^6 + \frac{139}{3072}E^5 + \frac{162721}{34560}E^4 - \frac{596467}{9216}E^3 + \frac{1653251}{6912}E^2 - \frac{253799}{768}E + \frac{145199}{960}\right)$$

$$C_4^{(11)}(E) = E\left(\frac{17}{41472}E^6 + \frac{895}{13824}E^5 + \frac{55025}{13824}E^4 - \frac{1505645}{41472}E^3 + \frac{19783}{192}E^2 - \frac{137875}{1152}E + \frac{1565}{32}\right)$$

$$C_4^{(12)}(E) = E\left(\frac{1}{497664}E^7 + \frac{11}{31104}E^6 + \frac{2431}{82944}E^5 + \frac{155735}{124416}E^4 - \frac{3942431}{497664}E^3 + \frac{249239}{13824}E^2 - \frac{250141}{13824}E + \frac{2575}{384}\right)$$

Appendix 6B

We want to calculate the integral

$$\hat{H}(\tau) \;=\; \frac{1}{2\pi i}\int_{-i\infty}^{i\infty} e^{f_\tau(z)}\,dz \quad , \quad f_\tau(z) = \frac{1}{\lambda^2}\left(e^{\lambda z} - 1 - \lambda z\right) - z\tau \;\; . \tag{6.128}$$

We will make use of the fact that

$$f_\tau\left(z + \frac{2\pi i n}{\lambda}\right) \;=\; f_\tau(z) - 2\pi i n\frac{1+\lambda\tau}{\lambda^2} \tag{6.129}$$

for all $n \in \mathbf{Z}$, so that

$$\hat{H}(\tau) \;=\; \frac{1}{2\pi i}\sum_{n\in\mathbf{Z}}\int_{\frac{(2n-1)\pi i}{\lambda}}^{\frac{(2n+1)\pi i}{\lambda}} e^{f_\tau(z)}\,dz \;=\; \frac{1}{2\pi i}\sum_{n\in\mathbf{Z}} e^{-2\pi i n\frac{1+\lambda\tau}{\lambda^2}}\int_{\frac{-\pi i}{\lambda}}^{\frac{\pi i}{\lambda}} e^{f_\tau(z)}\,dz \;\; . \tag{6.130}$$

Notice that the integral is independent of n, so that the sum can be interpreted as a sum of Dirac delta-distributions:

$$\sum_{n\in\mathbf{Z}} e^{-2\pi i n\frac{1+\lambda\tau}{\lambda^2}} \;=\; \sum_{n\in\mathbf{Z}}\delta\left(\frac{1+\lambda\tau}{\lambda^2} - n\right) \;=\; \sum_{n\in\mathbf{Z}}\lambda\delta\left(\tau - \left[n\lambda - \frac{1}{\lambda}\right]\right) \;\; . \tag{6.131}$$

These delta-distributions restrict the values that τ can take. If we use these restrictions and do the appropriate variable substitutions, the remaining integral in (6.130) can be reduced to

$$\int_{\frac{-\pi i}{\lambda}}^{\frac{\pi i}{\lambda}} e^{f_\tau(z)}\,dz \;=\; \frac{e^{-\frac{1}{\lambda^2}}}{\lambda}\int_{-\pi i}^{\pi i}\exp\left(\frac{e^\varphi}{\lambda^2}-n\varphi\right)\,d\varphi \;=\; \frac{e^{-\frac{1}{\lambda^2}}}{\lambda}\oint\frac{e^{\frac{1}{\lambda^2}w}}{w^{n+1}}\,dw \quad , \tag{6.132}$$

where $n \in \mathbf{Z}$ and the contour is closed around $w = 0$. According to Cauchy's theorem, the final integral is only non-zero if $n \in \mathbf{N}$, and in that case its value is $2\pi i\frac{1}{n!}(\frac{1}{\lambda^2})^n$. The combination of these results gives Eq.(6.84).

Chapter 7

Phase space integration

In particle physics, there is the need to integrate transition probabilities of particle processes over phase space, the space of all possible configurations of the final-state momenta (Section 1.2.2). This is usually done with the Monte Carlo method, and the first sections of this chapter deal with its basics and some useful techniques. The formalism converges towards the application for phase space in Section 7.4.

Contents

7.1 Monte Carlo integration

For the Monte Carlo (MC) method of numerical integration, the integral of a function F over an integration region $\mathbf{M}$ has to be reduced to the integral of a function f over an s-dimensional hypercube $\mathbf{K} := [0,1]^s$. In order to do so, a suitable mapping $\varphi : \mathbf{K} \mapsto \mathbf{M}$ and the normalization function g_φ have to be determined (Section 1.1.2). A conceptual help in the search for such mappings is considering them algorithms to generate random variables with a certain probability distribution. This probability distribution enters the integration problem as follows. Given a probability density G on $\mathbf{M}$, the integral of F over $\mathbf{M}$ can be written as

$$\langle F \rangle_{\mathbf{M}} := \int_{\mathbf{M}} F(y)\,dy = \int_{\mathbf{M}} \frac{F(y)}{G(y)}\,G(y)dy \quad , \tag{7.1}$$

so that the integral can be interpreted as the expectation value of F/G under the probability density G on $\mathbf{M}$. The only restriction on G is that its support should contain the support of F. The Monte Carlo method can then be directly applied to $\mathbf{M}$. Let us denote the average of a function w over the first N points of a sequence $y_1, y_2, \ldots$ in $\mathbf{M}$ distributed following G by

$$G_N[w] := \frac{1}{N}\sum_{k=1}^{N} w(y_k) \quad , \quad y_1, y_2, \ldots \text{ distributed with density } G(y). \tag{7.2}$$

If w is taken equal to F/G, then the expectation value $E(G_N[w]) = \langle F \rangle_{\mathbf{M}}$ and the variance $V(G_N[w]) = V_G[F]/N$, where

$$V_G[F] := \langle F^2/G \rangle_{\mathbf{M}} - \langle F \rangle_{\mathbf{M}}^2 \quad . \tag{7.3}$$

If $\langle F^2/G \rangle_{\mathbf{M}}$ exists, so that $V_G[F]$ is a finite number, then $G_N[w]$ converges in probability to $\langle F \rangle_{\mathbf{M}}$, and $V_G[F]/N$ can be interpreted as the expected squared error (Section 2.1.5.2). This number is positive by definition, and extremalization with respect to G leads to $G = |F/\langle F \rangle_{\mathbf{M}}|$, which minimizes $V_G[F]$ to zero if F is positive. Importance sampling can be interpreted as the effort to make G look like $|F|$ as much as possible. The squared error can be estimated with

$$G_N^{(2)}[w] := \frac{G_N[w^2] - G_N[w]^2}{N-1} \quad , \tag{7.4}$$

which satisfies $E(G_N^{(2)}[w]) = V(G_N[w])$. The integration is done most efficiently if the numbers $w(y_i)$ fluctuate as little as possible, so that $G_N^{(2)}[w]$ is as small as possible. That is what importance sampling should take care of. The expected squared error on the error can be estimated with the help of

$$G_N^{(4)}[w] := \frac{G_N[w^4] - 4G_N[w^3]G_N[w] + 3G_N[w^2]^2}{N(N-2)(N-3)} - \frac{(4N-6)G_N^{(2)}[w]^2}{(N-2)(N-3)} \quad , \tag{7.5}$$

which satisfies $E(G_N^{(4)}[w]) = V(G_N^{(2)}[w])$. If $\langle F^4/G^3 \rangle_{\mathbf{M}}$ exists, then $G_N^{(4)}[F/G]$ is a good estimator for the the expected squared error on the estimate of the expected squared integration error.

The integration problem is now for large part reduced to that of generating the sequence of points in $\mathbf{M}$ with the density G. In practice, the mapping φ still has to be made explicit, because algorithms usually start with the generation of numbers between 0 and 1, but the analysis of the whole algorithm can be done on a 'higher level' by considering the piece that generates the y-variables a given 'black box'. The connection with Section 1.1.2 can be established by taking $g_\varphi := G \circ \varphi$.

7.2 The unitary algorithm formalism

In general, it is hard to find an efficient algorithm to generate sequences with a given distribution. It is often even hard to determine the density under which a sequence, generated with a given algorithm, is distributed. For a certain class of algorithms the latter can be done analytically with the unitary algorithm formalism (UAF). This is the class of *unitary* algorithms, that is, algorithms which produce an output with probability one. This may sound a bit mysterious, and in order to explain what we mean, we introduce the class of *stepwise unitary* (SU) algorithms, of which all *steps* produce an output with probability one. We illustrate this with an example of a non-SU algorithm to generate a fair dice with five sides:

1. throw a fair dice, output $\leftarrow$ number of points;
2. if the number of points is less than six: output $\leftarrow$ number of points, else throw again.

The first step produces an output with probability one: if you throw a dice, it generates a number. The second step, however, produces an output with probability $\frac{5}{6}$, so that the algorithm is not SU. The whole algorithm, *is* unitary: the probability to produce no output is $\lim_{n\to\infty} \left(\frac{1}{6}\right)^n = 0$. Consequently, stepwise unitary is a relative concept. The steps may be "black boxes" that can be trusted to produce an output with probability one. Consider the following algorithm to generate numbers between 1 and 11:

1. throw a fair dice with five sides, output $\leftarrow$ number of points;
2. throw the dice again, output $\leftarrow$ number of points plus previous number of points.

This is a SU algorithm as long as we do not ask the question how the fair dice with five sides is generated.

7.2.1 Notation

We shall introduce the UAF with the help of two examples, but first we have to introduce some notation. We will frequently use the logical step function θ, which returns 1 if a statement Π is true, and 0 otherwise:

$$\theta(\Pi) := \begin{cases} 1 & \text{if } \Pi \text{ is true}, \\ 0 & \text{if } \Pi \text{ is false}. \end{cases} \tag{7.6}$$

A relation that is satisfied by this function and that we will often use is

$$\theta(\Pi) = 1 - \theta(\text{not}\,\Pi) \quad . \tag{7.7}$$

Also the Dirac delta-distribution will often appear, and we recall its most important features (cf. [4]): if F is a sufficiently regular function on $\mathbf{M}$, then

$$\int_{\mathbf{M}} F(y)\delta(y - y')\,dy \;=\; F(y') \quad , \tag{7.8}$$

and if $\varphi : x \mapsto y$ is an invertible and differentiable mapping, then

$$\delta(\varphi^{-1}(y) - x) \;=\; |J_\varphi(x)|\delta(\varphi(x) - y) \quad , \tag{7.9}$$

where J_φ is the determinant of the Jacobian matrix of φ. An integral over many variables will from now on start with a single $\int$-symbol, and for every variable z a dz means 'integrate z over the appropriate integration region'. The order in which the variables appear is irrelevant. If it is not evident what the 'appropriate integration region' is, we shall make it explicit with the help of θ-functions.

7.2.2 The UAF for SU algorithms

The following is an example of the use of the UAF for a SU algorithm. It is an algorithm to generate n numbers y_i, $i = 1, \ldots, n$ uniformly distributed in $[0, 1]$ such that their sum is equal to 1, and we are going to prove that it actually does. The algorithm goes as follows:

1. generate n numbers z_i, $i = 1, \ldots, n$ in $[0, \infty)$, distributed independently and with density e^{-z_i};
2. put $L \leftarrow \sum_{i=1}^{n} z_i$;
3. put $y_i \leftarrow z_i/L$ for $i = 1, \ldots, n$.

The algorithm clearly produces numbers the sum of which is equal to 1. The question is whether they are distributed uniformly, i.e., whether the density is, up to a normalization constant, equal to $\delta\,(1 - \sum_{i=1}^{n} y_i)$. The UAF can answer the question as follows. Write every generation of a variable in the algorithm as the integral over the density with which it is generated, and interpret every assignment as a generation with a density that is given by a Dirac delta-distribution. Only the assignment of the final output should not be written as an integral, but only with the delta-distributions. The integral obtained gives the generated density P. So in this case we have

$$P(y) \;=\; \int \Big(\prod_{i=1}^{n} dz_i\, e^{-z_i}\Big)\, dL\, \delta\Big(L - \sum_{i=1}^{n} z_i\Big)\Big(\prod_{i=1}^{n} \delta(y_i - z_i/L)\Big) \quad . \tag{7.10}$$

The unitarity of the algorithm is represented by the fact that integration over the y-variables of this equation gives the identity $1 = 1$. To find the density, we have to eliminate the z_i-and L-integrals. Application of the rules for the delta-distributions gives

$$P(y) \;=\; \int \delta\Big(1 - \sum_{i=1}^{n} y_i\Big)\, dL\, L^{n-1} e^{-L}\, \theta(0 \le L \le \infty) \;=\; \Gamma(n)\, \delta\Big(1 - \sum_{i=1}^{n} y_i\Big)\;, \qquad (7.11)$$

and we see that the the y_i-variables are generated with the correct density. We even calculated the normalization factor, which is $\Gamma(n) = (n-1)!$. The step 'generate z with density e^{-z}' is a black box in this example, but can be made explicit. Such variable can be obtained by generating x uniformly in $[0,1]$ and putting $z \leftarrow -\log(x)$, since

$$\int dx\, \delta(z + \log(x))\, \theta(0 \le x \le 1) \;=\; e^{-z}\;. \qquad (7.12)$$

7.2.3 The UAF for non-SU algorithms

As an application of the UAF to a non-SU algorithm, we show the correctness of the ratio-of-uniforms method for the generation of a random variable with a given density g. The algorithm goes as follows [5]. Let $b \ge \sup_y \sqrt{g(y)}$, $a_- \le \inf_y y\sqrt{g(y)}$ and $a_+ \ge \sup_y y\sqrt{g(y)}$. Then one has to

1. generate x_1 uniformly in $[0, b]$;
2. generate x_2 uniformly in $[a_-, a_+]$;
3. if $x_2^2 \le g(x_1/x_2)$ then put $y \leftarrow x_1/x_2$, else reject x_1, x_2 and start anew.

Just as our algorithm for the fair dice with five sides, it uses the rejection method, and the third step is not unitary. For this algorithm, we can write down a recursive equation for the probability density P that is generated. If we denote the volume of the space in which x_1 and x_2 are generated V, then this equation is then given by

$$P(y) = \int dx_1 dx_2\, \frac{1}{V} \Big[\theta\left(x_2^2 \le g(x_1/x_2)\right) \delta(y - x_1/x_2) + \theta\left(x_2^2 > g(x_1/x_2)\right) P(y)\Big]\;. \qquad (7.13)$$

Integration of the equation over y gives the identity $1 = 1$ again, expressing the unitarity of the algorithm. If we now use Eq. (7.7) and replace the variables x_1, x_2 by $t := x_1/x_2$ and $z := x_2^2$, we get the equation

$$P(y) \;=\; \int dt\, dz\, \frac{1}{V} \left\{\theta(z \le g(t))\, [\delta(y - t) - P(y)] + P(y)\right\}\;. \qquad (7.14)$$

The region in which x_1 and x_2 are generated are such that $\inf_y g(y) \le z \le \sup_y g(y)$. Furthermore is $\int dt\, dz = \int dx_1 dx_2 = V$, so that the equation becomes

$$0 \;=\; \int dt\, \frac{1}{V}\, g(t)\, [\delta(y - t) - P(y)] \quad\Longrightarrow\quad P(y) = \frac{g(y)}{\int dt\, g(t)}\;, \qquad (7.15)$$

and we see that the algorithm is correct. We even see that the function g, used in the algorithm, does not have to be normalized: the algorithm itself is unitary.

7.3 Some useful techniques

7.3.1 Inversion

The most straightforward way of generating random variables $y \in \mathbf{M}$ following a certain probability distribution G is with an invertible mapping $\varphi : \mathbf{K} \mapsto \mathbf{M}$, by generating $x \in \mathbf{K}$ and putting $y \leftarrow \varphi(x)$. The generated density P is given by

$$P(y) \;=\; \int_{\mathbf{K}} dx\, \delta(y - \varphi(x)) \;=\; |J_{\varphi^{-1}}(y)| \;\;, \tag{7.16}$$

so that $|J_{\varphi^{-1}}(y)|$ should be equal to $G(y)$. The search for φ is an integration and inversion problem, and is usually very hard to solve in practice, even for one-dimensional variables.

7.3.2 Crude MC

Sometimes, part of the difficulty of the integration problem lies in the shape of the integration region $\mathbf{M}$, which might be complicated. Usually, however, it can be seen as a subspace of a simpler manifold $\overline{\mathbf{M}}$ with the same dimension. One can look for a probability density G on $\overline{\mathbf{M}}$ then, and integrate the function $F\vartheta_{\mathbf{M}}$, where $\vartheta_{\mathbf{M}}$ is the characteristic function of $\mathbf{M}$. This just means that a density

$$\frac{G\vartheta_{\mathbf{M}}}{\langle G\vartheta_{\mathbf{M}}\rangle_{\overline{\mathbf{M}}}} \tag{7.17}$$

is used on $\overline{\mathbf{M}}$. The algorithm to generate a sequence of variables y following this density is very simple:

1. generate x in $\overline{\mathbf{M}}$ following G;
2. if $x \in \mathbf{M}$ then put $y \leftarrow x$, else reject x and start anew.

This is called *crude* or *hit-and-miss* MC. The proof of the correctness is also simple. In the UAF, the generated density P satisfies

$$P(y) \;=\; \int dx\, G(x)[\theta(x \in \mathbf{M})\delta(y - x) + \theta(x \notin \mathbf{M})P(y)] \;\;. \tag{7.18}$$

If we use Eq.(7.7) and evaluate the integrals, (7.17) is found as the solution to the equation.

In principle, this method always works, but can be inefficient if the volume of $\overline{\mathbf{M}}$ is much larger than the volume of $\mathbf{M}$. If the integrand is as simple as possible, i.e., $F(y) = 1$ so that the original problem was that of determining the volume $\mathrm{Vol}(\mathbf{M})$ of $\mathbf{M}$, and if one would take for G the uniform distribution on $\overline{\mathbf{M}}$, then

$$V_G[F] \;=\; \mathrm{Vol}(\mathbf{M})[\mathrm{Vol}(\overline{\mathbf{M}}) - \mathrm{Vol}(\mathbf{M})] \;\;. \tag{7.19}$$

So if the difference between the volumes is large, one better chooses a density G that is substantially larger on $\mathbf{M}$ than on $\overline{\mathbf{M}} - \mathbf{M}$.

7.3.3 Rejection

Crude MC is a special case of the rejection method to generate variables y following a density F on $\mathbf{M}$. One needs an algorithm to generate variables on $\mathbf{M}$ following some density G and a number c such that $cG(y) > F(y)$ for all $y \in \mathbf{M}$. To obtain the density F, one should

1. generate x following G, and ρ uniformly in $[0,1]$;
2. if $\rho cG(x) \leq F(x)$ then put $y \leftarrow x$, else reject x, ρ and start anew.

The generated density P satisfies

$$P(y) \;=\; \int dx G(x)\, d\rho\, [\theta(\,\rho cG(x) \leq F(x)\,)\,\delta(y-x) + \theta(\,\rho cG(x) > F(x)\,)P(y)]\;, \qquad (7.20)$$

and if we use Eq. (7.7) again and the fact that $\int_0^1 d\rho\,\theta(a\rho \leq b) = b/a$, the solution $P(y) = F(y)/\langle F\rangle_{\mathbf{M}}$ is found. In principle, this method works for any bounded F, since there are always an easy to generate density G and a c that will do the job: $G = 1/\mathrm{Vol}(\,\mathbf{M}\,)$ and $c \geq \mathrm{Vol}(\,\mathbf{M}\,)\sup_{y\in\mathbf{M}} F(y)$. However, the algorithm can become very inefficient. The efficiency can be expressed by $\langle F\rangle_{\mathbf{M}}/(c\langle G\rangle_{\mathbf{M}})$, and if this number is small, the variable x will often be rejected in step 2.

7.3.4 Sum of densities

As an example in which integer random variables have to be generated, we present a method to generate a density that is the normalized sum of a number of positive functions g_i with $i = 1,\ldots,n$. To generate the density

$$G(y) \;=\; \sum_{j=1}^{n} \bar{g}_i(y) \quad , \qquad \bar{g}_i(y) := \frac{g_i(y)}{\sum_{j=1}^{n}\langle g_j\rangle_{\mathbf{M}}} \;, \qquad (7.21)$$

one has to

1. generate an integer i with probability $\langle \bar{g}_i\rangle_{\mathbf{M}}$ and put $k \leftarrow i$;
2. generate x with density g_k and put $y \leftarrow x$.

To cast it into the UAF, a summation over the integer random variable has to be included into the equation for the density generated:

$$P(y) \;=\; \int \sum_{i=1}^{n} \langle \bar{g}_i\rangle_{\mathbf{M}}\, \delta_{i,k}\, dx\, g_k(x)\delta(y-x) \;. \qquad (7.22)$$

The assignment '$k \leftarrow i$' is represented by the Kronecker delta-symbol $\delta_{i,k}$. Evaluation of the integrals leads trivially to the correct density. To generate i, the unit interval $[0,1]$ can be dissected into n bins of size $\langle \bar{g}_i\rangle_{\mathbf{M}}$, and i becomes the number of the bin a random number z, distributed uniformly in $[0,1]$, falls in.

7.3.5 Adaptive MC

If one considers the actual calculation of a MC-integral a real random process, it is a small step to the question whether the density G may change during the process. The answer is yes (Section 2.1.5.2). If y_1 is generated following a density G_1, and then y_2 following G_2 which depends on y_1, and then y_3 following G_3 which depends on $\{y\}_2 := \{y_1, y_2\}$ and so on, then $N^{-1}\sum_{k=1}^{N} F(y_k)/G_k(\{y\}_k)$ converges in probability to $\langle F\rangle_{\mathbf{M}}$, with an estimated squared error given by $V_N[F]/N$, where

$$V_N[F] \;:=\; \frac{1}{N}\sum_{k=1}^{N}\langle \bar{G}_k^{-1}F^2\rangle_{\mathbf{M}} \;-\; \langle F\rangle_{\mathbf{M}}^2 \;\;, \tag{7.23}$$

with

$$\bar{G}_k^{-1}(x_k) \;:=\; \int_{\mathbf{M}^{k-1}} \frac{G_1(y_1)\cdots G_{k-1}(\{y\}_{k-1})}{G_k(\{y\}_k)}\, dy_1\cdots dy_{k-1} \;\;. \tag{7.24}$$

The explicit dependence on N of this expression shows that, by adapting the density for each integration point in the right way, the error may be reduced and the integration process optimized.

An example of a method to adapt the variance is weight optimization in multichannel-MC [30], in which a density $G_\alpha(y) := \sum_{i=1}^{n}\alpha_i g_i(y)$ is generated, where each function g_i is a probability density itself, and the parameters α_i are positive and satisfy $\sum_{i=1}^{n}\alpha_i = 1$. Let us define

$$W_i(\alpha) \;:=\; \int_{\mathbf{M}} \frac{F(y)^2}{G_\alpha(y)^2}\, g_i(y)\, dy \;\;, \tag{7.25}$$

so that $V_{G_\alpha}[F] = \sum_{i=1}^{n}\alpha_i W_i(\alpha) - \langle F\rangle_{\mathbf{M}}^2$. It is not difficult to see that the variance, as function of the parameters α_i, has a (local) minimum if the values of these parameters are such that $W_i(\alpha)$ has the same value for all $i = 1,\ldots,n$. Of course, the problem of finding these values is possibly even more difficult than the original integration problem, but with adaptive MC the values might be found approximately using an iterative procedure. The variance will then improve with each step.

In [30], the following is suggested: one starts with some (sensible) values for the parameters α_i and, after generating a number of N points y_k following the density G_α, one estimates $W_i(\alpha)$ with

$$E_i \;:=\; \frac{1}{N}\sum_{k=1}^{N}\frac{g_i(y_k)F(y_k)^2}{G_\alpha(y_k)^3} \tag{7.26}$$

for all $i = 1,\ldots,n$. These numbers are then used to improve the values of the parameters, for example through the prescription

$$\alpha_i \leftarrow c\alpha_i\sqrt{E_i} \tag{7.27}$$

where c is some constant. The plausibility of this prescription is supported by the example of stratified sampling, in which the functions g_i are normalized characteristic functions $\vartheta_i/\langle\vartheta_i\rangle_{\mathbf{M}}$ of non-overlapping subspaces of the integration region. In that case, $W_i(\alpha) = \alpha_i^{-2}\langle\vartheta_i\rangle_{\mathbf{M}}\langle\vartheta_i F^2\rangle_{\mathbf{M}}$, and we see that putting $\alpha_i \leftarrow c\alpha_i\sqrt{W_i(\alpha)}$ will give the local minimum immediately, starting from any configuration for the parameters α_i.

7.4 Random momenta beautifully organized

As mentioned in Section 1.2.2, particle physicists often need to integrate differential cross sections over phase space (PS), which is the space of all physically possible final-state momentum configurations. Usually, it depends on the transition amplitude which configurations are allowed, and here we mean by PS the space of all final-state momentum configurations for which the separate momenta sum up to a given momentum, and for which the particles have given masses. Because these restrictions reduce the dimension of the integration region, it has measure zero in the space of all momentum configurations so that the crude MC method is no option.

One way to generate PS is by sequential two-body decays, i.e., by the recursive splitting of each momentum generated so far into two momenta (cf. [31]). The drawback of this method is that the efficiency is poor if the number of momenta and the total energy become large (cf. [32]). The high-energy limit is equivalent with the limit in which the masses of the particles become negligible, and for this situation, `RAMBO` [32] can be used. It generates any number of massless momenta with a given total energy distributed uniformly in PS. We will not deal with the algorithm adapted for the generation of massive momenta [33]. Another approach to PS generation, which we will also not address, uses the help of the metropolis algorithm [34].

7.4.1 Notation

The relativistic momentum of an elementary particle is a vector in $\mathbf{R}^4$. Its first component, also called the 0-component, gives the energy of the particle [1], and the other three components give the real momentum in three-dimensional space:

$$p = (p^0, p^1, p^2, p^3) := (p^0, \vec{p}) \quad . \tag{7.28}$$

The momentum with the opposite 3-momentum is denoted by

$$\tilde{p} := (p^0, -\vec{p}) \quad . \tag{7.29}$$

The interpretation of $\mathbf{R}^4$ as a real vector space can be carried forward in the sense that a system of non-interacting particles has a momentum that is equal to the sum of the momenta of the separate particles. We shall need the first and the fourth canonical basis vectors, which we denote

$$e_0 := (1,0,0,0) \qquad \text{and} \qquad e_3 := (0,0,0,1) \quad . \tag{7.30}$$

[1] We use units with which the speed of light is equal to 1.

$\mathbf{R}^4$ becomes Minkowski space if it is endowed with the Lorentz invariant quadratic form

$$p^2 := (p^0)^2 - |\vec{p}|^2 \quad , \qquad |\vec{p}| := [(p^1)^2 + (p^2)^2 + (p^3)^2]^{1/2} \quad . \tag{7.31}$$

The same notation for the quadratic form and the 2-component will not lead to confusion, because the 2-component will not appear explicitly anymore after this section. The combination $(p+q)^2 - p^2 - q^2$ defines a bi-linear product of two momenta, which is two times the scalar product

$$(pq) := p \cdot q := p^0 q^0 - \vec{p} \cdot \vec{q} \quad , \qquad \vec{p} \cdot \vec{q} := p^1 q^1 + p^2 q^2 + p^3 q^3 \ . \tag{7.32}$$

The notation with the parentheses shall be used in the next chapter. For physical particles, p^2 has to be positive, and in that case, the square root gives the invariant mass of the particle:

$$m_p := \sqrt{p^2} \quad \text{if } \ p^2 \geq 0 \ . \tag{7.33}$$

The group of linear transformations on $\mathbf{R}^4$ that leave the quadratic form invariant, and the members of which have determinant 1 and leave the sign of the 0-component of a momentum invariant, is called the Lorentz group. It is generated by boosts, which are represented by symmetric matrices, and rotations, which are represented by orthogonal matrices. A boost that transforms a momentum p, with $p^2 > 0$, to $m_p e_0$ is denoted $\mathcal{H}_p$, so

$$\mathcal{H}_p p = m_p e_0 \qquad \text{and} \qquad m_p \mathcal{H}_p e_0 = \tilde{p} \ . \tag{7.34}$$

More explicitly, such a boost is given by

$$\mathcal{H}_p q = (a, \vec{q} - b\vec{p}) \qquad \text{where} \qquad a = \frac{p \cdot q}{m_p} \ , \quad b = \frac{q^0 + a}{p^0 + m_p} \ . \tag{7.35}$$

A rotation that transforms p to $p^0 e_0 + |\vec{p}| e_3$ is denoted $\mathcal{R}_p$, so

$$\mathcal{R}_p p = p^0 e_0 + |\vec{p}| e_3 \qquad \text{and} \qquad \mathcal{R}_p \tilde{p} = p^0 e_0 - |\vec{p}| e_3 \ . \tag{7.36}$$

Since rotations only change the 3-momentum, we shall use the same symbol if a rotation is restricted to three-dimensional space.

The physical PS of n particles is the $(3n-4)$-dimensional subspace of $\mathbf{R}^{4n}$, given by the restrictions that the energies of the particles are positive, the invariant masses squared p_i^2 are fixed to given positive values s_i, and that the sum

$$p_{(n)} := \sum_{i=1}^{n} p_i \tag{7.37}$$

of the momenta is fixed to a given momentum P. The restrictions for the separate momenta can be expressed with a 'PS characteristic distribution'

$$\vartheta_{s_i}(p) := \delta(p^2 - s_i)\, \theta(p^0 > 0) \quad , \qquad \text{and} \qquad \vartheta(p) := \vartheta_0(p) \quad . \tag{7.38}$$

The generic PS integral, of a function F of a set $\{p\}_n := \{p_1, \ldots, p_n\}$ of momenta, that has to be calculated is then given by

$$\int_{\mathbf{R}^{4n}} \Big(\prod_{i=1}^{n} d^4 p_i \vartheta_{s_i}(p) \Big) \, \delta^4(p_{(n)} - P) \, F(\{p\}_n) \quad . \tag{7.39}$$

We explicitly write down the number of degrees of freedom in the differentials and the delta-distributions in order to keep track of the dimensions. Each momentum component carries the dimension of a mass.

7.4.2 The algorithm

RAMBO was developed with the aim to generate the flat PS distribution of n massless momenta as uniformly as possible, and such that the sum of the momenta is equal to $\sqrt{s}\, e_0$ with s a given squared energy. This means that the system of momenta is in its center-of-mass frame (CMF), and that the density is proportional to the 'PS characteristic distribution'

$$\Theta_s(\{p\}_n) \;:=\; \delta^4(p_{(n)} - \sqrt{s}\, e_0) \prod_{i=1}^{n} \vartheta(p_i) \quad . \tag{7.40}$$

The algorithm consists of the following steps:

Algorithm 7.4.1 (RAMBO)

1. generate n massless vectors q_j with positive energy without constraints but under some normalized density $f(q_j)$;
2. compute the sum $q_{(n)}$ of the momenta q_j;
3. determine the Lorentz boost and scaling transform that bring $q_{(n)}$ to $\sqrt{s}\, e_0$;
4. perform these transformations on the q_j, and call the result p_j.

Trivially, the algorithm generates momenta that satisfy the various δ-constraints, but it is not clear a priori that the momenta have the correct distribution. To prove that they actually do, we apply the UAF. It tells us that the generated density Φ_s is given by

$$\begin{aligned} \Phi_s(\{p\}_n) = \int \Big(\prod_{j=1}^{n} d^4 q_j \vartheta(q_j) f(q_j) \Big) \, d^4 b \, \delta^4 \Big(b - \frac{q_{(n)}}{m_{q_{(n)}}} \Big) \, dx \, \delta \Big(x - \frac{\sqrt{s}}{m_{q_{(n)}}} \Big) \\ \times \prod_{i=1}^{n} \delta^4(p_i - x \mathcal{H}_b q_i) \quad . \end{aligned} \tag{7.41}$$

To calculate the distribution yielded by this algorithm, the integral has to be evaluated. First of all, some simple algebra using $p_{(n)} = x \mathcal{H}_b q_{(n)}$, $q_{(n)} = x^{-1} \mathcal{H}_b^{-1} p_{(n)}$ and the Lorentz and scaling properties of the Dirac δ-distributions leads to

$$\delta^4 \Big(b - \frac{q_{(n)}}{m_{q_{(n)}}} \Big) \, \delta \Big(x - \frac{\sqrt{s}}{m_{q_{(n)}}} \Big) \;=\; \frac{2 s^2}{x} \, \delta^4(p_{(n)} - \sqrt{s}\, e_0) \, \delta(b^2 - 1) \quad . \tag{7.42}$$

Furthermore, since we may write

$$d^4q_j\,\delta(q_j^2)\,\delta^4(p_j - x\mathcal{H}_b q_j) \;=\; \frac{1}{x^2}\,\delta(p_j^2) \tag{7.43}$$

under the integral, the l.h.s. of Eq.(7.41) becomes

$$\int \Theta_s(\{p\}_n)\,d^4b\,\delta(b^2-1)\,dx\frac{2s^2}{x^{2n+1}}\prod_{i=1}^{n} f(\frac{1}{x}\mathcal{H}_b^{-1}p_i)\,\theta(e_0\cdot\mathcal{H}_b^{-1}p_j>0)\;. \tag{7.44}$$

In the standard RAMBO algorithm, the following choice is made for f:

$$f(q) \;=\; \frac{c^2}{2\pi}\,\exp(-cq^0)\;, \tag{7.45}$$

where c is a positive number with the dimension of an inverse mass. Therefore, if we use that $p_{(n)} = \sqrt{s}\,e_0$ and that $q^0 = e_0\cdot q$ for any q, then

$$\begin{aligned}\prod_{i=1}^{n} f(\frac{1}{x}\mathcal{H}_b^{-1}p_i)\,\theta(e_0\cdot\mathcal{H}_b^{-1}p_i>0) \;&=\; \left(\frac{c^2}{2\pi}\right)^n \exp\left(-\frac{c}{x}\,e_0\cdot\mathcal{H}_b^{-1}p_{(n)}\right)\prod_{i=1}^{n}\theta(e_0\cdot\mathcal{H}_b^{-1}p_i>0)\\ &=\; \left(\frac{c^2}{2\pi}\right)^n \exp\left(-\frac{c\sqrt{s}}{x}\,b^0\right)\,\theta(b^0>0)\;.\end{aligned} \tag{7.46}$$

As a result of this, the variables p_i, $i = 1,\ldots,n$ only appear in Θ_s, as required. The remaining integral is calculated in the Appendix at the end of this section, with the result that RAMBO generates the density

$$\Phi_s(\{p\}_n) \;=\; \Theta_s(\{p\}_n)\left(\frac{2}{\pi}\right)^{n-1}\frac{\Gamma(n)\Gamma(n-1)}{s^{n-2}}\;. \tag{7.47}$$

Incidentally, we have computed here the volume of the PS for n massless particles:

$$\int_{\mathbf{R}^{4n}} d^{4n}p\,\Theta_s(\{p\}_n) \;=\; \left(\frac{\pi}{2}\right)^{n-1}\frac{s^{n-2}}{\Gamma(n)\Gamma(n-1)}\;. \tag{7.48}$$

Note, moreover, that c does not appear in the final answer; this is only natural since any change in c will automatically be compensated by a change in the computed value for x. Finally, it is important to realize that the 'original' PS has dimension $3n$, while the resulting one has dimension $3n-4$: there are configurations of the momenta q_j that are different, but after boosting and scaling end up as the same configuration of the p_j. It is this reduction of the dimensionality that necessitates the integrals over b and x.

The first step of the algorithm consists of generating massless momenta with positive energy. To generate such momenta, we use that

$$d^4p\vartheta(p) \;=\; d\varphi\,dz\,dp^0p^0\,\theta(p^0>0)\,\theta(0\le\varphi\le 2\pi)\,\theta(-1\le z\le 1)\;, \tag{7.49}$$

with $p = (\,p^0, p^0\hat{n}(z,\varphi)\,)$, where

$$\hat{n}_1(z,\varphi) := \sqrt{1-z^2}\sin\varphi\;,\quad \hat{n}_2(z,\varphi) := \sqrt{1-z^2}\cos\varphi\;,\quad \hat{n}_3(z,\varphi) := z\;. \tag{7.50}$$

From this we can directly see that, to generate p following a density proportional to $\vartheta(p)f(p^0)$, one should

Algorithm 7.4.2 (MASSLESS MOMENTUM)

1. generate p^0 in $[0,\infty)$ following a density $\sim p^0 f(p^0)$;
2. generate φ uniformly distributed in $[0,2\pi]$ and z uniformly in $[-1,1]$;
3. construct $\hat{n}(z,\varphi)$ and put $\vec{p} \leftarrow p^0 \hat{n}(z,\varphi)$.

To generate p^0 following the density $p^0 \exp(-p^0)$, one can

Algorithm 7.4.3 (0-COMPONENT)

1. generate x_1 and x_2 distributed uniformly in $[0,1]$;
2. put $p^0 \leftarrow -\log(x_1 x_2)$,

since

$$\int dx_1 dx_2\, \theta(0 \le x_{1,2} \le 1)\, \delta(\, p^0 + \log(x_1 x_2)\,) \;=\; \int_{e^{-p^0}}^1 dx\, \frac{e^{-p^0}}{x} \;=\; p^0 e^{-p^0}\;. \tag{7.51}$$

7.4.3 Appendix

We have to calculate the integral

$$2s^2 \left(\frac{c^2}{2\pi}\right)^n \int dx d^4b\, \delta(b^2-1)\, \theta(b^0>0)\, \frac{1}{x^{2n+1}}\, \exp\left(-\frac{c\sqrt{s}}{x}\, b^0\right) \;=\; \frac{2\Gamma(2n)\, B(n)}{(2\pi)^n s^{n-2}}\;,$$

where

$$B(n) \;:=\; \int d^4b\, \delta(b^2-1)\, \theta(b^0>0)\, (b^0)^{-2n} \;=\; 2\pi \int_1^\infty db^0\, (b^0)^{-2n}\, \sqrt{(b^0)^2-1}\;.$$

The 'Euler substitution' $b^0 := \frac{1}{2}\,(v^{1/2} + v^{-1/2})$ casts the integral in the form

$$B(n) \;=\; 2^{2n-2}\pi \int_1^\infty dv\, \frac{(v-1)^2 v^{n-2}}{(v+1)^{2n}}\;.$$

By the transformation $v \to 1/v$ it can easily be checked that the integral from 1 to ∞ is precisely equal to that from 0 to 1, so that we may write

$$B(n) \;=\; \frac{2^{2n-2}\pi}{2} \int_0^\infty dv\, \frac{v^n - 2v^{n-1} + v^{n-2}}{(1+v)^{2n}} \;=\; 4^{n-1}\pi\, \frac{\Gamma(n-1)\Gamma(n)}{\Gamma(2n)}\;,$$

where we have used, by writing $z := 1/(1+v)$, that

$$\int_0^\infty dv\, v^p (1+v)^{-q} \;=\; \int_0^1 dz\, z^{q-p-2}(1-z)^p \;=\; \frac{\Gamma(q-p-1)\Gamma(p+1)}{\Gamma(q)}\;.$$

Chapter 8

Generating QCD-antennas

An algorithm to generate random momenta, distributed with a density that contains the singular structure typically found in QCD-processes, is introduced. For the notation used we refer to Section 7.4.

Contents

8.1 Introduction

In future experiments with hadron colliders, such as the LHC, many multi-jet final states will occur, which have very high particle multiplicities. The initial states will consist of two hadrons

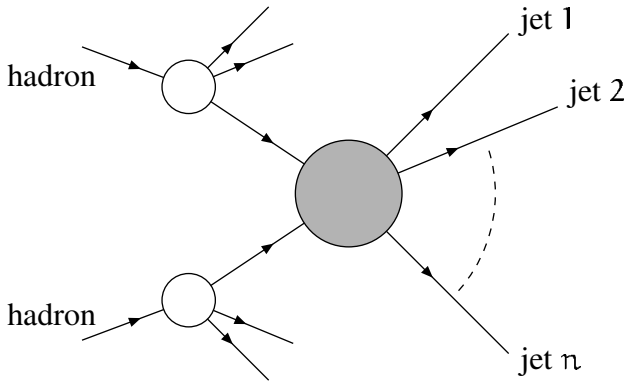

Figure 8.1: A generic multi-jet event

in the center-of-mass frame (CMF). The processes involved in one transition (one *event*) are very complicated, and are usually considered to consist of three steps. The generic situation is depicted schematically in Fig. 8.1. Time can be considered to flow from the left to the right in the picture. The hadrons start the interaction with the emission of partons. The transition of a hadron into the emitted parton and the leftover is represented by the white blobs. This is the first step. In the second step, represented by the grey blob, the partons interact, resulting in n new partons. In step three, these partons turn into jets with high particle multiplicities. The idea is that the contribution of the three steps more-or-less factorize in the transition amplitude of the whole event, and that the processes can be dealt with separately. In this chapter, we deal with step two, the grey blob.

The multi-jet events that will occur in hadron colliders can be divided into interesting events (IE) and very interesting events (VIE). The main difference between the two classes is that the existing model of elementary particles, the standard model, shall not have proven yet its capability of dealing with the description of the VIE at the moment when they are analyzed. The IE shall not manifest themselves as such a heavy test for the standard model. However, we still need to know the cross sections of the IE in order to compare the ratio of these and those of the VIE with the predictions of the standard model.

8.1.1 The problem

Large part of the IE can be described by quantum chromo dynamics (QCD), the formalism of quarks and gluons, with which multi-parton QCD-amplitudes are calculated. It is well known [35] that they contribute to the cross section with a singular behavior in phase space (PS), given by the so-called *antenna pole structure* (APS). In particular, for processes involving only n gluons the most important contribution comes from the sum of all permutations in the momenta of

$$\frac{1}{(p_1\cdot p_2)(p_2\cdot p_3)(p_3\cdot p_4)\cdots(p_{n-1}\cdot p_n)(p_n\cdot p_1)}\ , \tag{8.1}$$

single antenna integrated to 1% error		
number of momenta	cut-off / CM-energy	number of PS points
3	0.183	10,069
4	0.129	26,401
5	0.100	58,799
6	0.0816	130,591
7	0.0690	240,436
8	0.0598	610,570

evaluation amplitude in 1 PS point		
number of final gluons	cpu-time (seconds)	
	SPHEL	exact
3	2.83×10^{-5}	1.60×10^{-1}
4	9.76×10^{-5}	5.54×10^{-1}
5	4.88×10^{-4}	1.945
6	3.26×10^{-3}	6.06
7	2.57×10^{-2}	19.91
8		64.45

Table 8.1: Typical number of PS points and computing times.

and the singular nature stems from the fact that the scalar products $p_i \cdot p_j$ can become very small. If functions, containing this kind of kinematical structures, are integrated using the RAMBO (Section 7.4), which generates the momenta distributed uniformly in PS, then a large number of events is needed to reach a result to acceptable precision. As an illustration, we present in the left table of Tab. 8.1 the number of PS points needed to integrate the single antenna of Eq. (8.1), so not even the sum of its permutations, to an expected error of 1%. The antenna cannot be integrated over the whole of PS because of the singularities, so these have to be cut out. This is done through the restriction $(p_i + p_j)^2 \geq s_0$ for all $i, j = 1, \ldots, n$,[1] and in the table the ratio between $\sqrt{s_0}$ and the total energy $\sqrt{s}$ is given. These numbers are based on the reasonable choice $s_0/s = 0.2/[n(n-1)]$.

Performing MC integration with very many events is not a problem if the evaluation of the integrand in each PS point is cheap in computing time. This is, for example, the case for algorithms to calculate the squared multi-parton amplitudes based on the so called SPHEL-approximation, for which only the kinematical structure of (8.1) is implemented [35]. Nowadays, algorithms to calculate the *exact* matrix elements exist, which are far more time-consuming [37, 38]. As an illustration of what is meant by 'more time-consuming', we present the right table of Tab. 8.1 with the typical cpu-time needed for the evaluation in *one* PS point of the integrand for processes of two gluons going to more gluons, both for the SPHEL-approximation and the exact matrix elements [39]. It is expected, and observed, that the exact matrix elements reveal the same kind of singularity structures as the APS, so that, according to the tables, the PS integration for a process with 8 final gluons would take in the order of 400 days ...

8.1.2 The solution

The solution to this problem is importance sampling. Instead of RAMBO, a PS generator should be used which generates momenta with a density including the APS. The following sections show the construction of such a PS generator, called SARGE, which stands for Staggered Antenna Radiation GEnerator.

[1] Remember that $(p+q)^2 = 2p\cdot q$ since p and q are massless.

8.2 The basic antenna

As mentioned before, we want to generate momenta that represent radiated partons with a density that has the antenna structure $[(p_1p_2)(p_2p_3)(p_3p_4)\cdots,(p_{n-1}p_n)(p_np_1)]^{-1}$. Naturally, the momenta can be viewed as coming from a splitting process: one starts with two momenta, a third is radiated off creating a new pair of momenta of which a fourth is radiated off and so on. In fact, models similar to this are used in full-fledged Monte-Carlo generators like HERWIG. Let us therefore first try to generate a single massless momentum k, radiated from a pair of given massless momenta p_1 and p_2. In order for the distribution to have the correct infrared and collinear behavior, it should qualitatively be proportional to $[(p_1k)(kp_2)]^{-1}$. Furthermore, we want the density to be invariant under Lorentz transformations and scaling of the momenta, keeping in mind that the momenta are three out of possibly more in a CMF and that we have to perform these transformations in the end, like in RAMBO. This motivates us to define the *basic antenna* structure as

$$dA(p_1,p_2;k) \;:=\; d^4k\vartheta(k)\,\frac{1}{\pi}\,\frac{(p_1p_2)}{(p_1k)(kp_2)}\,g\left(\frac{(p_1k)}{(p_1p_2)}\right)g\left(\frac{(kp_2)}{(p_1p_2)}\right)\quad . \tag{8.2}$$

Here, g is a function that serves to regularize the infrared and collinear singularities, as well as to ensure normalization over the whole space for k: therefore, $g(\xi)$ has to vanish sufficiently fast for both $\xi\to 0$ and $\xi\to\infty$. To find out how k could be generated, we evaluate $\int dA$ in the CMF of p_1 and p_2. Writing

$$E := \sqrt{(p_1p_2)/2}\quad ,\qquad p := \mathcal{H}_{p_1+p_2}p_1\quad ,\qquad q := \mathcal{H}_{p_1+p_2}k\ , \tag{8.3}$$

we have

$$(p_1p_2) = 2E^2\quad ,\quad (p_1k) = Eq^0(1-z)\quad ,\quad (kp_2) = Eq^0(1+z)\ , \tag{8.4}$$

where $z=\vec{p}\cdot\vec{q}/(|\vec{p}||\vec{q}|)$. The azimuthal angle of $\vec{q}$ is denoted φ, so that $\vec{q}=|\vec{q}|\mathcal{R}_p^{-1}\hat{n}(z,\varphi)$, with $\hat{n}$ as in (7.50). We can write

$$d^4k\vartheta(k) \;=\; \tfrac{1}{2}\,q^0dq^0\,d\varphi\,dz \;=\; \tfrac{1}{2}(p_1p_2)\,d\varphi\,d\xi_1d\xi_2\ , \tag{8.5}$$

where,

$$\xi_1=\frac{(p_1k)}{(p_1p_2)}\qquad\text{and}\qquad \xi_2=\frac{(kp_2)}{(p_1p_2)}\ , \tag{8.6}$$

so that $z=(\xi_2-\xi_1)/(\xi_2+\xi_1)$ and $q^0=E(\xi_2+\xi_1)$. The integral over dA takes on the particularly simple form

$$\int dA(p_1,p_2;k) \;=\; \left(\int_0^\infty d\xi\,\frac{1}{\xi}\,g(\xi)\right)^2\quad . \tag{8.7}$$

The antenna $dA(p_1, p_2; k)$ will therefore correspond to a unitary algorithm when we let the density g be normalized by

$$\int_0^\infty d\xi \, \frac{1}{\xi} \, g(\xi) = 1 \quad . \tag{8.8}$$

Note that the normalization of dA fixes the overall factor uniquely: in particular the appearance of the numerator $(p_1 p_2)$ is forced upon us by the unitarity requirement.

For g we want to take, at this point, the simplest possible function we can think of, that has a sufficiently regularizing behavior. We introduce a positive non-zero number ξ_m and take

$$g(\xi) \; := \; \frac{1}{2 \log \xi_m} \, \theta(\xi_m^{-1} \leq \xi \leq \xi_m) \quad . \tag{8.9}$$

The number ξ_m gives a cut-off for the quotients ξ_1 and ξ_2 of the scalar products of the momenta, and not for the scalar products themselves. It is, however, possible to relate ξ_m to the total energy $\sqrt{s}$ in the CMF and a cut-off s_0 on the invariant masses, i.e., the requirement that

$$(p_i + p_j)^2 \geq s_0 \qquad \text{for all momenta } p_i \neq p_j. \tag{8.10}$$

This can be done by choosing

$$\xi_m \; := \; \frac{s}{s_0} - \frac{(n+1)(n-2)}{2} \quad . \tag{8.11}$$

With this choice, the invariant masses $(p_1 + k)^2$ and $(k + p_2)^2$ are regularized, but can still be smaller than s_0 so that the whole of PS, cut by (8.10), is covered. The s_0 can be derived from physical cuts p_T on the transverse momenta and θ_0 on the angles between the outgoing momenta:

$$s_0 \; = \; 2p_T^2 \cdot \min\left(1 - \cos\theta_0 \, , \, \left(1 + \sqrt{1 - p_T^2/s}\right)^{-1}\right) \quad . \tag{8.12}$$

With this choice, PS with the physical cuts is covered by PS with the cut of (8.10). To generate the physical PS, the method of crude Monte Carlo (Section 7.3.2) can be used, i.e., if momenta of an event do not satisfy the cuts, the whole event is rejected. We end this section with the piece of the PS algorithm that corresponds to the basic $dA(p_1, p_2; k)$:

Algorithm 8.2.1 (BASIC ANTENNA)

1. given $\{p_1, p_2\}$, put $p \leftarrow \mathcal{H}_{p_1+p_2} p_1$ and put $E \leftarrow \sqrt{(p_1 p_2)/2}$;
2. generate two numbers ξ_1, ξ_2 independently, each from the density $g(\xi)/\xi$, and φ uniformly in $[0, 2\pi)$;
3. put $z \leftarrow (\xi_2 - \xi_1)/(\xi_2 + \xi_1)$, $q^0 \leftarrow E(\xi_2 + \xi_1)$ and $\vec{q} \leftarrow q^0 \mathcal{R}_p^{-1} \hat{n}(z, \varphi)$;
4. put $k \leftarrow \mathcal{H}^{-1}_{p_1+p_2} q$.

8.3 A complete QCD antenna

The straightforward way to generate n momenta with the antenna structured density is by repeated use of the basic antenna. Let us denote

$$dA^i_{j,k} := dA(q_j, q_k; q_i) \ , \tag{8.13}$$

then

$$dA^2_{1,n}\, dA^3_{2,n}\, dA^4_{3,n} \cdots dA^{n-1}_{n-2,n} \ = \ \frac{(q_1 q_n)\, g_n(\{q\}_n)}{\pi^{n-2}(q_1q_2)(q_2q_3)(q_3q_4)\cdots(q_{n-1}q_n)} \prod_{i=2}^{n-1} d^4q_i\vartheta(q_i) \ ,$$

where

$$g_n(\{q\}_n) \ := \ g\left(\frac{(q_1q_2)}{(q_1q_n)}\right) g\left(\frac{(q_2q_n)}{(q_1q_n)}\right) g\left(\frac{(q_2q_3)}{(q_2q_n)}\right) g\left(\frac{(q_3q_n)}{(q_2q_n)}\right) \cdots g\left(\frac{(q_{n-1}q_n)}{(q_{n-2}q_n)}\right) \ . \tag{8.14}$$

So if we have two momenta q_1 and q_n, then we can easily generate $n-2$ momenta q_j with the antenna structure. Remember that this differential PS volume is completely invariant under Lorentz transformations and scaling transformations, so that it seems self-evident to force the set of generated momenta in the CMF with a given energy, using the same kind of transformation as in the case of RAMBO. If the first two momenta are generated with density $f(q_1, q_n)$, then the UAF tells us that generated density $A_s^{QCD}(\{p\}_n)$ satisfies

$$\begin{aligned} A_s^{QCD}(\{p\}_n) \ &= \int d^4q_1\vartheta(q_1) d^4q_n\vartheta(q_n)\, f(q_1,q_n)\, dA^2_{1,n}\, dA^3_{2,n}\, dA^4_{3,n} \cdots dA^{n-1}_{n-2,n} \\ &\quad \times d^4b\, \delta^4(b - q_{(n)}/m_{q_{(n)}})\, dx\, \delta(x - \sqrt{s}\,/m_{q_{(n)}}) \prod_{i=1}^{n} \delta^4(p_i - x\mathcal{H}_b q_i) \ . \end{aligned} \tag{8.15}$$

If we apply the same manipulations as in the proof of the correctness of RAMBO, we obtain the equation

$$\begin{aligned} A_s^{QCD}(\{p\}_n) \ &= \ \Theta_s(\{p\}_n) \frac{(p_1p_n)\, g_n(\{p\}_n)}{\pi^{n-2}(p_1p_2)(p_2p_3)(p_3p_4)\cdots(p_{n-1}p_n)} \\ &\quad \times \int d^4b\, \delta(b^2-1)\, dx\, \frac{2s^2}{x^5}\, f(x^{-1}\mathcal{H}_b^{-1}p_1 \, , \, x^{-1}\mathcal{H}_b^{-1}p_n) \ . \end{aligned} \tag{8.16}$$

Now we choose f such that q_1 and q_n are generated back-to-back in their CMF with total energy $\sqrt{s}$, i.e.,

$$f(q_1,q_n) \ = \ \frac{2}{\pi}\, \delta^4(q_1 + q_n - \sqrt{s}\, e_0) \ . \tag{8.17}$$

If we evaluate the second line of Eq.(8.16) with this f, we arrive at

$$\begin{aligned} &\frac{4s^2}{\pi} \int dx\, \frac{1}{x^5}\, d^4b\, \delta(b^2-1)\, \delta^4(x^{-1}\mathcal{H}_b^{-1}(p_1+p_n) - \sqrt{s}\, e_0) \\ &\qquad = \ \frac{4}{\pi}\int_0^\infty dx\, \frac{1}{x^5}\, \delta\left(\frac{(p_1+p_n)^2}{sx^2} - 1\right) \ = \ \frac{s^2}{2\pi(p_1p_n)^2} \ , \end{aligned} \tag{8.18}$$

so that the generated density is given by

$$A_s^{\text{QCD}}(\{p\}_n) \;=\; \Theta_s(\{p\}_n)\,\frac{s^2}{2\pi^{n-2}}\,\frac{g_n(\{p\}_n)}{(p_1p_2)(p_2p_3)(p_3p_4)\cdots(p_{n-1}p_n)(p_np_1)}\quad . \tag{8.19}$$

Note that, somewhat surprisingly, also the factor $(p_np_1)^{-1}$ comes out, thereby making the antenna even more symmetric. In fact, if the density $f(q_1,q_2) = c^4\exp(-cq_1^0 - cq_2^0)/4\pi^2$ is taken instead of the one we just used, the calculation can again be done exactly, with exactly the same result. The algorithm to generate n momenta with the above antenna structure is given by

Algorithm 8.3.1 (`QCD ANTENNA`)

1. generate massless momenta q_1 and q_n;
2. generate $n-2$ momenta q_j by the basic antennas $dA^2_{1,n}\,dA^3_{2,n}\,dA^4_{3,n}\cdots dA^{n-1}_{n-2,n}$;
3. compute $q_{(n)} = \sum_{j=1}^{n} q_j$, and the boost and scaling transforms that bring $q_{(n)}$ to $\sqrt{s}\,e_0$;
4. for $j = 1,\ldots,n$, boost and scale the q_j accordingly, into the p_j.

Usually, the event generator is used to generate cut PS. If a generated event does not satisfy the physical cuts, it is rejected. In the calculation of the weight coming with an event, the only contribution coming from the functions g is, therefore, their normalization. In total, this gives a factor $1/(2\log\xi_m)^{2n-4}$ in the density.

8.4 Incoming momenta and symmetrization

The density given by the algorithm above, is not quite what we want. First of all, we want to include the incoming momenta p_0 and $\tilde{p}_0$ in the APS, so that the density becomes proportional to $[(p_0p_1)(p_1p_2)\cdots(p_{n-1}p_n)(p_n\tilde{p}_0)]^{-1}$ instead of $[(p_1p_2)\cdots(p_{n-1}p_n)(p_np_1)]^{-1}$. Then we want the sum of all permutations of the momenta, including the incoming ones.

8.4.1 Generating incoming momenta

The incoming momenta can be generated after the antenna has been generated. To show how, let us introduce the following "regularized" scalar product:

$$(pq)_\delta \;:=\; (pq) + \delta p^0 q^0\quad , \tag{8.20}$$

where δ is a small positive number. This regularization is not completely Lorentz invariant, but that does not matter here. Important is that it is still invariant under rotations, as we shall see. Using this regularization, we are able to generate a momentum k with a probability density

$$\frac{1}{2\pi I_\delta(p_1,p_2)}\,\frac{\vartheta(k)\,\delta(k^0-1)}{(p_1k)_\delta(\tilde{k}p_2)_\delta}\quad . \tag{8.21}$$

To show how, we calculate the normalization $I_\delta(p_1,p_2)$. Using the Feynman-representation of $1/[(p_1k)_\delta(\tilde{k}p_2)_\delta]$, it is easy to see that

$$I_\delta(p_1,p_2) \;=\; \frac{1}{4\pi p_1^0 p_2^0}\int dz d\varphi \int_0^1 \frac{dx}{(1+\delta-|\vec{p}_x|z)^2} \quad , \tag{8.22}$$

where $\vec{p}_x = x\hat{p}_1 + (x-1)\hat{p}_2$. The integral over z and φ can now be performed, with the result that

$$I_\delta(p_1,p_2) \;=\; \frac{1}{p_1^0 p_2^0}\int_0^1 \frac{dx}{(1+\delta)^2-|\vec{p}_x|^2} \;=\; \frac{1}{2(p_1\tilde{p}_2)}\int_0^1 \frac{dx}{(x_+-x)(x-x_-)} \quad , \tag{8.23}$$

where $x_\pm$ are the solutions for x of the equation $1+\delta = |\vec{p}_x|$. Further evaluation finally leads to

$$I_\delta(p_1,p_2) \;=\; \frac{(p_1\tilde{p}_2)^{-1}}{x_+-x_-}\log\left|\frac{x_+}{x_-}\right| \quad , \quad x_\pm \;=\; \frac{1}{2}\pm\frac{1}{2}\sqrt{1+\frac{2p_1^0p_2^0(2\delta+\delta^2)}{(p_1\tilde{p}_2)}} \quad . \tag{8.24}$$

Notice that there is a smooth limit to the case in which p_1 and p_2 are back-to-back:

$$I_\delta(p,\tilde{p}) \;=\; \lim_{q\to\tilde{p}} I_\delta(p,q) \;=\; \frac{1}{(p^0)^2(2\delta+\delta^2)} \quad . \tag{8.25}$$

The algorithm to generate k can be derived by reading the evaluations of the integrals backwards.

Because k and $\tilde{k}$ are back-to-back, they can serve as the incoming momenta. To fix them to e_0+e_3 and e_0-e_3, the whole system of momenta can be rotated. If we generate momenta with the density A_s^{QCD}, use the first two momenta to generate the incoming momenta and rotate, we get a density

$$\begin{aligned} D_s(\{p\}_n) \;&=\; \int d^{4n}q\, A_s^{QCD}(\{q\}_n)\; d^4k\, \frac{1}{2\pi I_\delta(q_1,q_2)}\frac{\vartheta(k)\,\delta(k^0-1)}{(q_1k)_\delta(q_2\tilde{k})_\delta}\prod_{i=1}^{n}\delta^4(p_i-\mathcal{R}_k q_i) \\ &=\; A_s^{QCD}(\{p\}_n)\, I_\delta(p_1,p_2)^{-1}\int d^4k\vartheta(k)\,\delta(k^0-1)\,\frac{(2\pi)^{-1}}{(p_1\mathcal{R}_k k)_\delta(p_2\mathcal{R}_k\tilde{k})_\delta} \quad , \end{aligned} \tag{8.26}$$

where we used the fact that the whole expression is invariant under rotations, and that these are orthogonal transformations. The last line of the previous expression can be evaluated further with the result that

$$D_s(\{p\}_n) \;=\; A_s^{QCD}(\{p\}_n)\,\frac{I_\delta(p_1,p_2)^{-1}}{(p_1p_0)_\delta(\tilde{p}_0p_2)_\delta} \quad \text{with} \quad p_0 = e_0+e_3\ ,\ \ \tilde{p}_0 = e_0-e_3\ . \tag{8.27}$$

The algorithm to generate the incoming momenta is given by

Algorithm 8.4.1 (INCOMING MOMENTA)

1. given a pair $\{p_1,p_2\}$, calculate x_+ and x_-;
2. generate x in $[0,1]$ with density $\sim [(x_+-x)(x-x_-)]^{-1}$, and put $\vec{p}_x \leftarrow x\hat{p}_1+(x-1)\hat{p}_2$;

3. generate φ uniformly in $[0, 2\pi)$, z in $[-1, 1]$ with density $\sim (1 + \delta - |\vec{p}_x|z)^{-2}$;
4. put $\vec{k} \leftarrow \mathcal{R}_{p_x}^{-1}\hat{n}(z, \varphi)$ and $k^0 \leftarrow 1$;
5. rotate all momenta with $\mathcal{R}_k$;
6. put $p_0 \leftarrow \frac{1}{2}\sqrt{s}\,(e_0 + e_3)$ and $\tilde{p}_0 \leftarrow \frac{1}{2}\sqrt{s}\,(e_0 - e_3)$.

Notice that $I_\delta(p_1, p_2)(p_1p_0)_\delta(\tilde{p}_0p_2)_\delta$ is invariant under the scaling $p_1, p_2 \to cp_1, cp_2$ with a constant c, so that scaling of p_0 and $\tilde{p}_0$ has no influence on the density.

The pair (q_1, q_2) with which k is generated is free to choose because we want to symmetrize in the end anyway. We should only choose it such, that we get rid of the factor (q_1q_2) in the denominator of $A_s^{QCD}(\{q\}_n)$.

8.4.2 Choosing the type of antenna with incoming momenta

A density which is the sum over permutations can be obtained by generating random permutations, and returning the generated momenta with permutated labels. This, however, only makes sense for the outgoing momenta. The incoming momenta are fixed, and should be returned separately from the outgoing momenta by the event generator. Therefore, a part of the permutations has to be generated explicitly. There are two kinds of terms in the sum: those in which $(p_0\tilde{p}_0)$ appears, and those in which it does not.

Case 1: antenna with $(p_0\tilde{p}_0)$. To generate the first kind, we can choose a label i at random with weight $(p_ip_{i+1})/\Sigma_1(\{p\}_n)$ where $\Sigma_1(\{p\}_n)$ is the sum of all scalar products in the antenna [2]:

$$\Sigma_1(\{p\}_n) := \sum_{i=1}^{n}(p_ip_{i+1}) \quad . \tag{8.28}$$

This is a proper weight, since all scalar products are positive. The total density gets this extra factor then, so that (p_ip_{i+1}) cancels. The denominator of the weight factor does not give a problem, because its singular structure is much softer than the one of the antenna. The pair $\{p_i, p_{i+1}\}$ can then be used to generate the incoming momenta, as shown above. So in this case, a density $A_s^{QCD}(\{p\}_n)B_1(\{p\}_n)/\Sigma_1(\{p\}_n)$ is generated, where

$$B_1(\{p\}_n) := \sum_{i=1}^{n}\frac{(p_ip_{i+1})\,I_\delta(p_i, p_{i+1})^{-1}}{(p_ip_0)_\delta(\tilde{p}_0p_{i+1})_\delta} \quad . \tag{8.29}$$

Case 2: antenna without $(p_0\tilde{p}_0)$. To generate the second kind, we can choose two non-equal labels i and j with weight $(p_ip_{i+1})(p_jp_{j+1})/\Sigma_2(\{p\}_n)$, where

$$\Sigma_2(\{p\}_n) := \sum_{i\neq j}^{n}(p_ip_{i+1})(p_jp_{j+1}) \quad . \tag{8.30}$$

[2] Read $i + 1 \mod n$ when $i + 1$ occurs in this section

Next, a pair (k,l) of labels has to be chosen from the set of pairs

$$\{(i,j)\}_+ \;:=\; \{(i,j)\,,\,(i,j+1)\,,\,(i+1,j)\,,\,(i+1,j+1)\}\;. \tag{8.31}$$

If this is done with weight $I_\delta(p_k,p_l)/\Sigma_{i,j}(\{p\}_n)$, where

$$\Sigma_{i,j}(\{p\}_n) \;:=\; \sum_{(k,l)\in\{(i,j)\}_+} I_\delta(p_k,p_l)\;, \tag{8.32}$$

then the density $A_s^{QCD}(\{p\}_n)B_2(\{p\}_n)/\Sigma_2(\{p\}_n)$ is generated, where

$$\begin{aligned} B_2(\{p\}_n) \;&=\; \sum_{i\neq j}^{n}(p_ip_{i+1})(p_jp_{j+1}) \sum_{(k,l)\in\{(i,j)\}_+} \frac{I_\delta(p_k,p_l)}{\Sigma_{i,j}(\{p\}_n)}\cdot\frac{I_\delta(p_k,p_l)^{-1}}{(p_kp_0)_\delta(\tilde p_0p_l)_\delta} \\ &=\; \sum_{i\neq j}^{n}\frac{(p_ip_{i+1})(p_jp_{j+1})}{(p_ip_0)_\delta(p_{i+1}p_0)_\delta(\tilde p_0p_j)_\delta(\tilde p_0p_{j+1})_\delta}\cdot\frac{\sum_{(k,l)\in\{(i,j)\}_+}(p_kp_0)_\delta(\tilde p_0p_l)_\delta}{\sum_{(k,l)\in\{(i,j)\}_+}I_\delta(p_k,p_l)}\;. \end{aligned} \tag{8.33}$$

Before all this, we first have to choose between the two cases, and the natural way to do this is with relative weights $\frac{1}{2}s\Sigma_1(\{p\}_n)$ and $\Sigma_2(\{p\}_n)$, so that the complete density is equal to

$$S_s^{QCD}(\{p\}_n) \;=\; \frac{1}{n!}\sum_{\text{perm.}} A_s^{QCD}(\{p\}_n)\,\frac{\frac{1}{2}sB_1(\{p\}_n)+B_2(\{p\}_n)}{\frac{1}{2}s\Sigma_1(\{p\}_n)+\Sigma_2(\{p\}_n)}\;, \tag{8.34}$$

where the first sum is over all permutations of $(1,\ldots,n)$. One can, of course, try to optimize the weights for the two cases using the adaptive multichannel method (Section 7.3.5). The result of using the sum of the two densities is that the factors (p_ip_{i+1}) in the numerator of $B_1(\{p\}_n)$ and $(p_ip_{i+1})(p_jp_{j+1})$ in the numerator of $B_2(\{p\}_n)$ cancel with the same factors in the denominator of $A_s^{QCD}(\{p\}_n)$, so that we get exactly the pole structure we want. The 'unwanted' singularities in $B_1(\{p\}_n), B_2(\{p\}_n)$ and $\Sigma_1(\{p\}_n), \Sigma_2(\{p\}_n)$ are much softer than the ones remaining in $A_s^{QCD}(\{p\}_n)$, and cause no trouble. The algorithm to generate the incoming momenta and the permutation is given by

Algorithm 8.4.2 (`CHOOSE INCOMING POLE STRUCTURE`)

1. choose case 1 or 2 with relative weights $\frac{1}{2}s\Sigma_1(\{p\}_n)$ and $\Sigma_2(\{p\}_n)$;
2. in case 1, choose i_1 with relative weight $(p_{i_1}p_{i_1+1})$ and put $i_2 \leftarrow i_1+1$;
3. in case 2, choose (i,j) with $(i\neq j)$ and relative weight $(p_ip_{i+1})(p_jp_{j+1})$, and then choose (i_1,i_2) from $\{(i,j)\}_+$ with relative weight $I_\delta(p_{i_1},p_{i_2})$;
4. use $\{p_{i_1},p_{i_2}\}$ to generate the incoming momenta with Algorithm 8.4.1;
5. generate a random permutation $\sigma\in S_n$ and put $p_i \leftarrow p_{\sigma(i)}$ for all $i=1,\ldots,n$.

An algorithm to generate the random permutations can be found in [2]. An efficient algorithm to calculate a sum over permutations can be found in [36].

8.5 Improvements

When doing calculations with this algorithm on a PS, cut such that $(p_i + p_j)^2 > s_0$ for all $i \neq j$ and some reasonable $s_0 > 0$, we notice that a very high percentage of the generated events does not pass the cuts. An important reason why this happens is that the cuts, generated by the choices of g (Eq. (8.9)) and ξ_m (Eq. (8.11)), are implemented only on quotients of scalar products that appear explicitly in the generation of the QCD-antenna:

$$\xi_1^i := \frac{(p_{i-1}p_i)}{(p_{i-1}p_n)} \qquad \text{and} \qquad \xi_2^i := \frac{(p_i p_n)}{(p_{i-1}p_n)} \ , \quad i = 2,3\ldots,n-1 \ . \tag{8.35}$$

The total number of these ξ-variables is

$$n_\xi := 2n-4 \ , \tag{8.36}$$

and the cuts are implemented such that $\xi_m^{-1} \leq \xi_{1,2}^i \leq \xi_m$ for $i = 2,3\ldots,n-1$. We show now how these cuts can be implemented on *all* quotients

$$\frac{(p_{i-1}p_i)}{(p_{j-1}p_j)} \ , \quad \frac{(p_{i-1}p_i)}{(p_j p_n)} \quad \text{and} \quad \frac{(p_i p_n)}{(p_j p_n)} \ , \quad i,j = 2,3,\ldots,n-1 \ . \tag{8.37}$$

We define the m-dimensional convex polytope

$$\mathbf{P}_m := \{(x_1,\ldots,x_m) \in [-1,1]^m \,\big|\, |x_i - x_j| \leq 1 \ \forall\, i,j = 1,\ldots,m\} \ , \tag{8.38}$$

and replace the generation of the the ξ-variables by the following:

Algorithm 8.5.1 (`IMPROVEMENT`)

1. generate $(x_1, x_2, \ldots, x_{n_\xi})$ distributed uniformly in $\mathbf{P}_{n_\xi}$;
2. define $x_0 := 0$ and put,

$$\xi_1^i \leftarrow e^{(x_{2i-3}-x_{2i-4})\log\xi_m} \ , \quad \xi_2^i \leftarrow e^{(x_{2i-2}-x_{2i-4})\log\xi_m} \tag{8.39}$$

   for all $i = 2,\ldots,n-1$.

Because all the variables x_i are distributed uniformly such that $|x_i - x_j| \leq 1$, *all* quotients of (8.37) are distributed such that they are between ξ_m^{-1} and ξ_m. In terms of the variables x_i, this means that we generate the volume of $\mathbf{P}_{n_\xi}$, which is $n_\xi + 1$, instead of the volume of $[-1,1]^{n_\xi}$, which is 2^{n_ξ}. In Section 8.8, we give the algorithm to generate variables distributed uniformly in $\mathbf{P}_m$. We have to note here that this improvement only makes sense because the algorithm to generate these variables is very efficient. The total density changes such, that the function g_n in Eq. (8.19) has to be replaced by

$$g_n^{\mathbf{P}}(\xi_m;\{\xi\}) \ := \ \frac{1}{(n_\xi+1)(\log\xi_m)^{n_\xi}}\,\theta(\,(x_1,\ldots,x_{n_\xi}) \in \mathbf{P}_{n_\xi}\,) \ , \tag{8.40}$$

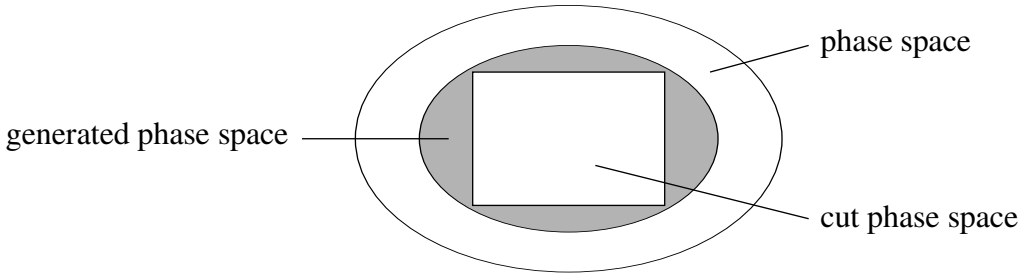

Figure 8.2: Schematic view on phase space.

where the variables x_i are functions of the variables $\xi^i_{1,2}$ as defined by (8.39). Because crude MC is used to restrict generated events to cut PS, again only the normalization has to be calculated for the weight of an event.

With this improvement, still a large number of events does not pass the cuts. The situation with PS is depicted in Fig. 8.2. Phase space contains generated phase space which contains cut phase space. The problem is that most events fall in the shaded area, which is the piece of generated PS that is not contained in cut PS. To get a higher percentage of accepted events, we use a random variable $\xi_\nu \in [0, \xi_m]$, instead of the fixed number ξ_m, to generate the variables $\xi^i_{1,2}$. This means that the size of the generated PS becomes variable. If this is done with a probability distribution such that ξ_ν can, in principle, become equal to ξ_m, then whole of cut phase space is still covered. We suggest the following, tunable, density:

$$h_\alpha(\xi_\nu) \;=\; \frac{\alpha n_\xi + 1}{(\log \xi_m)^{\alpha n_\xi + 1}} \cdot \frac{(\log \xi_\nu)^{\alpha n_\xi}}{\xi_\nu}\, \theta(1 \le \xi_\nu \le \xi_m) \quad , \quad \alpha \ge 0 \quad . \tag{8.41}$$

If $\alpha = 0$, then $\log \xi_\nu$ is distributed uniformly in $[0, \log \xi_m]$, and for larger α, the distribution peaks more and more towards $\xi_\nu = \xi_m$. Furthermore, the variable is easy to generate and the total generated density can be calculated exactly: $g^{\mathbf{P}}_n(\xi_m; \{\xi\})$ should be replaced by

$$\begin{aligned} G^{\mathbf{P}}_n(\alpha, \xi_m; \{\xi\}) \;&:=\; \int d\xi_\nu\, h_\alpha(\xi_\nu)\, g^{\mathbf{P}}_n(\xi_\nu; \{\xi\}) \\ &= \frac{1}{n_\xi + 1} \cdot \frac{\alpha n_\xi + 1}{(\log \xi_m)^{\alpha n_\xi + 1}} \int_{\log \xi_{low}}^{\log \xi_m} dx\, x^{(\alpha-1) n_\xi} \quad , \end{aligned} \tag{8.42}$$

where ξ_{low} is the maximum of the ratios of scalar products in (8.37).

8.6 Results and conclusions

We compare SARGE with RAMBO in the integration of the SPHEL-integrand for processes of the kind $gg \to ng$, which is given by

$$\sum_{perm.} \frac{2 \sum_{i \ne j}^{n+1} (p_i p_j)^4}{(p_1 p_2)(p_2 p_3)(p_3 p_4) \cdots (p_n p_{n+1})(p_{n+1} p_{n+2})(p_{n+2} p_1)} \quad , \tag{8.43}$$

n	4	5	6	7
$\tau_{\texttt{SPHEL}}(s)$	5.40×10^{-5}	2.70×10^{-4}	1.80×10^{-3}	1.41×10^{-2}
$\tau_{\text{exact}}(s)$	3.07×10^{-1}	1.08	3.35	10.92

Table 8.2: cpu-times ($\tau_{\texttt{SPHEL}}$) in seconds needed to evaluate the SPHEL-integrand one time with a 300-MHz UltraSPARC-IIi processor, and the cpu-times (τ_{exact}) needed to evaluate the exact integrand, estimated with the help of Tab. 8.1.

where p_1 and p_2 are the incoming momenta, and the first sum is over all permutations of $(2,3,\ldots,n+2)$ except the cyclic permutations. The results are presented in Tab. 8.3.

The calculations were done at a CM-energy $\sqrt{s} = 1000$ with cuts $p_T = 40$ on each transverse momentum and $\theta_0 = 30^\circ$ on the angles between the momenta. We present the results for $n = 4,5,6,7$, calculated with RAMBO and SARGE with different values for α (Eq. (8.42)). The value of σ is the estimate of the integral at an estimated error of 1% for $n = 4,5,6$ and 3% for $n = 7$. These numbers are only printed to show that different results are compatible. Remember that they are not the whole cross sections: flux factors, color factors, sums and averages over helicities, and coupling constants are not included. The other data are the number of generated events (N_{ge}), the number of accepted events (N_{ac}) that passed the cuts, the cpu-time consumed (t_{cpu}), and the cpu-time the calculation would have consumed if the exact matrix element had been used (t_{exa}), both in hours. This final value is estimated with the help of Tab. 8.2 and the formula

$$t_{exa} \;=\; t_{cpu} + N_{ac}(\tau_{exact} - \tau_{\texttt{SPHEL}}) \quad , \tag{8.44}$$

where τ_{exact} and $\tau_{\texttt{SPHEL}}$ are the cpu-times it takes to evaluate the squared matrix element once. Remember that the integrand only has to be evaluated for accepted events. The calculations have been performed with a single 300-MHz UltraSPARC-IIi processor.

The first conclusion we can draw is that SARGE outperforms RAMBO in computing time for all processes. This is especially striking for lower number of outgoing momenta, and this behavior has a simple explanation: we kept the CM-energy and the cuts fixed, so that there is less energy to distribute over the momenta if n is larger, and the cuts become relatively tighter. As a result, RAMBO gains on SARGE if n becomes larger. This effect would not appear if the energy, or the cuts, would scale with n like in Tab. 8.1. Another indication for this effect is the fact that the ratio N_{ac}/N_{ge} for RAMBO, which estimates the ratio of the volumes of cut PS and whole PS, decreases with n.

Another conclusion that can be drawn is that SARGE performs better if α is larger. Notice that the limit of $\alpha \to \infty$ is equivalent with dropping the improvement of the algorithm using the variable ξ_v (Eq. (8.42)). Only if the integrand becomes too flat, as in the case of $n = 7$ with the energy and the cuts as given in the table, smaller values are preferable. Then, too many events do not pass the cuts if α is large.

As an extra illustration of the performance of SARGE, we present in Fig. 8.3 the evaluation

$gg \to 4g$, 1% error	alg.	RAMBO	SARGE, $\alpha = 0.0$	SARGE, $\alpha = 0.5$	SARGE, $\alpha = 10.0$
	σ	4.30×10^8	4.31×10^8	4.37×10^8	4.32×10^8
	N_{ge}	4,736,672	296,050	278,702	750,816
	N_{ac}	3,065,227	111,320	40,910	23,373
	t_{cpu}(h)	0.198	0.0254	0.0172	0.0348
	t_{exa}(h)	262	9.52	3.51	2.03

$gg \to 5g$, 1% error	alg.	RAMBO	SARGE, $\alpha = 0.0$	SARGE, $\alpha = 0.5$	SARGE, $\alpha = 10.0$
	σ	3.78×10^{10}	3.81×10^{10}	3.80×10^{10}	3.81×10^{10}
	N_{ge}	4,243,360	715,585	1,078,129	6,119,125
	N_{ac}	1,712,518	167,540	36,385	21,111
	t_{cpu}(h)	0.286	0.133	0.0758	0.277
	t_{exa}(h)	514	51.6	11.7	9.10

$gg \to 6g$, 1% error	alg.	RAMBO	SARGE, $\alpha = 0.0$	SARGE, $\alpha = 0.5$	SARGE, $\alpha = 10.0$
	σ	3.07×10^{12}	3.05×10^{12}	3.13×10^{12}	3.05×10^{12}
	N_{ge}	3,423,981	2,107,743	6,136,375	68,547,518
	N_{ac}	700,482	276,344	34,095	17,973
	t_{cpu}(h)	0.685	1.32	0.471	3.17
	t_{exa}(h)	653	258	32.2	19.9

$gg \to 7g$, 3% error	alg.	RAMBO	SARGE, $\alpha = 0.0$	SARGE, $\alpha = 0.5$	SARGE, $\alpha = 10.0$
	σ	2.32×10^{14}	2.16×10^{14}	2.20×10^{14}	2.28×10^{14}
	N_{ge}	605,514	710,602	5,078,153	125,471,887
	N_{ac}	49,915	42,394	3,256	1,789
	t_{cpu}(h)	0.224	1.86	0.452	6.74
	t_{exa}(h)	152	130	10.3	12.2

Table 8.3: Results for the integration of the SPHEL-integrand. The CM-energy and the cuts used are $\sqrt{s} = 1000$, $p_T = 40$ and $\theta_0 = 30°$. Presented are the finial result (σ), the number of generated (N_{ge}) and accepted (N_{ac}) events, the cpu-time (t_{cpu}) in hours, and the cpu-time (t_{exa}) it would take to integrate the exact matrix element, estimated with the help of Tab. 8.2. In the calculation of this table, adaptive multichanneling in the two cases of Section 8.4.2 was used, and $\delta = 0.01$ (Section 8.4.1).

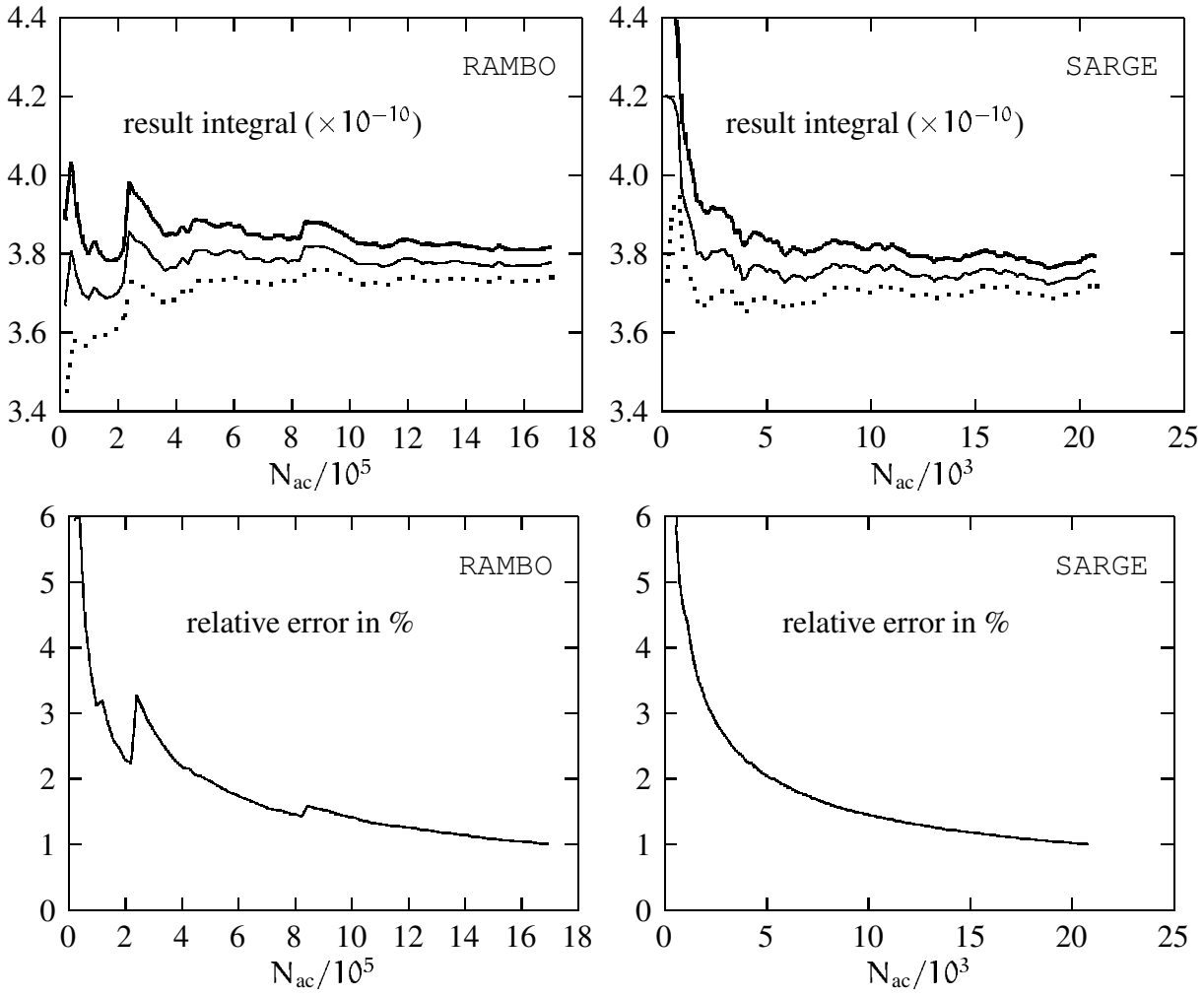

Figure 8.3: The convergence of the MC-process in the integration of the SPHEL-integrand for $n = 5$, with $\sqrt{s} = 1000$, $p_T = 40$ and $\theta_0 = 30°$. The upper graphs show the integral itself as function of the number of accepted events, together with the estimated bounds on the expected deviations. The lower graphs show the relative error. SARGE was used with adaptive multi-channeling in the two cases of Section 8.4.2, with $\delta = 0.01$ (Section 8.4.1) and without the variable ξ_v. The number of generated events was $6,699,944$, and the cpu-time was 0.308 hours.

of MC-integrals as function of the number of accepted events. Depicted are the integral σ with the bounds on the expected deviation coming from the estimated expected error, and the relative error. Especially the graphs with the relative error are illustrative, since they show that it converges to zero more smoothly for SARGE then for RAMBO. Notice the spike for RAMBO around $N_{ac} = 25000$, where an event obviously hits a singularity.

8.7 Other pole structures

The APS of (8.1) is not the only pole structure occurring in the squared amplitudes of QCD-processes; not even in purely gluonic processes. For example, in the case of $gg \to 4g$, also permutations of

$$\frac{1}{(p_1p_3)(p_2p_4)(p_0p_1)(\tilde{p}_0p_2)(p_0-p_1-p_2)^2} \tag{8.45}$$

occur [35]. If one is able to generate momenta with this density, it can be included in the whole density with the use of the adaptive multichannel technique. In the interpretation of the transition amplitude as a sum of Feynman diagrams, this kind of pole structures typically come from t-channel diagrams, which are of the type

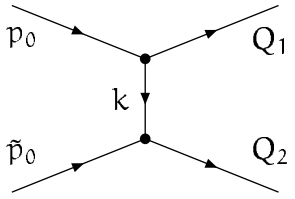

,

and where, for this case, $Q_1 = p_1 + p_3$ and $Q_2 = p_2 + p_4$, so that $k = p_0 - p_1 - p_3$. The natural way to generate a density with this pole structure is by generating $s_i := Q_i^2$ with a density proportional to $1/s_i$, a variable t that plays the role of $(p_0 - p_1 - p_3)^2$, construct with this and some generated angles the momenta Q_i, and then split new momenta from each of these. For $n = 4$, only two momenta have to split off each Q_i, and there is a reasonable simple algorithm to generate these.

We shall now just present the algorithm that generates the density (8.56), and then show its correctness using the UAF. If we mention the generation of some random variable x 'with a density $f(x)$' in the following, we mean a density that is proportional to $f(x)$, and we shall not always write down the normalization explicitly. Furthermore, s denotes the square of the CM-energy and $\lambda := \lambda(s, s_1, s_2)$ the usual Mandelstam variable

$$\lambda := s^2 + s_1^2 + s_2^2 - 2ss_1 - 2ss_2 - 2s_1s_2 \ . \tag{8.46}$$

Of course, a cut has to be implemented in order to generate momenta following (8.45), and we shall be able to put $(p_ip_j) > \frac{1}{2}s_0$ for the scalar products occurring in the denominator, where s_0 only has to be larger than zero. To generate the momenta with density (8.45), one should

Algorithm 8.7.1 (T-CHANNEL)

1. generate s_1 and s_2 between s_0 and s with density $1/s_1$ and $1/s_2$;
2. generate t between $s - s_1 - s_2 \pm \sqrt{\lambda(s, s_1, s_2)}$ with density $1/[t(t + 2s_1)(t + 2s_2)]$;
3. put $z \leftarrow (s - s_1 - s_2 - t)/\sqrt{\lambda}$ and generate φ uniformly in $[0, 2\pi)$;
4. put $Q_1 \leftarrow (\sqrt{s_1 + \lambda/(4s)}, \sqrt{\lambda/(4s)}\,\hat{n}(z, \varphi))$ and $Q_2 \leftarrow \sqrt{s}\,e_0 - Q_1$;
5. for $i = 1, 2$, generate $z_i > 1 - 4s_0/(t + 2s_i)$ with density $1/(1 - z_i)$ and φ_i uniformly in $[0, 2\pi)$, and put $q_i \leftarrow \frac{1}{2}\sqrt{s_i}\,(1, \hat{n}(z_i, \varphi_i))$;
6. for $i = 1, 2$, rotate q_i to the CMF of Q_i, then boost it to the CMF of $Q_1 + Q_2$ to obtain p_i, and put $p_{i+2} \leftarrow Q_i - p_i$;

As a final step, the incoming momenta can be put to $p_0 \leftarrow \frac{1}{2}\sqrt{s}\,(e_0 + e_3)$ and $\tilde{p}_0 \leftarrow \frac{1}{2}\sqrt{s}\,(e_0 - e_3)$. The variables s_i and z_i can easily be obtained by inversion (Section 7.3.1). The variable t can best be obtained by generating $x := \frac{1}{2}\log(4s_1s_2) - \log t$ with the help of the rejection method (Section 7.3.3). In the UAF, the steps of the algorithm read as follows. Denoting

$$\varepsilon_1 := e_0 + e_3 \quad , \qquad \varepsilon_2 := e_0 - e_3 \quad , \qquad h_\pm := s - s_1 - s_2 \pm \sqrt{\lambda} \quad , \tag{8.47}$$

and

$$\begin{aligned} \mathrm{nrm}(s, s_1, s_2) \;&:=\; \int \frac{dt}{t(t + 2s_1)(t + 2s_2)}\,\theta(h_- < t < h_+) \\ &= \frac{1/4}{s_1 - s_2}\left[\frac{1}{s_2}\log\frac{1 + 2s_2/h_-}{1 + 2s_2/h_+} - \frac{1}{s_1}\log\frac{1 + 2s_1/h_-}{1 + 2s_1/h_+}\right] \quad , \end{aligned} \tag{8.48}$$

we have

1. $\displaystyle\int \frac{ds_1}{s_1}\frac{ds_2}{s_2}\,\frac{\theta(s_0 < s_{1,2} < s)}{(\log\frac{s}{s_0})^2}$
2. $\displaystyle\int \frac{dt}{t(t + 2s_1)(t + 2s_2)}\,\frac{\theta(h_- < t < h_+)}{\mathrm{nrm}(s, s_1, s_2)}$
3. $\displaystyle\int dz\,\delta\left(z - \frac{s - s_1 - s_2 - t}{\sqrt{\lambda}}\right)\frac{d\varphi}{2\pi}$
4. $\displaystyle\int d^4Q_1\,\delta\left(Q_1^0 - \sqrt{s_1 + \tfrac{\lambda}{4s}}\right)\delta^3\left(\vec{Q}_1 - \sqrt{\tfrac{\lambda}{4s}}\,\hat{n}(z, \varphi)\right) d^4Q_2\,\delta^4(Q_1 + Q_2 - \sqrt{s}\,e_0)$
5. $\displaystyle\int \prod_{i=1}^{2} \frac{dz_i}{1 - z_i}\,\frac{\theta(1 - z_i > \frac{4s_0}{t+2s_i})}{\log\frac{t+2s_i}{2s_0}}\,\frac{d\varphi_i}{2\pi}\,d^4q_i\,\delta(q_i^0 - \tfrac{1}{2}\sqrt{s_i})\,\delta^3(\vec{q}_i - q_i^0\hat{n}(z_i, \varphi_i))$
6. $\displaystyle\int \prod_{i=1}^{2} d^4b_i\,\delta^4(b_i - \mathcal{H}_{Q_i}\varepsilon_i)\,\delta^4(p_i - \mathcal{H}_{Q_i}^{-1}\mathcal{R}_{b_i}^{-1}q_i)\,\delta^4(p_{i+2} + p_i - Q_i) \quad .$

The various assignments imply the following identities. First of all, we have

$$(p_i + p_{i+2})^2 = Q_i^2 = s_i \quad . \tag{8.49}$$

Using that $4ss_1 + \lambda = (s + s_1 - s_2)^2$ we find

$$\sqrt{4s}\,(\varepsilon_1 \cdot Q_1) = s + s_1 - s_2 - z\sqrt{\lambda} = t + 2s_1 \tag{8.50}$$

and the same for $(1 \leftrightarrow 2)$, so that

$$t = 4(p_0 \cdot Q_1) - 2(p_1 + p_3)^2 = -2(p_0 - p_1 - p_3)^2 \quad . \tag{8.51}$$

Denote $\mathcal{L}_{Q_i} := \mathcal{R}_{b_i}\mathcal{H}_{Q_i}$, so that $q_i = \mathcal{L}_{Q_i} p_i$. Because $\mathcal{L}_{Q_i}\varepsilon_i \sim \varepsilon_1$, we find that

$$1 - z_i = \frac{2(\varepsilon_1 \cdot q_i)}{\sqrt{s_i}} = 2\frac{(\varepsilon_1 \cdot \mathcal{L}_{Q_i} p_i)}{(\varepsilon_1 \cdot \mathcal{L}_{Q_i} Q_i)} = 2\frac{(\varepsilon_i \cdot p_i)}{(\varepsilon_i \cdot Q_i)} \quad , \tag{8.52}$$

so that

$$(t + 2s_1)(1 - z_1) = 8(p_0 \cdot p_1) \quad \text{and} \quad (t + 2s_2)(1 - z_2) = 8(\tilde{p}_0 \cdot p_2) \quad . \tag{8.53}$$

We can conclude so far that the algorithm generates the correct pole structure. For the further evaluation of the integrals one can forget about the factors s_i, t, $t + 2s_i$ and $1 - z_i$ in the denominators. Using that

$$d^4 q_i\, \delta(q_i^0 - \tfrac{1}{2}\sqrt{s_i}\,)\, \delta^3(\,\vec{q}_i - q_i^0 \hat{n}(z_i, \varphi_i)\,) \;=\; 2\, d^4 q_i \vartheta(q_i)\, \delta^3(\frac{2}{\sqrt{s_i}}\,\vec{q}_i - \hat{n}(z_i, \varphi_i)\,) \;, \tag{8.54}$$

and replacing step 4 by

$$\left(\prod_{i=1}^{2} 2\sqrt{s_1 + \tfrac{\lambda}{4s}}\, d^4 Q_i \vartheta_{s_i}(Q_i)\right) \delta(z(\vec{Q}_1) - z)\, \delta(\varphi(\vec{Q}_1) - \varphi)\, \delta^4(Q_1 + Q_2 - \sqrt{s}\, e_0) \;, \tag{8.55}$$

the integrals can easily be performed backwards, i.e., in the order q_i, φ_i, z_i, b_i, Q_i, φ, z, t, s_1, s_2. The density finally is

$$\begin{aligned}\Theta_s(\{p\}_4)\, &\frac{\theta(2(p_0p_1) > s_0)\,\theta(2(\tilde{p}_0p_2) > s_0)\,\theta(2(p_1p_3) > s_0)\,\theta(2(p_2p_4) > s_0)}{(p_0p_1)(\tilde{p}_0p_2)(p_1p_3)(p_2p_4)[-(p_0 - p_1 - p_3)^2]} \\ &\times \frac{s}{24(2\pi)^3}\left[\left(\log\frac{s}{s_0}\right)^2 \log\left(\frac{t + 2s_1}{2s_0}\right)\, \log\left(\frac{t + 2s_2}{2s_0}\right) \mathrm{nrm}(s, s_1, s_2)\right]^{-1} \quad , \end{aligned} \tag{8.56}$$

where $s_i := (p_i + p_{i+2})^2$ and $t := -2(p_0 - p_1 - p_3)^2$.

8.8 Generating a uniform distribution inside a polytope

We consider the m-dimensional convex polytope $\mathbf{P}_m$ defined in (8.38). The task is to generate m-dimensional points uniformly inside $\mathbf{P}_m$. A straightforward way is to generate points inside the hypercube $[-1,1]^m$ and implement the other conditions by rejection, with an efficiency given by $\mathrm{Vol}(\mathbf{P}_m)/2^m$, where $\mathrm{Vol}(\mathbf{P}_m)$ is the volume of the polytope. This may, however, become slow if $\mathrm{Vol}(\mathbf{P}_m)$ does not increase fast with m. Let us, therefore, compute $\mathrm{Vol}(\mathbf{P}_m)$. We distinguish positive and negative x_i values. Define

$$V_m(k) := \int_{\mathbf{P}_m} dx_1 \cdots dx_m \, \theta(x_{1,2,\ldots,k} \le 0)\, \theta(x_{k+1,\ldots,m} \ge 0) \quad . \tag{8.57}$$

We then have

$$\mathrm{Vol}(\mathbf{P}_m) = \sum_{k=0}^{m} \frac{m!}{k!(m-k)!} V_m(k) \quad . \tag{8.58}$$

In the calculation of $V_m(k)$ we notice that the only nontrivial constraints are of the type $x_i - x_j < 1$, with $i = k+1, k+2, \ldots, m$ and $j = 1, 2, \ldots, k$. Writing $x_i = -y_i$ for $i = 1, 2, \ldots, k$, we therefore have

$$V_m(k) = \int_0^1 dy_1 dy_2 \cdots dy_k dx_{k+1} dx_{k+2} \cdots dx_m \, \theta\left(\max_j x_j + \max_i y_i < 1 \right) \quad . \tag{8.59}$$

Relabeling such that $\max_i y_i = y_1$ and $\max_j x_j = x_m$ then leads us to

$$\begin{aligned} V_m(k) &= k(m-k) \int_0^1 dy_1 \int_0^{y_1} dy_2 \cdots dy_k \int_0^1 dx_m \int_0^{x_m} dx_{k+1} dx_{m-1} \theta(x_m + y_1 < 1) \\ &= k(m-k) \int_0^1 dy_1 \, y_1^{k-1} \int_0^{1-y_1} dx_m \, x_m^{m-k-1} \\ &= k \int_0^1 dy_1 \, y_1^{k-1} (1-y_1)^{m-k} = \frac{k!(m-k)!}{m!} \quad , \end{aligned} \tag{8.60}$$

so that we find

$$\mathrm{Vol}(\mathbf{P}_m) = m + 1 \quad . \tag{8.61}$$

Accordingly, the rejection algorithm will quickly become inefficient, below 1% for $n > 10$. The above calculation actually allows us to construct an optimal algorithm by working backwards. In the following each ρ_i stands for a new call to the random number source.

Algorithm 8.8.1 (`POLYTOPE`)

1. choose an integer k. Since $m!V_m(k)/k!(m-k)! = 1$, it should be chosen uniformly in $[0, m]$, so

$$k \leftarrow \lfloor (m+1)\rho_0 \rfloor \quad .$$

2. if $k = 0$ we simply have
$$x_i \leftarrow \rho_i \quad i = 1, m \quad .$$
If $k = m$ we use
$$x_i \leftarrow -\rho_i \quad i = 1, m \quad .$$

3. for $0 < k < m$, generate y_1 in $[0, 1]$ according to the distribution $y_1^{k-1}(1-y_1)^{m-k}$. An efficient algorithm to do this is Cheng's rejection algorithm BA for beta random variates (cf. [5])[3], but also the following works:
$$v_1 \leftarrow -\log\left(\prod_{i=1}^{k} \rho_i\right) \quad , \quad v_2 \leftarrow -\log\left(\prod_{j=1}^{m-k+1} \rho_j\right) \quad , \quad y_1 \leftarrow \frac{v_1}{v_1 + v_2} \quad .$$

4. generate x_m in $[0, 1-y_1]$ according to the distribution x_m^{m-k-1}. The algorithm to do this is
$$x_m \leftarrow (1-y_1)\rho_m^{1/(m-k)} \quad .$$

5. generate the $y_{2,\ldots,k}$ uniformly in $[0, y_1]$ and flip sign:
$$x_1 \leftarrow -y_1 \quad , \quad x_i \leftarrow -\rho_i y_1 \quad , i = 2, 3, \ldots, k \quad .$$

6. generate the $x_{k+1,\ldots,m-1}$ uniformly in $[0, x_m]$:
$$x_j \leftarrow \rho_j x_m \quad , j = k+1, k+2, \ldots, m-1 \quad .$$

7. Finally, perform a random permutation of the whole set of x values.

8.8.1 Computational complexity

The number usage S, that is, the expected number of calls to the random number source ρ per event can be derived easily. In the first place, 1 number is used to get k for every event. In a fraction $2/(m+1)$ of the cases, only m calls are made. In the remaining cases, there are $k + (m-k+1) = m+1$ calls to get y_1, and 1 call for all the other x values. Finally, the simplest permutation algorithm calls $m-1$ times [2]. The expected number of calls is therefore
$$S = 1 + \frac{2m}{m+1} + \frac{m-1}{m+1}(m+1+(m-1)+(m-1)) = \frac{3m^2 - m + 2}{m+1} \quad . \tag{8.62}$$
For large m this comes to about $3m-1$ calls per event. Using a more sophisticated permutation algorithm would use at least 1 call, giving
$$S = 1 + \frac{2m}{m+1} + \frac{m-1}{m+1}(m+1+(m-1)+(1)) = 2m \quad . \tag{8.63}$$

[3]There is an error on page 438 of [5], where "$V \leftarrow \lambda^{-1} U_1 (1-U_1)^{-1}$" should be replaced by "$V \leftarrow \lambda^{-1} \log[U_1 (1-U_1)^{-1}]$".

We observed that Cheng's rejection algorithm to obtain y_1 uses about 2 calls per event. Denoting this number by C the expected number of calls becomes

$$S = \frac{2m^2 + (C-1)m - C + 3}{m+1} \sim 2m + C - 1 \tag{8.64}$$

for the simple permutation algorithm, while the more sophisticated one would yield

$$S = \frac{m^2 + (C+2)m - C + 1}{m+1} \sim m + C + 2 \ . \tag{8.65}$$

We see that in all these cases the algorithm is uniformly efficient in the sense that the needed number of calls is simply proportional to the problem's complexity m, as m becomes large. An ideal algorithm would of course still need m calls, while the straightforward rejection algorithm rather has $S = m2^m/(m+1) \sim 2^m$ expected calls per event.

In the testing of algorithms such as this one, it is useful to study expectation values of, and correlations between, the various x_i. Inserting either x_i or $x_i x_j$ in the integral expression for $V(P)$, we found after some algebra the following expectation values:

$$E(x_i) = 0 \quad , \quad E(x_i^2) = \frac{m+3}{6(m+1)} \quad , \quad E(x_i x_j) = \frac{m+3}{12(m+1)} \ \ (i \neq j) \ , \tag{8.66}$$

so that the correlation coefficient between two different x's is precisely 1/2 in all dimensions! This somewhat surprising fact allows for a simple but powerful check on the correctness of the algorithm's implementation.

As an extra illustration of the efficiency, we present in Tab. 8.4 the cpu-time (t_{cpu}) needed to generate 1000 points in an m-dimensional polytope, both with the algorithm just presented (`OURALG`) and the rejection method (`REJECT`). In the latter, we just

1. put $x_i \leftarrow 2\rho_i - 1$ for $i = 1, \ldots, m$;
2. reject x if $|x_i - x_j| > 1$ for any $i = 1, \ldots, m-1$ and $j = i+1, \ldots, m$.

The computations were done using a single 300-MHz UltraSPARC-IIi processor, and the random number generator used was `RANLUX` on level 3. For $m = 2$ and $m = 3$, the rejection method is quicker, but from $m = 4$ on, the cpu-time clearly grows linearly for `OURALG` and exponentially for the rejection method.

8.8.2 Extension

Let us, finally, comment on one possible extension of this algorithm. Suppose that the points x are distributed on the polytope $\mathbf{P}_m$, but with an additional (unnormalized) density given by

$$F(x) = \prod_{i=1}^{m} \cos(\tfrac{1}{2}\pi x_i) \ , \tag{8.67}$$

	t_{cpu}(sec)	
m	OURALG	REJECT
2	0.03	0.01
3	0.03	0.02
4	0.03	0.04
5	0.04	0.08
6	0.05	0.17
7	0.06	0.32
8	0.07	0.67
9	0.08	1.33
10	0.09	2.76

m	OURALG	REJECT
11	0.09	5.15
12	0.10	10.94
13	0.11	21.71
14	0.12	44.06
15	0.13	87.90
16	0.14	169.65
17	0.15	336.67
18	0.16	671.46
19	0.17	1383.33
20	0.18	2744.82

Table 8.4: The cpu-time (in seconds) needed to generate 1000 points in $\mathbf{P}_m$.

so that the density is suppressed near the edges. It is then still possible to compute $V_m(k)$ for this new density. Writing $s(x) := \sin(\frac{1}{2}\pi x)$ and $c(x) := \cos(\frac{1}{2}\pi x)$, we have

$$\begin{aligned} V_m(k) &= k(m-k)\int_0^1 dy_1 c(y_1)\int_0^{1-y_1} dx_m c(x_m)\left(\int_0^{y_1} dy\, c(y)\right)^{k-1}\left(\int_0^{x_m} dx\, c(x)\right)^{m-k-1} \\ &= k(m-k)\left(\frac{2}{\pi}\right)^m \int_0^1 ds(y_1)\, s(y_1)^{k-1}\int_0^{c(y_1)} ds(x_m)\, s(x_m)^{m-k-1} \\ &= \frac{2^{m-1}k}{\pi^m}\int_0^1 ds\, s^{k/2-1}(1-s)^{(m-k)/2} \;=\; \left(\frac{2}{\pi}\right)^m \frac{\Gamma(1+\frac{k}{2})\Gamma(1+\frac{m-k}{2})}{\Gamma(1+\frac{m}{2})}\quad , \end{aligned} \tag{8.68}$$

where we used $s := s(y_1)^2$. Therefore, a uniformly efficient algorithm can be constructed in this case as well, along the following lines. Using the $V_m(k)$, the relative weights for each k can be determined. Then s is generated as a β-distribution. The generation of the other x_i's involves only manipulations with sine and arcsine functions. Note that, for large m, the weighted volume $V(\mathbf{P}_m)$ is

$$V(\mathbf{P}_m) \;=\; \sum_{k=0}^{m}\left(\frac{2}{\pi}\right)^m \frac{\left(\frac{k}{2}\right)!\left(\frac{m-k}{2}\right)!}{\left(\frac{m}{2}\right)!}\frac{m!}{k!(m-k)!} \;\sim\; m\sqrt{\frac{\pi}{8}}\left(\frac{8}{\pi^2}\right)^{m/2}\quad , \tag{8.69}$$

so that a straightforward rejection algorithm would have number usage

$$S \sim \sqrt{\frac{8}{\pi}}\left(\frac{\pi^2}{2}\right)^{m/2}\quad , \tag{8.70}$$

and a correspondingly decreasing efficiency.

Bibliography

[1] W.H. Press, B.P. Flannery, S.A. Teukolsky and W.T. Vetterling, *Numerical Recipes* (Cambridge 1986).

[2] D.E. Knuth, *The Art of Computer Programming, Vol.2. 2d ed.* (Princeton, 1991).

[3] H. Niederreiter, *Random number generation and Quasi-Monte Carlo methods,* (SIAM, 1992).

[4] Y. Choquet-Bruhat, C. DeWitt-Morette with M. Dillard-Bleick, *Analysis, Manifolds and Physics. Part I: Basics* (North-Holland).

[5] L. Devroye, *Non-Uniform Random Variate Generation* (Springer, 1986).

[6] R.F. Tichy and M. Drmota, *Sequences, Discrepancies and Applications,* (Springer, 1997).

[7] S. Weinberg, *The Quantum Theory of Fields, Volume I* (Cambridge, 1995).

[8] R.J. Rivers, *Path integral methods in quantum field theory* (Cambridge, 1987).

[9] S. Coleman, *Aspects of Symmetry* (Cambridge, 1993).

[10] R.G. Laha and V.K. Rohatgi, *Probability Theory* (Wiley, 1979).

[11] P. Billingsley, *Convergence of Probability Measures* (Wiley, 1968).

[12] P. Hall and C.C. Heyde, *Martingale limit theory and its application* (Academic Press, 1980).

[13] L.D. Landau and E.M. Lifshitz, *Mechanics Third Edition* (Pergamon Press, 1976).

[14] G.H. Hardy, E.M. Wright, *An introduction to the Theory of Numbers* (Oxford, 1988).

[15] F. James, *Monte Carlo theory and practice*, Rep. Prog. Phys. 43 (1980) 1145-1189.

[16] S. Tezuka, *Polynomial arithmetic analogue of Halton sequences*, ACM Trans. Modeling and Computer Simulation 3 (1993) 99-107,
S. Ninomiya and S. Tezuka, *Toward real-time pricing of complex financial derivatives*, Applied Mathematical Finance 3 (1996) 1-20.

[17] H. Woźniakowski, *Average-case complexity of multivariate integration,* Bull. AMS 24 (1991) 185-194.

[18] T.W. Anderson, *Goodness of fit tests for spectral distributions*, Ann. Statist. 21 (1993) 830-847.

[19] P. Hellekalek and H. Niederreiter, *The weighted spectral test: Diaphony*, ACM Trans. Model. Comput. Simul. 8, No.1 (1998), 43-60.

[20] P. Hellekalek and H. Leeb, *Dyadic diaphony*, Acta Arith. 80, No.2 (1997), 187-196.

[21] M. Berblinger, Ch. Schlier, T. Weiss, *Monte Carlo integration with quasi-random numbers: experience with discontinuous integrands*, Comp. Phys. Comm. 99 (1997) 151-162.

[22] F. James, J. Hoogland, and R. Kleiss, *Multidimensional sampling for simulation and integration: measures, discrepancies and quasi-random numbers,* Comp. Phys. Comm. 99 (1997) 180-220.

[23] J. Hoogland and R. Kleiss, *Discrepancy-based error estimates for Quasi-Monte Carlo. I: General formalism*, Comp. Phys. Comm. 98 (1996) 111-127.

[24] J. Hoogland and R. Kleiss, *Discrepancy-based error estimates for Quasi-Monte Carlo. II: Results for one dimension*, Comp. Phys. Comm. 98 (1996) 128-136.

[25] J. Hoogland and R. Kleiss, *Discrepancy-based error estimates for Quasi-Monte Carlo. III: Error distributions and central limits*, Comp. Phys. Comm. 101 (1997) 21-30.

[26] H. Leeb, *Weak limits for diaphony,* Proceedings of the *2nd International Conference on Monte Carlo and Quasi-Monte Carlo Methods in Scientific Computing,* edited by H. Niederreiter, P. Hellekalek, G. Larcher, and P. Zinterhof Lecture notes in statistics, (Springer).

[27] E.N. Argyres, R. Kleiss, C.G. Papadopoulos, *Amplitude estimates for multi-Higgs production at high-energies*, Nucl. Phys. B391:42-56 (1993);

[28] R. Hagedorn and J. Rafelski, *Analytic Structure and Explicit Solution of an Important Implicit Equation*, Commun. Math. Phys. 83:563-578 (1982).

[29] N.N. Khuri and O.A. McBryan, *Explicit solutions for the 't Hooft transformation*, Phys. Ref. D20:881-886 (1979).

[30] R. Kleiss and R. Pittau, *Weight optimization in multichannel Monte Carlo*, Comp. Phys. Comm. 83 (1994) 141-146.

[31] E. Byckling and K. Kajantie, *Particle Kinematics* (Wiley, 1973).

[32] W.J. Stirling, R. Kleiss and S.D. Ellis, *A new Monte Carlo treatment of multiparticle phase space at high energy*, Comp. Phys. Comm. 40 (1986) 359.

[33] R. Kleiss and J. Stirling, *Massive multiplicities and Monte Carlo*, Nucl. Phys. B385 (1992) 413-432.

[34] H. Kharraziha and S. Moretti, *The metropolis algorithm for on shell momentum phase space*, Comp. Phys. Comm. 127 (2000) 242-260.

[35] J.G.M. Kuijf, *Multiparton production at hadron colliders*, PhD thesis, University of Leiden, 1991.

[36] F. Berends and H. Kuijf, *Jets at the LHC*, Nucl. Phys. B353 (1991) 59-86.

[37] P. Draggiotis, R. Kleiss and C.G. Papadopoulos, *On the computation of multigluon amplitudes*, Nucl. Phys. B439 (1998) 157-164.

[38] F. Caravaglios, M.L. Mangano, M. Moretti and R. Pittau, *A new approach to multi-jet calculations in hadron collisions*, Nucl. Phys. B539 (1999) 215-232.

[39] P. Draggiotis, private communication.

Summary

Since particle physicists consider themselves scientists, they apply the scientific method in their exploration of nature, which means that they perform experiments and have a model that tries to reproduce the results of the experiments. Furthermore, as the scientific method demands, they make predictions derived from the model, which are believed to be testable in the (near) future. The model gives the best description of nature on the most fundamental level that is currently accessible by the experiments, and is called the Standard Model. It is based on the physical concept of quantum mechanical particles and the mathematical construction of quantum field theory.

Quantum theories describe nature by the dynamics of states, and for a model of quantum particles, these are states of particles. At one time, this state with these particles is appropriate to a physical situation, and at another time, that state with those particles is appropriate. An important piece of information provided by the model comes from the *transition probabilities*, which give the probability to get, in a certain situation, from one certain particle state to another certain particle state. These probabilities are interpreted as the ratios of the number of times the different states should appear, starting from the same state every time. In an experiment, one particular state is prepared millions of times, and then it is counted how often it goes over into which other state. These numbers are then compared with the probabilities predicted by the model in order to check its validity.

transition probabilities

Conceptually, the connection between model and experiments with the help of the transition probabilities is easy. Practically, however, it is difficult. One of the difficulties lies in the fact that, among other things, the *momenta* of the particles belong to the characteristics of a state. These include the information in which directions the particles are moving, and it is possible that states only differ in these directions. The types and numbers of particles involved may be exactly the same; if the momenta are just slightly different, the states are different. The problem is that it is impossible to interpret the probabilities as described before, if the number of different states is so large. If a state with a definite momentum configuration for the particles appears at all, it will appear at most one time, and the model predicts probability zero for the state to occur. One can only speak about a non-zero probability for the direction of a particle, if it concerns a certain (small) range of directions within which the particular direction is predicted to be. The set of all possible momentum configurations is a continuum, called *phase space*, and transition probabilities are probability densities over phase space.

momenta

phase space

The solution to the problem is to consider states that only differ in momentum configuration as equivalent. In an experiment, this just means that such states should not be counted separately, but should be collected together. For the model, this means that the average of the transition probabilities over the momentum configurations, over phase space, has to be calculated, and has to be multiplied by the total magnitude, the volume, of phase space. This is an example of the mathematical procedure of integration. It asks for a measure on phase space, which is given by the model of quantum particles. The quantity of which the average has to be calculated, in this case the probability density, is called the *integrand*. The integration problem is again difficult to solve, but its solution is accessible, especially with the help of computers.

integrand

Monte Carlo

points

A popular method to integrate an integrand over phase space is the *Monte Carlo* method, and the idea behind it is, again, simple; just do the same as the experimentalists. Take the average over a (finite) number of momentum configurations, or phase space *points*, chosen at random, and hope that the result comes close to the exact average. Probability theory tells us that, if the points are chosen according to a uniform distribution, and their number becomes larger and larger, then the result converges to the exact average. To understand what is meant by 'chosen according to a uniform distribution', it is helpful to consider the process of choosing points in phase space as the delivery of points by phase space itself. If the points are *distributed uniformly*, then the probability for each region of phase space to deliver the following point is proportional to the volume of that region; at each instance in the process, all regions should get a fair chance to deliver a point. The volumes are measured by the measure mentioned before. The number of points, needed to get a result that is as close to the exact average as demanded, can be derived from a formula for the expected deviation at each number of used points. This formula is supplied by probability theory, and shows an expected deviation which becomes smaller with larger number of used points.

uniform distribution

The Monte Carlo method almost always works. There are some restrictions on the integrand, but the number of degrees of freedom over which it has to be averaged, the number of dimensions, does not matter. The only drawback of the method is that it can be rather slow, because the number of phase space points often has to be large. In those cases, it pays to 'load the dice', and not to give all regions a fair chance to deliver points.

The reason why the Monte Carlo method works is that enough information about the integrand is obtained to make a good estimate of its average. The points get distributed uniformly over phase space, so that information is obtained that is diverse enough for a trustworthy average. However, if it is known for which regions of phase space the integrand shows its most diverse behavior, one would like to use more points in that region, and less in the less interesting regions. This can be achieved by giving a larger (than fair) probability to the interesting regions to deliver points. These probabilities have to be known exactly, in order to compensate for the cheating when the average is calculated: points coming from uninteresting regions should get a higher weight, since less of them are used. This improvement of the Monte Carlo method is called *importance sampling*, and the second part of this thesis deals with an explicit application to specific kinds of transition probabilities.

importance sampling

Calculations of the kind described above are usually done with the help of computers, for which there are 'standard' algorithms to deliver, or *generate*, numbers between 0 and 1. These can be considered distributed 'as good as' randomly according to the uniform distribution. They are called *(pseudo) random numbers*, where the 'pseudo' represents the 'as good as' in the previous sentence. A computer cannot do things at random, but it can run algorithms that deliver randomly looking results, and for the purpose of Monte Carlo integration, this suffices. With the algorithms mentioned above, all other kind of random points in spaces, needed for the application of Monte Carlo method, have to be constructed, and in practice, this is almost always possible. Every problem of calculating an average with the Monte Carlo method has to be reduced to a problem of taking the average of a (complicated) integrand over many degrees of freedom that all range from 0 to 1. This is also the case for importance sampling, where one just chooses a smart integrand. So eventually, one always applies the ordinary Monte Carlo method on a space of variables between 0 and 1, called a *hypercube*, using configurations of random numbers, again called *points*.

random numbers

hypercube

As noted before, the Monte Carlo method works because the points get distributed uniformly over the hypercube. However, random numbers will not necessarily deliver points that are distributed as uniformly as possible over the hypercube, and there is room for improvement. This sounds confusing, but there is a difference between the uniform distribution in the probabilistic sense, with fair probabilities for all regions of the hypercube to deliver a point, and the uniformity of the distribution over the hypercube of a given set of points; one only uses the same words. In the first case, there are fair probabilities at each instance in the process, so that two following points can still get close together, and this is something one would like to avoid happening. If there is a region where a few points have shown up already, and another which is still empty, then it is time that the latter region delivers a point. As a result of this kind of 'fudging', the points are not chosen independently anymore, but one might need less of them for a good estimate of the average. This method is called the *Quasi Monte Carlo* method, and the points are called *quasi random*.

Quasi Monte Carlo

The Quasi Monte Carlo method also has its drawbacks. First of all, it is easier to let a computer choose the points with fair chances than distributed as uniformly as possible. Secondly, the formula for the expected deviation of the result only works for the normal Monte Carlo method. So the Quasi Monte Carlo result may be better, you only do not know how much. There are formulas that can be used, and they ask for the rate of non-uniformity, the *discrepancy*, of the set of used points. These formulae, however, are very complicated.

discrepancy

One way to compare the normal and the Quasi Monte Carlo method is by calculating the probability for a set of points, consisting of random numbers, to have a certain discrepancy. If there is a large probability for the discrepancy to be equally small, compared with a quasi random set of points, then the two methods are equally good. If this probability is small, then one better uses the Quasi Monte Carlo method. The first part of this thesis is devoted to the calculation of such probability distributions.

Samenvatting

Aangezien deeltjesfysici zichzelf als wetenschappers beschouwen, hanteren zij de wetenschappelijke methode bij hun onderzoek van de natuur. Dit betekent dat ze experimenten doen en een model hebben dat de resultaten van de experimenten tracht te reproduceren. Bovendien doen ze voorspellingen aan de hand van het model, waarvan geloofd wordt dat ze verifieerbaar zijn in de (nabije) toekomst, zoals de wetenschappelijke methode verlangt. Dit model geeft de beste beschrijving van de natuur op het meest fundamentele niveau dat toegankelijk is met de huidige experimenten en wordt het Standaard Model genoemd. Het is gebaseerd op het fysische concept van quantummechanische deeltjes en het wiskundige formalisme van de quantumveldentheorie.

Quantumtheorieën beschrijven de natuur met behulp van de dynamica van toestanden en voor een model van quantumdeeltjes zijn dit deeltjestoestanden. Op het ene ogenblik is deze toestand met deze deeltjes van toepassing op een fysische situatie en op een ander ogenblik die toestand met die deeltjes. Belangrijke informatie, die door het model geleverd wordt, komt van de *overgangswaarschijnlijkheden*, die de waarschijnlijkheid geven om, in een bepaalde situatie, van de ene toestand over te gaan in de andere toestand. Deze waarschijnlijkheden worden geïnterpreteerd als de verhoudingen van het aantal keren dat de verschillende toestanden zouden verschijnen, wanneer er telkens met dezelfde toestand gestart wordt. In een experiment wordt één en dezelfde toestand miljoenen keren geprepareerd en dan wordt er geteld hoe vaak deze over gaat in welke andere toestanden. Deze getallen worden dan vergeleken met de door het model voorspelde waarschijnlijkheden, zodat zijn geldigheid nagegaan kan worden.

overgangswaarschijnlijkheden

Conceptueel is het verband tussen het model en de experimenten met behulp van de overgangswaarschijnlijkheden gemakkelijk te leggen. Praktisch is het echter moeilijk. Eén van de moeilijkheden ligt in het feit dat de impulsen van de deeltjes deel uit maken van de karakteristieken van een toestand. Deze bevatten o.a. de richtingen in welke de deeltjes zich bewegen en het is mogelijk dat toestanden alleen verschillen in deze richtingen. De types en aantallen deeltjes mogen precies hetzelfde zijn; als de impulsen verschillen, dan verschillen de toestanden. Het probleem is dat het onmogelijk is om de waarschijnlijkheden te interpreteren zoals zojuist beschreven, als het aantal toestanden zo groot is. Als een toestand met een bepaalde impulsconfiguratie zich überhaupt voor doet, dan hoogstens één keer en het model voorspelt een kans gelijk aan nul dat hij zich voor doet. Men kan met betrekking tot de richting van een deeltje alleen over een kans spreken die niet nul is, als het een bepaald bereik van richtingen betreft waarbinnen de richting voorspeld wordt te liggen. De verzameling van alle mogelijke impulsconfiguraties

faseruimte is een continüum dat de *faseruimte* genoemd wordt, en de overgangswaarschijnlijkheden zijn waarschijnlijkheidsdichtheden op de faseruimte.

De oplossing voor het probleem is het equivalent beschouwen van toestanden die alleen in impulsconfiguratie verschillen. In een experiment betekent dit eenvoudigweg dat zulke toestanden niet apart geteld moeten worden, maar bij elkaar genomen moeten worden. Voor het model betekent dit dat het gemiddelde van de overgangswaarschijnlijkheden over de faseruimte genomen moet worden, en vermenigvuldigd moet worden met de totale uitgebreidheid, het volume, van de faseruimte. Dit is een voorbeeld van de wiskundige procedure van integratie. Er is een maat op de faseruimte voor nodig, die geleverd wordt door het model van quantumdeeltjes. De grootheid van welke het gemiddelde uitgerekend moet worden, in dit geval de overgangswaarschijnlijkheid, wordt de *integrand* genoemd. Het integratieprobleem is weerom moeilijk op te lossen, maar de oplossing is bereikbaar, in het bijzonder met behulp van computers.

integrand

Monte Carlo Een populaire methode om een integrand over de faseruimte te integreren is de *Monte Carlo* methode en de gedachte erachter is, weerom, eenvoudig; doe maar hetzelfde als de experimentatoren. Neem het gemiddelde over een (eindig) aantal willekeurig gekozen impulsconfiguraties, ook wel *punten* in de faseruimte genoemd, en hoop dat het resultaat dicht bij het exacte gemiddelde komt. De waarschijnlijkheidsleer vertelt ons dat het resultaat naar het exacte gemiddelde convergeert als de punten gekozen worden volgens een uniforme verdeling en hun aantal groter en groter wordt. Om te begrijpen wat er bedoeld wordt met 'gekozen worden volgens een uniforme verdeling' is het nuttig om het proces van het kiezen van punten in de faseruimte te zien als het leveren van punten door de faseruimte zelf. Als de punten *uniform verdeeld* zijn, dan is voor ieder gebied van de faseruimte de waarschijnlijkheid om het volgende punt te leveren evenredig aan het volume van dat gebied: op ieder moment van het proces behoren alle gebieden een eerlijke kans te krijgen om een punt te leveren. De volumes worden gemeten met de eerder genoemde maat. Het aantal punten dat nodig is om een resultaat te verkrijgen dat dicht genoeg bij het exacte gemiddelde ligt kan afgeleid worden van een formule voor de verwachte afwijking na ieder aantal gebruikte punten. Deze formule komt uit de waarschijnlijkheidsleer en laat een verwachte afwijking zien die afneemt met het aantal gebruikte punten.

punten

uniforme verdeling

De Monte Carlo methode werkt bijna altijd. Er zijn een paar restricties op de integrand, maar het aantal vrijheidsgraden waarover het gemiddelde genomen moet worden, het aantal dimensies, maakt niet uit. Het enige nadeel van de methode is dat hij nogal traag kan zijn, omdat het aantal benodigde punten vaak groot is. In die gevallen loont het zich om 'vals te spelen' en niet alle gebieden een eerlijke kans te geven.

De reden waarom de Monte Carlo methode werkt is dat er voldoende informatie over de integrand wordt verkregen om een goede schatting van zijn gemiddelde te doen. De punten worden gelijkmatig over de faseruimte verdeeld, zodat de informatie afwisselend genoeg is voor een betrouwbaar gemiddelde. Echter, als het bekend is in welke gebieden van de faseruimte de integrand zijn meest afwisselende gedrag vertoont, dan zou men daar meer punten willen gebruiken dan in de minder interessante gebieden. Dit kan bereikt worden door de interessante gebieden een grotere (dan eerlijke) kans te geven om punten te leveren. Deze kansen moeten wel exact bekend zijn, zodat er gecompenseerd kan worden voor het 'vals spelen' wanneer het gemiddelde

importance sampling

uitgerekend wordt: punten uit de oninteressante gebieden moeten een hoger gewicht krijgen, want er worden er minder van gebruikt. Deze verbetering van de Monte Carlo methode wordt *importance sampling* genoemd en het tweede deel van dit proefschrift behandelt een expliciete toepassing op een specifiek soort overgangswaarschijnlijkheden.

Het boven beschreven soort van berekeningen wordt gewoonlijk gedaan met behulp van computers, waarvoor 'standaard' algorithmes bestaan die getallen tussen 0 en 1 leveren. Deze kunnen beschouwd worden als 'zo goed als' willekeurig verdeeld volgens de uniforme verdeling. Ze worden *(pseudo) toevalsgetallen* genoemd, waar het 'pseudo' het 'zo goed als' in de vorige zin representeert. Een computer kan geen willekeurige dingen doen, maar hij kan wel algorithmes uitvoeren die resultaten leveren die er willekeurig uit zien en voor het doel van Monte Carlo integratie voldoen. Met de bovengenoemde algorithmes moeten alle andere soorten van willekeurige punten in ruimtes, benodigd voor de toepassing van de Monte Carlo methode, geconstrueerd worden en dit is in de praktijk bijna altijd mogelijk. Ieder probleem van de berekening van een gemiddelde met behulp van de Monte Carlo methode moet gereduceerd worden tot het nemen van het gemiddelde van een (ingewikkelde) integrand over veel vrijheidsgraden, die allemaal lopen van 0 tot 1. Dit is ook het geval voor importance sampling, waarbij men enkel een slimme integrand kiest. Dus uiteindelijk past men altijd de gewone Monte Carlo methode toe op een ruimte van variabelen die lopen van 0 tot 1, een *hyperkubus* genoemd, waarbij configuraties van toevalsgetallen, weerom *punten* genoemd, gebruikt worden.

toevals-getallen

hyperkubus

Zoals zojuist beschreven werkt de Monte Carlo methode, omdat de punten gelijkmatig over de hyperkubus verdeeld worden. Toevalsgetallen geven echter niet noodzakelijk de meest gelijkmatige verdeling die mogelijk is en er is ruimte voor verbetering [4]. Met de toevalsgetallen zijn er gelijke kansen op ieder ogenblik in het proces en kan het gebeuren dat twee opeenvolgende punten vlak bij elkaar komen te liggen, wat men zou willen proberen te verhinderen. Als er een gebied is waar reeds enige punten zijn verschenen en een ander waar er nog geen zijn, dan wordt het tijd dat dit laatste gebied een punt levert. Als resultaat van dit 'geknoei' worden de punten niet meer onafhankelijk van elkaar gekozen, maar zijn er mogelijk minder nodig voor een goede schatting van het gemiddelde. Deze methode wordt de *Quasi Monte Carlo* methode genoemd en de punten worden *quasi toevallig* genoemd.

Quasi Monte Carlo

De Quasi Monte Carlo methode heeft ook zijn nadelen. Ten eerste is het gemakkelijker om een computer punten te laten kiezen met gelijke kansen dan zo gelijkmatig mogelijk verdeeld. Ten tweede werkt de formule voor de verwachte afwijking alleen voor de gewone Monte Carlo methode. Dus het Quasi Monte Carlo resultaat mag dan wel beter zijn, je weet alleen niet hoeveel. Er zijn formules die wel gebruikt kunnen worden en ze vragen naar de mate van niet-gelijkmatigheid, de *discrepantie*, van de verzameling van gebruikte punten. Deze formules zijn echter erg ingewikkeld.

discrepantie

Een manier om de normale en de Quasi Monte Carlo methode te vergelijken is door de waarschijnlijkheid uit te rekenen dat een verzameling van punten, bestaande uit toevalsgetallen,

[4] In het Engels kan hierover verwarring ontstaan, omdat voor het woord 'gelijkmatig' ook het woord 'uniformly' gebruikt wordt.

een bepaalde discrepantie vertoont. Als er een grote kans is voor de discrepantie om even klein te zijn als voor een quasi toevallige verzameling, dan zijn de twee methoden even goed. Als deze kans klein is, dan kan de Quasi Monte Carlo methode beter gebruikt worden. Het eerst gedeelte van dit proefschrift is gewijd aan de berekening van zulke waarschijnlijkheidsverdelingen.

List of publications

1. A. van Hameren, R. Kleiss and J. Hoogland, *Gaussian limits for discrepancies: I. Asymptotic results*, Comp. Phys. Comm. 107 (1997) 1-20.

2. A. van Hameren, R. Kleiss and J. Hoogland, *Gaussian limits for discrepancies*, Nucl. Phys. B (Proc. Suppl.) 63A-C (1998) 988-990.

3. A. van Hameren and R. Kleiss, *Quantum field theory for discrepancies*, Nucl. Phys. B 529 [PM] (1998) 737-762.

4. A. van Hameren and R. Kleiss, *Computer-aided analysis of Riemann sheet structures*, Comp. Phys. Comm. 116 (1999) 311-318.

5. A. van Hameren, R. Kleiss and C.G. Papadopoulos, *Quantum field theory for discrepancies II: 1/N corrections using fermions*, Nucl. Phys. B 558 [PM] (1999) 604-620.

6. A. van Hameren and R. Kleiss, *Scaling limits for the Lego discrepancy*, Nucl. Phys. B 558 [PM] (1999) 621-636.

7. A. van Hameren and R. Kleiss, *A fast algorithm for generating a uniform distribution inside a high-dimensional polytope*, Comp. Phys. Comm. 133 (2000) 1-5.

8. A. van Hameren, R. Kleiss and P. Draggiotis, *SARGE: an algorithm for generating QCD-antennas*, Phys. Lett. B 483 (2000) 124-130.

9. A. van Hameren and R. Kleiss, *Generating QCD-antennas*, Eur. Phys. J. C 17, (2000) 611-621.

Curriculum vitae

4-12-1973:	geboren te Horst.
1992:	gymnasium diploma behaald aan het Boschveld College te Venray.
1996:	doctoraal examen in de opleiding natuurkunde met lof afgelegd aan de Katholieke Universiteit Nijmegen.
1997-2000:	promotie onderzoek verricht onder Prof. Dr. R.H.P. Kleiss aan de Katholieke Universiteit Nijmegen.